UC Riverside

UC Riverside Electronic Theses and Dissertations

Title

Artemia franciscana as a Model for Stress in Saltwater Lakes: An Environmental Metabolomics Approach

Permalink

https://escholarship.org/uc/item/4w93x87t

Author

Morgan, Melissa Ann

Publication Date

2018

Copyright Information

This work is made available under the terms of a Creative Commons Attribution License, availalbe at https://creativecommons.org/licenses/by/4.0/

Peer reviewed|Thesis/dissertation

eScholarship.org Powered by the California Digital Library
University of California

UNIVERSITY OF CALIFORNIA
RIVERSIDE

Artemia franciscana as a Model for Stress in Saltwater Lakes: an Environmental Metabolomics Approach

A Dissertation submitted in partial satisfaction
of the requirements for the degree of

Doctor of Philosophy

in

Chemistry

by

Melissa Ann Morgan

September 2018

Dissertation Committee:
Dr. Cynthia K. Larive, Chairperson
Dr. Wenwan Zhong
Dr. De-en Jiang

Copyright by
Melissa Ann Morgan
2018

The Dissertation of Melissa Ann Morgan is approved:

_____

_____

_____

Committee Chairperson

University of California, Riverside

Acknowledgements

I'd like to acknowledge the following people, organizations, and services for their help in completing this dissertation: My advisor, Cindy Larive, for her support, guidance, and all of the edits. My labmates, Corey Griffith, Meredith Dinges, and Andrew Green, for their support and companionship and for providing a positive learning environment, especially Corey and Meredith with whom I worked side by side and who taught me so much. Justin Peng for his help as an undergraduate researcher and for bringing so much positive energy to the lab, I'm so lucky that I was your TA our first year at UCR. Yana Lyon for being a great listener and bike buddy, also I'm really grateful for the mass spectrometry help. Ryan Julian for allowing us the use of his instrument. Dan Borchardt and the ACIF for his help with instruments and method development. Jay Kirkwood and the UCR Metabolomics Core for their instrument use and analysis. Professor David Volz for taking time to help me with my research, providing me guidance, and allowing me the use of his instrument. The NSF IGERT WaterSENSE Fellowship for their funding, all the opportunities that they provided, and all the amazing people in the group. The Chemistry Department for supporting me for 5 years and the staff for taking care of us graduate students. Emily Li for her friendship, hotpot, and our dog, Sokka, the best pup in the world. Professor Paul Edmiston at the College of Wooster for encouraging me to pursue graduate research and for always being there to give a positive word. My Wooster friends for staying in touch and helping me stay sane while we struggle through graduate school and life and for making every effort to get together.

All the great friends I've made over my 5 years at UCR and Riverside through GradSuccess, sports, dog parties, physical therapy, and conference planning. Sylvia O'Neill for healing me and for being a great friend and role model as a strong, independent woman. Mick and Mimi for welcoming me to their family and letting me use their home for writing retreats. My parents for their love and support and for never trying to influence me. My sisters for being fun and goofy and making me regret the long distance. The little baby in my belly that is making me sick and miserable, I can't wait to meet you. And my husband, Matt, for his love, for always making me laugh, and for motivating me to finish as fast as possible so that we could be together again.

Dedication

To Women and Women First

ABSTRACT OF THE DISSERTATION

Artemia franciscana as a Model for Stress in Saltwater Lakes: an Environmental Metabolomics Approach

by

Melissa Ann Morgan

Doctor of Philosophy, Chemistry
University of California, Riverside, September 2018
Dr. Cynthia K. Larive, Chairperson

Due to rising salinity of freshwater systems and the lack of information about contaminants in saltwater lakes, there is a need for new methods to identify stressors and their effects in saline environments. We propose the use of the saltwater aquatic crustacean, *Artemia franciscana*, as a model organism for environmental metabolomics analysis of stressors for saltwater ecosystems. *Artemia* is an ideal indicator species because it is well-studied, have short life-cycles, and are robust. Their hemolymph has a high concentration of small molecule metabolites in an open circulatory system that is susceptible to environmental conditions and amenable to metabolomics analysis. Environmental metabolomics methods use analytical techniques, such as nuclear magnetic resonance (NMR) and mass spectrometry (MS), with chemometric analysis to characterize the interactions of an organism with its environment. When exposed to a stressor, these methods are used to identify biomarkers of exposure and assess the biochemical pathways that are impacted.

The small molecule metabolite profile of *Artemia* was characterized using 1D and 2D NMR and GC-MS and 43 metabolites were identified. Environmental metabolomics methods were developed using untargeted ^{1}H NMR and GC-MS analysis coupled with high-content

imaging to assess *Artemia* exposed to established and emerging stressors, which included temperature stress, Roundup® herbicide, and tris(1,3-dichloro-2-propyl) phosphate (TDCIPP) flame retardant. Targeted metabolomics analysis with LC-MS/MS was introduced to study the effects of perfluorooctanesulfonic acid (PFOS) and perfluorooctanoic acid (PFOA), 118 metabolites were identified with this method. Multivariate and univariate statistical analysis was used to identify biomarkers of exposure for each stressor and pathway analysis identified biochemical pathways that were likely affected. Although each stressor had a unique effect, it was determined that sugars, which are important for energy pathways such as glycolysis, and osmolytes, such as betaine and gadusol, play an important role in *Artemia* stress response.

Table of Contents

***Artemia franciscana* as an Indicator for Stress in Saltwater Lakes: An Environmental Metabolomics Approach**

Environmental metabolomics methods for experiments with *Artemia franciscana*

Evaluating sub-lethal stress from Roundup® exposure in *Artemia* franciscana using ^{1}H NMR and GC-MS

CHAPTER THREE

TDCIPP exposure affects *Artemia* growth and osmoregulation

CHAPTER FOUR

Metabolic perturbations from PFOS and PFOA in *Artemia franciscana*

CHAPTER FIVE

Conclusions and Future Work

CHAPTER SIX

List of Figures

List of Tables

Artemia franciscana as an Indicator for Stress in Saltwater Lakes: An Environmental Metabolomics Approach

CHAPTER ONE

1 Introduction

The work presented in this dissertation aims to establish *Artemia franciscana* as an indicator species for stress in saltwater lakes. Inland saltwater lakes are understudied and undervalued, but they are important ecosystems that are increasingly stressed from drought conditions and human interference.[1–3] Therefore, this work aimed to develop an ecosystem stress test for saltwater lakes to increase our understanding of the types of stress that affect these environments. This stress test was modeled after established *Daphnia magna* toxicity tests but used metabolite expression as an endpoint.[4] By measuring changes in metabolite expression in response to stress, the metabolic perturbation can be traced to discover the biochemical modes of action of the stressor. This approach to studying ecosystem stressors is called environmental metabolomics. We believe that an environmental metabolomics assay with *Artemia* as a model species can offer a rapid and simple, yet comprehensive, method to identify and characterize stressors in saltwater ecosystems.

The objectives of this thesis are as follows:

Objective 1. Develop and optimize environmental metabolomics methods using *Artemia franciscana.*

Objective 2. Establish the validity of *Artemia* environmental metabolomics for characterizing the effects of known and emerging contaminants in saltwater lakes.

Objective 3. Develop novel multiplatform assays to inform and drive metabolomics hypotheses.

Chapter one introduces the challenges facing saltwater lakes and the methods in use to identify environmental stressors. In chapter two, the exposure, instrumental analysis, and statistical analysis methods developed for environmental metabolomics using *Artemia franciscana* under temperature stress are presented as a proof of concept. This chapter also reports the *Artemia* metabolome as determined from *Artemia* extracts measured using gas chromatography-mass spectrometry (GC-MS) and ^{1}H nuclear magnetic resonance (NMR). Chapter three reports my findings on the impact of the Roundup® herbicide on the *Artemia* metabolome. In chapter four the effects of the organophosphate flame retardant, tris(1,3-dichloro-2-propyl) phosphate (TDCIPP), on the *Artemia* metabolome are reported along with a high-throughput imaging assay that provides phenotypic insights to augment our metabolomics findings. Chapter five describes the correlation between perfluorooctanesulfonic acid (PFOS) and perfluorooctanoic acid (PFOA) bioaccumulation and metabolic perturbation. Here, targeted metabolomics with liquid chromatography-mass spectrometry will be introduced with the findings presented for PFOA and PFOS metabolic perturbation. Chapter six includes conclusions and future directions of this work.

1.1. Environmental health and assessment

Global freshwater salinization is a major threat to aquatic ecosystems, drinking water availability, and recreation.[1–3,5,6] A recent study shows that many of the freshwater lakes in

the U.S. Midwest are suffering from rising salinity, largely from over-application and poor management of road salt in lakeside areas that are becoming increasingly urbanized. With the current chloride trends, the study projects that salinity levels will exceed the aquatic life threshold for many ecosystems in 50 years' time.[6] The impact of salinization in arid and semi-arid regions of the world is compounded by increased human pressures and scarcity of resources. In these regions, salinization is most often caused by diverting water for irrigation, which mobilizes salt in the soil and reduces inflows to catchment basins.[1,2]

Inland saltwater lakes account for a large percentage of the surface water in the Western U.S. and are critical habitats.[3] These lakes are naturally saline, but they are increasingly struggling from rapid increases in salinity due to anthropogenic interference.[1,7,8] Mono Lake and the Salton Sea are critical habitats for the Pacific Flyway and for agriculture in California.[7] At the Salton Sea, diversions for agriculture, reduced inflows from the Colorado River, and reduced rainfall are causing the lake to shrink and the salinity to increase rapidly. As this lake dries up and the shoreline becomes exposed, toxic dust pollutes the air and contaminates agriculture, and migratory birds lose one of their last sanctuaries to safely rest and fuel up on tilapia.[7–10]

In addition to rising salinity, the Salton Sea and many freshwater lakes in the US have long suffered from the effects of nonpoint source agricultural pollution, such as eutrophication from fertilizer, animal waste, and pesticide runoff.[11–14] Eutrophication, caused by excess nutrients, leads to hypoxia, dead zones, and toxic algae blooms that threaten human and

animal health. The decimation of the Mississippi River Delta ecosystem by seasonal algae blooms and dead zones as a result of agricultural pollution from the Corn Belt all along the Mississippi River is an unfortunate example of the harmful effects of eutrophication.[15–17] Non-point source pollution is difficult to curtail because its origin is diffuse. Many states now encourage cropland management strategies such as precision and no-till farming or tile drainage with filtration systems to prevent environmental release.[18–20] Clean-up methods, such as dredging lakebed sediment and applying adsorbent treatment for nutrient sequestration, may be applied at the back end after pollution is extreme; however, these methods are expensive and disruptive to the ecosystem.[15,21,22,22–24]

Although there are many methods in use to prevent or clean-up pollution once it has been identified, challenges with identifying environmental contaminants remain.[25] The environmental movement began with vivid and dramatic examples of the risks of pollution, such as the Cuyahoga River catching on fire.[26] This occurred many times over 100 years between 1868 and 1969 as a result of industries dumping untreated waste into the river. It was not always obvious that industrial waste would negatively affect human and environmental health, but once this was realized the source of the problem was not difficult to identify. Thanks to the establishment of the Environmental Protection Agency shortly after the 1969 Cuyahoga River fire, society has made a significant headway towards recognizing and preventing overt signs of pollution. However, cause and effect are not always easy to determine for non-point source pollutants when the effect occurs in an environment that is seemingly unrelated to the application.[25,27] In the cases of DDT

decimating the bald eagle population, the feminization of frogs from atrazine, and even the accumulation of plastic beads in marine vertebrates, it took many years to connect the dots because it was not clear how these contaminants came into contact with the affected non-target organism.[28–31] Many studies today focus on identifying emerging contaminants and determining their effects on human and environmental health.[25,27]

Environmental stress is caused by a stressor that reduces the performance or fitness of an organism or ecosystem.[32] Stressors may be endogenous (salinity or temperature) or exogenous (pharmaceuticals or agrochemicals), but typically result from anthropogenic influence, be it climate change or nonpoint source pollution. Many different aspects of an ecosystem may be studied in order to identify these stressors. Water quality is one such parameter that is measured and monitored using standardized tests developed by the EPA and USGS.[33–35] Regular monitoring of natural parameters like total dissolved solids, salinity, dissolved oxygen, temperature, and pH, provides insight on seasonal and yearly changes in different regions of the country in response to climate change or human interference.[34] However, these changes may not be important unless there is a corresponding effect on the biota. Therefore, environmental stress may be better evaluated using bioindicators.[36]

Bioindicators include biological organisms, communities, or processes that can be used to evaluate the state of an ecosystem. The canary in the coal mine is the most well-known example of a bioindicator.[36] In this situation, the death of the canary was an indicator of

unsafe levels of carbon monoxide, giving miners time to escape a hazardous situation. Other examples of bioindicators include the presence of lichen indicating poor air quality, declining honey bee populations reflecting insecticide pollution, low earthworm populations indicating poor soil quality, and low *Daphnia magna* populations reflecting degraded freshwater quality.[36,37] These examples of bioindicators involve regular environmental sampling to identify population trends. Environmental sampling is essential for evaluating long term trends, but it is time-consuming, costly, potentially disruptive to the environment, and data collection may be interrupted due to natural phenomena or when funding is limited. Therefore, in vitro and high-throughput screening assays using bioindicators are promising for less costly, rapid, specific, and quantitative evaluation of chemical effects on biota.[38,39]

In vitro studies with *Daphnia magna* have been established as standardized ecotoxicity assays.[4,40] Ecotoxicity testing refers both to the assessment of chemical effects on organisms and the testing of media for the presence of toxic compounds.[39] The Toxic Substances Control Act requires chemical manufacturers to conduct ecotoxicity testing prior to approval of products for commercial release.[41] The Organization for Economic Cooperation and Development (OECD) Guidelines for the testing of chemicals includes internationally accepted specifications under which new chemicals must comply. These tests fall into five categories: physical and chemical properties, effects on biotic systems, degradation and accumulation, health effects, and other.[42] The OECD *Daphnia* sp., Acute Immobilisation and Reproduction Test as well as the EPA freshwater *daphnids* aquatic

invertebrate acute toxicity test and daphnid chronic toxicity tests are widely used and accepted tests under the "effects on biotic systems" category.[4,40,42,43]

These *Daphnia* acute and chronic ecotoxicological assays rely on *Daphnia magna* for toxicity information for freshwater ecosystems, however, *Daphnia* are highly sensitive to salinity and would not be a suitable model for stressors for ecosystems with rising chloride levels.[44,45] Therefore, we propose *Artemia franciscana* as an alternative indicator for saltwater stress. *Artemia franciscana* are closely related to *Daphnia magna* but they are known to live in environments with a salinity range up to 300 ppm and thus may be used to study saltwater lakes, marine aquatic systems, and freshwater systems that are increasing in salinity.[46,47] *Artemia* fulfill all of criteria of a good indicator; they are abundant and common, well-studied, economically important, and they provide measurable responses to environmental stress.[36]

1.2. *Artemia* as an indicator for saltwater stress

The genus *Artemia* is an ancient and primitive aquatic crustacean that is found worldwide in inland saltwater lakes. The species *Artemia franciscana* is found in North America at the Great Salt Lake and the San Francisco Salt Pond. *Artemia* are an interesting biological model due to their unique development. In favorable environmental conditions, females will give birth to live, free-swimming *Artemia* nauplii, but when environmental conditions are poor, encysted gastrula embryos ("cysts") are released. These cysts are metabolically inactive but hatch once favorable environmental conditions return.[48–51] The Great Salt Lake

has a booming brine shrimp industry that relies on the formation of cysts that are collected and sold as fish food for aquacultures and aquariums all over the world. This phenomenon makes *Artemia* cysts ideal for ecotoxicity assays because the cysts are inexpensive, easy to hatch, and have a long shelf-life.[52]

Artemia also have a short life cycle, allowing life-stage and generation specific testing.[53] Metabolically inactive cysts are encysted in the gastrula phase of development while they are in the maternal brood sac.[49] Once released to the environment, they remain dormant until favorable conditions return. These dormant cysts are frozen in a vitrified state that makes them highly tolerant to environmental extremes.[54] The disaccharide sugar, trehalose, is responsible for their robust nature because it replaces water in cysts to form glass-like structures that protect the internal membranes from dehydration damage.[55] Favorable conditions trigger post-diapause development by activating the enzyme trehalase, which stimulates the metabolism of trehalose via the glycolytic pathway and Krebs cycle.[54] Metabolism and development is rapidly re-initiated with respiration, RNA and protein synthesis beginning within minutes of rehydration. Embryos emerge from the shell as swimming nauplius larva.[54]

For the first few days of life, nauplii utilize internal yolk platelet organelles for energy. These yolk platelets store glycogen and act as a protective structure for mitochondria during diapause and through the naupliar stage.[49,54,56] Yolk platelets are the source of the orange hue of nauplii, which disappears with the platelets as the *Artemia* develop to the

juvenile stage. *Artemia* begin to feed after depleting their yolk reserves and their digestive system matures. Their naupliar eye guides them towards light to find food. They use their antennae for swimming and for pushing food towards their mouth and they will eat algae and bacteria, or whatever detritus is found in the water.[46,50,57] *Artemia* molt, shedding their exoskeleton through several naupliar stages and then to the juvenile and adult stages. As they develop, their trunk grows longer, they develop swimming appendages called thoracopods and two compound eyes. The adult males develop claspers for mating and the females develop a brood sac for housing eggs and forming cysts (Figure 1.1).[54,57,58]

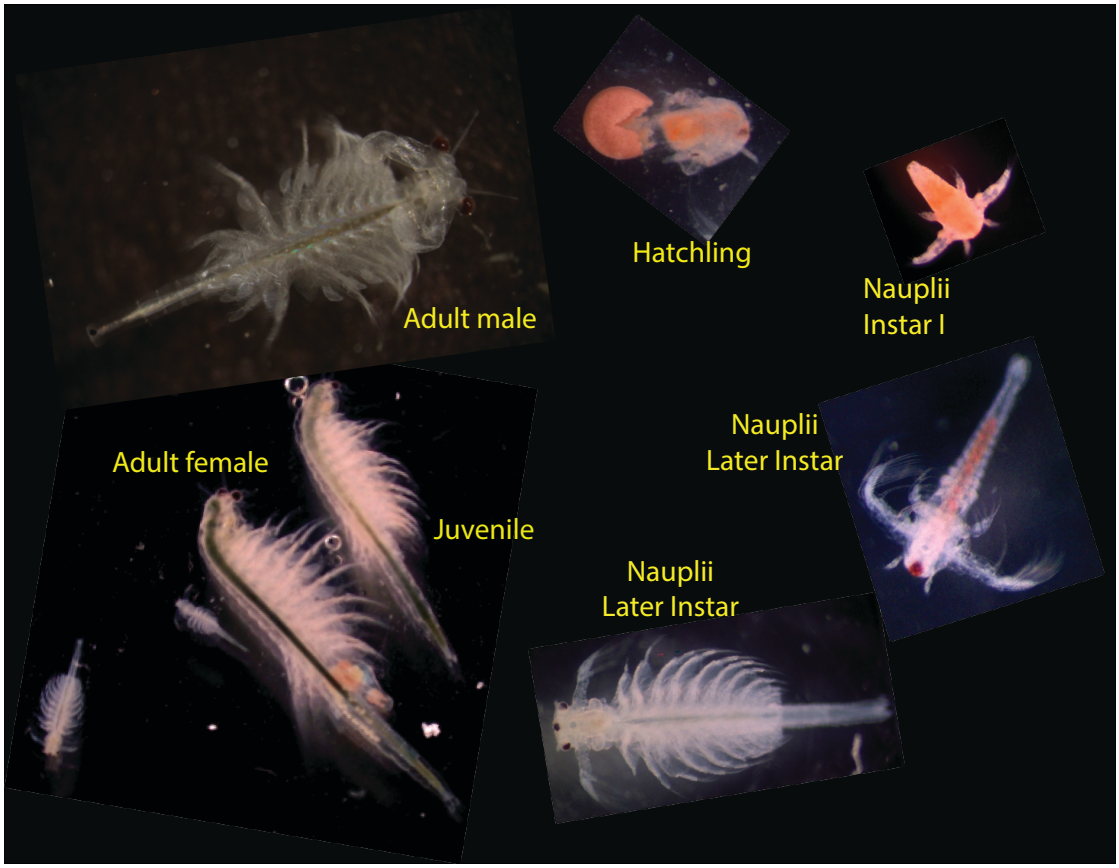

Figure 1.1. Life cycle of *Artemia* from hatchling to adulthood. Images taken with 10x Leica MZIII Pursuit Stereoscope with SPOT camera.

Developing embryos have several stress response pathways that contribute to their extreme robustness. For diapause and post-diapause embryos, the pH switch determines whether an embryo will hatch or resume dormancy. The activity of enzymatic processes for development are completely dependent on intracellular pH. At high pH, development may proceed, but at low pH, embryos will either remain dormant or revert to a dormant state.[49] Development is reversible for developing embryos up until the hatching processes begin. Trehalase and stress response proteins, like p26, Hsp70 and 90, are pH dependent and are important for countering protein damage due to thermal or environmental stress.[54,59,60]

Free swimming *Artemia* are more susceptible to environmental conditions than encysted gastrula but they are uniquely adapted for environmental extremes and they are the best osmoregulators in the animal kingdom.[54] *Artemia* often are 10 times less susceptible to toxic agents than *Daphnia* under similar test conditions, as is the case for Roundup® and TDCIPP, as described in Chapters 3 and 4. However, *Artemia* are susceptible to environmental conditions due to their open circulatory system. In the open circulatory system, the hemolymph circulates through the body and remains in direct contact with the animal's tissue which leads to greater exchange with the surrounding environment. This hemolymph contains a high concentration of free amino acids that are involved in primary metabolism and osmoregulation.[61,62]

Ecotoxicity tests with *Daphnia magna* use mortality, heart rate, and fecundity as assay endpoints. These endpoints are useful for identifying an effective concentration of a

contaminant, but in order to identify the toxic mode of action, further targeted testing is typically required.[40,63–66] Recent metabolomics studies have demonstrated the potential of monitoring metabolite shifts during sublethal stress in identifying toxic modes of action.[67] As *Artemia* are considered too robust for standard mortality tests, the potential for environmental metabolomics studies offers a new opportunity for *Artemia* use in ecotoxicity assays for studying saltwater stressors.[46,52,63,68]

1.3. Omics approaches for studying environmental stress

The omics revolution began with the Human Genome Project (HGP) that was completed in 2003. The goal of the HGP was to sequence the human genome and to identify the function of each gene.[69] This endeavor was a mega-scale, multi-disciplinary project that demonstrated the potential of big science for tackling global challenges.[70] The advancements made during the HGP have had far reaching implications for science and medicine. Technological advancements included the generation of new techniques for whole genome sequencing, the creation of publicly available databases to store biological information, and the development of approaches for handling and analyzing large datasets.[69,71] At the conclusion of the HGP, these new tools inspired and made possible new omics methodology to tackle additional biomolecules and biological systems.

The central dogma of biology says that DNA transcribes RNA which translates proteins that regulate the levels of downstream small molecule metabolites. These steps of the central dogma have corresponding omics fields that provide both novel and complementary

insights into biological questions. While science historically has tackled questions from a reductionist approach by isolating the problem as a means of simplifying the question, the HGP made it possible to study systems from a global, holistic, top-down approach.[70,72] Instead of targeting one or several genes for a mutation or variation, genomics looks for effects on the whole genome. The advances in genomics have led to commercial ventures that have drastically reduced the cost of genetic and carrier testing, as is the case for the company 23&Me, Inc. Transcriptomics, the study of total mRNA in an organism, proteomics, the study of all expressed proteins in an organism, and metabolomics, the study of the metabolite profile of an organism, are developing omics fields that measure the downstream products of gene expression and provide insights on biological conditions.[72] These omics approaches have been used to study disease progression, compare crop varietals, and illuminate the effects of environmental stress.[73–75] Whereas genomics, transcriptomics, and proteomics give partial insight into the systems-level status, metabolomics reflects how an organism obtains and utilizes basal building blocks and maintains energy balance. Metabolomics is arguably a more direct measure of organismal health and the utilization of environmental resources than other omics approaches.[76]

Metabolomics measures small molecule metabolites in complex biological samples. Small molecule metabolites are low molecular weight (< 900 Dalton) organic compounds that are the products of enzyme-catalyzed reactions in the cell. They regulate biological processes through intercellular biochemical pathways and are the building blocks of macromolecules, including proteins, lipids, polysaccharides, and nucleic acids.[77] There are approximately

5000 known human primary and secondary metabolites that have critical roles in maintaining homeostasis.[72] Metabolomics aims to profile the metabolite fingerprint of organisms under different biological conditions in order to identify differences in biochemical pathway activity. The variation in metabolite profiles measured under different experimental conditions provides information about metabolic modes of action that are triggered under these conditions.[78,79] Metabolomics has emerged as a powerful tool for biomarker discovery, especially for disease detection and environmental exposure.[72,74,78,80]

Environmental metabolomics is an emerging method for identifying ecosystem stressors by analyzing metabolite shifts in model organisms. These studies monitor changes to an organism's small-molecule metabolite profile before and after exposure to a stressor with the purpose of elucidating the toxicological mode of action.[78,81,82] Advances in analytical platforms, sample preparation protocols, hyphenated techniques, metabolite databases, and statistical analysis methods have enabled metabolic measurements to address increasingly complex environmental challenges in new model species. These advances are enabling a deeper understanding of the metabolic responses of organisms to environmental perturbations.[78,79,81]

1.4. Tools for metabolomics

The first step in environmental metabolomics experiments is to characterize the metabolome of the model organism. An organism's metabolome is its small molecule

fingerprint. This fingerprint is defined by the sample, which may be the whole body, one organ, one type of cell, etc. Once the sample is defined, isolation, extraction and derivatization steps are usually necessary to prepare the sample for instrumental analysis and metabolite profiling.[81,83] For living biological samples, prior to sample acquisition, all metabolic processes have to be halted to prevent sample degradation or post-experiment metabolism.[83,84] In many cases, this is accomplished by flash freezing in liquid nitrogen or in a -80 ºC freezer. For organisms that are tolerant of low temperatures, heat treatment may be necessary to quench enzymatic reactions. Halting metabolism as close to the end of the experiment as possible provides a snapshot of all metabolic processes occurring prior to death and leads to the identification of affected processes.[83]

1.4.1. Sample Preparation

Homogenization is used in experiments where the model organism has a tough exterior that needs to be disrupted to release the metabolites for analysis. Some of these methods include bead beating, sonication, and grinding with a mortar and pestle.[83] Rice is particularly challenging to homogenize, but bead beating with a cryo-cooled vacuum breaks apart the tissue and prevents the sample from heating and degrading.[85] After homogenization, solvent extractions isolate the desired small molecules from the unwanted biological material. In most cases, metabolomics studies seek to measure polar and semi-polar small molecules that are involved in primary metabolism. Commonly used solvent extraction methods include solid phase extraction (SPE) and liquid-liquid extraction (LLE). SPE methods use a solid stationary phase to which the molecules of interest bind.

They are eluted step wise using liquid solvents.[83] In liquid-liquid extraction, a biphasic method, such as the methanol:water:chloroform (MWC) method, is used for separating polar and non-polar molecules into two phases. In this method, polar metabolites are extracted into the methanol/water solvent layer, and unwanted lipids are extracted into the chloroform layer.[83,84] Some studies use a simple buffer or water extraction to study water soluble metabolites.[86] Other solvent conditions are used depending on experimental considerations, for example acetonitrile has been found to precipitate proteins better than methanol and cold methanol is important for some experiments to prevent metabolite degradation.[87,88] Further isolation and purification may involve centrifugation or filtration with high molecular weight centrifuge filters to remove proteins that could interfere with analysis. Metabolite solvent extracts may be dried using a vacuum centrifuge or lyophilizer to increase stability during storage or to reconstitute the sample into a different medium for analysis.[89]

1.4.2. Instrumental Analysis

The analytical instrumentation used for analysis of metabolite extracts plays a major role in metabolome characterization. Nuclear magnetic resonance spectroscopy (NMR) and mass spectrometry (MS) are common tools used for metabolomics. MS is a highly sensitive method for detection, quantitation, and structure elucidation. Hundreds of metabolites can be detected in a single run from very little sample. NMR is a powerful tool that is quantitative, reproducible, and suitable for complex mixtures. NMR is a non-destructive technique, so samples can be recovered for further analysis; however, the detection limits

are generally higher than MS. Numerous techniques within MS and NMR offer multifaceted approaches to detect and identify a variety of metabolites and accurately measure their concentrations.[78,90,91]

1.4.2.1. Nuclear Magnetic Resonance Spectroscopy

1.4.2.1.1. Nuclear Spin and Resonance

Nuclear magnetic resonance (NMR) spectroscopy is a spectroscopic technique that measures the absorbance of radio frequency radiation by atomic nuclei exposed to high magnetic fields. NMR is dependent on a quantum property called spin. A spinning charged nucleus generates a magnetic field. The resulting spin-magnet has a magnetic moment (μ) oriented along the axis of spin and proportional to the angular momentum (p). The proportionality constant, γ, is the gyromagnetic ratio and is different for every type of nucleus (Equation 1.1).

Equation 1.1

$$\mu = \gamma p$$

When an external magnetic field (B_0) is applied, the nucleus may orient into $2I + 1$ possible spin states depending on its spin quantum number. Nuclei may have integer spins (I = 1, 2, 3 ...) like ^{2}H, fractional spins (I = ½, 3/2, 5/2…) like ^{1}H, or no spin (I = 0) like ^{12}C. Those with I = 0 possess no nuclear spin and therefore cannot exhibit NMR. For a spin ½ nucleus such as the proton, there are two possible states alpha (+½) and beta (–½), and for I = 1,

such as deuterium, the states are +1, 0 and –1. For most nuclei with I = ½, the magnetic moment of the lower energy alpha state is aligned with the external field, but that of the higher energy beta spin state is opposed to the external field. However, this also depends on whether γ is positive or negative. In the case of ^{15}N, the beta spin is aligned with B_0. The difference in energy between these two states is demonstrated in Equation 1.2, where h is Planck's constant. This energy difference depends on the gyromagnetic ratio and the external magnetic field.[92,93]

Equation 1.2

$$\Delta E = \frac{\gamma h}{4\pi} B_0$$

The lack of sensitivity in NMR experiments is due to the small energy difference between the excited and ground states which leads to small population differences (Equation 1.3). In this equation, N_α = the population of spins in the alpha state, N_β= the population in the beta state, T is temperature, and k_B= the Boltzmann constant. When combining Equation 1.2 and Equation 1.3, we can see that a larger B_0 leads to a larger ΔE, which leads to a greater population ratio, therefore, higher magnetic fields are ideal for increased sensitivity.[94] However, sensitivity and signal-to-noise (S/N) is also dependent on the sample size, n, the gyromagnetic ratio of the excited spin, γ_e, the gyromagnetic ratio of the spin being detected, γ_d, and the acquisition time of the experiment, t (Equation 1.4). Increasing the magnetic field may reduce the resolution for some nuclei that have high chemical shift anisotropy, such as ^{31}P, for which peaks broaden at high fields.[92,94] Modern

NMR spectrometers have magnetic fields from 1-23 tesla (T). By convention, in NMR this energy difference is given as a frequency in units of MHz, ranging from 20-900 MHz, depending on the magnetic field strength and the nucleus being studied.

Equation 1.3

$$\frac{N_\alpha}{N_\beta} = e^{\Delta E/k_B T}$$

Equation 1.4

$$\frac{S}{N} \propto n\gamma_e \sqrt{\gamma_d^2 B_0^3 t}$$

Proton NMR (^{1}H NMR) is the most common type of NMR experiment, especially for high-throughput metabolomics. However, ^{13}C, ^{19}F, and ^{31}P are also important nuclei that have been widely used because they are biologically and pharmaceutically relevant.[78]

1.4.2.1.2. The NMR spectrum

In pulsed-NMR experiments, nuclei in a strong magnetic field are subjected to periodic pulses of radio frequency (RF) radiation. During the interval between pulses, the nuclei oscillate until the population distribution is restored. This oscillation produces a time-domain RF signal, called the free-induction decay (FID). The FID is detected with a radio receiver coil and converted to a frequency-domain NMR spectrum by Fourier transformation.[95,96]

The NMR spectrum is a plot of absorption versus frequency (Hz), labeled from right to left by convention. Frequency on the x-axis is usually converted to parts-per-million (ppm) by referencing the frequencies of the sample resonance (ν_s) to an internal reference standard (ν_r), such as tetramethylsilane for proton NMR, and dividing this by the spectrometer frequency in megahertz. This new value is referred to as chemical shift (σ). The unit ppm is dimensionless and is the same for any magnetic field, so it is consistent across instruments (Equation 1.5). The ^{1}H NMR spectrum of *Artemia* metabolite extracts is shown in Figure 1.2A. The resonance of 2,2-dimethyl-2-silapentane-5-sulfonic acid-d6 (DSS) is used as an internal chemical shift reference (0 ppm).

Equation 1.5

$$Chemical\ Shift\ \sigma\ (ppm) = \frac{\nu_s - \nu_r}{spectrometer\ frequency} x\ 10^6$$

1.4.2.1.3. Chemical shift

The spectrum for each molecule is unique because the frequency of RF radiation that is absorbed by a given nucleus is affected by its chemical environment, which includes nearby electrons and nuclei. The two main environmental effects are chemical shift and spin-spin coupling. Chemical shifts arise from local magnetic fields generated by the circulation of electrons in a molecule. This field opposes the primary field and shields the nucleus from the full effect of the primary field. The degree of shielding is proportional to electron density, so shielding decreases with increasing electronegativity of adjacent

groups. Nuclei in a molecule that experience high degrees of shielding resonate upfield (right, close to zero) and nuclei that are deshielded resonate downfield (left) on an NMR spectrum.[92,95,96] In the molecular structure of taurine (Figure 1.2B), there are four carbon bound protons that give rise to two resonances (3.25 and 3.43 ppm) detected in ^{1}H NMR. The protons H_8 and H_9 (3.25 ppm), resonate upfield from protons H_{10} and H_{11} (3.43 ppm) because they are adjacent to an electron donating amine group that shields their nuclei from the external magnetic field. Protons H_{10} and H_{11} are adjacent to an electron withdrawing sulfonate group that deshields their nuclei (Figure 1.2C, red). Chemical shift information is extremely useful for structural elucidation because it is well characterized for known organic functional groups.

1.4.2.1.4. Spin-Spin coupling

As can be seen in the ^{1}H NMR spectrum of taurine (Figure 1.2A and C, red), each resonance (3.25 and 3.43 ppm) consists of three narrow peaks. These resonances split into a triplet pattern because the angular momentum of H_8/H_9, and H_{10} /H_{11} are coupled, meaning the spins of one set of nuclei exert an effect on the resonance behavior of the other set. The spacing between each resonance is called the coupling constant, and this value is characteristic of different types of bond orientations for adjacent nuclei, such as 10 Hz for protons in the cis location on a carbon-carbon double bond.[95] The peak splitting, or multiplicity, occurs because coupled nuclei have more possible spin orientations than uncoupled nuclei. The number of different orientations is reflected in the integral under each peak. In a triplet, the middle peak is twice as large as the outside peaks because there

are twice as many possible spin orientations with respect to B_0. The multiplicity is equal to the number *n* of magnetically equivalent protons on adjacent atoms plus one. The taurine protons H_8/H_9 have two neighboring equivalent protons H_{10}/H_{11} so they have a multiplicity of three. Coupling constants are useful for the structural elucidation of organic molecules because they provide information about how nuclei are connected. In this example, only proton coupling is shown, but coupling can occur between any NMR-active nuclei.

1.4.2.1.5. Resolution of NMR spectra

One challenge with NMR is spectral crowding, especially in complex mixtures as spectra are usually measured on the whole sample without a hyphenated separation method. Complex metabolomics samples with hundreds of metabolites have overlapping resonances in regions of the spectra for which molecules have similar chemical shifts. As illustrated in Figure 1.2A and C, resonances for taurine are obscured by resonance overlap in the ^{1}H NMR spectrum of *Artemia* metabolite extracts.

Performing NMR metabolomics measurements using the highest available magnetic field is advisable for most nuclei as both sensitivity and dispersion increase with increasing field strength.[97] In addition, two-dimensional NMR experiments create improved resolution in a second dimension. Homonuclear 2D NMR experiments, such as correlation spectroscopy (COSY) and total correlation spectroscopy (TOCSY), are useful tools for structure elucidation because these experiments identify proton resonances that are connected along a carbon backbone.[92] In a COSY spectrum of *Artemia* extracts (Figure 1.2D), a cross-peak

is evident at 2.25-2.43 ppm and 2.43-2.25 ppm, which confirms that the taurine protons H_8/H_9 and H_{10}/H_{11} are coupled.

The most common heteronuclear 2D NMR experiment is $^{1}H:^{13}C$ heteronuclear single quantum coherence (HSQC). In this experiment, cross peaks correlate protons connected thru one bond to ^{13}C. In the HSQC spectrum of *Artemia* extracts (Figure 1.2E), cross peaks are evident at 3.25-51.0 ppm for H_8/H_9 and C_2 and at 3.43-38.0 ppm for H_{10}/H_{11} and C_3 to confirm the taurine resonances. Multiplicity edited-HSQC has the added functionality of providing C-H multiplicity information, where the color indicates whether the bond is a CH/CH_3 or a CH_2. The Homonuclear Multiple Bond Correlation (HMBC) experiment correlates proton and ^{13}C resonances along a carbon backbone that are separated by 3-4 bonds. Used in tandem, 2D NMR techniques are pivotal tools for characterizing metabolites in a complex metabolome.[78,98]

1.4.2.1.6. Metabolite Identification

Due to the robust and reproducible nature of NMR and the well-characterized chemical shift and coupling information for organic functional groups, there are many available resources for identifying metabolites in a sample. Spectral matching libraries, such as Chenomx, and NMR spectral databases, such as the Human Metabolome Database (HMDB) and the Biological Magnetic Resonance Data Bank (BMRB), have thousands of reference spectra for which metabolites can be searched based on chemical shift.[99–101] When there is a lack of reference data, NMR can be used for de novo structural elucidation

using a combination of 1D and 2D techniques, and since it is a non-destructive technique, many different experiments can be performed without concern for sample loss.[92,97,102]

For metabolomics applications, NMR is exceptionally useful because it is an inherently quantitative technique. An NMR signal is proportional to the number of protons (or other nuclei) in the molecule, so with a calibrated reference, exact quantitation is possible.[102] However, for environmental metabolomics, relative quantitation is often suitable because metabolite levels are considered within the context of experimental conditions, such as control versus treatment.[81] Although quantitation is possible, NMR generally has higher limits of detection than MS-based methods. Metabolites that are present at trace levels (sub-micromolar) may not be detected by NMR using the currently available technology.[83]

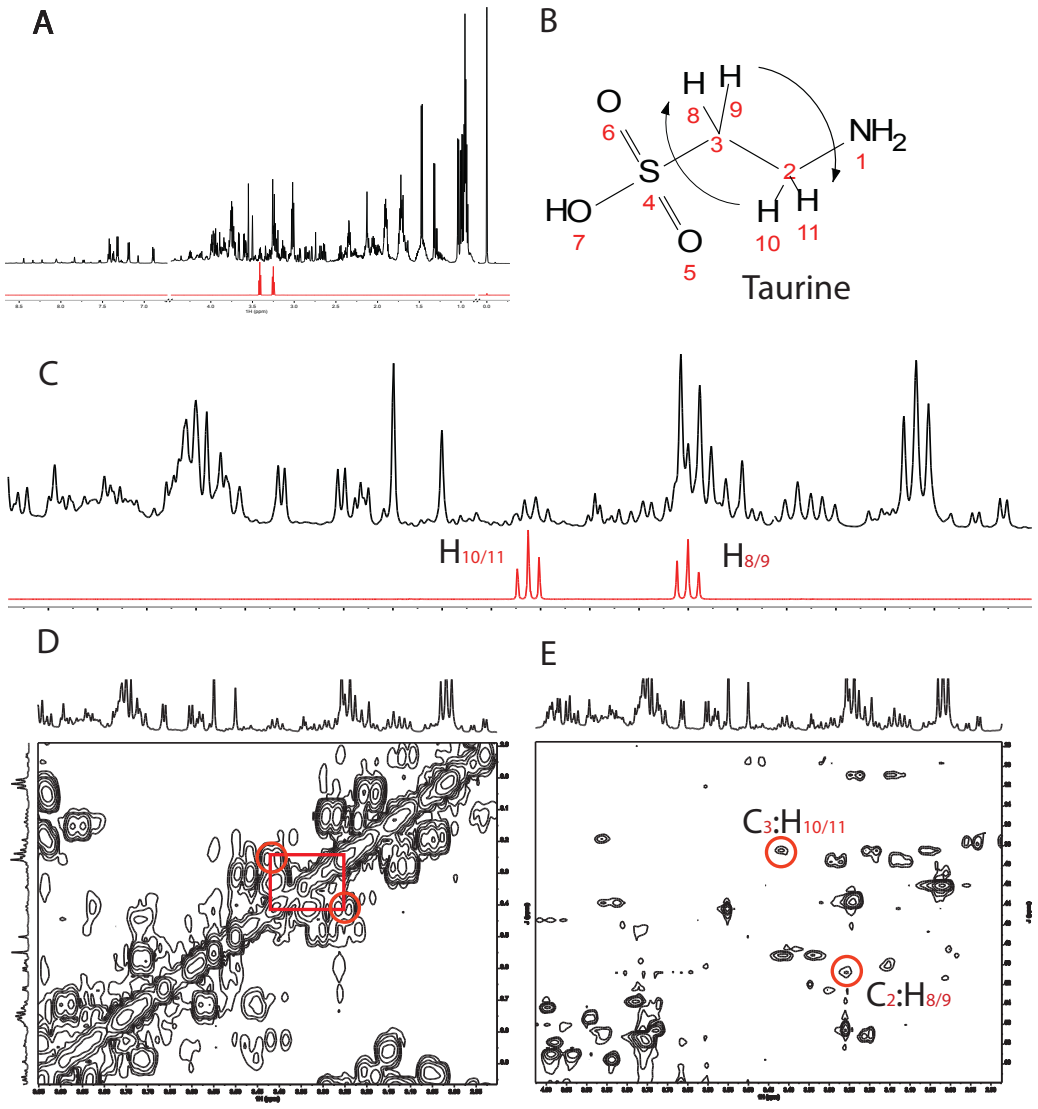

Figure 1.2. (A) Full ^{1}H NMR spectra (0-9.0 ppm) of a taurine standard (red) overlaid with *Artemia* metabolite extracts (black). (B) Taurine structure with arrows indicate coupled protons. (C) ^{1}H NMR spectra magnified to show the taurine proton resonances (2.95 ppm to 3.95 ppm). (D) Homonuclear ^{1}H:^{1}H COSY spectra indicating correlated taurine resonances. (E) Heteronuclear ^{1}H:^{13}C HSQC indicating correlated taurine resonances.

1.4.2.1.7. Mass Spectrometry

Mass spectrometry-based metabolomics methods are typically coupled with gas (GC) or liquid chromatography (LC) prior to sample introduction into the mass analyzer. In these methods, a complex metabolite sample is separated along the length of the column by chemical properties like volatility, solubility, and size such that metabolites are resolved prior to detection.[103] Metabolites are ionized by electron impact, electrospray, or chemical ionization prior to introduction to the mass spectrometer which detects mass-to-charge ratios (m/z). Mass spectrometers are classified by their mass analyzer. Time-of-flight and quadrupole mass analyzers are common, however, ion trap mass analyzers, including the Orbitrap, have advanced detection capabilities.[104] Additionally, tandem mass spectrometry (MS/MS, or MS^n), for which ions pass through multiple mass analyzers, leads to highly resolved and accurate MS/MS spectra which allows enhanced mass resolution and detection.[90,105] For many metabolomics applications, a researcher's choice is driven by whether a gas or liquid chromatography separation will be employed and what mass analyzers are available locally.[104]

1.4.2.1.8. Chromatographic Methods

Metabolomics studies with mass spectrometry analysis introduce the sample into the mass analyzer through direct infusion (DIMS), gas chromatography (GC-MS), or liquid chromatography (LC-MS).[103] Direct-infusion mass spectrometry is a rapid identification method because sample workup steps are avoided, however, challenges remain with identifying metabolites based solely on mass-to-charge ratio and with matrix

interferences.[103,104,106,107] A chromatographic separation prior to MS analysis provides better spectral resolution and reduces matrix effects for improved quantification and identification of metabolites based on retention time and mass-to-charge ratio. However, separations introduce additional variables for method development, such as column selection and gradient optimization.

Primary metabolites can be challenging to separate with traditional LC methods. Reversed phase (RP) separations are most common for liquid chromatography. In a RP separation, molecules elute along a nonpolar stationary phase, such as C18. Polar molecules are poorly retained on a C18 column, so derivatization or alternative separation methods can be used to improve chromatographic resolution.[108] Different column chemistries also aid in chromatographic resolution, such as aqueous normal phase, hydrophilic interaction liquid, and ion-exchange chromatography. Additionally, column chemistries can be combined to form multidimensional-LC, such as RP-HILIC and ion-exchange-RP.[90,109] Although these methods may lead to better resolution for polar metabolites, they are more expensive, less reproducible, and method development is complex.[90,105]

Gas chromatography separates molecules along a capillary column based on volatility, but many polar molecules, like amino acids, have low volatility and decompose at high temperatures, therefore, chemical derivatization is necessary to stabilize the molecule and increase volatility.[83,110] Chemical derivatization can also be used in liquid chromatography to increase retention along the non-polar, reversed phase (RP) column.[111] Derivatizations

methods such as ion-pairing reagents, like diamyl ammonium, and chemical derivatizing agents, like 2-hydrazinoquinoline, have been used in in RP separations for LC-MS in metabolomics studies to improve retention along the non-polar stationary phase.[111,112] For both LC and GC, derivatization reagents are likely not compatible with all metabolites and, inevitably, not all metabolites will be detected. Derivatization also introduces variability that can affect the reproducibility of quantitation. Derivatization, however, is not only useful for chromatographic resolution, but also for ionization.[108]

1.4.2.1.9. Electron Ionization

After chromatographic separation or direct infusion, metabolites must be ionized at the ion source before they can be resolved in the mass analyzer. The ion source turns neutral molecules into charged, gas phase ions. In GC, the mobile phase is an inert carrier gas and the metabolites are volatile, so these molecules are already in the gas phase. GC is typically coupled with electron impact ionization (EI). Electron impact is a hard ionization technique because it uses high energy collisions with an electron beam to create ions. The collision creates a radical molecular ion ($M^{+\bullet}$ - $2e^-$) that contains excess energy from the collision. This excess energy dissipates through the molecule and causes further fragmentation.[83,96] Fragmentation patterns are compound specific and can be used to identify known metabolites or to deduce the structure of unknown molecules. However, since EI mass spectra contain many fragment ions, it can be challenging to identify which peak is the molecular ion, information that is important for verifying the mass. This creates a challenge for correctly labeling metabolites. Also certain molecules, such as dipeptides or

disaccharides, fragment in such a way that could lead to misinterpretation of the metabolic pathway.[83,108,113]

In LC, the molecules are in the liquid phase so electrospray (ESI) or atmospheric pressure chemical ionization (APCI) is used to convert the neutral liquid molecules into gaseous ions. In ESI, the ion source generates an "electrospray" of charged droplet from the solvent carrier liquid, this liquid is then evaporated by a heated nitrogen gas to create the charged molecule.[83] In APCI, ions are generated by vaporizing the solvent carrier liquid and the sample by spraying them into a heater using an inert gas. Solvent molecules are ionized by corona discharge to generate stable reaction ions. These reaction ions undergo proton-transfer reactions with the sample molecules. ESI and APCI are the most common ionization method for LC-MS because they are soft ionization methods that produce mostly protonated $M+H^+$ ions in positive mode or $M-H^-$ ions in negative mode with few fragments. This is advantage for identifying peaks by their mass, but it does not help for structural elucidation of an unknown.[90] However, tandem mass spectrometry (MS/MS, or MS^n) is often utilized to address this challenge.[105] The development of new ionization sources and dissociation methods are major areas of innovation in mass spectrometry, that aim to improve structural elucidation.[114]

1.4.2.1.10. Mass Analyzers

Molecules must be ionized prior to mass analysis because mass analyzers can only manipulate atoms or molecules based on their mass-to-charge ratio (m/z). Ions in a time-of-flight (TOF) mass analyzer are detected based on their velocity when accelerated through an electric field. TOF analyzers are fast and they have high ion transmission but limited dynamic range.[90,104] Quadrupoles are considered mass filters because the quadrupole rods use DC and RF potentials such that only ions with a selected mass-to-charge ratio pass through the channel. These mass analyzers are relatively inexpensive, have good reproducibility, and are ideal for MS/MS analysis because of their selectivity for a precursor ion.[83] There are several different types of ion trap mass analyzers, including ion cyclotron resonance and quadrupole ion trap. The Orbitrap uses ion cyclotron to trap ions in orbit around a spindle shaped quadrupole. As the ions revolve around the axis, they also oscillate which generates an image current that the instrument records.[83] This image current frequency depends on ion mass-to-charge ratio. Ion cyclotron traps have the highest reported mass resolution and are powerful for MS/MS experiments, but they have a limited dynamic range and are too costly for routine analysis.[103,104,107]

Mass analyzers can be used in tandem for added selectivity and resolution. In tandem mass spectrometry, ions are formed in the source and separated by m/z in the first stage of mass spectrometry (MS1). Precursor ions of interest with a particular m/z are selected and fragmented to create product ions. These are then separated and detected in the second stage of mass spectrometry (MS2).[105] The triple quadrupole, QqQ, which consist of two

quadrupole mass analyzers in sequence connected by a quadrupole collision cell, and the quadrupole-Time of Flight, q-TOF, a quadrupole and a TOF in sequence, are tandem-in-space instruments. Whereas, linear triple quad (LTQ)-Orbitrap, and ion-trap-TOF, instruments are tandem-in-time. Tandem-in-space mass analyzers are physically separated by space but connected by high vacuum. Tandem-in-time mass analyzers trap ions in place with multiple stages of separation (MS^n). Modern high-resolution mass analyzers can provide accurate mass measurements for metabolite identification and quantitation and MS/MS analysis can further aid in the identification of metabolites. However, MS/MS spectra have poor reproducibility compared to electron impact ionization and may vary greatly across instruments, which creates a challenge for spectral matching databases.[90]

1.4.2.1.11. Metabolite Identification by GC-MS

A major advantage of NMR metabolomics is the availability of many databases for metabolite identification; this is also an advantage of GC-MS. Due to standardized acquisition parameters, large libraries, such as NIST, Wiley, and Golm, are available to rapidly assign spectral features and ion fragments to a metabolite identity.[99,115,116] Internal standards, such as fatty acid methyl ester (FAMEs) or n-alkanes, are used to increase the accuracy of assignments and calculate a retention index for each spectral peak. The retention index (I) of a chemical compound is its retention time ($t_{r(unknown)}$) normalized to the retention times of adjacently eluting n-alkanes or FAMEs (t_n and t_N), where N is the retention index of the reference that elutes before the compound and n is the retention index of the reference that elutes after the compound (Equation 1.6).[117–119] A molecules' retention

index is a more accurate metric than retention time for comparison to library results because it accounts for differences from column length and temperature gradients.[117] For example, the metabolite assignments for *Artemia* extracts derivatized with trimethylsilane (TMS) were verified by calculating the retention index in AMDIS (Equation 1.6) and comparing the results with reported literature values (Figure 1.3). Sample derivatization is not standardized, but most libraries account for commonly used derivatization reagents. Derivatization of amine and carboxylate groups is usually achieved with silylation reactions that covalently bond an alkyl-silyl group to the acidic or basic functional group (Scheme 1). This silyl group decreases the boiling point of polar molecules and increases their stability for high temperature gradient elutions.[106]

Equation 1.6

$$I = 100 \times \left[n + (N - n) \frac{t_{r(unknown)} - t_{r(n)}}{t_{r(N)} - t_{r(n)}} \right]$$

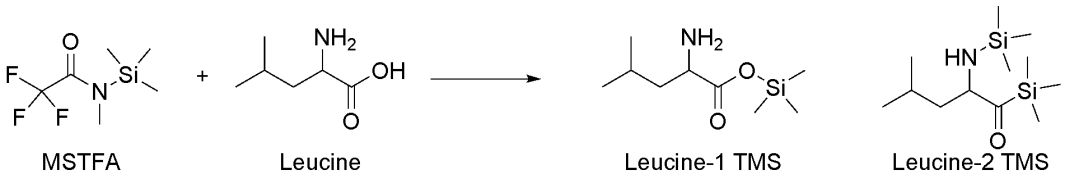

Scheme 1. Trimethylsilane derivatization reaction mechanism. N-Methyl-N-(trimethylsilyl)trifluoroacetamide (MSTFA) reacts with the amine and carboxyl functional groups of leucine to create Leucine-1 TMS and Leucine-2 TMS.

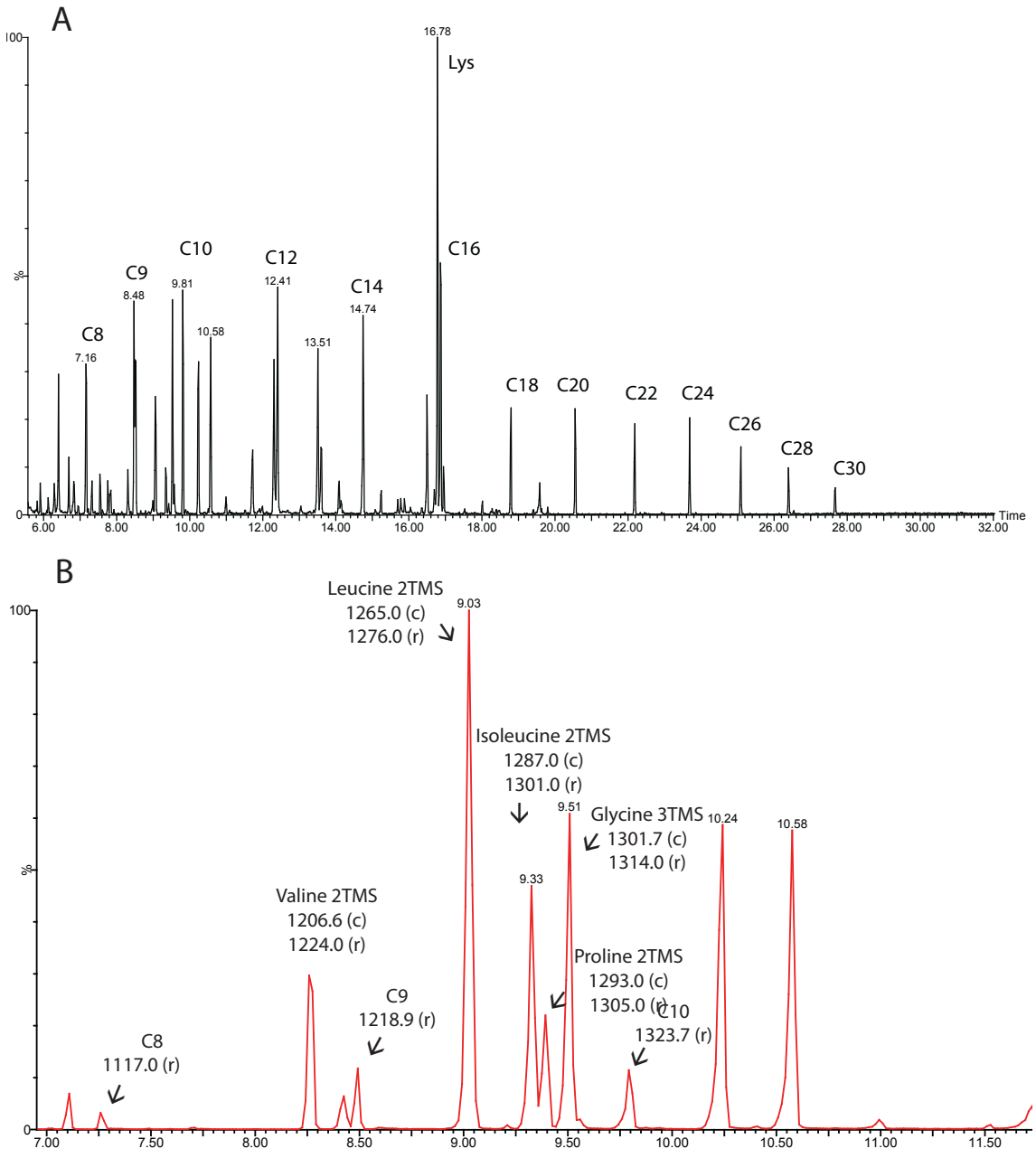

Figure 1.3. (A) GC-MS spectrum of an *Artemia* metabolite extract and FAMES internal standards derivatized with silylation reagents. (B) Region of the GC spectrum labeled with FAMES carbon number (C#), metabolite identity, retention index calculated in AMDIS with equation 1(c), and reported literature retention index values (r)

1.4.2.1.12. Metabolite Identification by LC-MS

The use of LC-MS for metabolomics applications is growing rapidly because of the broad coverage of metabolite classes it achieves due to the availability of different column chemistries, low limits of detection, and high mass resolution.[83,90,105] However, unlike GC and NMR, standard acquisition methods have not been adopted for LC, which currently creates a challenge for developing robust spectral matching databases. For untargeted LC-MS/MS metabolomics, metabolite identification is typically achieved through mass-based searching followed by verification with an authentic standard and MS/MS analysis.[90,105,120] Many labs or university's build in-house libraries of authentic standards and their product ions. Once these libraries are built, rapid and specific metabolite identification is simple. However, even with access to an in-house library, unknown identification still remains a challenge. It has been demonstrated that it might be possible to create a universal product ion mass spectral library from fragments created by collision-induced dissociation.[121,122] This would aid in identification of known and unknown metabolites when combined with structural elucidation chemometric platforms.

1.4.2.1.13. Multiplatform metabolome coverage

Most metabolomics studies use either mass spectrometry or NMR based methods, but with multiplatform analysis greater metabolome coverage is achievable. NMR is a robust and quantitative technique that requires minimal sample preparation.[123] GC-MS requires derivatization, but it has low limits of detection and well-established libraries. LC-MS has low limits of detection and can detect a broad range of metabolite classes, but unknown

identification is challenging. Amino acids, sugars, sugar phosphates, nucleotide-sugars, polyamines, nucleosides, organic acids, and short chain fatty acids among other compounds are detectable and quantifiable in metabolomics samples by using these three methods.[83] These are great complementary techniques that can achieve comprehensive analysis of the *Artemia* metabolome.[85]

1.4.2.2. Chemometric methods for metabolomics

Instrumental analysis is followed by a computational workflow including annotation, preprocessing, post-processing, statistical analysis, and pathway analysis.[124–127] This workflow can also be described as chemometrics, or the science of extracting information from chemical systems by data-driven means.[120,126,128] Metabolomics experiments involve dozens of samples, potentially with hundreds to thousands of features per spectrum; therefore, chemometrics is necessary to manage the large datasets and extract meaningful biological information. The initial steps of preprocessing and annotation are instrument-dependent, but these steps should prepare the dataset for instrument-independent post-processing and statistical analysis. The computational workup can be a major bottleneck for omics studies due to the lack of statistics training for bench scientists, poor standardization of these methods, and confusion about which statistical tests are most important or relevant depending on the experimental context. Bioinformaticists are developing commercial and open source software to streamline metabolomics workups for the bench researcher, but there is still uncertainty about processing metabolomics data in different contexts.[127]

Annotation does not have to be the first step in the computational workflow, but it is important to identify the regions of interest in an instrumental spectrum. For example, in ^{1}H NMR, water suppression methods do not entirely remove the HOD peak, so the region from 4.55 to 4.88 ppm may be excluded from the spectrum. For GC-MS analysis where derivatization steps were used, there will likely be silylation byproducts or contaminants in the spectrum that should be identified and excluded from analysis. For NMR and GC-MS analysis, a single metabolite often has multiple peaks, either from multiple unique proton resonances or from incomplete derivatization. In some cases, these peaks will either be summed to represent one metabolite or only one peak will be selected for analysis and the others excluded. Open source and commercial software is available for NMR and GC-MS to identify these peaks and convert the spectra into data points.[127]

The pre-processing step involves converting instrumental spectra into data points. For NMR and chromatographic methods, this usually involves measuring individual peak integrals, also known as peak fitting, or binning the spectra.[129,130] Peak fitting is essential for quantifying metabolites, but it can be a tedious process even with the assistance of a software tool.[129] With programs like Mestrenova (Mestrelab Research), a curve is fit to the NMR peak and the area of the fitted curve is recorded in a spreadsheet for chemical shift or each time point. Mestrenova is even able to identify and integrate poorly resolved peaks (Figure 1.4). Each spectrum has to be fit individually, which necessitates further manual steps to identify the integrals that represent each metabolite in each spectrum.

Data binning is a technique to group a series of continuous values into one representative value or one bin.[129] For example, a ^{1}H NMR spectrum from 0-12 ppm can be divided into bins or intervals, for example 0.05 ppm, to produce an averaged integral for each bin to reduce the number of variables (Figure 1.5). In order to bin the data, all the spectra in a dataset have to be transferred to one document or file and aligned perfectly or the bins will not accurately reflect metabolite shifts between control and treatment. This can be challenging because some metabolites are highly pH sensitive which causes their location in the spectrum to shift slightly from sample to sample.[130] Since binning arbitrarily segments a portion of a spectrum, individual metabolite shifts cannot be quantified, but this process greatly speeds up pre-processing and is beneficial for high-throughput analysis.[123]

For untargeted mass spectrometry methods, absolute quantitation is challenging because each metabolite has a different response in a mass analyzer, necessitating calibration curves for each metabolite of interest. Relative quantitation is usually sufficient for GC and LC-MS metabolomics. After the spectrum is collected, programs such as MarkerLynx (Waters Inc) or Skyline (MacCoss Lab Software) can be used to deconvolute and identify overlapping metabolite peaks and report an ion count for each mass. The mass will be labeled with a corresponding metabolite and the ion count for each metabolite is compiled and normalized to the total ion count for the spectra.

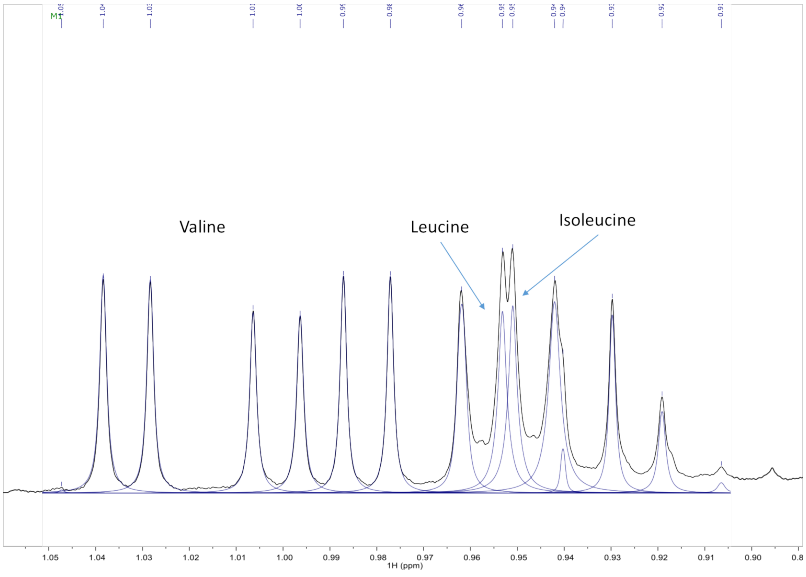

Figure 1.4. Expanded region of the 700 MHz ^{1}H NMR spectrum of an *Artemia* metabolite extract showing the branched chain amino acid resonances (black) and the Lorentzian curves fitted to the peaks (blue). The overlapped isoleucine and leucine resonances at 0.95 ppm were resolved with peak-fitting.

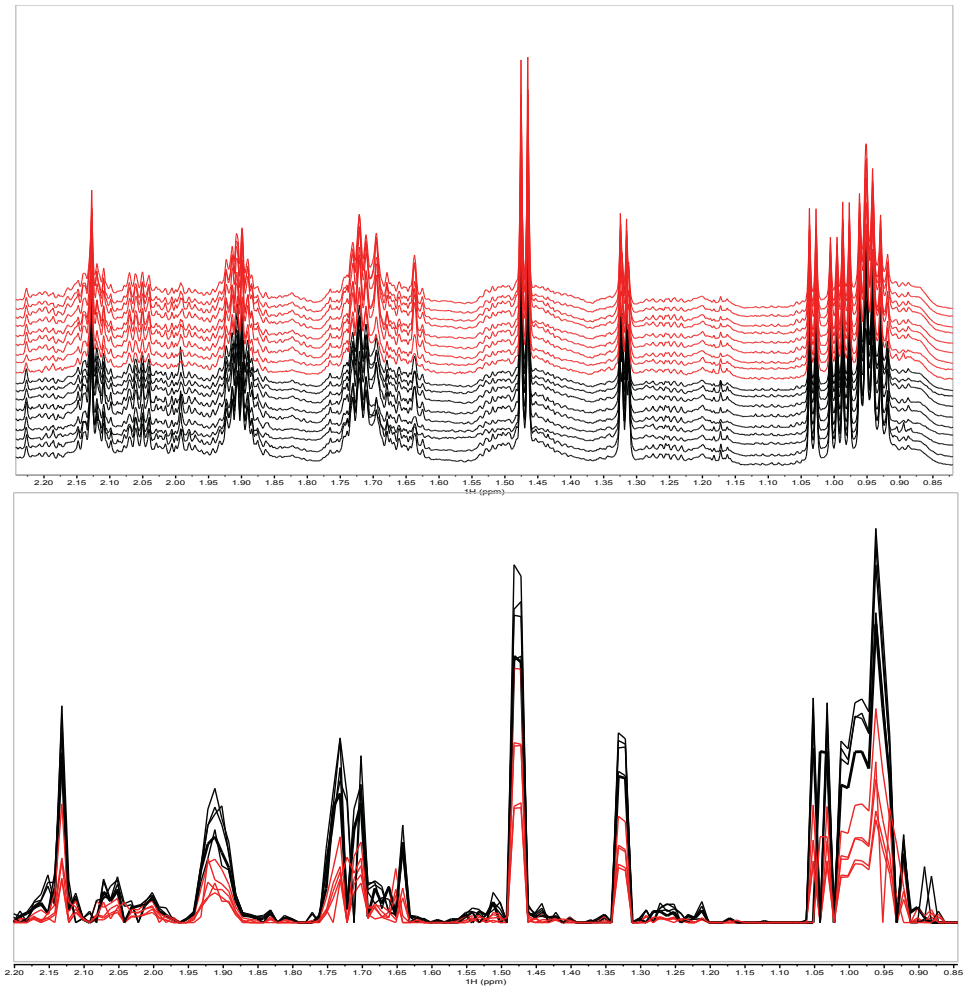

Figure 1.5. ^{1}H NMR spectra of *Artemia* metabolite extracts showing control (black) versus cold stress (red) from 0.85 to 2.20 ppm (top) and the spectra after processing by 0.01 ppm peak binning.

Post-processed data are consolidated into one spreadsheet, normalized, transformed, and ready for statistical analysis. This spreadsheet is usually arranged with the sample number, treatment, and metabolite identity in individual columns with each row containing replicates.[126,131] Ideally, metabolomics data is normally distributed around a Gaussian curve. Most statistical tests, including ANOVA, are designed for normally distributed data. When data are not normally distributed, normalizations and transformations can be used to manipulate the data into a usable format or other statistical tests can account for non-normally distributed data. Normalization to the total spectral area, the area of an internal standard, or the sample mass reduces inter-sample variance.[131] Further logarithmic or exponential transformations make highly skewed distributions less skewed. The Shapiro test can determine if a dataset is normally distributed and is useful in determining the best transformation for the dataset.[124,126,131]

Normalized and transformed data arranged in a spreadsheet are now ready for statistical analysis. Both multivariate and univariate statistical methods are valuable for extracting information from metabolomics data. Multivariate analysis can indicate that the treatment or stress causes a difference in metabolite levels and univariate analysis can identify those differences.[124,128,132] Multivariate analysis looks at the dataset as a whole and helps visualize variance between treatments and populations. Multivariate analysis methods involve the manipulation of many different variables and simplification of the variables down to the important components. Principal component analysis (PCA) and partial least squares discriminant analysis (PLS-DA) are common strategies for visualizing sample

behavior in a dataset. The difference between these techniques is that PCA is unsupervised and PLS-DA is supervised, meaning treatment membership is defined in PLS-DA but not in PCA. Samples that cluster together on a PCA or PLS-DA score plot have similar metabolite profiles, and this helps identify inter-treatment variance.[125,133] A PCA and PLS-DA loading plot identifies which metabolites drive the variance between treatments. After these important metabolites are identified, univariate analysis can measure how these metabolites change in different treatment conditions.

Following the multivariate analyses, univariate analysis of the features identified as important leads to quantitative information about changes in the metabolite levels under different treatments. Analysis of Variance, also known as ANOVA, is a statistical method to compare sample means and determine if the differences are statistically significant.[126,134] ANOVA followed by a post-hoc analysis, such as Tukey's HSD, will identify if there is a statistical difference between control and treatment conditions for each metabolite. For non-normally distributed data, analogous statistical tests can be used, such as the Kruskal-Wallis-test, to compare means and calculate p-values. Volcano plots and box and whisker plots are popular visualizations for individual variables. In a volcano plot, the fold change is plotted on the x-axis and p-value is plotted on the y-axis. Similar to a PCA loading plot, significant metabolites will be furthest from the axis origin. A metabolite is deemed significant if it has a fold change greater than 1.2 or less than 0.8 and statistically significant p-values (usually $p < 0.05$).[132] Box and whisker plots show the median and range of

metabolite replicates, which is useful to exhibit data integrity and treatment-dependent trends. Ideally, univariate analysis leads to a biological interpretation.

Many statistical programs are available to help with choosing the correct tests and constructing the best plots. The open-source platform R has free packages specifically for metabolomics researchers.[127,135] The muma R package automatically completes PCA, PLS-DA, Kruskal-Wallis test, volcano plots, and box plots from a post-processed metabolomics spreadsheet.[132] The metabolomics R package has scripts for normalization and log transformation in addition to PCA and box plots.[127] R is an important tool but there is a curve to learning the language and interpreting error codes. Commercial programs such as GraphPad Prism and SPSS are more user-friendly and include decision trees to help novice statisticians choose the statistical tests that best suit their data and produce useful figures. SIMCA Umetrics is another useful program for multivariate statistics because it can perform multiblock multivariate statistics, which integrates data from multiple analytical pathways for PCA or PLS-DA. Combining multiple analytical techniques, such as NMR and GC-MS or LC-MS, into one dataset can validate the trends in the data collected by both techniques to identify important metabolites.[136]

1.4.2.3. Biological interpretation of metabolite shifts

Biological interpretation is the final step of metabolomics analysis. The large number of variables produced by metabolomics experiments creates an added challenge for biological interpretation. The reductionist approach to determining the biological effect is to focus on

the significant variables that were identified by univariate analysis. Relating the changes observed for these significant variables, or biomarkers, to known biochemical pathways can help to identify affected pathways. For example, if the levels of succinate, fumarate, and malate are affected by a treatment it can be deduced that the stress has an effect on the TCA cycle. Similarly, if a treatment is known to target a certain biochemical pathway, such as the shikimate pathway for glyphosate, shifts in the metabolites related to that pathway may be observed.[137]

Open source bioinformatics platforms for correlating metabolite trends and biochemical pathway profiles are promising tools for biological interpretation. The metabolomics R package includes statistical total correlation spectroscopy (STOCSY) analysis and ratio analysis spectroscopy (RANSY) for binned NMR data. These analyses identify spectral bins within a spectrum that have the same ratio or follow the same trend, and therefore elucidates metabolites from the same pathway that is affected.[97,123,138,139] The R package Pathway Activity Profiling (PAPi) correlates metabolite levels to the activity of metabolic pathways within biological systems.[140] Using the metabolomics data and the Kyoto Encyclopedia of Genes and Genomes, PAPi predicts which pathways are affected and compares the activity of these pathways across experimental conditions. An open source platform in Java, called Cytoscape, similarly identifies affected pathways through metabolic network profiling.[127] These programs are useful for hypothesis generation, but they can be misleading as they only account for metabolites and pathways that can be found

in their databases and are often only meant for human or *saccharomyces* biochemical pathways.

1.4.3. Environmental relevance of Artemia metabolomics

The primary goal of this dissertation is to develop an ecosystem stress test for saltwater lakes. In the following pages I will show that *Artemia franciscana* is a promising model organism because of its salt tolerance, ease of use for in situ and in vitro studies, and suitable biology for metabolomics analysis. Through thorough experimentation all areas of the metabolomics workflow have been tested, from organism growth to pathway analysis, to identify the established methods that best suit the questions asked and develop new methods when necessary. Considerable effort was placed into accurately and thoroughly reporting the *Artemia* metabolome as determined by NMR, GC-MS, and LC-MS. As the following chapters demonstrate, environmental metabolomics is an invaluable data driven method for identifying and studying known and emerging environmental stressors.

The use of *Artemia* in environmental metabolomics is demonstrated through several applications of increasing complexity. The first environmental metabolomics application studies cold stress with ^{1}H NMR and GC-MS followed by chemometric analysis as a proof of concept (Chapter 2). Temperature stress is well characterized in arthropod species, including *Artemia* and other extremophiles such as the Arctic midge and tardigrades, therefore many of the metabolite shifts can be predicted, including increases in the levels of glucose and glycerol, which are known cryoprotectants.[54,55,141] The second application

studies the ubiquitous herbicide, glyphosate, also known as Roundup® (Chapter 3). The effects of this herbicide are well characterized in the environment and in several aquatic species, but have not been studied in *Artemia* or saltwater lakes.[142–144] From this study, I validated our exposure protocol and elucidated the effects of glyphosate and the Roundup® formulation ingredients on *Artemia*.[145] The study of the emerging contaminant, tris(1,3-dichloro-2-propyl)phosphate (TDCIPP) demonstrates that *Artemia* metabolomics can provide novel information about the mode of action of emerging pollutants and that metabolomics can be coupled with high-throughput imaging analysis for multidimensional phenotyping of environmental stress (Chapter 4).[146] The last study reported in this work emphasizes the versatility of NMR metabolomics and importance of *Artemia* as a model species. Perfluorooctanesulfonic acid (PFOS) and perfluorooctanoic acid (PFOA) are fluorinated surfactants that are known to bioaccumulate in aquatic species. Using ^{1}H NMR and LC-MS, PFOS and PFOA bioaccumulation are measured and the resulting metabolic perturbation analyzed in *Artemia* (Chapter 5).[147] As *Artemia* are at the bottom of the food chain, this study provides insight onto the potential for these molecules to biomagnify in the saltwater ecosystem. The dissertation is concluded with an overview of conclusions and future work (Chapter 6).

2 References

1. Williams, W. D. Salinisation: A major threat to water resources in the arid and semi-arid regions of the world. *Lakes Reserv. Res. Manag.* **4,** 85–91 (1999).

2. Williams, W. d. Environmental threats to salt lakes and the likely status of inland saline ecosystems in 2025. *Environ. Conserv.* **null,** 154–167 (2002).

3. Williams, W. D. Conservation of salt lakes. *Hydrobiologia* **267,** 291–306 (1993).

4. OECD. *Test No. 211: Daphnia magna Reproduction Test*. (Organisation for Economic Co-operation and Development, 2012).

5. Kaushal, S. S. *et al.* Increased salinization of fresh water in the northeastern United States. *Proc. Natl. Acad. Sci. U. S. A.* **102,** 13517–13520 (2005).

6. Dugan, H. A. *et al.* Salting our freshwater lakes. *Proc. Natl. Acad. Sci.* **114,** 4453–4458 (2017).

7. Cohen et al. *Haven or Hazard: The Ecology and Future of the Salton Sea*. (Pacific Institute, 1999).

8. Cohen, M. *Hazard's Toll: The Cost of Inaction at the Salton Sea*. (Pacific Institute, 2014).

9. Cohen, M.; Hyun, K. Hazard: The Future of the Salton Sea With No Restoration Project. (2006).

10. Glenn, E. P., Cohen, M. J., Morrison, J. I., Valdés-Casillas, C. & Fitzsimmons, K. Science and policy dilemmas in the management of agricultural waste waters: the case of the Salton Sea, CA, USA. *Environ. Sci. Policy* **2,** 413–423 (1999).

11. Chapter 1: Introduction to agricultural water pollution. Available at: http://www.fao.org/docrep/w2598e/w2598e04.htm. (Accessed: 9th March 2018)

12. Nonpoint source pollution - an overview | ScienceDirect Topics. Available at: https://www.sciencedirect.com/topics/agricultural-and-biological-sciences/nonpoint-source-pollution. (Accessed: 9th March 2018)

13. US EPA, O. What is Nonpoint Source? *US EPA* (2015). Available at: https://www.epa.gov/nps/what-nonpoint-source. (Accessed: 29th October 2017)

14. Watson, S. B. *et al.* The re-eutrophication of Lake Erie: Harmful algal blooms and hypoxia. *Harmful Algae* **56,** 44–66 (2016).

15. Twilley, R. R. & Rivera-Monroy, V. Sediment and Nutrient Tradeoffs in Restoring Mississippi River Delta: Restoration vs Eutrophication. *J. Contemp. Water Res. Educ.* **141,** 39–44 (2009).

16. The Gulf of Mexico Dead Zone. *Dead Zone* Available at: https://serc.carleton.edu/microbelife/topics/deadzone/index.html. (Accessed: 9th March 2018)

17. Yuan, Y., Locke, M. A., Bingner, R. L. & Rebich, R. A. Phosphorus losses from agricultural watersheds in the Mississippi Delta. *J. Environ. Manage.* **115,** 14–20 (2013).

18. Best Management Practices for Georgia Agriculture | Georgia Soil and Water Conservation Commission. Available at: https://gaswcc.georgia.gov/best-management-practices-georgia-agriculture. (Accessed: 10th March 2018)

19. Smith, C., Williams, J., Nejadhashemi, A. P., Woznicki, S. & Leatherman, J. Cropland management versus dredging: An economic analysis of reservoir sediment management. *Lake Reserv. Manag.* **29,** 151–164 (2013).

20. Cropland and Hayland Management Systems | NRCS Vermont. Available at: https://www.nrcs.usda.gov/wps/portal/nrcs/detail/vt/home/?cid=nrcs142p2_010551. (Accessed: 10th March 2018)

21. *Six Municipalities, One Watershed: A Collaborative Approach to Remove Phosphorus in the Assabet River Watershed*. (US EPA, 2015).

22. Burger, J. The Effect on Ecological Systems of Remediation to Protect Human Health. *Am. J. Public Health* **97,** 1572–1578 (2007).

23. Jacquemin, S. J., Johnson, L. T., Dirksen, T. A. & McGlinch, G. Changes in Water Quality of Grand Lake St. Marys Watershed Following Implementation of a Distressed Watershed Rules Package. *J. Environ. Qual.* **47,** 113–120 (2018).

24. Cost-Sharing Soil Conservation Practices: Economic Pros and Cons from a Lake Management Perspective: Lake and Reservoir Management: Vol 4, No 2. Available at: https://www.tandfonline.com/doi/abs/10.1080/07438148809354832. (Accessed: 9th March 2018)

25. Emerging pollutants in the environment: A challenge for water resource management - ScienceDirect. Available at:

https://www.sciencedirect.com/science/article/pii/S2095633915000039. (Accessed: 10th March 2018)

26. Grant, J. How a Burning River Helped Create the Clean Water Act. *The Allegheny Front* (2017). Available at: https://www.alleghenyfront.org/how-a-burning-river-helped-create-the-clean-water-act/. (Accessed: 10th March 2018)

27. Development, O. of R. &. Early Warning Program to Detect and Identify Contaminants of Emerging Concern and Their Effects to Fish and Wildlife. Available at: https://cfpub.epa.gov/ (Accessed: 1st February 2018)

28. Wright, S. L., Thompson, R. C. & Galloway, T. S. The physical impacts of microplastics on marine organisms: A review. *Environ. Pollut.* **178,** 483–492 (2013).

29. News, B. B., Environmental Health & News, B. B., Environmental Health. DDT Still Killing Birds in Michigan. *Scientific American* Available at: https://www.scientificamerican.com. (Accessed: 10th March 2018)

30. Feminization of male frogs in the wild: Nature News. Available at: https://www.nature.com/news/2002/021031/full/news021028-7.html. (Accessed: 10th March 2018)
31. How Important Was Rachel Carson's Silent Spring in the Recovery of Bald Eagles and Other Bird Species? - Scientific American. Available at: https://www.scientificamerican.com/ (Accessed: 10th March 2018)

32. Schulte, P. M. What is environmental stress? Insights from fish living in a variable environment. *J. Exp. Biol.* **217,** 23–34 (2014).

33. US EPA, O. National Primary Drinking Water Regulations. *US EPA* (2015). Available at: https://www.epa.gov. (Accessed: 1st June 2017)

34. USGS Water-Quality Data for the Nation. Available at: https://waterdata.usgs.gov/nwis/qw. (Accessed: 10th March 2018)

35. US EPA, O. What EPA is Doing to Reduce Nutrient Pollution. *US EPA* (2013). Available at: https://www.epa.gov/nutrient-policy-data/what-epa-doing-reduce-nutrient-pollution. (Accessed: 10th March 2018)

36. Bioindicators: Using Organisms to Measure Environmental Impacts | Learn Science at Scitable. Available at: https://www.nature.com/. (Accessed: 10th March 2018)

37. Bioindicators: the natural indicator of environmental pollution: Frontiers in Life Science: Vol 9, No 2. Available at: https://www.tandfonline.com/. (Accessed: 10th March 2018)

38. Vaal, M. A. & Folkerts, A. J. Suitability of microscale ecotoxicity tests for environmental monitoring. in *New Microbiotests for Routine Toxicity Screening and Biomonitoring* 253–260 (Springer, Boston, MA, 2000). doi:10.1007/978-1-4615-4289-6_28

39. Ecotoxicity Testing. Available at: https://ntp.niehs.nih.gov/. (Accessed: 10th March 2018)

40. Guilhermino, L., Diamantino, T., Silva, M. C. & Soares, A. M. Acute toxicity test with Daphnia magna: an alternative to mammals in the prescreening of chemical toxicity? *Ecotoxicol. Environ. Saf.* **46,** 357–362 (2000).

41. US EPA, O. Summary of the Toxic Substances Control Act. *US EPA* (2013). Available at: https://www.epa.gov/. (Accessed: 10th March 2018)

42. Books / OECD Guidelines for the Testing of Chemicals, Section 2:Effects on Biotic Systems. Available at: http://www.oecd-ilibrary.org. (Accessed: 10th March 2018)

43. US EPA, O. Series 850 - Ecological Effects Test Guidelines. *US EPA* (2015). Available at: https://www.epa.gov/. (Accessed: 10th March 2018)

44. Martínez-Jerónimo, F. & Martínez-Jerónimo, L. Chronic effect of NaCl salinity on a freshwater strain of Daphnia magna Straus (Crustacea: Cladocera): a demographic study. *Ecotoxicol. Environ. Saf.* **67,** 411–416 (2007).

45. Schuytema, G. S., Nebeker, A. V. & Stutzman, T. W. Salinity tolerance of Daphnia magna and potential use for estuarine sediment toxicity tests. *Arch. Environ. Contam. Toxicol.* **33,** 194–198 (1997).

46. Nunes, B. S., Carvalho, F. D., Guilhermino, L. M. & Van Stappen, G. Use of the genus Artemia in ecotoxicity testing. *Environ. Pollut. Barking Essex 1987* **144,** 453–462 (2006).

47. Kerster, H. W. & Schaeffer, D. J. Brine shrimp (Artemia salina) nauplii as a teratogen test system. *Ecotoxicol. Environ. Saf.* **7,** 342–349 (1983).

48. Sura, S. A. & Belovsky, G. E. Impacts of harvesting on brine shrimp (Artemia franciscana) in Great Salt Lake, Utah, USA. *Ecol. Appl.* **26,** 407–414 (2016).

49. Clegg, James & Trotman, Clive. Physiological and Biochemical Aspects of Artemia Ecology. in *Artemia Basic and Applied Biology* **1,** (Kluwer Academic Publisher, 2002).

50. Gajardo, G. M. & Beardmore, J. A. The Brine Shrimp Artemia: Adapted to Critical Life Conditions. *Front. Physiol.* **3,** (2012).

51. Warner, A. *Cell and Molecular Biology of Artemia Development*. (Springer Science & Business Media, 2013).

52. Libralato, G. The case of Artemia spp. in nanoecotoxicology. *Mar. Environ. Res.* **101,** 38–43 (2014).

53. Loretta Rodriquez, Elisa J Livengood, Richard D. Miles, Frank A Chapman. Uptake of Metronidazole in Artemia at Different Developmental Life Stages. *J. Aquat. Anim. Health* **23,** 100–102 (2011).

54. *Artemia: Basic and Applied Biology | Th.J. Abatzopoulos | Springer*.

55. Teets, N. M., Kawarasaki, Y., Lee, R. E. & Denlinger, D. L. Expression of genes involved in energy mobilization and osmoprotectant synthesis during thermal and dehydration stress in the Antarctic midge, Belgica antarctica. *J. Comp. Physiol. B* **183,** 189–201 (2013).

56. Ezquieta, B. & Vallejo, C. G. The trypsin-like proteinase of Artemia: Yolk localization and developmental activation. *Comp. Biochem. Physiol. Part B Comp. Biochem.* **82,** 731–736 (1985).

57. Brine Shrimp Life Cycle. Available at: http://learn.genetics.utah.edu/. (Accessed: 10th March 2018)

58. Heath, H. The external development of certain phyllopods. *J. Morphol.* **38,** 453–483 (1924).

59. Qiu, Z., Tsoi, S. C. M. & MacRae, T. H. Gene expression in diapause-destined embryos of the crustacean, Artemia franciscana. *Mech. Dev.* **124,** 856–867 (2007).

60. Kasturi, S. R., Hazlewood, C. F., Yamanashi, W. S. & Dennis, L. W. The Nature and Origin of Chemical Shift for Intracellular Water Nuclei in Artemia Cysts. *Biophys. J.* **52,** 249–256 (1987).

61. Nakamura, K., Iwaizumi, K. & Yamada, S. Hemolymph patterns of free amino acids in the brine shrimp Artemia franciscana after three days starvation at different salinities. *Comp. Biochem. Physiol. A. Mol. Integr. Physiol.* **147,** 254–259 (2007).

62. Helland, S. *et al.* Modulation of the free amino acid pool and protein content in populations of the brine shrimp Artemia spp. *Mar. Biol.* **137,** 1005–1016 (2000).

63. Libralato, G., Prato, E., Migliore, L., Cicero, A. M. & Manfra, L. A review of toxicity testing protocols and endpoints with Artemia spp. *Ecol. Indic.* **69,** 35–49 (2016).

64. OECD. *Test No. 211: Daphnia magna Reproduction Test*. (Organisation for Economic Co-operation and Development, 2008).

65. Liu, Y. D., Wu, F. C., Ji, C. W. & Chon, T. S. Movement Patterning of Daphnia magna Treated with Copper Based on Self-Organizing Map. *Procedia Environ. Sci.* **13,** 994–1002 (2012).

66. Watson, S. B., Jüttner, F. & Köster, O. Daphnia behavioural responses to taste and odour compounds: ecological significance and application as an inline treatment plant monitoring tool. *Water Sci. Technol. J. Int. Assoc. Water Pollut. Res.* **55,** 23–31 (2007).

67. Le, Q.-A. V., Sekhon, S. S., Lee, L., Ko, J. H. & Min, J. Daphnia in water quality biomonitoring - "omic" approaches. *Toxicol. Environ. Health Sci.* **8,** 1–6 (2016).

68. Persoone, G.; Wells, P. Artemia in aquatic toxicology: a review. in *Artemia research and its applications* **1,** 259–275 (Universa Press, 1987).

69. All About The Human Genome Project (HGP). *National Human Genome Research Institute (NHGRI)* Available at: https://www.genome.gov/. (Accessed: 10th March 2018)

70. Hood, L. & Rowen, L. The Human Genome Project: big science transforms biology and medicine. *Genome Med.* **5,** 79 (2013).

71. Human Genome Project: Sequencing the Human Genome | Learn Science at Scitable. Available at: https://www.nature.com/. (Accessed: 10th March 2018)

72. Horgan, R. P. & Kenny, L. C. 'Omic' technologies: genomics, transcriptomics, proteomics and metabolomics. *Obstet. Gynaecol.* **13,** 189–195 (2011).

73. Whole transcriptome profiling of Late-Onset Alzheimer's Disease patients provides insights into the molecular changes involved in the disease | Scientific Reports. Available at: https://www.nature.com/. (Accessed: 11th March 2018)

74. Lankadurai, B. P. Environmental metabolomics: an emerging approach to study organism responses to environmental stressors. *Environ. Rev.* **21,** 180–205 (2013).

75. Rossouw, D., Dool, A. H. van den, Jacobson, D. & Bauer, F. F. Comparative Transcriptomic and Proteomic Profiling of Industrial Wine Yeast Strains. *Appl. Environ. Microbiol.* **76,** 3911–3923 (2010).

76. Fiehn, O. Metabolomics - the link between genotypes and phenotypes. *Plant Mol Biol* **48,** (2002).

77. Harris, E. D. *Biochemical Facts behind the Definition and Properties of Metabolites*. (FDA).

78. Larive, C. K., Barding, G. A. & Dinges, M. M. NMR Spectroscopy for Metabolomics and Metabolic Profiling. *Anal. Chem.* **87,** 133–146 (2015).

79. Schuhmacher, R., Krska, R., Weckwerth, W. & Goodacre, R. Metabolomics and metabolite profiling. *Anal. Bioanal. Chem.* **405,** 5003–5004 (2013).

80. Xia, J., Broadhurst, D. I., Wilson, M. & Wishart, D. S. Translational biomarker discovery in clinical metabolomics: an introductory tutorial. *Metabolomics* **9,** 280–299 (2013).

81. Lankadurai, Brian P, Nagato, Edward G & Simpson, M. J. Environmental metabolomics: an emerging approach to study organism responses to environmental stressors. *Environ. Rev.* **21,** 180–205 (2013).

82. Bundy, J. G., Ramløv, H. & Holmstrup, M. Multivariate Metabolic Profiling Using 1H Nuclear Magnetic Resonance Spectroscopy of Freeze-Tolerant and Freeze-Intolerant Earthworms Exposed to Frost. *Cryoletters* **24,** 347–358 (2003).

83. Villas-Bôas, S. G. *Metabolome Analysis: An Introduction*. (John Wiley & Sons, Ltd, 2007).

84. Sapcariu, S. C. *et al.* Simultaneous extraction of proteins and metabolites from cells in culture. *MethodsX* **1,** 74–80 (2014).

85. Barding, G. A., Béni, S., Fukao, T., Bailey-Serres, J. & Larive, C. K. Comparison of GC-MS and NMR for Metabolite Profiling of Rice Subjected to Submergence Stress. *J. Proteome Res.* **12,** 898–909 (2013).

86. Nagato, E. G. *et al.* (1)H NMR-based metabolomics investigation of Daphnia magna responses to sub-lethal exposure to arsenic, copper and lithium. *Chemosphere* **93,** 331–337 (2013).

87. Polson, C., Sarkar, P., Incledon, B., Raguvaran, V. & Grant, R. Optimization of protein precipitation based upon effectiveness of protein removal and ionization effect in liquid chromatography–tandem mass spectrometry. *J. Chromatogr. B* **785,** 263–275 (2003).

88. Ser, Z., Liu, X., Tang, N. N. & Locasale, J. W. Extraction parameters for metabolomics from cell extracts. *Anal. Biochem.* **475,** 22–28 (2015).

89. Griffith, C. M. *et al.* 1H NMR Metabolic Profiling of Earthworm (Eisenia fetida) Coelomic Fluid, Coelomocytes, and Tissue: Identification of a New Metabolite Malylglutamate. *J. Proteome Res.* **16,** 3407–3418 (2017).

90. Zhou, B., Xiao, J. F., Tuli, L. & Ressom, H. W. LC-MS-based metabolomics. *Mol. Biosyst.* **8,** 470–481 (2012).

91. Betts, K. *Chemistry is Driving Discovery in Metabolomics*. (American Chemical Society, 2018).

92. Claridge, T. D. W. Chapter 2 - Introducing High-Resolution NMR. in *High-Resolution NMR Techniques in Organic Chemistry (Third Edition)* 11–59 (Elsevier, 2016). doi:10.1016/B978-0-08-099986-9.00002-6

93. NMR Spectroscopy. Available at: https://www2.chemistry.msu.edu/faculty/reusch/virttxtjml/spectrpy/nmr/nmr1.htm. (Accessed: 13th May 2018)

94. JAMES, T. L. Chapter 1 Fundamentals of NMR. 31 (1998).

95. Wade, L. *Organic Chemistry*. (Pearson Education, Inc, 2010).

96. Skoog, D. *Principals of Instrumental Analysis*. (Thomson Brooks/Cole, 2007).

97. Nagana Gowda, G. A. & Raftery, D. Can NMR Solve Some Significant Challenges in Metabolomics? *J. Magn. Reson.* doi:10.1016/j.jmr.2015.07.014

98. Simpson, M. J. NMR spectroscopy in environmental research: From molecular interactions to global processes. *Prog. Nucl. Magn. Reson. Spectrosc.* **58,** 97–175 (2011).

99. Wishart, D. S. *et al.* HMDB: the Human Metabolome Database. *Nucleic Acids Res.* **35,** D521-526 (2007).

100. Chenomx Inc | Metabolite Discovery and Measurement.

101. Biological Magnetic Resonance Data Bank. Available at: http://www.bmrb.wisc.edu/metabolomics/. (Accessed: 14th May 2018)

102. Barding, G. A., Salditos, R. & Larive, C. K. Quantitative NMR for bioanalysis and metabolomics. *Anal. Bioanal. Chem.* **404,** 1165–1179 (2012).

103. Dettmer, K., Aronov, P. A. & Hammock, B. D. MASS SPECTROMETRY-BASED METABOLOMICS. *Mass Spectrom. Rev.* **26,** 51–78 (2007).

104. Summary of the characteristics of different mass analyzers. *Jeol* (2018). Available at: https://www.jeolusa.com/. (Accessed: 5th March 2018)

105. Xiao, J. F., Zhou, B. & Ressom, H. W. Metabolite identification and quantitation in LC-MS/MS-based metabolomics. *Trends Anal. Chem. TRAC* **32,** 1–14 (2012).

106. Dona, A. C. Chapter 5 - High-Throughput Metabolic Screening. in *Metabolic Phenotyping in Personalized and Public Healthcare* 111–136 (Academic Press, 2016). doi:10.1016/B978-0-12-800344-2.00005-7

107. Finehout, E. J. & Lee, K. H. An introduction to mass spectrometry applications in biological research. *Biochem. Mol. Biol. Educ.* **32,** 93–100 (2004).

108. Chemical derivatization-based LC–MS for metabolomics: advantages and challenges | Bioanalysis. Available at: https://www.future-science.com/doi/full/10.4155/bio-2016-0192. (Accessed: 12th May 2018)

109. Bell, David S. Retention and Selectivity of Stationary Phases Used in HILIC. *LCGC North America* **33,** 90

110. LC-MS Metabolomics Analysis. Available at: https://www.thermofisher.com. (Accessed: 12th May 2018)

111. Lu, Y., Yao, D. & Chen, C. 2-Hydrazinoquinoline as a Derivatization Agent for LC-MS-Based Metabolomic Investigation of Diabetic Ketoacidosis. *Metabolites* **3,** 993–1010 (2013).

112. Knee, J. M., Rzezniczak, T. Z., Barsch, A., Guo, K. Z. & Merritt, T. J. S. A novel ion pairing LC/MS metabolomics protocol for study of a variety of biologically relevant polar metabolites. *J. Chromatogr. B* **936,** 63–73 (2013).

113. Halket, J. M. *et al.* Chemical derivatization and mass spectral libraries in metabolic profiling by GC/MS and LC/MS/MS. *J. Exp. Bot.* **56,** 219–243 (2005).

114. McLuckey, S. A. & Mentinova, M. Ion/Neutral, Ion/Electron, Ion/Photon, and Ion/Ion Interactions in Tandem Mass Spectrometry: Do We Need Them All? Are They Enough? *J. Am. Soc. Mass Spectrom.* **22,** 3–12 (2011).

115. Hummel Jan *et al.* Mass Spectral Search and Analysis Using the Golm Metabolome Database. *Handb. Plant Metabolomics* (2013). doi:10.1002/9783527669882.ch18

116. Johnson, S. G. NIST Standard Reference Database 1A v17. *NIST* (2014). Available at: https://www.nist.gov/srd/nist-standard-reference-database-1a-v17. (Accessed: 12th May 2018)

117. Strehmel, N., Hummel, J., Erban, A., Strassburg, K. & Kopka, J. Retention index thresholds for compound matching in GC-MS metabolite profiling. *J. Chromatogr. B Analyt. Technol. Biomed. Life. Sci.* **871,** 182–190 (2008).

118. Chemistry, I. U. of P. and A. IUPAC Gold Book - retention index, I in column chromatography. doi:10.1351/goldbook.R05360

119. The Kováts Retention Index System. *Anal. Chem.* **36,** 31A-41A (1964).

120. Lai, Z. *et al.* Identifying metabolites by integrating metabolome databases with mass spectrometry cheminformatics. *Nat. Methods* **15,** 53–56 (2018).

121. Hopley, C. *et al.* Towards a universal product ion mass spectral library – reproducibility of product ion spectra across eleven different mass spectrometers. *Rapid Commun. Mass Spectrom.* **22,** 1779–1786 (2008).

122. Vinaixa, M. *et al.* Mass spectral databases for LC/MS- and GC/MS-based metabolomics: State of the field and future prospects. *TrAC Trends Anal. Chem.* **78,** 23–35 (2016).

123. Markley, J. L. *et al.* The future of NMR-based metabolomics. *Curr. Opin. Biotechnol.* **43,** 34–40 (2017).

124. Worley, B. & Powers, R. Multivariate Analysis in Metabolomics. *Curr. Metabolomics* **1,** 92–107 (2013).

125. Grootveld, M. CHAPTER 1:Introduction to the Applications of Chemometric Techniques in 'Omics' Research: Common Pitfalls, Misconceptions and 'Rights and Wrongs'. in *Metabolic Profiling* 1–34 (2014). doi:10.1039/9781849735162-00001

126. De Livera, A., Olshansky, M. & Speed, T. Statistical Analysis of Metabolomics Data. in *Metabolomics Tools for Natural Product Discovery* (eds. Roessner, U. & Dias, D. A.) 291–307 (Humana Press, 2013). doi:10.1007/978-1-62703-577-4_20

127. Spicer, R., Salek, R. M., Moreno, P., Cañueto, D. & Steinbeck, C. Navigating freely-available software tools for metabolomics analysis. *Metabolomics Off. J. Metabolomic Soc.* **13,** 106–106 (2017).

128. Madsen, R., Lundstedt, T. & Trygg, J. Chemometrics in metabolomics—A review in human disease diagnosis. *Anal. Chim. Acta* **659,** 23–33 (2010).

129. Vu, T. N. & Laukens, K. Getting Your Peaks in Line: A Review of Alignment Methods for NMR Spectral Data. *Metabolites* **3,** 259–276 (2013).

130. Liebeke, M., Hao, J., Ebbels, T. M. D. & Bundy, J. G. Combining Spectral Ordering with Peak Fitting for One-Dimensional NMR Quantitative Metabolomics. *Anal. Chem.* **85,** 4605–4612 (2013).

131. De Livera, A. M. *et al.* Normalizing and Integrating Metabolomics Data. *Anal. Chem.* **84,** 10768–10776 (2012).

132. Gaude, E. *et al.* muma, An R Package for Metabolomics Univariate and Multivariate Statistical Analysis. *Current Metabolomics* (2013). Available at: http://www.eurekaselect.com/107837/article. (Accessed: 29th October 2017)

133. van den Berg, R. A., Hoefsloot, H. C., Westerhuis, J. A., Smilde, A. K. & van der Werf, M. J. Centering, scaling, and transformations: improving the biological information content of metabolomics data. *BMC Genomics* **7,** 142 (2006).

134. Box, G. E. P. & Cox, D. R. An Analysis of Transformations. *J R Stat. Soc B* **26,** (1964).

135. Grace, S. C. & Hudson, D. A. Processing and Visualization of Metabolomics Data Using R. *Metabolomics - Fundam. Appl.* (2016). doi:10.5772/65405

136. Multiblock principal component analysis: an efficient tool for analyzing metabolomics data which contain two influential factors | SpringerLink. Available at: https://link.springer.com/article/10.1007/s11306-011-0361-9. (Accessed: 11th March 2018)

137. Jeff Schuette. *Environmental Fate of Glyphosate*. (Department of Pesticide Regulation, 1998).

138. Cloarec, O. *et al.* Statistical total correlation spectroscopy: an exploratory approach for latent biomarker identification from metabolic 1H NMR data sets. *Anal. Chem.* **77,** 1282–1289 (2005).

139. Wei, S. *et al.* Ratio Analysis Nuclear Magnetic Resonance Spectroscopy for Selective Metabolite Identification in Complex Samples. *Anal. Chem.* **83,** 7616–7623 (2011).

140. Aggio, R. B. M. Pathway Activity Profiling (PAPi): A Tool for Metabolic Pathway Analysis. in *Yeast Metabolic Engineering* 233–250 (Humana Press, New York, NY, 2014). doi:10.1007/978-1-4939-0563-8_14

141. Kletetschka, G. & Hruba, J. Dissolved Gases and Ice Fracturing During the Freezing of a Multicellular Organism: Lessons from Tardigrades. *BioResearch Open Access* **4,** 209–217 (2015).

142. Howe, C. M. *et al.* Toxicity of glyphosate-based pesticides to four North American frog species. *Environ. Toxicol. Chem.* **23,** 1928–1938 (2004).

143. Avigliano, L. *et al.* Effects of Glyphosate on Growth Rate, Metabolic Rate and Energy Reserves of Early Juvenile Crayfish, Cherax quadricarinatus M. *Bull. Environ. Contam. Toxicol.* **92,** 631–635

144. Battaglin, W. a., Meyer, M. t., Kuivila, K. m. & Dietze, J. e. Glyphosate and Its Degradation Product AMPA Occur Frequently and Widely in U.S. Soils, Surface Water, Groundwater, and Precipitation. *JAWRA J. Am. Water Resour. Assoc.* **50,** 275–290 (2014).

145. Erickson, B & Bomgardner, M. Rocky Road for Roundup. *Chemical & Engineering News* **93,** 10–15 (2015).

146. Chemicals, N. R. C. (US) S. on F.-R. *Tris (1,3-dichloropropyl-2) Phosphate*. (National Academies Press (US), 2000).

147. Ji, K. *et al.* Toxicity of perfluorooctane sulfonic acid and perfluorooctanoic acid on freshwater macroinvertebrates (Daphnia magna and Moina macrocopa) and fish (Oryzias latipes). *Environ. Toxicol. Chem.* **27,** 2159–2168 (2008).

Environmental metabolomics methods for experiments with *Artemia franciscana*

CHAPTER TWO

Abstract

Environmental metabolomics methods were developed for studying aquatic stress in *Artemia franciscana*. Cysts were hatched for 48 hours in hatching vessels and the nauplii were transferred to saltwater aquariums for 48 hours before they were sacrificed. The metabolites are extracted and prepared for NMR and GC-MS analysis. The *Artemia* metabolome was characterized from a pooled sample and 43 metabolites were identified using 1D and 2D NMR and GC-MS. The metabolite gadusol was identified after SPE clean-up and further 2D NMR analysis, the identity was verified with LC-MS/MS. Environmental metabolomics methods were tested on cold stressed *Artemia*. Cold stress led to increased accumulation of sugars and cryoprotectants such as glycerol, trehalose, glucose, and maltose. Pathways related to protein synthesis and energy storage were also affected. These results agree with known metabolic pathways related to *Artemia* growth and development and are also consistent with other extremophile organisms.

1 Introduction

In this chapter, environmental metabolomics methods are developed to study stress in *Artemia franciscana*. Metabolomics is the study of small-molecule metabolites that comprise a biological sample. The metabolite profile is a representation of the biochemical processes that are important for the sample, such as photosynthesis or glycolysis. For metabolomics analysis, the metabolite profile is measured in using nuclear magnetic

resonance (NMR) or mass spectrometry (MS).[1–3] These high-throughput analytical methods generate large volumes of complex information that provide insights into the metabolic state of the sample.[4] Metabolomics has been identified as a powerful tool for biomarker discovery and has many potential applications in studying disease progression, medicine, and exposure to toxins.[1,2,5,6]

Metabolomic technologies are increasingly being applied to study biological questions related to the environment.[1,3,4,7,8] Environmental metabolomics has been used to answer questions about sublethal stress, pollutant mode of action, and the effects of climate change.[9,10] For environmental metabolomics, the metabolite profile of an organism is monitored before and after exposure to a stressor.[1,7] The biochemical mode of action of the stressor can be elucidated by analysis of changes in metabolite levels resulting from the exposure.

Environmental metabolomics studies are conducted by first, designing the experiment – this involves selecting the stressor, the organism, and the mode of exposure, such as *in vitro* or *in situ*.[1] Specimen selection and mode of exposure are important aspects of experimental design because the results should accurately and realistically represent the impact of the stressor. Since *Daphnia magna* is a freshwater species, it should not be used in studies focused on saltwater stressors, and if daphnids are raised in the lab, aquarium conditions should closely match environmental conditions.[11–13] Due to a growing interest in the environmental challenges at the Salton Sea, we were interested in identifying a model

for studying stress in saltwater lakes.[14–16] *Artemia* was identified as a potential bioindicator species because it thrives in saltwater lakes, such as the Great Salt Lake and Mono Lake, and it is closely related to *Daphnia magna*, which has already been established for environmental metabolomics for freshwater systems.[9,17–19] In order to study the effects of isolated stressors on *Artemia*, the mode of exposure is *in vitro* with conditions that are relevant for saltwater lakes.

The second step is to obtain a biological sample – this involves either collecting specimens in the environment or exposing the specimen to a stressor *in vitro* and isolating the samples for extraction.[1] Since *Artemia* are aquatic organisms, the mode of collection ultimately involves removing them from the water. Since they cannot survive outside of water, the most logical method involves sacrificing them while they are in water and then removing the water via lyophilization. Liquid nitrogen is a fast and easy way to sacrifice the organism and also halt metabolism without adding more stress. Metabolomics represents a snapshot of global metabolic processes, in order to identify metabolic processes that are affected by experimental conditions, it is important to suspend metabolic processes during or just after exposure to the stressor.[2]

Third, sample preparation – this includes metabolite extraction from the organism.[1] In order to isolate the metabolites from the specimen and from unwanted macromolecules, steps such as homogenization, solid or liquid extraction, and filtration might be used.[2] These methods free metabolites from the tissue and isolate them from other unwanted

macromolecules. Samples are then prepared for instrumental analysis, which may involve derivatization or pH adjustment.[2] In this study, each sample is analyzed using GC-MS and NMR, therefore the sample extraction method has to be suitable for both methods.

Fourth, data acquisition – measuring the metabolite profile using NMR or MS. Samples are analyzed by one or multiple instruments depending on the experimental considerations or instrument availability.[1] The use of multiple instrumental methods leads to greater metabolome coverage because no single method can detect every metabolite; however, added instrumental measurements adds more time, complexity, and cost to the experiment.[2] NMR and GC-MS have well established databases that are useful for metabolomics profiling. NMR is robust and highly reproducible. This method has been the gold standard for structural elucidation of organic molecules for many years and this ability is highly useful for untargeted metabolomics and unknown identification.[7,20] NMR, however, has higher limits of detection than MS-based methods.[3,8] GC-MS has standardized derivatization and acquisition methods, which has led to large and robust databases, such as NIST, which can be used for untargeted metabolomics.[21–23] However, GC-MS is only useful for metabolites that are volatile or can be derivatized, so some classes of molecules will not be suitable for this method, it is also not ideal for unknown identification because the mass spectrum is typically too fragmented to obtain a molecular ion.[10,24]

Fifth, data processing – metabolite identification and chemometrics. Metabolites are identified using metabolomics databases, such as the Human Metabolome Database,

Chenomx, NIST, and the Golm Metabolome Database.[21,22,25–29] Uncharacterized peaks or resonances may remain labeled as an unknown or further investigation with 2D NMR or MS/MS may lead to an identification.[20,30] Often, metabolite identity is tentatively assigned via a database match and is verified by comparing elution times, mass spectra or NMR chemical shift to an authentic standard. Once identified, peak area or bins are collected for chemometric analysis, which involves multivariate and univariate analysis.[6,31] Principal Component Analysis (PCA) and Partial Least Squares-Discriminant Analysis (PLS-DA) dimension reduction methods are important visualizations for identifying the variation in the whole dataset. PCA is an unsupervised exploratory dataset analysis that identifies the variation between groups and PLS-DA is a supervised pattern recognition technique that identifies variation within groups.[32] Univariate analysis is used for pairwise comparisons between treatments to identify significant variables in the dataset, such tests include *t*-test and ANOVA.[32,33]

Lastly, biological interpretation – identifying biomarkers of exposure or metabolic perturbation.[1,3,7] Biological interpretation of metabolite shifts may be performed a number of ways. Some studies using multi-omics methods to use metabolomics to give insight to genomic data from their own study or from published results.[31,34] Researchers may compare the metabolite profile to the KEGG database or other biochemical pathway databases and draw conclusions based on changes to metabolites in the same pathway.[19,35] Bioinformatics packages are also available for this purpose, however, many of the available

databases are only relevant for humans or yeast and the results for other organisms may be inaccurate.[36–38]

These six steps in the environmental metabolomics workflow were optimized to study environmental stress in *Artemia franciscana*. The main questions to be answered include: is *Artemia* a suitable model, how should the exposures be performed, how should the metabolites be extracted, what instruments will be used for analysis, and how are the data best analyzed? Methods that had been previously reported for metabolomics or small molecule analysis were applied and optimized for our conditions when needed. For this study, the growth and exposure parameters, sample preparation, and instrumental analysis were optimized and the *Artemia* metabolome was characterized using NMR and GC-MS. Additionally, the optimized environmental metabolomics methods were used to study the effect of cold stress on *Artemia*.

2 Experimental

Herein, the methods for optimizing metabolomics using *Artemia franciscana* are detailed. In addition, the optimized methods used for cold stress as a proof of concept for *Artemia* metabolomics are presented.

2.1 *Artemia* growth and hatching conditions

We attempted to establish an *Artemia* aquaculture multiple times by hatching *Artemia* cysts in an aquarium of saltwater, letting the shrimp grow, and reproduce, with the goal of having

access to different life stages to study instead of starting each experiment from a cyst. We also developed metabolomics methods that start from the cyst stage.

2.1.1 Attempts at an *Artemia* aquaculture

A brine shrimp aquarium kit was purchased from Lighthouse Educational Products. This kit included a 10-gallon tank, aquarium air pump, incandescent light bulb, cysts, sea salt, turkey baster, and spirulina algae for food. The aquarium was filled with 10 gallons of 35 g/L sea salt and the cysts were added to the tank. The aquarium had constant aeration and constant light for the first 48 hours. After the initial hatch period, the aquarium had constant aeration and a 16:8-hour light cycle. The *Artemia* were fed a pinch of spirulina algae every 48 hours after the initial 48-hour growth period. A third of the aquarium water was replaced each week with fresh salt water. Empty cysts that float to the surface and dead specimens that sink to the bottom of the aquarium were removed as needed using a plastic turkey baster or plastic 1 mL transfer pipet. The aquarium was maintained for 2 months until all the *Artemia* had died.

A second aquarium was set up from an aquarium kit from Elliots' for Pets (Riverside, CA). This included a 20-gallon glass tank, fluorescent overhead light, aquarium heater, and aquarium pump. The aquarium was filled with 35 g/L Oceanic Natural Sea Salt Mix (Amazon.com, Seattle, WA) mixed with ultrapure water (EMD Millipore, Burlington, MA). Grade A brine shrimp cysts (Brine Shrimp Direct, Ogden, UT) were used for this

tank. The same aquarium directions were followed as with the 10-gallon tank with similarly poor results.

Since neither of these methods were successful, we did not continue any attempts to establish a permanent aquarium. From this point, only temporary aquariums were prepared and used for the duration of each experiment.

2.1.2 *Artemia* hatching

An *Artemia* hatching vessel was assembled with a 2 L soda bottle, the San Francisco Bay Brand Hatchery kit (Newark, CA), and the Marina aquarium air pump. Oceanic Natural Sea Salt Mix (35 g/L) mixed with ultrapure water was added to the hatching vessel. This vessel was placed in an incubator with 2 inches of water, an aquarium heater, an aquarium air pump, and an overhead light source. 1 oz Grade A brine shrimp cysts were hatched in a hatching vessel at 80 °F with constant aeration. During the 48 hr hatching period, the cysts are exposed to constant fluorescent light. The hatched nauplii are then transferred to new tanks for growth in fresh media or exposure for environmental metabolomics studies.

2.1.3 "Control" conditions

Many of the initial experiments for parameter optimization were conducted on *Artemia* raised under control conditions. These samples were prepared in bulk and stored for later use. Control conditions are hatched following the procedure outlined in section 2.1.2. Hatched nauplii were next transferred from the hatching vessel into a 1 L beaker with fresh

salt water and stored in a temperature (80 °F) and light (16:8 hr cycle) controlled environment for a 48 hr growth period.

2.2 Sample preparation optimization

After a 48 hr growth or exposure period, *Artemia* are collected for analysis. To collect the nauplii, we take advantage of their phototaxis behavior which causes them to swim towards light sources to find food. When a point source of light is shone through the aquarium, the nauplii crowd around the light, making it easy to pipet the nauplii as a dense mass. They are transferred into cold-resistant microvials using a transfer pipet. The microvials containing *Artemia* are submerged in liquid nitrogen for several seconds to flash freeze the specimen. The samples are then thawed in room temperature, so that excess media can be removed and exchanged three times with ultrapure water to remove dosed media and excess salt prior to metabolite extraction. These samples are then re-frozen and lyophilized. The dehydrated samples are stored in a –80 ºF freezer until analysis.

2.2.1 Solvent extraction and homogenization

Dehydrated *Artemia* are homogenized to disrupt and release metabolites from cells and tissues. Solvent extraction transfers the metabolites from the tissue to the solvent so that it can be used for instrumental analysis. These can be done in sequence or simultaneously depending on the homogenization. Tip sonication and bead beating methods were tested to determine the most effective homogenization technique. Grinding with a mortar and pestle was also attempted, but this method was not feasible because the lyophilized shrimp

were too small and had too much static to grind manually, so this method was not pursued further. Tip sonication and bead beating are conducted in solvents, so solvent extraction is done simultaneously with homogenization. In our experiments, all extractions were done using the established biphasic liquid-liquid methanol/water/chloroform method that extracts both aqueous and polar metabolites and separates the non-polar metabolites into the chloroform phase that is ultimately discarded.[261,2,39]

2.2.1.1 Tip sonication

640 µL methanol and 240 µL water was added to dehydrated control *Artemia* in a 2 mL microvial and placed in an ice bath. The tip of the sonicator (Branson Sonifier 250, Branson Ultrasonics, San Dimas, CA) was submerged in the solvent and pulsed for 30 s at a duty cycle of 30s and an output of 2V. The tip was cleaned with methanol and a Kimwipe (Kimberly-Clark, Roswell, GA) between samples. Additional water (240 µL) and chloroform (640 µL) was added to each sample.

2.2.1.2 Vortex mixer bead mill

Control *Artemia* were collected and flash frozen in 2 mL XXTuff reinforced polypropylene microvials (Biospec Products, Bartlesville, OK). Zirconia beads (500.0-700.0 mg), 640 µL methanol, and 240 µL water were added to each vial. Samples were mechanically homogenized in a ThermoMixer C vortex mixer at 4 °C for 1 min (Eppendorf, Hauppauge, New York).

2.2.1.3 Solvent extraction

Aqueous and polar metabolites were extracted from lyophilized *Artemia* samples using a methanol: water: chloroform method.[2,39] To each sample 640 μL cold methanol (Fisher Scientific) and 240 μL cold D_2O (Sigma Aldrich) and the samples were homogenized. The remaining 240 μL cold D_2O and 640 μL chloroform (Macron Fine Chemicals, Center Valley, PA) were added to each sample followed by centrifugation at 15.7 g for 20 min at 4 °C (Eppendorf). The top layer of the supernatant was transferred to a 1 mL microvial which was evaporated at room temperature using a Savant SC110 speedvac equipped with a refrigerator vapor trap (RVT400) (ThermoFisher Scientific, Waltham, MA). The dried samples were stored at -80°C.

2.3 Metabolome characterization

The *Artemia* metabolome for 48 hr nauplii was characterized from *Artemia* raised under control conditions. In addition, a concentrated sample was prepared for ^1H NMR analysis from a pooled sample of specimens exposed to the herbicide, Roundup®. This sample was used for many two-dimensional NMR experiments to identify an exogenous compound.

2.3.1 Roundup® exposure conditions for metabolome characterization

Artemia were hatched following the procedure reported in section 2.1.2. Hatched nauplii were transferred from the hatching vessel into three beakers containing 300 mL of 100 ppm glyphosate (Roundup Weed & Grass Killer Concentrate Plus, The Home Depot®) in 35

g/L sea salt, adjusted to pH 8.00, and maintained in an incubator for a 48 hr exposure and growth period.

2.3.2 Sample preparation for pooled metabolome characterization samples

After a 48 hr exposure, living brine shrimp from each beaker were collected in 2 mL microvials and flash frozen in liquid nitrogen. The samples were thawed, and the dose solution was exchanged with ultrapure water to remove salt and Roundup®. After lyophilization, the dehydrated specimens were combined to make a 29.0 mg pooled sample. The metabolites were homogenized using a bead beater (section 2.2.1.2) and extracted following the protocol from section 2.2.1.3.

2.3.3 NMR for metabolome characterization

Dried metabolite extracts were reconstituted in 200 μL 50 mM phosphate buffer (pD 7.45) in D_2O (D, 99.9%) (Cambridge Isotope Laboratories, Tewksbury, MA) containing 0.4 mM sodium 2,2-dimethyl-2-silapentane-5-sulfonic acid-d_6 (DSS-d_6) and 0.2 mM ethylenediaminetetraacetic acid-d_{16} (Cambridge Isotope Laboratories, Tewksbury, MA). ^{1}H NMR spectra were acquired with a Bruker Avance 600 NMR (Billerica, MA) spectrometer equipped with a BBI probe operating at 599.58 MHz. ^{1}H survey spectra were measured by coaddition of 256 transients using 32 dummy scans, a relaxation delay of 2 s and acquisition time of 3.0 s. Water suppression was performed using 1D NOESY with presaturation (noesypr1d) during the 120 ms mixing time and 2 s relaxation delay. A

spectral width 11.6808 ppm was used with 32768 complex data points acquired using digital quadrature detection.

2.3.4 Identifying metabolites with 2D NMR

Metabolites were identified in the ^{1}H NMR profile of naupliar *Artemia* extracts using the metabolomics databases, Chenomx (Chenomx Inc, Edmonton, Alberta), the Human Metabolome Database, and by comparison with spectra measured for authentic standards from our in-house library.[25–28] Two-dimensional NMR experiments, including ^{1}H-^{1}H TOCSY and ^{1}H-^{1}H COSY, were performed to verify the assignments. At 600 MHz, the double quantum filtered COSY spectra (cosygpprqf) were measured with a 45° pulse, while the TOCSY spectra (mlevgpphw5) were measured using a mixing time of 120 ms. Both experiments were performed with 32 scans and 16 dummy scans, with 2048 points acquired in F2 and 512 in F1. The ^{1}H−^{13}C edited HSQC spectra (hsqcedetgpsisp2.2) were acquired with 2048 by 128 points in F2 and F1, respectively. These spectra were zero filled to 4096 by 2048 points. The 2D *J*-Resolved spectra (jresgpprqf) were acquired at 600 MHz with 8192 points in F2 and 64 in F1 with 64 scans and 16 dummy scans. *J*-resolved spectra were zero filled to 16384 by 128 points. The TOCSY and HSQC spectra were apodized using a cosine function in both dimensions, while the COSY and 2D J-resolved spectra were apodized with a sine bell function.

2.3.5 Identifying gadusol

Before the identity of gadusol was verified, two singlet peaks at 3.501 and 4.107 ppm and two doublet peaks at 2.379 and 2.686 ppm remained unidentified in the NMR after initial 1D and 2D NMR experiments. From ^{1}H-^{1}H COSY and TOCSY, it was clear that 2.379 and 2.686 ppm were equivalent, but no bond correlations were apparent between the other peaks. Therefore, we conducted several experiments to identify these peaks. A pH titration was performed to identify the pKa for each peak to identify likely functional groups, solid phase extraction was used to resolve and isolate the peaks, and ^{1}H NMR and HSQC were used on the cleaned-up *Artemia* extracts to identify any previous unresolved peaks, ^{1}H-^{13}C homonuclear multiple bond correlation (HMBC) spectroscopy was used to elucidate the molecular structure by identifying long range coupling, and mass spectrometry was used for mass identification.

2.3.5.1 pH titration

A pH titration was conducted to determine the pKa of the unknown peaks. The pH of 10 control samples of metabolite extracts reconstituted in phosphate buffer were titrated from pH 2 to 7.34. One-dimensional ^{1}H NMR spectra were acquired for each sample with 125 scans coadded and 16 dummy scans. The chemical shift of each resonance was recorded at each pH. The pKa of the four peaks was determined by plotting chemical shift (y) against pH (x) and performing a nonlinear regression curve fit in GraphPad Prism version 7.03 (GraphPad Software, La Jolla, CA). The nonlinear regression (Equation 2. 1) used for this

analysis was a Dose-Response (log[agonist] vs normalized response - variable slope). The pKa was reported as LogEC50 and the Hill Slope was set to 1.0.

Equation 2.1. Nonlinear Regression

$$Y = \frac{100}{1 + 10^{((LogEC50 - X) * Hill\ Slope))}}$$

2.3.5.2 Gadusol isolation

The structure and identity of gadusol was verified by isolating the molecule from the control *Artemia* metabolome using solid phase extraction. Oasis® mixed cation exchange 3cc extraction cartridges (Waters Corporation, Millford, MA) were conditioned with 3.0 mL methanol followed by 3.0 mL ultrapure water. The methanol and water were discarded after passing through the cartridge. *Artemia* extracts were reconstituted in 1 mL ultrapure water, adjusted to pH 3.00, and loaded onto the cartridge. This load solution was passed through the cartridge and collected for analysis and evaporated at room temperature using a speedvac.

2.3.5.3 Gadusol elucidation with NMR

The structure of gadusol was confirmed by one and two-dimensional NMR and mass spectrometry from the mixed cation exchange *Artemia* extracts. ^{1}H NMR and HSQC experimental parameters are found in sections 2.3.3 and 2.3.4, respectively. Homonuclear multiple bond correlation (HMBC) spectroscopy was acquired at 600 MHz with 32 scans and 16 dummy scans, a spectral width of 13.9848 ppm in F2 and 210.0 ppm in F1, a two

or three bond coupling constant (cnst13) of 10 Hz, and 2048 points in F2 and 512 points in F1.

2.3.5.4 Gadusol verification with mass spectrometry

Analyte of ~20 μM in 50:50 methanol/water was directly infused into an LTQ mass spectrometer (Thermo Fisher Scientific, San Jose, CA) at 3 μL/min. Negative ion mode was utilized for Full MS and MS2 analysis. Source voltage was 3.5 kV, capillary temperature was 275°C, and tube lens voltage was -33 V. For MS2 analysis, an isolation window of 3 Da was used along with a normalized collision energy of 23.7.

2.3.6 GC-MS derivatization and experimental parameters

Artemia metabolite extracts were derivatized by adding 20 μL of 20 mg/mL methoxyamine (Sigma-Aldrich, St. Louis, MO) in pyridine (Thermo Scientific, Bellefonte, PA) and mixing at 300 rpm for 90 min at 37°C.[40] A 90 μL aliquot of *N*-methyl-*N*-(trimethylsilyl)trifluoroacetamide (MSTFA)(Sigma-Aldrich) was added to each sample and reacted for 30 min at 37°C. A 2 μL aliquot of a fatty acid methyl ester (FAMES) standard containing 0.8 mg/mL C8, C9, C10, C12, C14, and C16 and 0 .4 mg/mL C18, C20, C22, C24, C26, C28, and C30 was added to each sample as a retention time reference and the vial was immediately sealed with a crimp cap.

Samples were injected in pulsed splitless mode on an Agilent J&W DB-5MS UI 30 m x 0.25 mm x 0.25 μm column (Santa Clara, CA) using an Agilent 7890A gas chromatograph

coupled to a Waters GCT Premier mass spectrometer. Samples were introduced at initial oven temperature of 60 °C held for 1 min, ramped at 10 °C/min to a final temperature of 320 °C with a final 5 min hold. The injector, transfer line, and source were maintained at 230°C, 320°C, and 220°C, respectively, and the liner was changed after every 25 injections. Instrument operations were controlled by Waters MassLynx software version 4.1 (Waters Corporation, Milford, MA).

2.3.7 Identifying metabolites from GC-MS

The data were collected in the Waters file format (*.raw) and converted to NetCDF (*.cdf) for compatibility with the Automated Mass Spectral Deconvolution and Identification System (AMDIS, NIST, Gaithersburg, MD). Deconvolution parameters were set to a component width of 17 scans, high resolution, high sensitivity, and medium shape. Retention indices (RIs) were calculated for each peak by AMDIS using an internal standard library and calibration standard library. Compounds were identified using the Golm Metabolome Database (Max Planck Institute of Molecular Plant Physiology, Potsdam, Germany) and NIST 2017 Mass Spectral Library (National Institute of Standards, Gaithersburg, MD).

2.4 Cold Stress metabolomics

As a proof of concept for the application of *Artemia* in metabolomics we exposed newly hatched nauplii to 48 hr cold stress prior to metabolite extraction and metabolome analysis.

2.4.1 Cold Stress exposures

Cysts were hatched following the procedure outlined in section 2.1.2. Hatched nauplii were transferred from the hatching vessel into twenty 50 mL tanks with 20 mL fresh salt water. Ten tanks were maintained at control conditions at 80 °F and ten tanks were kept at 4 °C in a cold room, all were maintained with a 16:8h light cycle. After the 48 hr exposure, living brine shrimp from each jar were collected in 2 mL microvials and flash frozen in liquid nitrogen. The samples were thawed, and the dose solution was exchanged with ultrapure water to remove salt. The samples were lyophilized and stored in -80 °C. The metabolites were extracted following the procedure outlined in sections 2.2.1.2 and 2.2.1.3 for bead beating and solvent extraction.

2.4.2 ^{1}H NMR parameters for Cold Stress metabolomics experiments

^{1}H NMR spectra were acquired following the procedure outlined in section 2.3.3 but using a Bruker Avance III NMR spectrometer equipped with a 5 mm TCI CryoProbe operating at 700.23 MHz.

2.4.2.1 ^{1}H NMR data processing parameters

Spectra were processed using Bruker Topspin 3.2 to phase and reference to DSS (0 ppm). Spectral deconvolution and line fitting was performed using MestReNova 11 (Mestrelab Research, Escondido, CA). FIDs were apodized by multiplication with an exponential function equivalent to 1.5 Hz line broadening, zero-filled to 131072 points, and baseline corrected using a Whittaker Smoother function set to autodetect. Peak fitting was

conducted using a generalized Lorentzian peak shape, a lower width constraint of 0 Hz, an upper width constraint of 30 Hz, position constraint within ± 5%, maximum number of fine iterations of 100, and local minima filter of 0. The peak fitting results were exported to Excel (Microsoft Office 2017) and the results of each spectrum were normalized to the sum of the total area between 0.8-9.0 ppm, excluding the HOD peak between 4.6-5.2 ppm. One well-resolved resonance of each metabolite was selected for statistical analysis (Table 2.2).

2.4.3 GC-MS parameters for Cold Stress metabolomics experiments

A 2 μL aliquot of 3.45 mM Triclosan (Fisher Scientific, Hanover Park, Il) in chloroform was added to the GC-MS aliquots as derivatization surrogate. The samples were derivatized following the procedure reported in section 2.3.6 with methoxyamine and MSTFA with 1% TMCS. Instead of adding FAMES to each sample, between every 10 samples, a FAMES calibration standard containing a 2 μL aliquot of a fatty acid methyl ester (FAMES) standard containing 0.8 mg/mL C8, C9, C10, C12, C14, and C16 and 0.4 mg/mL C18, C20, C22, C24, C26, C28, and C30 was run to account for retention time drift. GC-MS samples were run following the same procedure reported in section 2.3.6.

2.4.3.1 GC-MS processing parameters

MarkerLynx XS (Waters Corporation) was used for data preprocessing to collect integration values for identified metabolites. Peaks were detected without smoothing from an initial retention time of 7.00 min and a final retention time of 32.00 min, with a low-mass cutoff of 73.5 Da, a high-mass cutoff of 600 Da, and a mass accuracy of 0.10 Da. A

peak-to- peak baseline noise value of 1.0, a marker intensity threshold of 25 counts, and a mass and retention time window of 0.1 Da/min, with 3.0 noise elimination were used. The results were exported to Excel where the retention times and m/z values were matched with identified metabolites. One mass−retention time pair with the corresponding area for each metabolite was taken for data normalization and statistical analysis. For metabolites with more than one silylation product, the most abundant mass-retention time pair for each retention time was summed to obtain one value for each metabolite. The mass−retention time pair with the highest relative abundance was chosen to represent each metabolite (Table 2.2).

2.4.4 Statistical analysis for Cold Stress metabolomics experiments

Statistical analysis and data visualization was performed using SIMCA 14.1 (Umetrics, Malmo, Sweden) and the muma R package in R Studio (v 1.0.136).[33] ^{1}H NMR and GC-MS results for each sample were combined in SIMCA for multiblock PCA and PLS-DA. Univariate statistical analysis was performed using the muma R package and used to identify significant variables in the dataset. This package calculates fold change and p-value and constructs boxplots and volcano plots from imported metabolite concentrations. Using a decision tree, muma runs the Shapiro test to determine which metabolites are normally distributed and then runs either the Welch's t-test for normally distributed data and the Wilcoxon-Mann Whitney U Test for non-normally distributed data to calculate a p-value.[32,33] A significant variable for our purpose is defined as a metabolite that has a

measured fold change (fc) 1.2 > fc < 0.8 and p-value < 0.05 when comparing two conditions, in this case control versus cold stress.[33]

3 Results & Discussion

Environmental metabolomics methods using *Artemia franciscana* were optimized for analysis with NMR and GC-MS. These methods were then used to characterize the *Artemia* metabolome and to study the effect of cold stress on the naupliar *Artemia* metabolome.

3.1 Optimizing *Artemia* growth conditions

At the onset of this project, I set out to determine the most feasible option for conducting environmental metabolomics experiments on *Artemia franciscana*. The initial questions included: what conditions are optimal for *Artemia growth*, what life stage should we study, what duration should exposure studies be, and what kind of toxicity tests should we perform? We started by following OECD and EPA guidelines for testing *Daphnia magna*.[41–43] The OECD chronic and acute toxicity tests for *Daphnia* use specimens that are all at the same life stage. These specimens are often obtained from established aquarium colonies. Therefore, we began by attempting to set up an aquarium in which we would hatch and grow out the shrimp.

The advantage of a colony of brine shrimp is that we would be able to potentially test different life stages and also study fecundity and progeny.[44–46] We tested a 10 gallon and 20 gallon aquarium, each with a 16:8 hr life cycle, constant aeration, 80 °F, and 35 g/L sea

salt. Conditions that were suggested from online forums and commercial sea monkey kits were followed. These included feeding the shrimp algae every 48 hrs and partially or completely exchanging the water every three days. After multiple attempts, we determined that our 10 gallon and 20-gallon saltwater aquarium setups would not be sufficient. The shrimp that did manage to survive to adulthood, which took 2 months, did not reproduce, therefore, a colony was not able to be established. We also experimented with growing shrimp in miniature aquariums with only 50 mL, but this also resulted in poor survival for longer than a few weeks and would not be suitable for obtaining the repetitions and amount of sample necessary for metabolomics experiments. Our conclusion from these attempts was that establishing a colony was not going to be simple and that we should consider different testing option.

From that point, we initiated cyst-based assays. *Artemia* cysts are dormant gastrula embryos. Female *Artemia* produce young through either ovoviparous or oviparous reproduction. Ovoviparous reproduction occurs during favorable environmental conditions and leads to live young nauplii hatched from the mother's brood sac.[18,47] Oviparous reproduction occurs when environmental conditions are poor, causing embryonic development to be suspended and a hard shell to encase the embryo. This cyst is released from the brood sac and floats to the surface of the water until favorable conditions return. At the Great Salt Lake, colder temperatures cause female brine shrimp to undergo oviparous reproduction and a large harvest occurs every season during which shrimp farmers collect the floating eggs which are sold for live food for aquacultures and fish

tanks.[47] Upon the return of warmer temperatures, the embryo becomes re-hydrated, metabolism is kick-started, and the embryo resumes development.[17,18]

Artemia cysts offer many advantages as a starting point for toxicological assays compared to free swimming nauplii. For one, they can easily be used for lab-based and field-based experiments.[44,46,48] These desiccated brine shrimp cysts can be purchased in bulk and stored in a freezer for decades. The standard protocol for hatching shrimp is to use a hatching vessel, which is simply any apparatus which produces aggressive bubbles from the bottom of the container. Millions of brine shrimp are typically hatched at the same time. A 48 hr hatching period maximizes the number of shrimp that breach the shell. After the 48 hr hatch period, the OECD *Daphnia* acute and chronic toxicity tests for 48-hour exposures and longer may easily be modified for *Artemia*.

We have optimized the use of two different tanks for *Artemia* exposures: 50 mL (jars) and 300 mL (beaker) tanks (Figure 2.1). In both set-ups, the tanks are housed in a 20-gallon aquarium that serves as an incubator to maintain a consistent 80 °F that is standard for saltwater aquariums (Figure 2.1a). Oxygen exchange is an important parameter for maintaining a healthy tank. The surface area of the 50 mL tanks allowed enough aeration, but an air pump was used for the 300 mL tanks. The swimming motion of *Artemia* also stir up the water and contribute to air exchange, which was sufficient for the 50 mL tank, but without enough aeration, many of the shrimp in the 300 mL tanks die.[49] The other important factor for each tank was the distribution of specimens. Standard protocols for *Daphnia* call

for 20 animals per 100 mL media.[41] However, it was found that *Artemia* were still able to thrive in a much higher density, which is fortunate as 20 shrimp were insufficient to comprise a metabolomics sample. Instead of counting individual shrimp, it was found that starting from 1 oz cysts, the hatched nauplii could be distributed into twenty 50 mL, and six 300 mL tanks. These parameters were sufficient for an exposure up to 1 week in duration.

The different tank types were useful for different applications. The 50 mL tanks could provide higher replicates with one sample per tank; therefore, multiple doses or conditions could be tested at one time. However, these experiments typically resulted in smaller sample volumes and managing more tanks created logistical challenges. The 50 mL tanks were also used for range-finding experiments and lethal concentration experiments. With the 300 mL tanks, fewer conditions could be tested simultaneously, but for each tank, multiple large samples could be taken.

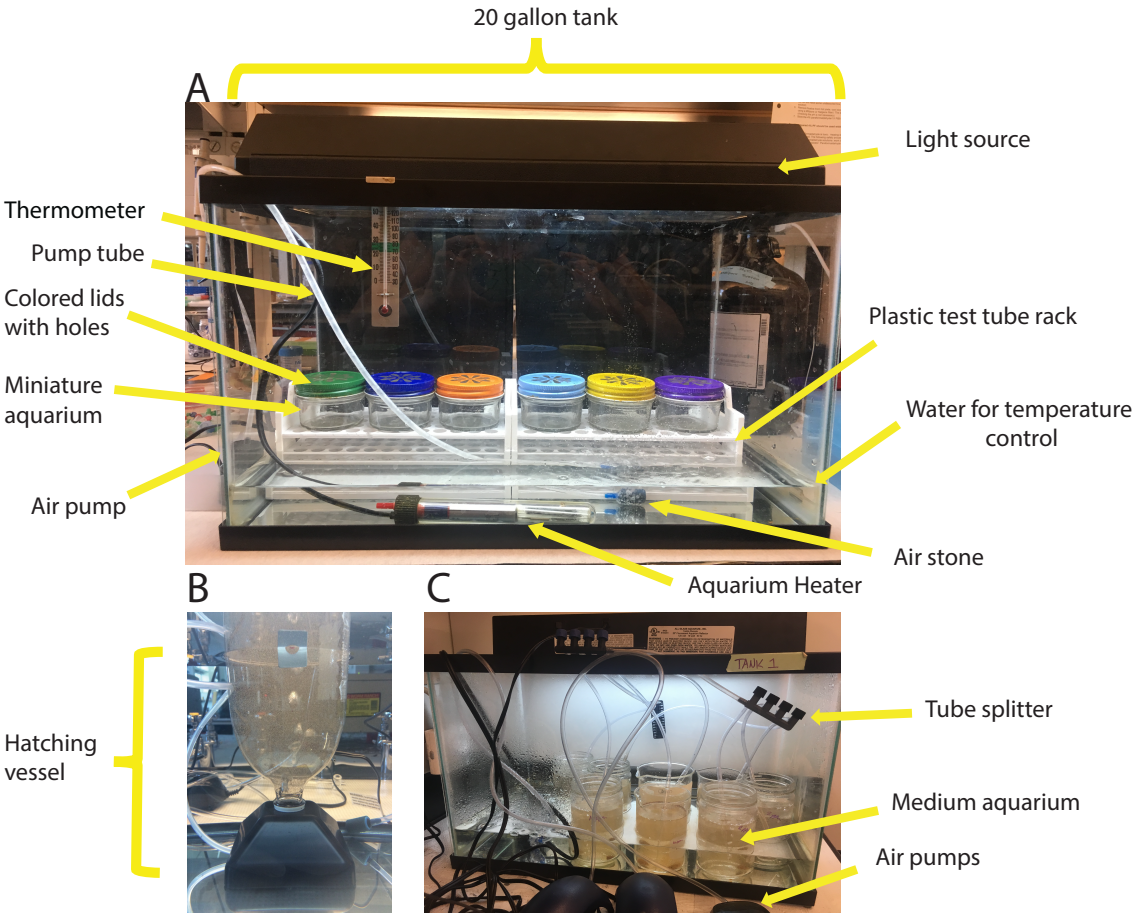

Figure 2.1. Aquarium set up labeled with parts. (A) Incubator with 50 mL (jar) tanks (B) hatching vessel (C) incubator with 300 mL (beaker) tanks.

3.2 Optimizing sample preparation

Sample preparation is a critical step for metabolomics studies because it affects the quality of the data and puts the sample into a form that is suitable for the instrument to be used. In order to have consistent and comparable results with other metabolomics studies, the commonly used methanol: water: chloroform, two-step extraction method was used to extract metabolites from *Artemia*. This is a liquid-liquid biphasic extraction that isolates polar and aqueous classes of compounds from lipophilic compounds.[1] This method is suitable for NMR and MS analysis. Some studies that solely use NMR for analysis use a D_2O buffer extraction.[19,50] This is suitable for many metabolites such as amino acids and sugars but could exclude more polar and polar aprotic metabolites.[1,2] The chloroform extraction step is also important for removing unwanted lipid molecules that create broad peaks that obscure other alkyl resonances. The organic layer can also be analyzed separately for lipidomics, but this was not pursued in our study.

Homogenization methods were briefly tested to identify an effective procedure. Tip sonication seemed to thoroughly disrupt the tissue, by visual inspection, but it introduced heat which was a concern for sample degradation. Additionally, each sample had to be homogenized individually because the apparatus is only equipped with one tip, which was a concern for reproducibility, cross-contamination from the tip, and the time required for sample preparation. The bead beater approach also appeared to disrupt the sample. With bead beating homogenization, zirconia beads were added to each sample vial, which was placed in a temperature controlled shaking apparatus. This method can also introduce heat,

but the temperature-controlled unit prevented this. Twenty-four samples can be homogenized simultaneously so we determined that this streamlined approach was the most feasible option for reducing the time for sample extraction and for reproducibility.

3.3 *Artemia* metabolome

The *Artemia* metabolome was characterized from a pooled sample of *Artemia* exposed to 100 ppm Roundup® to achieve improved detection of low abundance metabolites for both 1D and 2D NMR analysis. The metabolic impacts of Roundup® exposure are discussed in Chapter 3. The metabolites reported in ^{1}H NMR spectra (Figure 2.5, Table 2.1) include amino acids, organic acids, osmolytes, sugars, nucleic acids, and one exogenous compound. These molecules were verified with HSQC, COSY, and TOCSY as well as GC-MS (Figure 2.3, Table 2.1) for some metabolites. NMR and GC-MS together resulted in the identification of 43 metabolites in our naupliar *Artemia* extracts. These metabolites fall under the classification of amino acid, osmolyte, sugar, nucleic acid, and polyamine. Alanine, betaine, formate, lactate, taurine, homarine, glycerophosphocholine, phosphocholine, methanol, guanosine, uridine, cytidine, and gadusol were only detected by NMR. There are several reasons why low molecular weight compounds can be better measured NMR, for example given the experimental parameters used they may have eluted in the GC void volume, are unstable at the separation temperatures employed, fragment under electron impact ionization to the degree that their mass-retention time might not be discernible or are nonvolatile and lack the functional groups that allow them to be derivatized. L dopa, cholesterol, linolenic acid, urea, spermidine, putrescine, uracil, and

myo-inositol were only detected by GC-MS. These compounds are present in quantities below the limit of detection for NMR or are poorly resolved in the NMR spectrum. Sugars, such as glucose, were better resolved in GC-MS but identified by both methods.

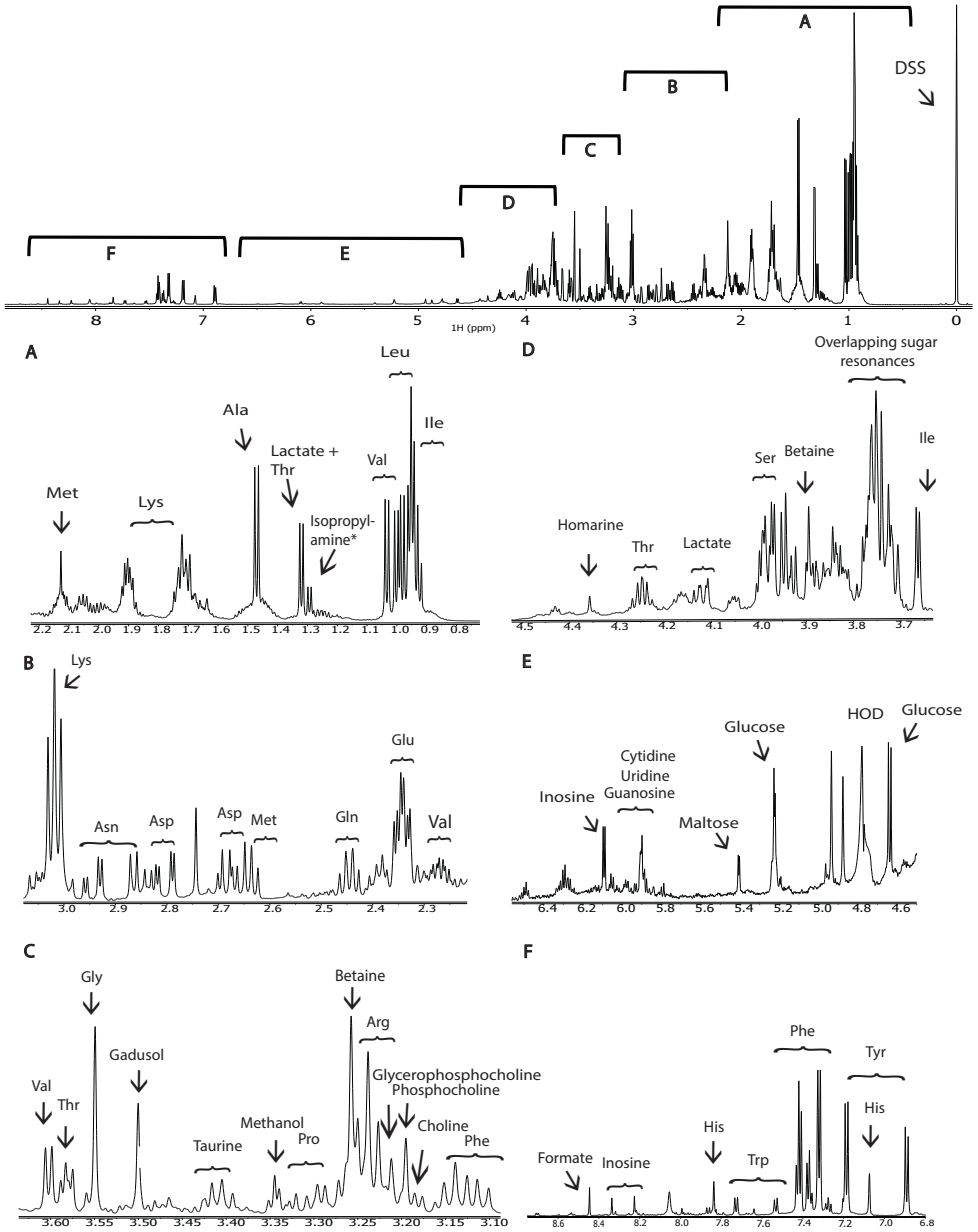

Figure 2.2. [1]H NMR spectra of naupliar *Artemia* extracts labeled with identified metabolites. The chemical shift reference DSS at 0 ppm is shown in the full spectrum, A, with each region of the spectrum magnified to show spectral detail. The chemical shift range for each inset include: A. 0.8 to 2.2 ppm, B. 2.3 to 3.1 ppm, C. 3.1 to 3.7 ppm, D. 3.7 to 4.5 ppm, E. 4.5 to 6.5 ppm, F. 6.8 to 8.7 ppm.

Table 2.1. ^{1}H NMR and GC-MS metabolite profile of *Artemia* extracts

Metabolites	^{1}H Chemical Shift (ppm)	R.I.
Amino Acid		
Alanine (Ala)	1.464d, 3.77*	
Arginine (Arg)	1.900m, 3.238m	1821.6
Asparagine (Asn)	2.840m, 2.943dd, 3.99*	1496.9; 1589.2
Aspartate (Asp)	2.667m, 2.802dd, 3.89*	1511.8
Glutamate (Glu)	2.051m, 2.139m, 2.342m	1615.4
Glutamine (Gln)	2.123m, 2.440q, 3.76*	1723.1; 1769
Glycine (Gly)	3.556s	1303
Histidine (His)	3.103m, 3.23*, 3.98*, 7.073s, 7.837s	1914.2
Isoleucine (Ile)	0.929m, 1.002d, 1.252m, 1.461m	1180.3; 1290.5
Leucine (Leu)	0.952t, 1.708m, 3.72*	1159.7
Lysine (Lys)	1.470m, 1.714m, 1.907m, 3.018m, 3.75*	1702; 1916
Methionine (Met)	2.126m, 2.637t, 3.840*	1511.4
Phenylalanine (Phe)	3.117m, 3.276, 3.983*, 7.318d, 7.372t, 7.418t	1621.3
Proline (Pro)	2.027m, 2.347m, 3.330m, 3.414, 4.119dd	1295.4; 1573
Serine (Ser)	3.83*, 3.952m	1356.8
Threonine (Thr)	1.323d, 4.245m	1381.4
Tryptophan (Trp)	7.189t, 7.276t, 7.534d, 7.724d	2204.7
Tyrosine (Tyr)	3.037*, 3.182*, 3.927*, 6.885d, 7.184d	1933.4
Valine (Val)	0.982d, 1.034d, 2.264m, 3.603*	1213.5
Osmolyte		
Betaine	3.258s, 3.894s	
Choline	3.185s, 3.51*, 4.052m	
Formate	8.445s	
Glycerol	3.550m, 3.641m	
Glycerophosphocholine	3.212s, 3.40*, 3.47*, 3.75*, 3.98*	
Homarine	4.357s, 8.534dd, 8.77*	
Lactate	1.322d, 4.124m	
Methanol	3.345s	
Phosphocholine	3.195s, 3.58*, 4.17*	
Taurine	3.417m, 3.33*	1660.9
Sugar		
Gadusol	2.379d, 2.686d, 3.502s, 3.567, 3.718, 4.107s	
Glucose	3.24*, 13.40*, 3.44*, 4.635d, 5.223d	1887.4
Maltose	4.636d, 5.223d, 5.406d	
Myo-inositol		2072.8
N-acetylglucosamine	5.196d	2059.2
Trehalose	5.196d	
Nucleic Acid		
Cytidine	5.899d, 6.093d	
Guanosine	5.899d, 7.899s	
Inosine	4.428m, 6.093d, 8.224s, 8.329s	2566.5
Uracil	5.794d, 7.528d	1334.1
Uric acid		2085.1
Uridine	3.85*, 4.12*, 4.22*, 5.902m, 7.855d	
Polyamine		
Ornithine	3.053t	1610.5;1811.7
Ornithine-1,5-lactam		1452.6
Putrescine		1729.1

Urea		1240.6
Other		
L-Dopa		2081.6
Glycyl-proline		1973.8
Pyroglutamate	2.03*, 2.39*, 2.501m, 4.168dd	
Exogenous		
Isopropylamine	1.294d, 3.48*	

Asterisk (*) indicates resonances that were identified in COSY or TOCSY spectra. These values are reported to two decimal places due to reduced resolution in 2D spectra.

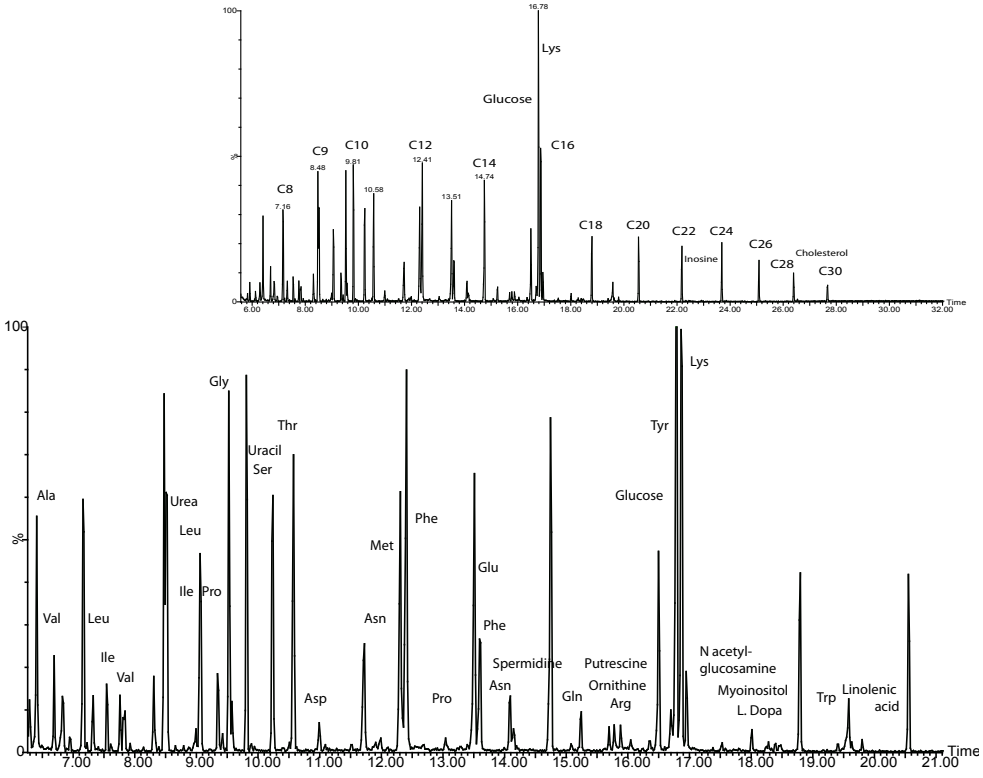

Figure 2.3. Gas Chromatography-Mass Spectrometry Total Ion Chromatogram (TIC) of *Artemia* extract labeled with selected metabolites labeled.

Several peaks and resonances were not able to be identified using metabolomics libraries. Isopropylamine, homarine, and gadusol were identified by comparison to published spectra after an extensive literature search.[51–54] The identities of isopropylamine and homarine were confirmed by recording the NMR spectra of authentic standards. Isopropylamine is an exogenous compound that is an important ingredient in the Roundup® formulation, and it therefore, was not considered part of the *Artemia* metabolome. Homarine has not previously been reported in *Artemia* but it has been reported in other crustaceans, such as the American oyster.[53] Homarine has been determined to be an important methyl donor and possibly serves as a methyl group reservoir in crustaceans.[55,56]

Gadusol was more challenging to identify because many of its resonances were masked by spectral interference. Gadusol has been reported in *Artemia* and zebrafish, it is an interesting compound with a UV-protective function.[51,52,57,58] Only the singlet at 3.502 ppm was clearly resolved in the 1D ^{1}H NMR spectrum (Figure 2.2) and because of the limited ^{1}H-^{1}H coupling the COSY and TOCSY spectra were of limited use in completing the spectra assignments. Initially, four intense resonances, 2.379 ppm (d), 2.686 ppm (d), 3.502 ppm (s), and 4.107 ppm (s), remained unidentified in the NMR spectra after using the metabolomics libraries and the in-lab collection of standards. The resonances at 2.379 and 2.686 were suspected to be equivalent protons because they had identical coupling and had similar structural features to citrate. Therefore, we performed a pH titration on control samples to verify this connection and to elucidate other structural features (Figure 2.4). It was found from a nonlinear regression of the changing chemical shifts versus pH, that these

four peaks had the same pK_a (4.1) suggesting that the molecule had only one ionizable group, perhaps a carboxylate.[58] Next, using mixed cation exchange SPE, we were able to clean up the spectrum and clearly resolve the resonances at 2.379 (H-2), 2.686 (H-2), 3.501 (H-9), 3.567 (H-12), 3.718 (H-12), and 4.107 (H-6) ppm (Figure 2.5). ^{1}H-^{1}H coupling with COSY and TOCSY verified that the H-2 resonances were equivalent with a 17.10 Hz coupling and also revealed that the H-12 resonances were equivalent with a 12.21 Hz coupling, but no other coupling was identified (Figure 2.6).

Using ^{1}H-^{13}C heteronuclear single quantum correlation spectroscopy (HSQC), the carbon resonance for each proton resonance was identified. The carbon shift for H-2 protons (C-2) occurs at 43.3 ppm, C-9 occurs at 62.5 ppm, C-12 occurs at 66.2 ppm, and C-6 occurs at 78.3 ppm (Figure 2.4, Figure 2.7), however, the arrangement of carbons and protons was till not apparent. Homonuclear multiple bond correlation (HMBC) aided in the structural elucidation of gadusol by showing long range ^{1}H-^{13}C couplings (Figure 2.8). In this spectrum, cross peaks that are aligned vertically and horizontally are connected within 2-3 bonds. This experiment verified that H-2 is connected to C-6, C-12, and C-9, H-6 is connected to C-2 and C-12, H-9 is connected to C-2, and H-12 is connected to C-6 and C-2.

Finally, the identity of gadusol was verified in our extracts from a mass spectrum (Figure 2.9). The mass and molecular formula for gadusol is reported as 204.178 g/mol and $C_8H_{12}O_6$. Using LC-MS/MS in negative ion mode, the parent ion [M-H] was measured at

202.92 m/z, this constitutes the loss of one proton ($C_8H_{11}O_6$). Collision induced dissociation of the parent ion resulted in losses and ring cleavage products. Loss of the hydroxyl group at C-12 converts it to a methyl group with the formula $C_8H_9O_5$, loss of this methyl group at C-1 leads to $C_7H_7O_5$, ring cleavage leads to $C_4H_3O_3$. These fragments were confirmed against predicted LC-MS/MS spectra in the HMDB database.[27]

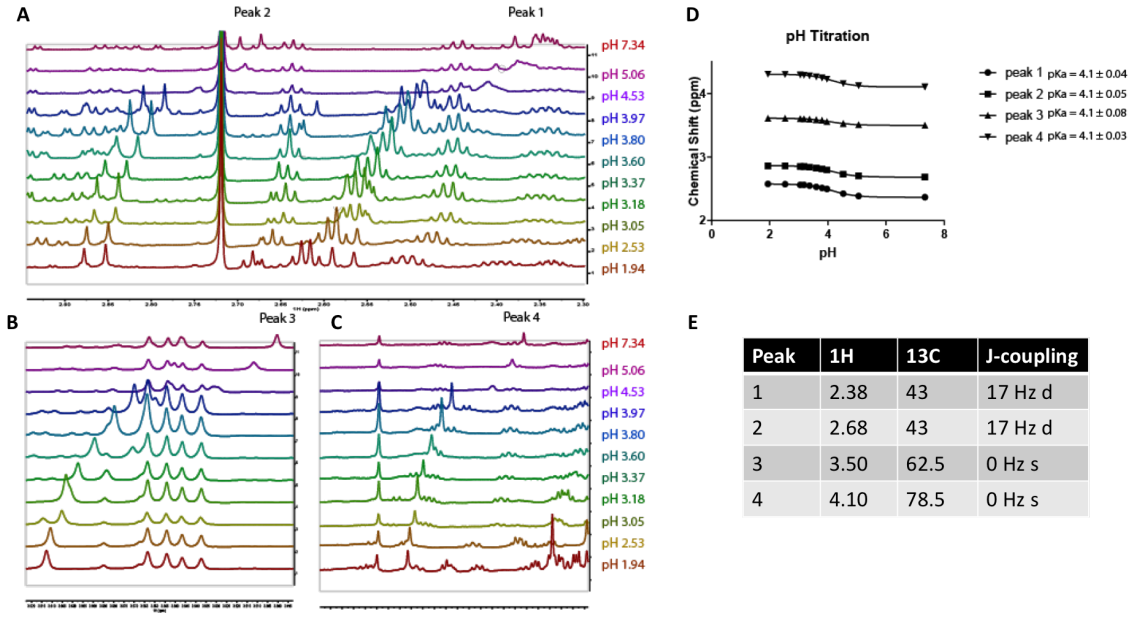

Peak	1H	13C	J-coupling
1	2.38	43	17 Hz d
2	2.68	43	17 Hz d
3	3.50	62.5	0 Hz s
4	4.10	78.5	0 Hz s

Figure 2.4. Stacked 1H NMR spectra of *Artemia* extracts titrated from pH 1.94 to 7.34 with four well-resolved gadusol resonances labeled. (A) 2.30 to 2.95 ppm showing peaks 1 and 2 (B) 3.45 to 3.62 ppm showing peak 3 (C) 4.03 to 4.41 ppm showing peak 4. (D) Non-linear regression of the resonances with respect to pH revealed that these four resonances had the same pKa =4.1. (E) Table of peaks, with ^{1}H and ^{13}C chemical shift, J-coupling constant in Hz, and multiplicity.

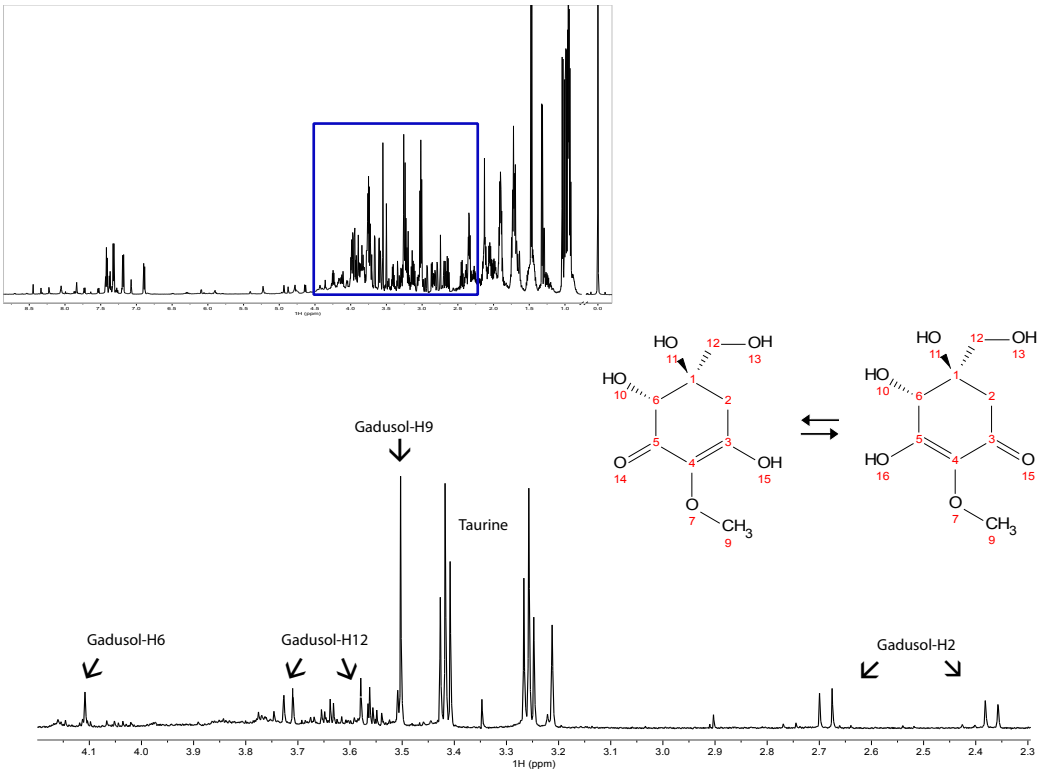

Figure 2.5. ^{1}H NMR spectrum of *Artemia* extracts (0 – 9.5 ppm). The expanded region shows the extracts after mixed cation exchange clean-up (2.3 – 4.2 ppm), gadusol and taurine resonances are labeled. Gadusol-H2 refers to the doublet of doublets at 2.379 and 2.686 ppm (J = 17.10 Hz), H-9 refers to the singlet at 3.501 ppm, H-12 refers to the doublet of doublets at 3.567 and 3.718 ppm (12.21 Hz), and H-6 refers to the singlet at 4.107 ppm.

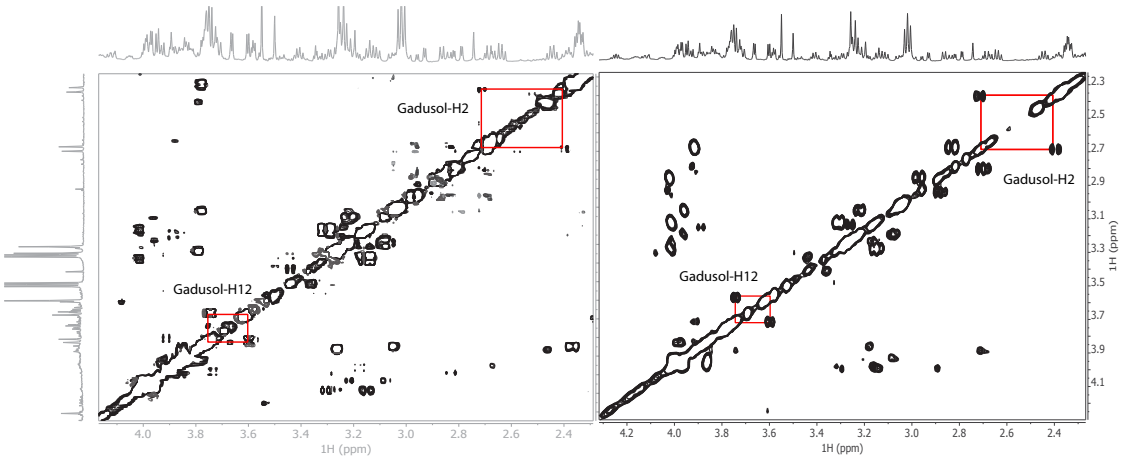

Figure 2.6. Two-dimensional homonuclear NMR spectra (left) TOCSY and (right) COSY of Artemia extracts labeled with gadusol resonances. Cross peaks represent ^{1}H-^{1}H coupling, which was observed for H-2 protons (J = 17.10 Hz) and H-12 protons (J = 12.21 Hz), but no further coupling was observed for gadusol.

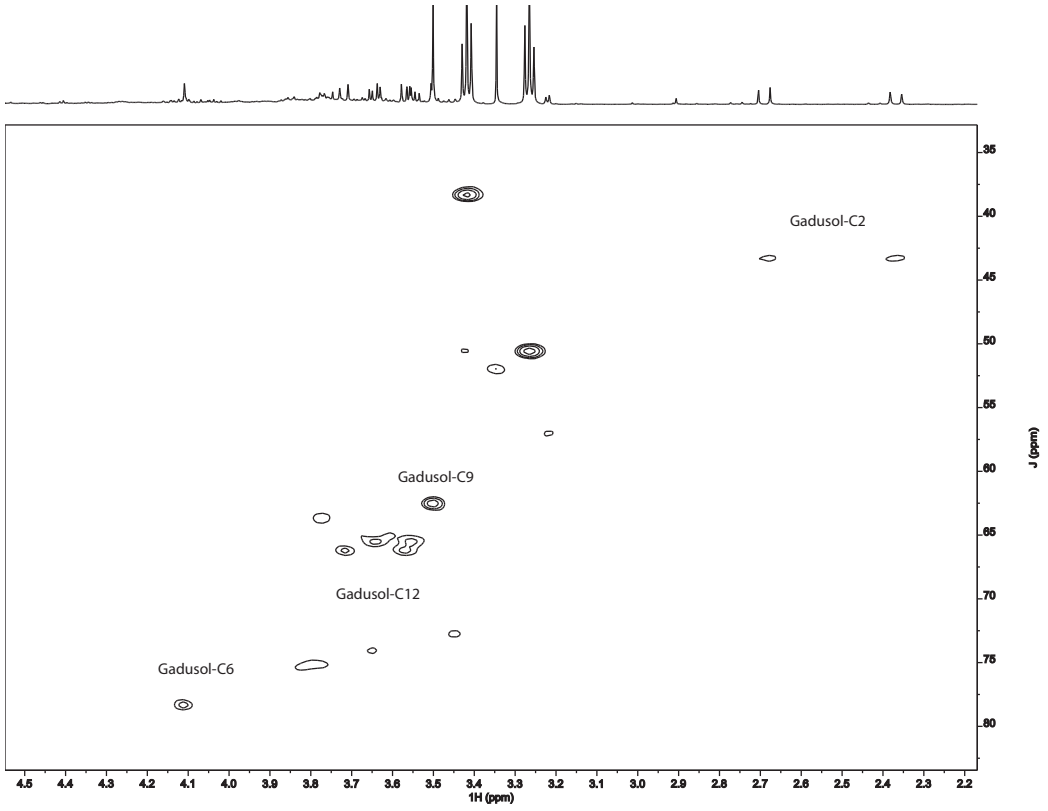

Figure 2.7. ^{1}H-^{13}C HSQC spectrum of *Artemia* extracts after mixed cation exchange clean-up. Gadusol resonances for C-2 (43.3 ppm), C-9 (62.5 ppm), C-12 (66.2 ppm), and C-6 (78.3 ppm) are labeled.

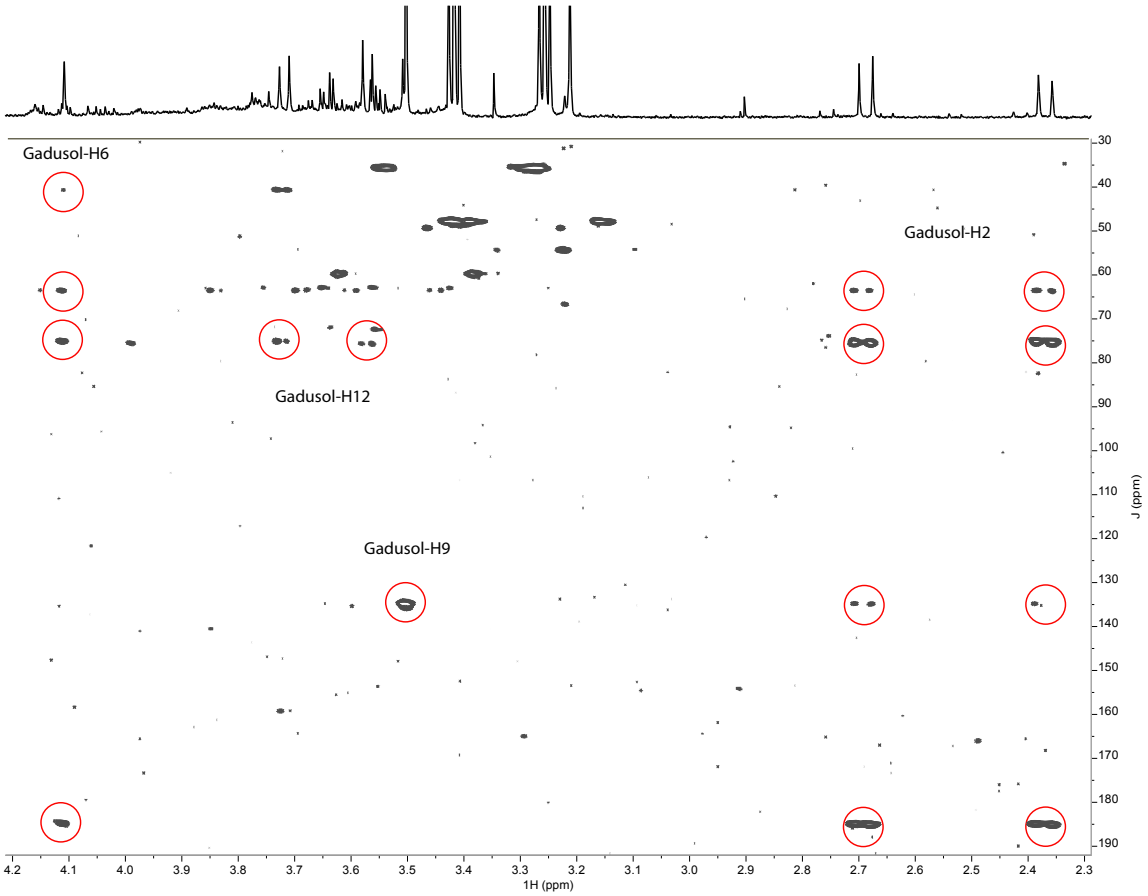

Figure 2.8. ^{1}H-^{13}C HMBC spectrum of *Artemia* extracts with the gadusol resonances labeled. Cross peaks that are aligned vertically and horizontally are connected through 2-3 bond long-range ^{1}H-^{13}C coupling.

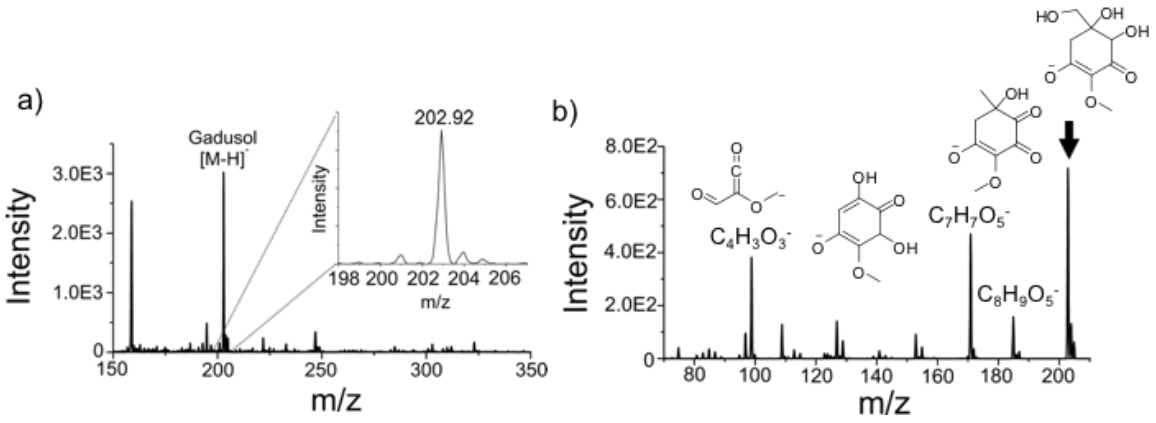

Figure 2.9. LC-MS/MS of *Artemia* extracts. a) Full mass spectrum of gadusol in negative ion mode. Inset shows expanded region of parent ion. b) Collision induced dissociation of parent ion yields various losses and ring cleavage products.

3.4 Cold Stress metabolomics

Cold stress was chosen for the environmental metabolomics proof of concept experiment because it is a known stressor for *Artemia* and the effects have previously been studied in *Artemia* and other invertebrates and extremophile species.[18,59–61] Seasonal weather changes in the Great Salt Lake have an effect on *Artemia* reproduction. During unfavorable environmental conditions, such as cold or hypoxic water, female *Artemia* lay dormant cysts instead of live young. These dormant cysts will only hatch once conditions become more favorable. At times when conditions seem favorable, cysts will start to reactivate, but if conditions reverse, the developing embryos will resume dormancy.[17,18] In our study, the naupliar *Artemia* are unable to revert to the dormant state because they have already hatched; still our observations of the changes in metabolite levels are related to many of the important metabolites for the developing cysts. As shown in the example control and cold stress NMR spectra (Figure 2.10) and GC-MS TIC (Figure 2.11), the metabolites that appear to be important for responding to cold stress include glucose, trehalose, maltose, and glycerol. These molecules are important for gluconeogenesis which leads to downstream metabolic processes and for stabilizing the lipid bilayer during temperature extremes.[62] However, to examine whether these observed changes are significant, statistical analyses are required.

The identifying information for each metabolite used for statistical analysis can be found in Table 2.2. Due to small sample sizes (1 – 4 mg), not all metabolites in the previously reported *Artemia* metabolome (Table 2.1) were used for statistical analysis. Using SIMCA,

GC-MS and NMR results for each sample were combined for multiblock multivariate analysis (Figure 2.12). For PCA, 58.5% of the variance between the cold stress and control data can be explained by PC 1 (43.9%) and PC 2 (14.6%). OPLS-DA predicts 49.7% class discrimination between the cold and control conditions. Choline, methanol, alanine, glucose, maltose, trehalose, glycerol, arginine, and AMP were identified by both OPLS-DA and PCA loading plots in the cold stress quadrants, indicating that these metabolites are strongly affected.

Univariate statistical analysis was used for pairwise comparisons to identify significant variables in the dataset. A significant variable is defined as a metabolite that has a measured fold change (fc) $1.2 > fc < 0.8$ and p-value < 0.05 when comparing two conditions, control vs cold stress. The significant variables for GC-MS are isoleucine, lysine, methionine, phenylalanine, serine, threonine, tryptophan, tyrosine and glucose. The NMR significant variables include arginine, aspartate, histidine, leucine, lysine, methionine, acetylcholine, phosphocholine, glucose, trehalose, and AMP. In both datasets, glucose is the driving variable for the difference between the cold and control conditions with a 4-fold increase in concentration under cold stress. Maltose could not be evaluated by univariate analysis because it was not detected under control conditions and a fold change cannot be calculated from a zero value.

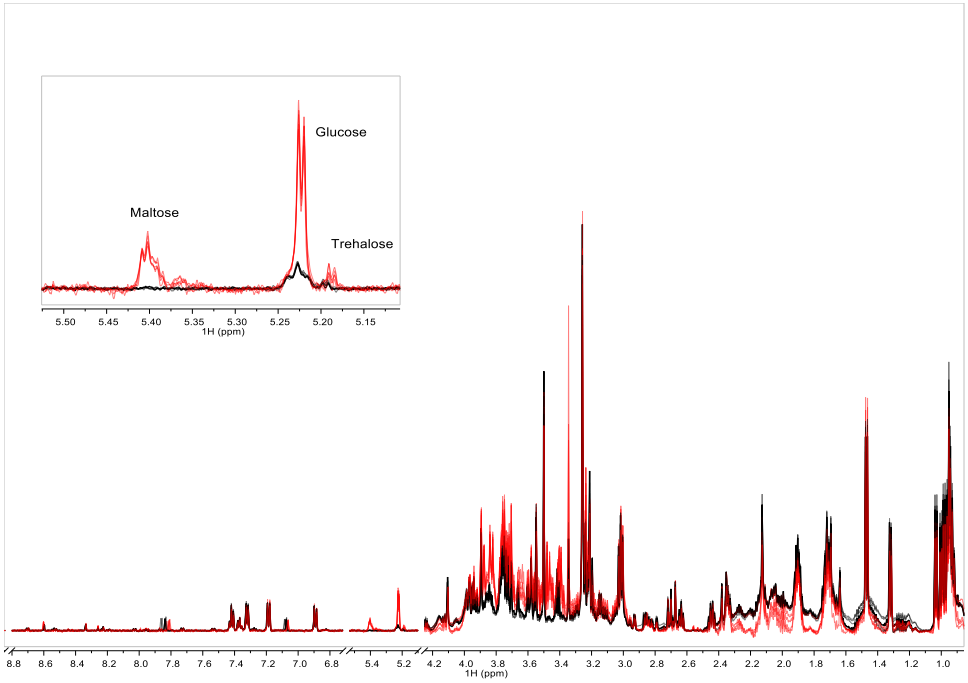

Figure 2.10. ^{1}H NMR spectra of *Artemia* extracts from organisms treated with cold (red) and control (black) overlaid. The insert shows the anomeric sugar resonances of maltose, glucose, trehalose, which are expressed in higher concentrations for the cold stress samples.

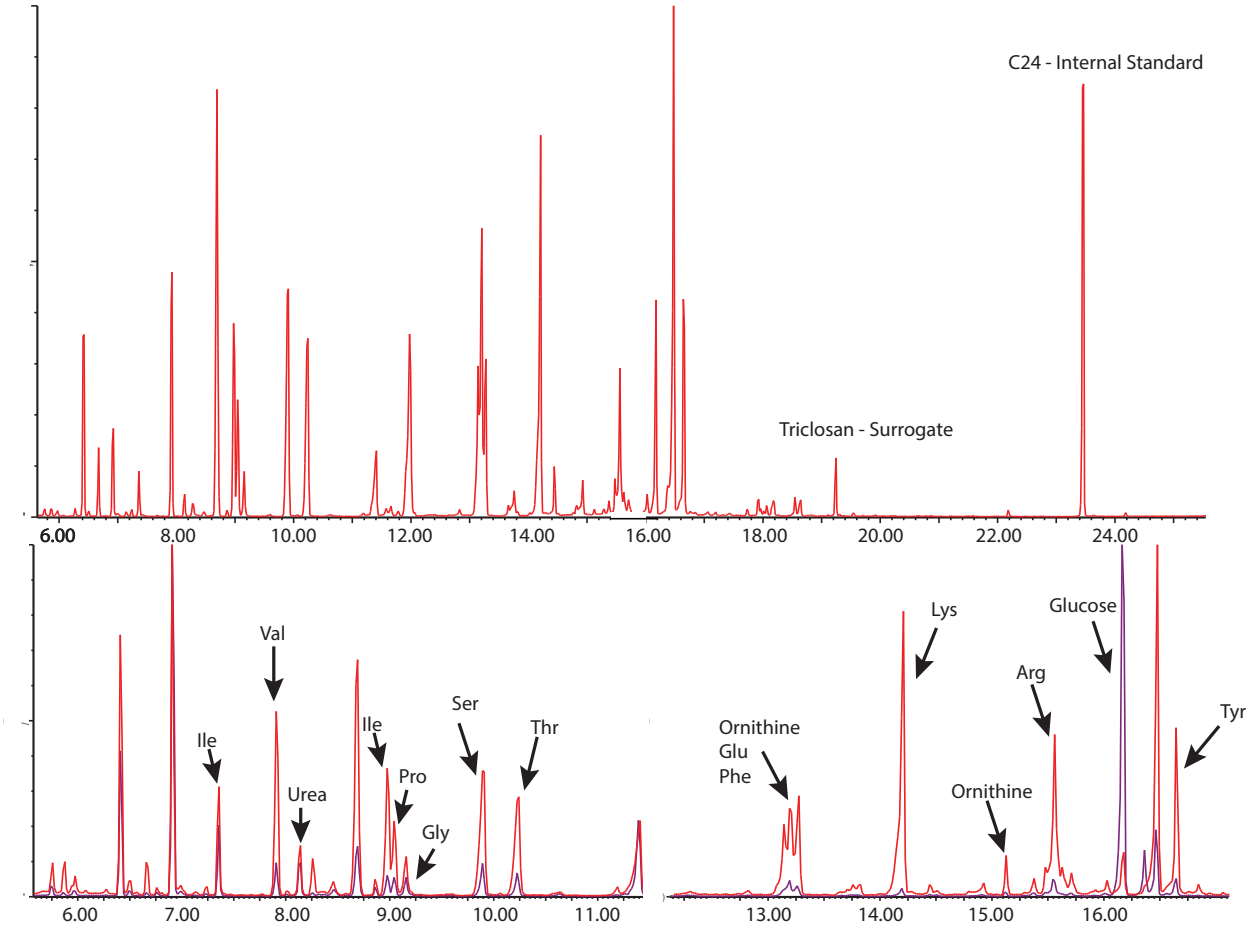

Figure 2.11. (Top) Full GC-MS spectrum for control Artemia extracts, the triclosan derivatization surrogate and C24 FAMES internal standard are labeled. (Bottom) Magnified region of the spectrum with a control spectrum (red) overlaid with a cold spectrum (purples). Prominent metabolites are labeled.

Table 2.2. Metabolites used for statistical analysis

Metabolite	^{1}H Chemical Shift (ppm)	GC-MS Peaks	R.I.	m/z
Amino Acid				
Alanine (Ala)	1.464			
Arginine (Arg)	3.245	Arginine 3TMS	1822.2	256.21
		Arginine 3TMS	1822.2	157.14
Asparagine (Asn)	2.930	Asparagine 2TMS	1497.2	115.1
		Asparagine 2TMS	1497.2	100.07
		Asparagine 3TMS	1663.8	116.11
Aspartate (Asp)	2.790	Aspartate 3TMS	1512.2	232.15
Glutamate (Glu)	2.050	Glutamate 3TMS	1616.4	246.17
Glutamine (Gln)	2.427	Glutamine 3TMS	1769.4	156.11
Glycine (Gly)	3.546	Glycine 3TMS	1302.7	174.14
Histidine (His)	7.056	Histidine (3TMS)	1914.6	254.18
Isoleucine (Ile)	0.919	Isoleucine 1TMS	1180.3	75.04
		Isoleucine 1TMS	1180.3	86.11
		Isoleucine 2TMS	1259.6	158.16
		Isoleucine 2TMS	1259.6	218.14
Leucine (Leu)	0.961	Leucine 1TMS	1158.5	75.04
		Leucine 1TMS	1158.5	86.11
		Leucine 2TMS	1238.4	158.16
Lysine (Lys)	3.016	Lysine 4TMS	1919.1	174.14
		Lysine 4TMS	1919.1	317.27
Methionine (Met)	2.127	Methionine 2TMS	1511.4	176.11
Phenylalanine (Phe)	7.315	Phenylalanine 2TMS	1622.3	91.07
		Phenylalanine 2TMS	1622.3	218.14
Proline (Pro)	3.336	Proline 1TMS	1176.9	172.11
		Proline 2TMS	1264.3	142.12
		Proline 2TMS	1264.3	186.13
		Proline 2TMS	1264.3	142.13
Serine (Ser)	3.946	Serine 3TMS	1356.7	132.1
		Serine 3TMS	1356.7	218.13
Threonine (Thr)	4.238	Threonine 3TMS	1381.5	117.09
		Threonine 3TMS	1381.5	218.17
Tryptophan (Trp)	7.722	Tryptophan 3TMS	2205.6	202.14
		Tryptophan 3TMS	2205.6	291.2
Tyrosine (Tyr)	6.885	Tyrosine 3TMS	1934	218.14
Valine (Val)	1.027	Valine 1TMS	1098	75.04
		Valine 2TMS	1212.3	218.14
		Valine 2TMS	1212.3	144.14
Osmolyte				
Acetylcholine	3.182			
Betaine	3.255			
Choline	3.191			
Glycerol	3.641			
Glycerophosphocholine	3.218			
Phosphocholine	3.201			
Sugar				
Glucose	5.223	Glucose 5TMS	1888.8	147.09
		Glucose 5TMS	1888.8	319.21
		Glucose 5TMS	1888.8	205.14

		Glucose 5TMS	1888.8	205.14
Gadusol	3.500			
Maltose	5.402			
Trehalose	5.196			
Nucleic Acid				
Inosine	8.329	Inosine 4TMS	2566.5	217.15
		Inosine 4TMS	2566.5	230.15
Polyamine				
Urea		Urea	1280.7	189.12
		Urea	1280.7	171.11
Other				
AMP	8.239			
Homarine	4.355			
Taurine	3.422			

a

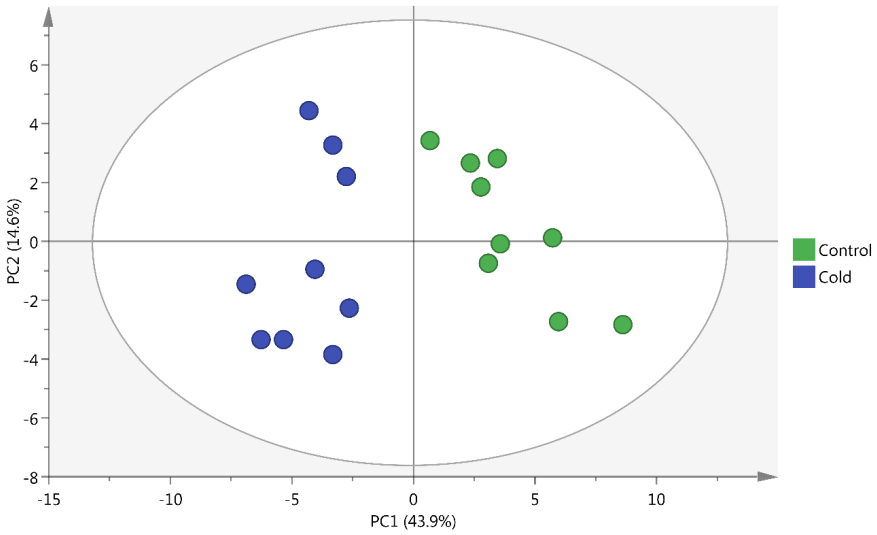

b

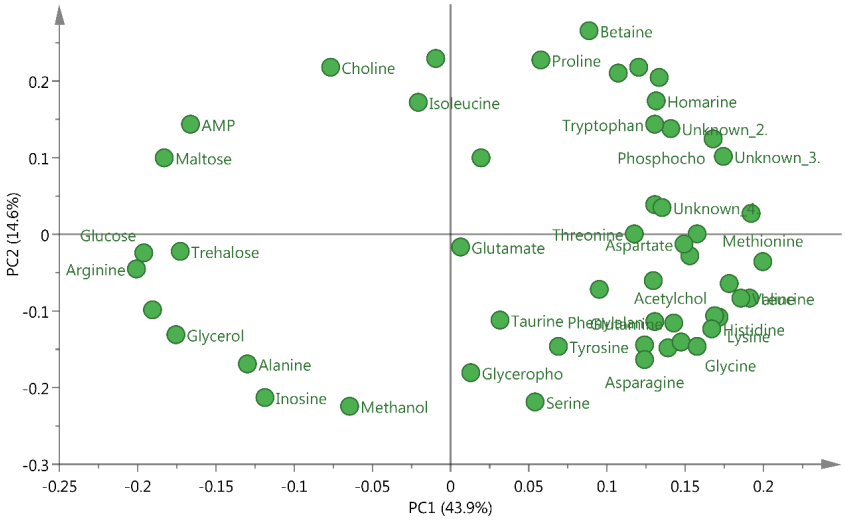

Figure 2.12. (a) PCA score plot and (b) PCA loadings plot showing 43.9% variance in PC1 and 14.6% variance in PC2. Maltose, glucose, trehalose, AMP, choline, arginine, and glycerol driving much of the variance.

Table 2.3. Cold Stress Significant Variables

Metabolite	NMR		GC-MS	
Amino Acid	p-value	Fold Change	p-value	Fold Change
Alanine	0.039	0.9224		
Arginine	**0.008**	0.5791		
Asparagine	**0.095**	1.2568		
Aspartate	0.025	1.3173		
Glutamate	**0.310**	1.1017	0.053	1.3203
Glutamine	**0.095**	1.0963		
Glycine	0.016	1.1161		
Histidine	0.009	1.3273		
Isoleucine	0.999	0.9999	0.000	1.8714
Leucine	0.000	1.2732		
Lysine	0.013	1.2578	0.024	4.0316
Methionine	0.002	1.3258	0.003	1.8697
Phenylalanine	0.020	1.1712	0.040	1.3717
Proline	0.665	1.1282	0.796	1.0842
Serine	0.644	1.0309	0.001	1.9914
Threonine	0.131	1.1366	0.000	2.1946
Tryptophan	0.091	1.9527	0.010	2.6442
Tyrosine	0.308	1.0471	0.023	1.6544
Valine	0.000	1.1986	0.546	1.7960
Osmolyte				
Acetylcholine	0.010	2.1620		
Betaine	0.371	1.0615		
Choline	**0.421**	0.7557		
Glycerophosphocholine	0.974	1.0052		
Phosphocholine	0.007	1.2170		
Sugar				
Glucose	0.001	0.3791	0.005	0.04612
Gadusol	0.054	1.1324		
Trehalose	0.000	0.0444		
Nucleic Acid				
Inosine	0.059	0.8510		
Polyamine				
Urea			0.085	3.9008
Other				
AMP	0.001	0.5686		
Homarine	0.205	1.0816		
Taurine	**0.151**	0.9750		

*** Wilcoxon-Mann-Whitney U Test P-Value**

*Statistically Significant P-Value ($P < 0.05$)

*Fold change between 0.8 and 1.2

The biomarkers, or significant variables, that were identified in the *Artemia* metabolome exhibited statistically significant ($p < 0.05$) fold changes that were greater than 1.2 or less than 0.8. Glucose is the metabolite that contributes most to the variance between the control and cold conditions. The 1D ^{1}H NMR spectra (Figure 2.10) clearly indicate a large increase in the glucose resonances at 4.6 and 5.2 ppm. A similar increase is observed in the GC-MS TIC (Figure 2.11) at 16.11 min. The large increase also affects the "sugar" region of the NMR spectra between 3 ppm and 4 ppm where the sugar resonances have obscured the signals from other metabolites in that region, such as the taurine triplet at 3.422 ppm. Maltose (5.40 ppm) and trehalose (5.19 ppm) also show notable increases in the ^{1}H NMR spectrum of cold stressed *Artemia*. These metabolites are important for cryoprotection in many invertebrate organisms that live in extreme environments.

Certain extremophiles, including *Artemia*, utilize cryoprotectant molecules to protect their internal structures from harsh environmental conditions.[59,63–65] The freeze tolerant frog, *Rana sylvatica*, the Antarctic midge, *Belgica antarctica,* and the tardigrade, *Milnesium tardigradum*, utilize similar mechanisms to protect internal structures from cold and dehydration. Freezing induced rapid glucose accumulation in *Rana sylvatica* along with a decline in ATP and aspartate, glutamate, and glutamine.[63] The Antarctic midge utilizes trehalose, glycerol, glucose, and proline to combat dehydration and extreme cold.[59] Maltose, glucose, glycerol, and trehalose play an important role in stabilizing the phospholipid bilayer for tardigrades in freezing temperatures.[62,64,65] In the encysted *Artemia* embryo, energy is stored in the form of trehalose. As the embryo emerges and

develops through the naupliar stages, trehalose is converted to glucose with the help of the proteolytic trehalase enzyme.[17,18] Trehalase and the other proteolytic enzymes that are involved in *Artemia* development are highly sensitive to environmental conditions, such as temperature, hypoxia, and pH.[17] Glucose accumulation may indicate suspended development and increased energy storage in response to the cold temperature.

In addition to the effects on cryoprotectant sugars, there was an observed decrease in total amino acid concentration, which may be explained by suspension of gluconeogenesis in response to poor environmental conditions. This would cause the developing organism to enter a state of energy conservation, such that amino acid metabolism slows, protein and lipid synthesis and metabolism is inhibited, and organismal growth slows. The significant variables are also related to these processes. Lysine and arginine are involved in protein synthesis. AMP is an energy molecule. Acetylcholine and phosphocholine are involved in glycerophospholipid metabolism.[66] The branched chain amino acids, leucine and isoleucine, are involved in stress, energy and muscle metabolism.[29] Other pathways that may have been affected include the phenylalanine, tyrosine, and tryptophan biosynthesis pathway and the glycine, serine, threonine metabolism pathway, these metabolites were expressed at lower levels under cold stress.[67,68]

4 Conclusions

We have developed growth, sample preparation and instrumental methods for using *Artemia franciscana* as a model organism for environmental metabolomics and we have

applied these methods to study cold stress as a proof-of-concept experiment. Using multivariate and univariate analysis of ^{1}H NMR and GC-MS data we determined that cold stress led to increased accumulation of sugars and cryoprotectants such as glycerol, trehalose, glucose, and maltose. We also measured a general decrease in amino acids related to protein synthesis and energy storage. These results agree with known metabolic pathways related to *Artemia* growth and development and are also consistent with other studies on freeze tolerant frogs, midges, and tardigrades. These results suggest that *Artemia franciscana* can be used as a model species for environmental metabolomics analysis of saltwater pollutants and in future studies we will study the effects of aquatic contaminants on the *Artemia* metabolome in order to identify stressors and determine their toxic mode of action.

5 References

1. Lankadurai, B. P. Environmental metabolomics: an emerging approach to study organism responses to environmental stressors. *Environ. Rev.* **21,** 180–205 (2013).

2. Villas-Bôas, S. G. *Metabolome Analysis: An Introduction*. (John Wiley & Sons, Ltd, 2007).

3. Bundy, J. G., Davey, M. P. & Viant, M. R. Environmental metabolomics: a critical review and future perspectives. *Metabolomics* **5,** 3 (2009).

4. Morrison, N. *et al.* Standard reporting requirements for biological samples in metabolomics experiments: environmental context. *Metabolomics* **3,** 203–210 (2007).

5. Jeon, J., Kurth, D. & Hollender, J. Biotransformation pathways of biocides and pharmaceuticals in freshwater crustaceans based on structure elucidation of metabolites using high resolution mass spectrometry. *Chem. Res. Toxicol.* **26,** 313–324 (2013).

6. Madsen, R., Lundstedt, T. & Trygg, J. Chemometrics in metabolomics—A review in human disease diagnosis. *Anal. Chim. Acta* **659,** 23–33 (2010).

7. Larive, C. K., Barding, G. A. & Dinges, M. M. NMR Spectroscopy for Metabolomics and Metabolic Profiling. *Anal. Chem.* **87,** 133–146 (2015).

8. Simpson, M. J. NMR spectroscopy in environmental research: From molecular interactions to global processes. *Prog. Nucl. Magn. Reson. Spectrosc.* **58,** 97–175 (2011).

9. Kariuki, M. N., Nagato, E. G., Lankadurai, B. P., Simpson, A. J. & Simpson, M. J. Analysis of Sub-Lethal Toxicity of Perfluorooctane Sulfonate (PFOS) to Daphnia magna Using 1H Nuclear Magnetic Resonance-Based Metabolomics. *Metabolites* **7,** (2017).

10. Barding, G. A., Béni, S., Fukao, T., Bailey-Serres, J. & Larive, C. K. Comparison of GC-MS and NMR for Metabolite Profiling of Rice Subjected to Submergence Stress. *J. Proteome Res.* **12,** 898–909 (2013).

11. Bioindicators: the natural indicator of environmental pollution: Frontiers in Life Science: Vol 9, No 2. Available at: https://www.tandfonline.com/doi/full/10.1080/21553769.2016.1162753. (Accessed: 10th March 2018)

12. Siciliano, A., Gesuele, R., Pagano, G. & Guida, M. How Daphnia (Cladocera) Assays may be used as Bioindicators of Health Effects? *J. Biodivers. Endanger. Species* **0,** (2015).

13. Martínez-Jerónimo, F. & Martínez-Jerónimo, L. Chronic effect of NaCl salinity on a freshwater strain of Daphnia magna Straus (Crustacea: Cladocera): a demographic study. *Ecotoxicol. Environ. Saf.* **67,** 411–416 (2007).

14. Cohen et al. *Haven or Hazard: The Ecology and Future of the Salton Sea*. (Pacific Institute, 1999).

15. Cohen, M. *Hazard's Toll: The Cost of Inaction at the Salton Sea*. (Pacific Institute, 2014).

16. Cohen, M.; Hyun, K. Hazard: The Future of the Salton Sea With No Restoration Project. (2006).

17. Warner, A. *Cell and Molecular Biology of Artemia Development*. (Springer Science & Business Media, 2013).

18. Clegg, James & Trotman, Clive. Physiological and Biochemical Aspects of Artemia Ecology. in *Artemia Basic and Applied Biology* **1,** (Kluwer Academic Publisher, 2002).

19. Kovacevic, V., Simpson, A. J. & Simpson, M. J. 1H NMR-based metabolomics of Daphnia magna responses after sub-lethal exposure to triclosan, carbamazepine and ibuprofen. *Comp. Biochem. Physiol. Part D Genomics Proteomics* **19,** 199–210 (2016).

20. Barding, G. A., Salditos, R. & Larive, C. K. Quantitative NMR for bioanalysis and metabolomics. *Anal. Bioanal. Chem.* **404,** 1165–1179 (2012).

21. Johnson, S. G. NIST Standard Reference Database 1A v17. *NIST* (2014). Available at: https://www.nist.gov/srd/nist-standard-reference-database-1a-v17. (Accessed: 12th May 2018)

22. Hummel Jan *et al.* Mass Spectral Search and Analysis Using the Golm Metabolome Database. *Handb. Plant Metabolomics* (2013). doi:10.1002/9783527669882.ch18

23. Strehmel, N., Hummel, J., Erban, A., Strassburg, K. & Kopka, J. Retention index thresholds for compound matching in GC-MS metabolite profiling. *J. Chromatogr. B Analyt. Technol. Biomed. Life. Sci.* **871,** 182–190 (2008).

24. Halket, J. M. *et al.* Chemical derivatization and mass spectral libraries in metabolic profiling by GC/MS and LC/MS/MS. *J. Exp. Bot.* **56,** 219–243 (2005).

25. Wishart, D. S. *et al.* HMDB: the Human Metabolome Database. *Nucleic Acids Res.* **35,** D521-526 (2007).

26. Wishart, D. S. *et al.* HMDB 3.0--The Human Metabolome Database in 2013. *Nucleic Acids Res.* **41,** D801-807 (2013).

27. Wishart, D. S. *et al.* HMDB 4.0: the human metabolome database for 2018. *Nucleic Acids Res.* **46,** D608–D617 (2018).

28. HMDB: a knowledgebase for the human metabolome. - PubMed - NCBI. Available at: https://www.ncbi.nlm.nih.gov/pubmed/18953024. (Accessed: 14th April 2018)

29. Chenomx Inc | Metabolite Discovery and Measurement.

30. Xiao, J. F., Zhou, B. & Ressom, H. W. Metabolite identification and quantitation in LC-MS/MS-based metabolomics. *Trends Anal. Chem. TRAC* **32,** 1–14 (2012).

31. Grootveld, M. CHAPTER 1:Introduction to the Applications of Chemometric Techniques in 'Omics' Research: Common Pitfalls, Misconceptions and 'Rights and Wrongs'. in *Metabolic Profiling* 1–34 (2014). doi:10.1039/9781849735162-00001

32. De Livera, A., Olshansky, M. & Speed, T. Statistical Analysis of Metabolomics Data. in *Metabolomics Tools for Natural Product Discovery* (eds. Roessner, U. & Dias, D. A.) 291–307 (Humana Press, 2013). doi:10.1007/978-1-62703-577-4_20

33. Gaude, E. *et al.* muma, An R Package for Metabolomics Univariate and Multivariate Statistical Analysis. *Current Metabolomics* (2013). Available at: http://www.eurekaselect.com/107837/article. (Accessed: 29th October 2017)

34. Horgan, R. P. & Kenny, L. C. 'Omic' technologies: genomics, transcriptomics, proteomics and metabolomics. *Obstet. Gynaecol.* **13,** 189–195 (2011).

35. Kanehisa, M. & Goto, S. KEGG: Kyoto Encyclopedia of Genes and Genomes. *Nucleic Acids Res* **28,** (2000).

36. MetaboAnalyst. Available at: http://www.metaboanalyst.ca/MetaboAnalyst/faces/ModuleView.xhtml. (Accessed: 27th May 2018)

37. Aggio, R. B. M. Pathway Activity Profiling (PAPi): A Tool for Metabolic Pathway Analysis. in *Yeast Metabolic Engineering* 233–250 (Humana Press, New York, NY, 2014). doi:10.1007/978-1-4939-0563-8_14

38. Gao, J. *et al.* Metscape: a Cytoscape plug-in for visualizing and interpreting metabolomic data in the context of human metabolic networks. *Bioinformatics* **26,** 971–973 (2010).

39. Theodoridis, G. *et al.* LC-MS based global metabolite profiling of grapes: solvent extraction protocol optimisation. *Metabolomics* **8,** 175–185 (2012).

40. Optimization of silylation using N-methyl-N-(trimethylsilyl)-trifluoroacetamide, N,O-bis-(trimethylsilyl)-trifluoroacetamide and N-(tert-butyldimethylsilyl)-N-methyltrifluoroacetamide for the determination of the estrogens estrone and 17alpha-ethinylestradiol by gas chromatography-mass spectrometry. | Sigma-Aldrich. Available at: https://www.sigmaaldrich.com/. (Accessed: 26th May 2018)

41. OECD. *Test No. 211: Daphnia magna Reproduction Test*. (Organisation for Economic Co-operation and Development, 2012).

42. Books / OECD Guidelines for the Testing of Chemicals, Section 2:Effects on Biotic Systems. Available at: http://www.oecd-ilibrary.org/environment/oecd-guidelines-for-the-testing-of-chemicals-section-2-effects-on-biotic-systems_20745761. (Accessed: 10th March 2018)

43. US EPA, O. Series 850 - Ecological Effects Test Guidelines. *US EPA* (2015). Available at: https://www.epa.gov/test-guidelines-pesticides-and-toxic-substances/series-850-ecological-effects-test-guidelines. (Accessed: 10th March 2018)

44. Libralato, G. The case of Artemia spp. in nanoecotoxicology. *Mar. Environ. Res.* **101,** 38–43 (2014).

45. Kerster, H. W. & Schaeffer, D. J. Brine shrimp (Artemia salina) nauplii as a teratogen test system. *Ecotoxicol. Environ. Saf.* **7,** 342–349 (1983).

46. Libralato, G., Prato, E., Migliore, L., Cicero, A. M. & Manfra, L. A review of toxicity testing protocols and endpoints with Artemia spp. *Ecol. Indic.* **69,** 35–49 (2016).

47. Brine Shrimp: Parthenogenesis and shrimp genetics.

48. Nunes, B. S., Carvalho, F. D., Guilhermino, L. M. & Van Stappen, G. Use of the genus Artemia in ecotoxicity testing. *Environ. Pollut. Barking Essex 1987* **144,** 453–462 (2006).

49. PennisiApr. 18, E., 2018 & Pm, 1:00. Tiny shrimp may be mixing ocean water as much as the wind and waves. *Science | AAAS* (2018). Available at: http://www.sciencemag.org/news/2018/04/tiny-shrimp-may-be-mixing-ocean-water-much-wind-and-waves. (Accessed: 27th May 2018)

50. Nagato, E. G. *et al.* (1)H NMR-based metabolomics investigation of Daphnia magna responses to sub-lethal exposure to arsenic, copper and lithium. *Chemosphere* **93,** 331–337 (2013).

51. Grant, P. T., Middleton, C., Plack, P. A. & Thomson, R. H. The isolation of four aminocyclohexenimines (mycosporines) and a structurally related derivative of cyclohexane-1:3-dione (gadusol) from the brine shrimp, Artemia. *Comp. Biochem. Physiol. Part B Comp. Biochem.* **80,** 755–759 (1985).

52. Mycosporine-Like Amino Acids and Related Gadusols: Biosynthesis, Accumulation, and UV-Protective Functions in Aquatic Organisms | Annual Review of Physiology. Available at: http://www.annualreviews.org/. (Accessed: 23rd January 2018)

53. Tikunov, A. P., Johnson, C. B., Lee, H., Stoskopf, M. K. & Macdonald, J. M. Metabolomic Investigations of American Oysters Using 1H-NMR Spectroscopy. *Mar. Drugs* **8,** 2578–2596 (2010).

54. Cartigny, B. *et al.* Quantitative determination of glyphosate in human serum by 1H NMR spectroscopy. *Talanta* **74,** 1075–1078 (2008).

55. Netherton, J. C. & Gurin, S. Biosynthesis and physiological role of homarine in marine shrimp. *J. Biol. Chem.* **257,** 11971–11975 (1982).

56. Berking, S. Homarine (N-methylpicolinic acid) and trigonelline (N-methylnicotinic acid) appear to be involved in pattern control in a marine hydroid. *Dev. Camb. Engl.* **99,** 211–220 (1987).

57. Plack, P. A. *et al.* Gadusol, an enolic derivative of cyclohexane-1,3-dione present in the roes of cod and other marine fish. Isolation, properties and occurrence compared with ascorbic acid. *Biochem. J.* **199,** 741–747 (1981).

58. Carreto, J. I. & Carignan, M. O. Mycosporine-Like Amino Acids: Relevant Secondary Metabolites. Chemical and Ecological Aspects. *Mar. Drugs* **9,** 387–446 (2011).

59. Teets, N. M., Kawarasaki, Y., Lee, R. E. & Denlinger, D. L. Expression of genes involved in energy mobilization and osmoprotectant synthesis during thermal and

dehydration stress in the Antarctic midge, Belgica antarctica. *J. Comp. Physiol. B* **183,** 189–201 (2013).

60. Bundy, J. G., Ramløv, H. & Holmstrup, M. Multivariate Metabolic Profiling Using 1H Nuclear Magnetic Resonance Spectroscopy of Freeze-Tolerant and Freeze-Intolerant Earthworms Exposed to Frost. *Cryoletters* **24,** 347–358 (2003).

61. Kletetschka, G. & Hruba, J. Dissolved Gases and Ice Fracturing During the Freezing of a Multicellular Organism: Lessons from Tardigrades. *BioResearch Open Access* **4,** 209–217 (2015).

62. Pereira, C. S. & Hünenberger, P. H. Interaction of the Sugars Trehalose, Maltose and Glucose with a Phospholipid Bilayer: A Comparative Molecular Dynamics Study. *J. Phys. Chem. B* **110,** 15572–15581 (2006).

63. Storey, K. B. & Storey, J. M. Freeze tolerant frogs: cryoprotectants and tissue metabolism during freeze–thaw cycles. *Can. J. Zool.* **64,** 49–56 (1986).

64. Boothby, T. C. *et al.* Tardigrades Use Intrinsically Disordered Proteins to Survive Desiccation. *Mol. Cell* **65,** 975-984.e5 (2017).

65. Tsujimoto, M., Imura, S. & Kanda, H. Recovery and reproduction of an Antarctic tardigrade retrieved from a moss sample frozen for over 30 years. *Cryobiology* **72,** 78–81 (2016).

66. KEGG PATHWAY: Glycerophospholipid metabolism - Reference pathway. Available at: http://www.genome.jp/. (Accessed: 10th January 2018)

67. KEGG PATHWAY: map00400. Available at: http://www.genome.jp/dbget-bin/www_bget?map00400. (Accessed: 28th May 2018)

68. KEGG PATHWAY: Glycine, serine and threonine metabolism - Reference pathway. Available at: http://www.genome.jp/kegg-bin/show_pathway?map00260. (Accessed: 10th January 2018)

Evaluating sub-lethal stress from Roundup® exposure in *Artemia* franciscana using ^{1}H NMR and GC-MS

CHAPTER THREE

Abstract

We have developed an environmental metabolomics method for the exposure of *Artemia franciscana* to the broad-spectrum herbicide, glyphosate, and the analysis of their metabolite extracts using ^{1}H NMR and GC-MS. It was determined that unformulated glyphosate did not have a detectable effect on *Artemia* hatch rate, mortality, or metabolic perturbation, and that the polyethoxylated tallow amine (POEA) adjuvant and isopropylamine stabilizing salt likely contribute to toxic effects. The LC_{50} for a 48 hr exposure of Roundup® was determined to be 237 ± 23 ppm glyphosate in the Roundup® formulation. *Artemia* cysts were hatched and exposed to sub-lethal glyphosate concentrations of 1, 10, 50, or 100 ppm glyphosate in Roundup®. Dose-dependent metabolic perturbation was evident from principal component analysis and partial least squares-discriminant analysis. Metabolites that change significantly from Roundup® exposure include aspartate, formate, betaine, glucose, tyrosine, phenylalanine, gadusol, and isopropylamine. Biochemical pathway analysis with the KEGG database indicates impairment of carbohydrate and energy metabolism, folate-mediated one-carbon metabolism, *Artemia* molting and development, and microbial metabolism.

1. Introduction

Glyphosate is the most widely used pesticide with an estimated 250 million pounds applied in the United States in 2015.[1] In California alone, it is one of the top five pesticides used in each county for landscape management and crops such as grapes, alfalfa, avocado, citrus, and almonds.[2] The most common use of Roundup® is post-emergent application on Roundup Ready® corn and soybeans. These seeds are genetically modified to be resistant to Roundup®; therefore, every living plant except for corn and soybeans in an agricultural field will be killed after application of this herbicide.[3,4] Glyphosate-based products are also widely applied on a smaller scale for gardening and landscaping. Glyphosate is not generally considered a harmful contaminant because it is minimally toxic to animals, is readily degraded by soil microbes, and has low leach potential.[4,5] However, due to poor management of this herbicide, it and its primary metabolite, aminomethylphosphonic acid (AMPA) is detected at sublethal levels in many water systems.[5–7] Roundup® is a well-characterized environmental contaminant and has been thoroughly studied in soil and freshwater systems, but there are few studies on the effects of Roundup® in saltwater lakes.[8,9] Many studies have found that glyphosate products affect aquatic organisms, therefore, we hypothesize that glyphosate may impact saltwater organisms such as *Artemia franciscana*.[8,10–12]

Monsanto commercialized Roundup Ready® seeds in 1996, since this time, the volume of glyphosate applied on crops annually has increased from 30 to 250 million pounds in the US.[2,13] This growth is due to both increased use of genetically modified crops and also

glyphosate-resistant weeds cropping up all over the country, which necessitates applying larger volumes.[10,13] Glyphosate's primary action is the inhibition of the enzyme 5-enolpyruvylshikimate-3-phosphate synthase (EPSPS), which is located in chloroplasts and is a critical part of the shikimate pathway. Inhibition of this enzyme prevents the production of chorsimate, which is needed for aromatic amino acid biosynthesis pathways as well as the synthesis of other aromatic compounds such as salicylic acid, an important plant hormone, Vitamin K and folate.[14] This pathway is present in plants and bacteria, but not in animals, with the exception of bacteria that reside in gut microbiota.[14]

Glyphosate is a small, polar molecule that is highly soluble in water. Glyphosate is resistant to chemical degradation, is stable in sunlight, and has a low tendency to runoff (Table 3.1). It is relatively immobile in most soil environments because it adsorbs strongly to soil particles. The field dissipation half-life for glyphosate is approximately 44 days and its primary metabolite is aminomethylphosphonic acid (AMPA). AMPA is further broken down into smaller constituents such as ammonium, carbon dioxide, and phosphate (Figure 3.1). However, despite its' low-leachability, in a 2002 study completed by the USGS, out of 154 water samples, glyphosate was detected in 36% and AMPA was detected in 69% of samples.[15] The highest measured concentration for glyphosate was 8.7 ppb, which is well below the maximum contaminant level (MCL) of 700 ppm, and the highest concentration measured for AMPA was 3.6 ppb. Glyphosate run-off occurs as a result of poor agricultural management due to overapplication and application on rainy days. It also occurs from poor management of household applications.[9,13,15]

Many people are concerned about potential side-effects from widespread detection of glyphosate in terrestrial and aquatic environments.[5,13] Toxicity testing has revealed that there are minimal risks to oral and dermal glyphosate exposure in mammals and it is unlikely carcinogenic or teratogenic for humans.[10] AMPA was found to be even less toxic than the parent compound. However, long-term exposure to glyphosate led to reduced body weight, liver toxicity, and loose stool in dogs and rats.[10] Toxicity results for aquatic species differ from those of terrestrial species.[4,11] Bluegill sunfish and rainbow trout were susceptible to glyphosate exposures below the MCL (Table 3.2).[4] Also, trace levels of glyphosate affected growth, metabolism, and energy utilization in juvenile crayfish.[16] There is no reported toxicity information for *Artemia franciscana*.

Several studies have shown that the formulation of glyphosate is more toxic than the active ingredient. Roundup® is the Monsanto company's formulation of the active ingredient glyphosate (Figure 3.2).[13] This active ingredient needs other components for stabilization and for delivery through plant cuticles. The formulation used in this study uses isopropylamine as the stabilizing salt, other formulations use potassium or dimethylamine.[2] Different adjuvant compositions are also used for Roundup® but the exact chemical formulas are proprietary.[17] The adjuvant is a polyethoxylated tallow amine (POEA) with different side chains and oxide:tallow amine ratios.[17,18] POEA and isopropylamine have been reported to be more toxic than the glyphosic acid, and POEA varieties have been found to be highly toxic to North American frogs and fairy shrimp.[12,17] Due to the reported

toxicity of the Roundup® ingredients, these different ingredients were individually tested for their effect on the *Artemia* metabolome.

This study uses gas chromatography-mass spectrometry (GC-MS) and nuclear magnetic resonance (NMR) to evaluate changes in *Artemia* metabolite levels in response to exposure to the Roundup® herbicide. NMR is a rapid, robust, and quantitative technique that requires minimal sample preparation.[19,20] GC-MS requires derivatization, but its lower limits of detection and well-established libraries provide greater coverage of the metabolome.[21–24] The complementarity of NMR and GC-MS produce a more comprehensive analysis of the *Artemia* metabolome than could be obtained with either method alone. [24,25]

The aims of this study are to identify the lethal concentration (LC_{50}) of Roundup® in *Artemia*, characterize the metabolite profile of *Artemia* 48 hr after hatching using NMR and GC-MS, characterize the molecular response of *Artemia* to sub-lethal Roundup® exposure, and to ascertain how the Roundup® ingredients contribute to the metabolic perturbation. Analysis with principal component analysis (PCA) and univariate statistical methods helped identify biomarkers of sub-lethal Roundup® exposure providing insights about the mode of action.

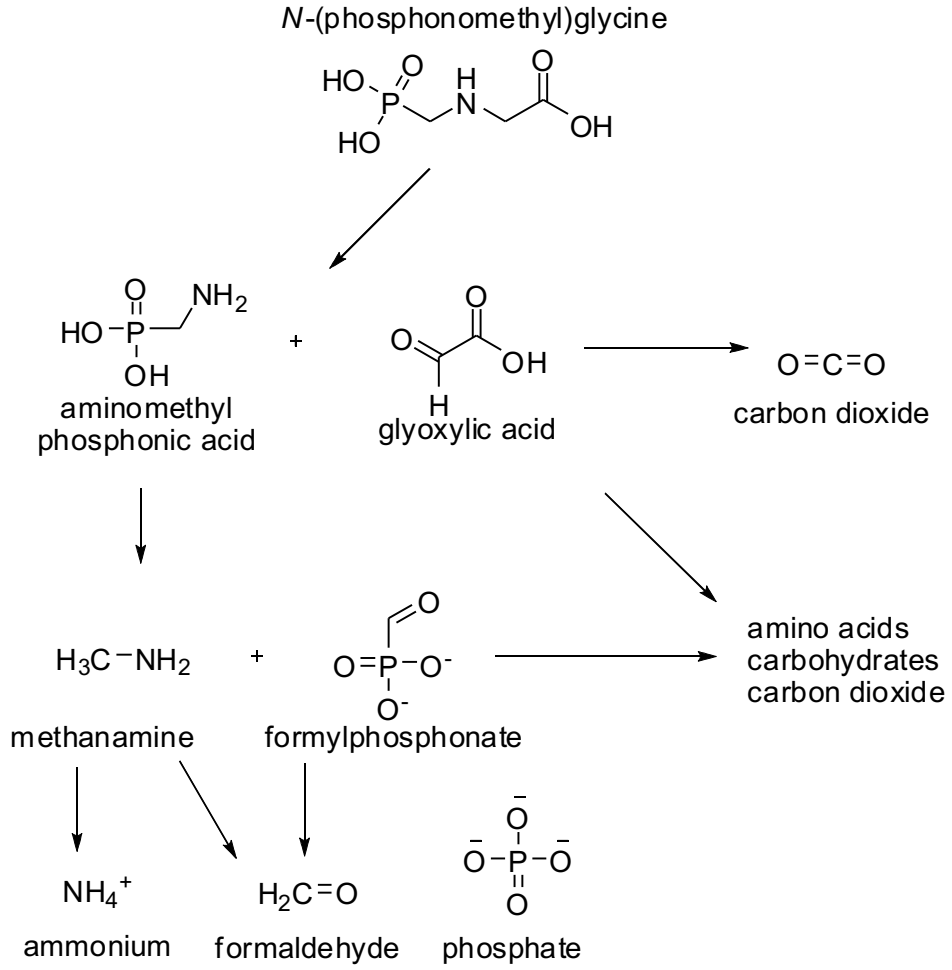

Figure 3.1. Glyphosate (N-(Phosphonomethyl)glycine) degradation pathways. The primary degradants are aminomethyl phosphonic acid (AMPA) and glyoxylic acid.

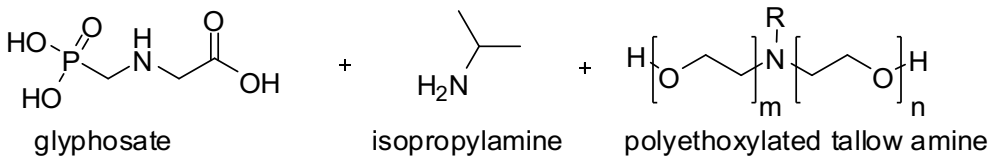

Figure 3.2. Ingredients for the Roundup® formulation: the active ingredient glyphosate, the stabilizing salt isopropylamine, and the adjuvant polyethoxylated tallow amine (POEA)

Table 3.1. Physical and chemical properties of glyphosate

Molecular weight	169.08 g/mol
Water solubility	11,600 ppm (25 ºC)
Soil adsorption coefficient (K_d)	61 g/m^3
Octanol-water coefficient log (K_{ow})	-3.5
Field dissipation half-life	44 days
Half-life (aquatic, freshwater)[3]	2-91 days
Half-life (aquatic, freshwater)[8]	47 days at 25 ºC in low light 315 days at 31 ºC in dark

Table 3.2. Glyphosate toxicity information for select terrestrial and aquatic organisms

Rat (oral)	LD_{50} 4320 mg/kg[4]
Rat (oral) 90-day	NOAEL 300 mg/kg bw per day[10]
Mallard duck 8-day	LC_{50} > 4640 ppm[4]
Bobwhite quail	LD_{50} > 3851 mg/kg[4]
Bluegill sunfish (96 hr)	LC_{50} ~ 78 ppm[4]
Rainbow trout (96 hr)	LC_{50} 38 ppm[4]
Daphnia magna (48 hr)	LC_{50} 930 ppm[4]
Honeybee	LD_{50} > 100 µg/bee[4]

2. Materials and Methods

2.1. Roundup® effect on hatch rate

The effect of Roundup®, glyphosate and AMPA on brine shrimp hatch rate was determined using petri dish experiments (described below).[26] Roundup Weed & Grass Killer Concentrate Plus purchased from The Home Depot® was used for analysis of the glyphosate formulation, 96% *N*-(Phosphonomethyl)glycine (Sigma-Aldrich, St. Louis, MO) was used for authentic glyphosate, and 99% (Aminomethyl)phosphonic acid (Sigma-Aldrich) was used for AMPA. The Roundup® formulation contains 18.00 % glyphosate isopropylamine salt, which converts to 142600 ppm glyphosate in Roundup®. Stock solutions of Roundup® (0 to 7000 ppm glyphosate in Roundup®), glyphosate (0 to 400 ppm), and AMPA (0 to 400 ppm) were prepared in 35 g/L Oceanic Natural Sea Salt Mix mixed in ultrapure water, the solutions were adjusted to pH 8.0. Glyphosate and AMPA could not be dissolved at concentrations higher than 400 ppm in saltwater.

Grade A brine shrimp cysts (Brine Shrimp Direct, Ogden, UT) were immobilized on glass slides using a small paint brush with double sided sticky tape. The slide was immersed in a petri dish (Eppendorf) filled with 15 mL of media dosed with Roundup®, glyphosate, or AMPA. For each dose, there were three replicate petri dishes containing 15-20 immobilized cysts. The petri dishes were stacked in an incubator maintained at 80 °F with constant light. After a 48 hr hatch period the number of hatched nauplii and unhatched shrimp were counted under a dissecting microscope at 10x magnification (Nikon SMZ 2B)

equipped with a Low-Noise Illuminator light source (Cole Palmer Model 9741-50). The petri dishes were returned to the incubator for an additional 48 hrs, but now maintained at a 16:8 hr light cycle. At the end of this period, the shrimp were counted again, this time accounting for living and dead shrimp that had hatched.

2.2. Glyphosate Exposures

Brine shrimp cysts were hatched according to the procedure presented in Chapter 2, section 2.1.2. To determine the Roundup® LC_{50}, 20 nauplii (early life stage of *Artemia*) were transferred into each jar for 10 replicates per dose ranging from 0 to 300 ppm glyphosate in Roundup®. Solutions were adjusted to pH 8.0 for all doses. The numbers of dead and living brine shrimp in each jar were recorded after 48 hr. A sigmoidal curve was fit to the morality data points in OriginLab (OriginLab Corporation, Northampton, MA), and the lethal concentration for 50 % of the population (LC_{50}) was determined from the inflection point of the curve.

For sub-lethal Roundup® exposures, cysts (1 oz) were hatched and nauplii were evenly distributed into fifty 50 mL jars for dose-response exposures (0 ppm, 1.00 ppm, 10.0 ppm, 50.0 ppm, 100 ppm). After a 48 hr exposure, living brine shrimp from each jar were collected in 2 mL microvials and flash frozen in liquid nitrogen. The samples were thawed, and the dose solution was exchanged with ultrapure water to remove salt and Roundup®. The samples were lyophilized and stored at -80 °C.

To assess the effect of Roundup® exposure and identify which formulation ingredients contribute to toxicity, in separate experiments *Artemia* were exposed for 48 hr to 100 ppm glycine (Fisher Scientific, Hanover Park, Il) as a positive control, 50.0 and 100 ppm glyphosate (Sigma Aldrich), and 50.0 ppm isopropylamine (Acros Organics, Morris, NJ), and samples were collected for GC-MS and NMR analysis.

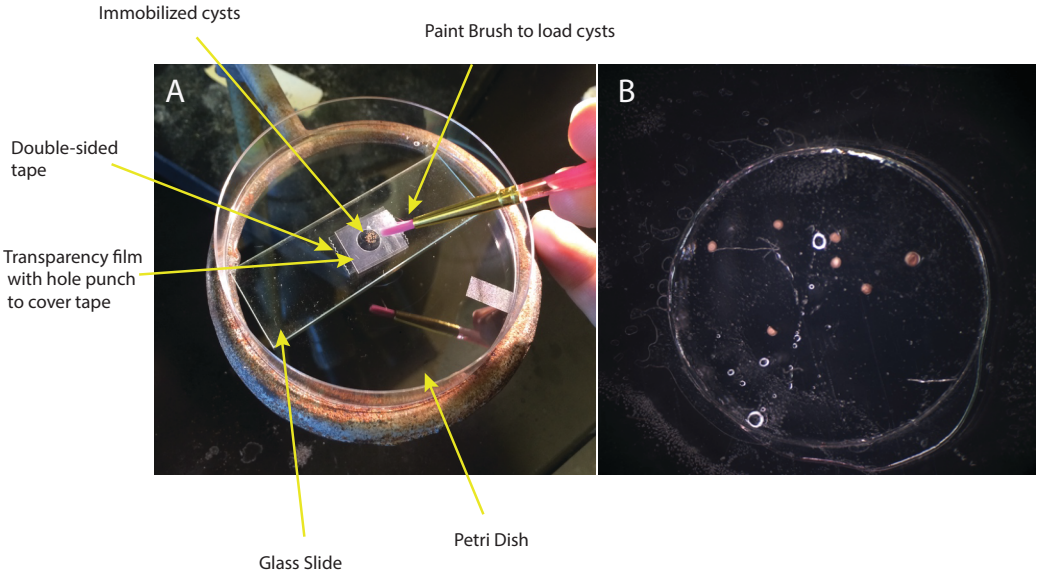

Figure 3.3. Petri dish experiments. (A) The cysts are loaded onto a glass slide using a paintbrush. They are immobilized onto double-sided tape that is partially covered by a piece of transparency film. (B) Magnified region showing immobilized cysts submerged in water. The cysts are approximately 200 µm in diameter.

2.3. Sample preparation and Instrumental Analysis

Dehydrated *Artemia* samples were extracted according to the protocol in Chapter 2, section 2.2.1.3. ^{1}H NMR spectra were acquired with a Bruker Avance III NMR spectrometer (Billerica, MA) equipped with a 5 mm TCI CryoProbe operating at 700.23 MHz. The protocol for NMR acquisition and processing are found in Chapter 2, sections 2.3.3 and 2.4.2.1. The protocols for derivatization, GC separation, and MS analysis are found in Chapter 2, section 2.3.6.

2.4. Data Analysis

Statistical analysis and data visualization was performed using SIMCA 14.1 (Umetrics, Malmo, Sweden) and the muma R package in R Studio (v 1.0.136).[27] NMR and GC-MS results for each sample were combined in SIMCA for multiblock PCA. Univariate statistical analysis was performed using the muma R package. This package calculates fold change and p-value and constructs boxplots and volcano plots from imported metabolite concentrations.

The R package PAPi was used for pathway analysis of *Artemia* metabolites and their measured responses to Roundup® exposure.[28] Spreadsheets were constructed according to the specifications of the PAPi package with metabolite identity, 2 sample treatments (control and 100 ppm Roundup®), and sample replicates in separate columns. PAPi queries the Kyoto Encyclopedia of Genes and Genomes database (KEGG, Kyoto University, Japan) to first convert metabolite names to KEGG codes and then to extract biochemical

pathway information. An activity score is calculated from the number of metabolites identified from each pathway and the relative abundance of each metabolite in a sample. A line graph of the activity score of significant pathways ($p < 0.05$) is plotted with the control group and the Bonferroni correction set as a reference.

3. Results and Discussion

The metabolomics analysis of sublethal exposure to Roundup® led to the identification of seven potential endogenous metabolite biomarkers of Roundup® exposure and one potential exogenous biomarker. Additionally, pathway analysis of the metabolite shifts indicated biochemical pathways that might be perturbed by Roundup® exposure.

3.1. Hatch Rate

Artemia cysts are highly susceptible to the environment and will not hatch in unfavorable conditions, such as low pH, hypoxia, or low temperatures.[29,30] In order to determine if Roundup® creates an unfavorable environment, hatch rate tests were conducted with Roundup®, glyphosate, and AMPA.[29] Initial range-finding studies from 0 – 7000 ppm Roundup®, 0-400 ppm glyphosate, and 0 – 400 ppm AMPA revealed that none of these compounds influenced the *Artemia* hatch rate. It was also determined that glyphosate nor AMPA had any effect on *Artemia* post-hatch mortality. However, significant post-hatch mortality was observed for nauplii hatched in 100 ppm – 7000 ppm glyphosate in Roundup® (Figure 3.4). This result was followed up with further mortality tests to identify the LC_{50} for Roundup® exposure.

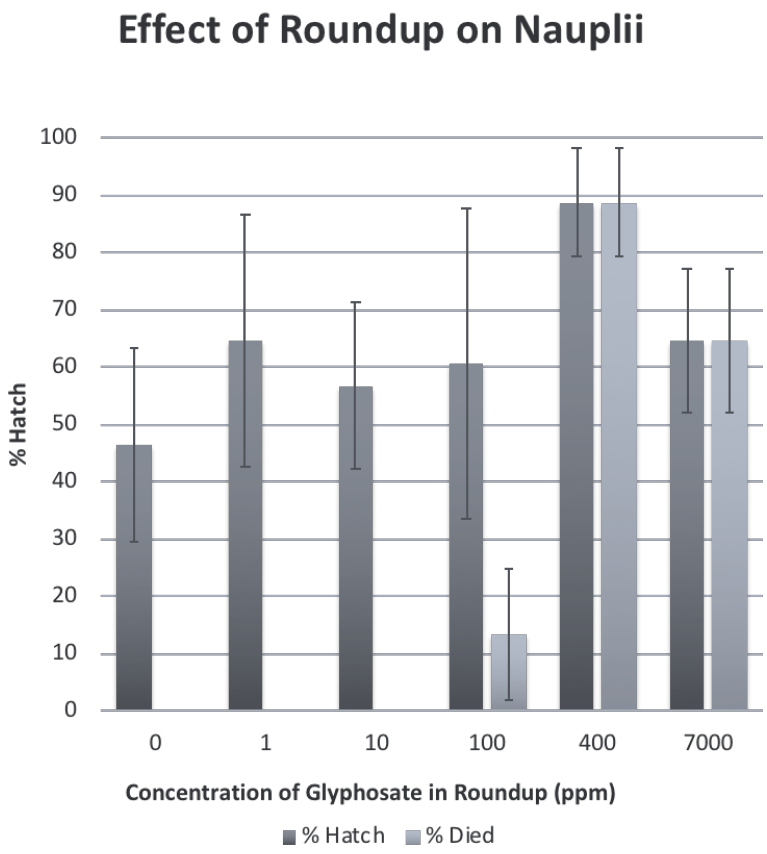

Figure 3.4. Hatch Rate and mortality for cysts hatched in 0-7000 ppm glyphosate in the Roundup® formulation, three replicates per dose with n=15-20 cysts per dish. There was not a statistical difference in hatch rate (dark), but post-hatch mortality was observed for high dose Roundup® exposures (light).

3.2. Glyphosate lethal concentration

Mortality studies for a 48 hr exposure were conducted to identify the concentrations of glyphosate in Roundup® that cause mortality. Seven concentrations ranging from 0 to 500 ppm glyphosate in Roundup® were evaluated with 10 replicate tanks per dose each containing 20 nauplii. There was a slight decrease in mortality for low dose Roundup® exposures (0-100 ppm) compared to control conditions and then increasing mortality was observed until complete mortality was reached at the highest dose after 48 hours (Figure 3.5). The lethal concentration for 50 % of the starting population of nauplii (LC_{50}) was determined from the inflexion point of the sigmoidal curve and was determined to be 237 ± 23 ppm glyphosate in Roundup®. This value was determined to find a starting point for testing the sublethal effects of Roundup® for metabolomics studies with glyphosate. The remainder of the Roundup® exposures were conducted below the calculated LC_{25} (~118 ppm).

The lethal concentration determined for Roundup® is lower than the reported toxicity of glyphosate for *Daphnia magna* and higher than the toxicities reported in sunfish and trout (Table 3.2). We were unable to determine a lethal concentration for glyphosate because no mortality was observed when the solubility limits were reached at 400 ppm. Saltwater organisms may be less susceptible to Roundup® due to the solubility limits of this compound, especially in saltwater lakes where salinity levels can reach over 300 ppm.[31] The glyphosate formulation of Roundup® had toxic effects in naupliar *Artemia* so this was the focus of the remaining exposures.

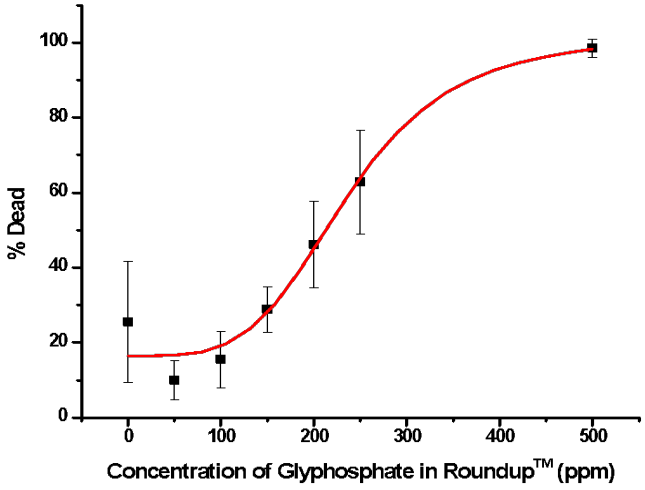

Figure 3.5. Dose-Response Plot for *Artemia* mortality with exposure to Roundup®. The LC_{50} is determined to be 237 ± 23 ppm glyphosate in Roundup® (Origin Lab).

3.3. Dose-dependent metabolite changes

3.3.1. Roundup® Exposures

The lethal concentration for 50% of the *Artemia* population was determined to be 237 ± 23 ppm glyphosate in the Roundup® formulation (Figure 3.5). Metabolomics analysis was conducted on *Artemia* exposed to 0, 1, 10, 50, and 100 ppm Roundup® concentrations to elucidate the sublethal dose-dependent metabolic impacts. A representative spectrum for NMR (Figure 3.6) and total ion chromatogram GC-MS (Figure 3.7) with control versus 100 ppm Roundup® show peaks that correspond to metabolites that change significantly. Isopropylamine, aspartate, betaine, gadusol, tyrosine, and formate have a noticeable difference in ^{1}H NMR peak height. The peak area for glucose is also considerably different in the GC-MS TIC.

Using multiblock multivariate analysis, the results for NMR and GC-MS were combined for each sample to better visualize the variation in the whole dataset and confirm the identification of metabolites that contribute to the variation between groups. The metabolites reported in the *Artemia* metabolome (Table 2.1) were not all considered for metabolomics analysis because larger pooled sample quantities were used for profiling than were possible in the experiments. The metabolites that were measurable in the experimental procedure are reported in Table 3.3. Multivariate analysis results indicate dose-dependent separation. PCA (Figure 3.8) indicates that 35.6 % of variance can be explained by PC 1 (23.2 %) and PC 2 (12.4 %). PCA reveals dose-dependent grouping but considerable overlap is evident among the control, 1 ppm and 10 ppm doses which suggests that the

metabolite profile within these samples is similar. The higher Roundup® doses (50 ppm and 100 ppm) have greater separation from the control and lower Roundup® doses (1 and 10 ppm) indicating that there is more variation in the metabolite profile for these samples.

The loading plot (Figure 3.8b) for PCA shows how the metabolites contribute to each component. In the score plots, PC1 and component 1 contributes to the separation between control and 100 ppm Roundup®. The PCA loading plot shows that tyrosine, aspartate, formate, glutamate, lysine, and arginine are plotted furthest from the origin in PC1. Loading plots can be challenging to decipher when comparing multiple groups, so in order to better understand how individual metabolite levels change with exposure, univariate analyses were conducted on each metabolite.

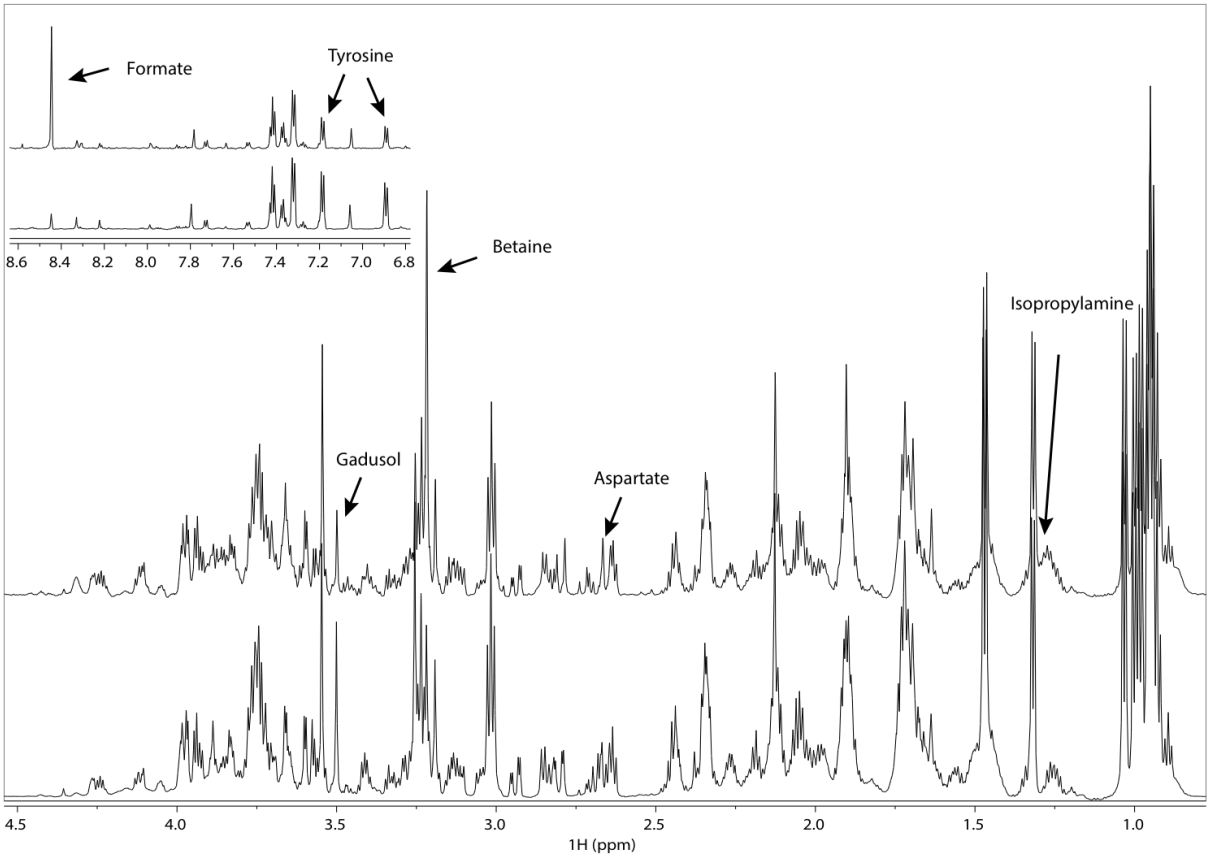

Figure 3.6. ^{1}H NMR spectra (0.92 - 4.50 ppm and 6.80 - 8.60 ppm) for *Artemia* exposed to control (bottom) versus 100 ppm Roundup® (top). Spectra are labeled with metabolites that were significantly affected by exposure.

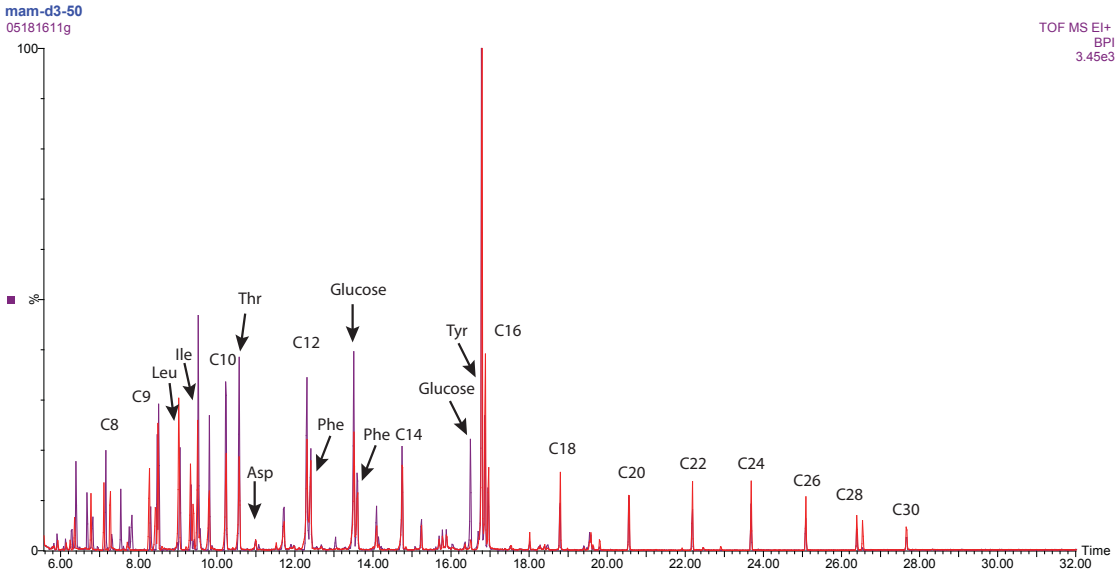

Figure 3.7. GC-MS total ion chromatogram for *Artemia* exposed to control (red) or 100 ppm Roundup® (purple) labeled with FAMES internal standards and significant metabolites.

Table 3.3. ^{1}H NMR resonances and GC-MS peaks used for statistical analysis

Metabolite	^{1}H Chemical Shift (ppm)	GC-MS Peaks	R.I.	m/z
Amino Acid				
Alanine (Ala)	1.464			
Arginine (Arg)	3.245	Arginine 3TMS	1822.2	256.21
		Arginine 3TMS	1822.2	157.14
Asparagine (Asn)	2.930	Asparagine 2TMS	1497.2	115.1
		Asparagine 2TMS	1497.2	100.07
		Asparagine 3TMS	1663.8	116.11
Aspartate (Asp)	2.790	Aspartate 3TMS	1512.2	232.15
Glutamate (Glu)	2.050	Glutamate 3TMS	1616.4	246.17
Glutamine (Gln)	2.427	Glutamine 3TMS	1769.4	156.11
Glycine (Gly)	3.546	Glycine 3TMS	1302.7	174.14
Histidine (His)	7.056	Histidine (3TMS)	1914.6	254.18
Isoleucine (Ile)	0.919	Isoleucine 1TMS	1180.3	75.04
		Isoleucine 1TMS	1180.3	86.11
		Isoleucine 2TMS	1259.6	158.16
		Isoleucine 2TMS	1259.6	218.14
Leucine (Leu)	0.961	Leucine 1TMS	1158.5	75.04
		Leucine 1TMS	1158.5	86.11
		Leucine 2TMS	1238.4	158.16
Lysine (Lys)	3.016	Lysine 4TMS	1919.1	174.14
		Lysine 4TMS	1919.1	317.27
Methionine (Met)	2.127	Methionine 2TMS	1511.4	176.11
Phenylalanine (Phe)	7.315	Phenylalanine 2TMS	1622.3	91.07
		Phenylalanine 2TMS	1622.3	218.14
Proline (Pro)	3.336	Proline 1TMS	1176.9	172.11
		Proline 2TMS	1264.3	142.12
		Proline 2TMS	1264.3	186.13
		Proline 2TMS	1264.3	142.13
Serine (Ser)	3.946	Serine 3TMS	1356.7	132.1
		Serine 3TMS	1356.7	218.13
Threonine (Thr)	4.238	Threonine 3TMS	1381.5	117.09
		Threonine 3TMS	1381.5	218.17
Tryptophan (Trp)	7.722	Tryptophan 3TMS	2205.6	202.14
		Tryptophan 3TMS	2205.6	291.2
Tyrosine (Tyr)	6.885	Tyrosine 3TMS	1934	218.14
Valine (Val)	1.027	Valine 1TMS	1098	75.04
		Valine 2TMS	1212.3	218.14
		Valine 2TMS	1212.3	144.14
Osmolyte				
Betaine	3.255			
Choline	3.191			
Glycerophosphocholine (GPC)	3.218			
Formate	8.446			
Lactate	4.130			
Sugar				
Glucose		Glucose 5TMS	1888.8	147.09
		Glucose 5TMS	1888.8	319.21
		Glucose 5TMS	1888.8	205.14
		Glucose 5TMS	1888.8	205.14

Gadusol	3.500			
Myoinositol		Myo-Inositol	2073.3	147.09
		Myo-Inositol	2073.3	217.14
		Myo-Inositol	2073.3	305.2
N-acetylglucosamine		N-acetylglucosamine	2058.8	319.21
		N-acetylglucosamine	2058.8	205.14
Nucleic Acid				
Inosine	8.329	Inosine 4TMS	2566.5	217.15
		Inosine 4TMS	2566.5	230.15
Uracil		Uracil 2TMS	1334.5	99.04
		Uracil 2TMS	1334.5	241.13
Polyamine				
Butanediamine		Putrescine 4TMS	1729.3	174.14
Urea		Urea	1280.7	189.12
		Urea	1280.7	171.11
Other				
L-Dopa		L-Dopa	2081.6	267.16
Cholesterol		Cholesterol	2812	129.1
Linolenic Acid		Linolenic acid	2241.4	79.07
Homarine	4.355			

a

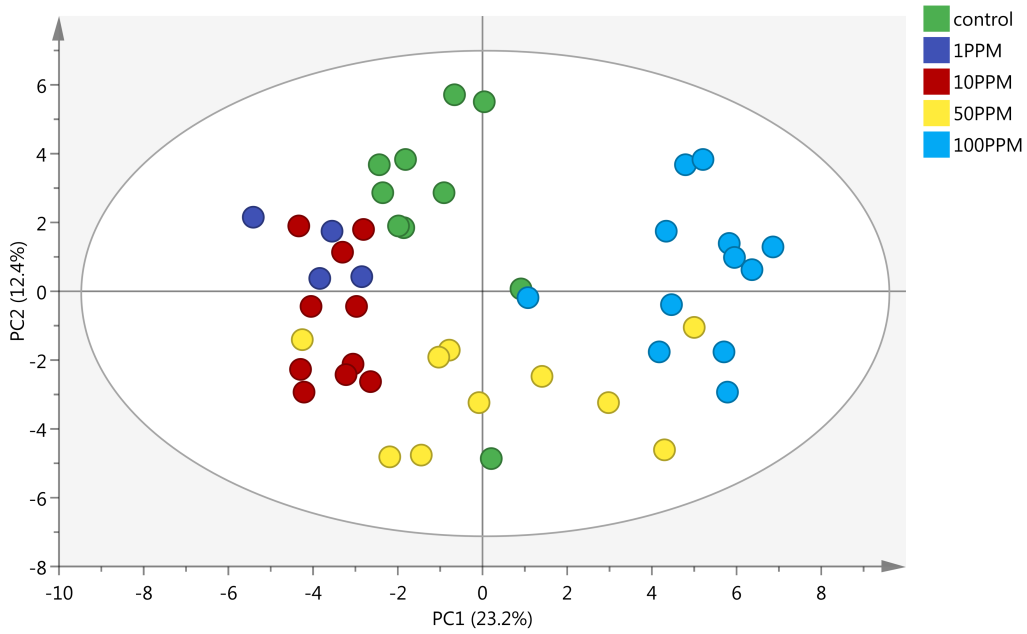

b

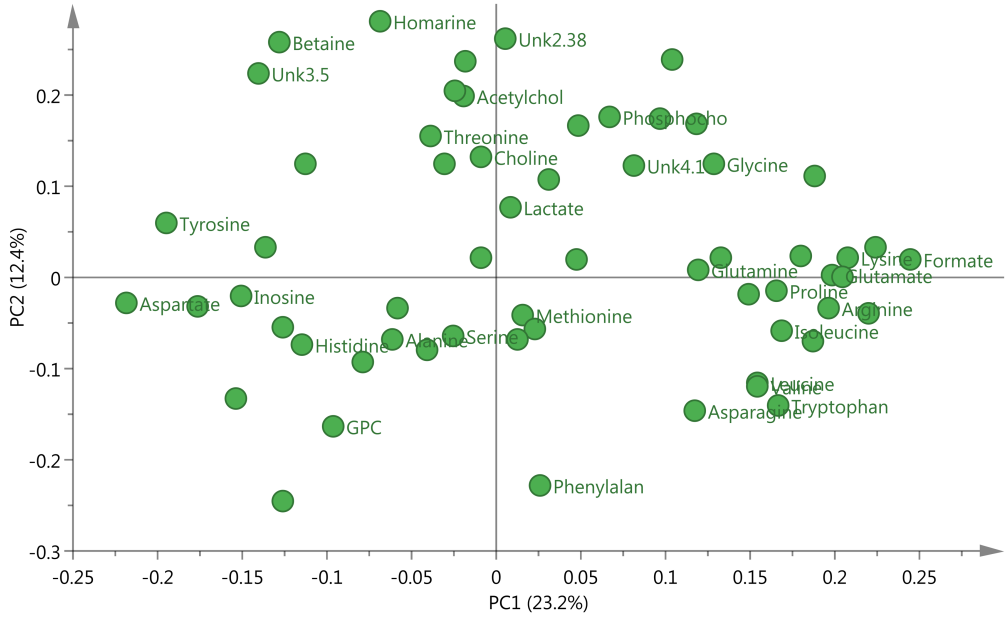

Figure 3.8. Multivariate analysis of GC-MS and NMR dose-dependent results compiled in SIMCA. (a) Multiblock-PCA Score Plot with PC1 = 23.2% and PC2 = 12.4% explained variance for control (green), 1 ppm (purple), 10 ppm (red), 50 ppm (yellow), and 100 ppm (blue) Roundup®. (b) Loading plot indicating how metabolites from GC-MS and NMR contribute to the variance in PC1 and PC2.

Univariate analysis was conducted with the muma package to determine which metabolites change significantly with Roundup® exposure, these metabolites might be considered biomarkers. The fold change and p-value for each metabolite in control and 100 ppm Roundup® dataset were plotted to generate a volcano plot. These plots provide a way of visualizing the metabolites that change most significantly from exposure, these are plotted furthest from the origin. The volcano plots indicate that much of the difference between the high dose (100 ppm Roundup®) and the control can be attributed to formate, aspartate, glucose, betaine, phenylalanine, tyrosine, and gadusol (Figure 3.9). Several of the metabolites identified in both GC-MS and NMR, such as aspartate and tyrosine, are significant in both datasets, indicating consistency between the techniques.

Dose-response box and whisker plots of the normalized spectral area for each significant variable were plotted for ^{1}H NMR and GC-MS (Figure 3.10) for each metabolite identified by volcano plots. According to ^{1}H NMR: aspartate, betaine, gadusol, and tyrosine decrease with exposure and formate increases with exposure. According to GC-MS: aspartate and tyrosine decrease, and glucose increases with Roundup® exposure. The trend for aspartate and tyrosine is consistent between the instrument measurements but the error bars in GC-MS data indicates more response variability. Threonine, glucose, phenylalanine, and isoleucine are able to be measured by GC-MS and NMR but were only identified as significant by GC-MS. These metabolites have similar trends for both measurements but did not have a statistically significant p-value for NMR due to resonance overlap. Although

other metabolites were affected by Roundup® exposure, we focused on the significant variables because they contribute most to the metabolic variation and might be reliable biomarkers of Roundup® exposure.

The p-value for all remaining metabolites are reported in Table 3.4 for both GC-MS and NMR results for each dose compared to control conditions. The cells highlighted in blue are statistically significant ($p < 0.05$) and the bolded text represents a p-value that was calculated with a U-test instead of a t-test because the metabolite concentrations were non-normally distributed. In addition to the significant metabolites, from GC-MS, urea, L dopa, linolenic acid, uracil, inosine, and myo-inositol had statistically significant p-values for at least one dose. For NMR, valine, proline, lysine, leucine, histidine, glycine, glutamine, and alanine were statistically significant for at least one dose. These metabolites had statistically significant p-values ($p < 0.05$) but did not have a fold change > 1.2 or < 0.8 and several metabolites were significant in other doses, but not for control and 100 ppm Roundup®, so these were not identified in the volcano plots.

a

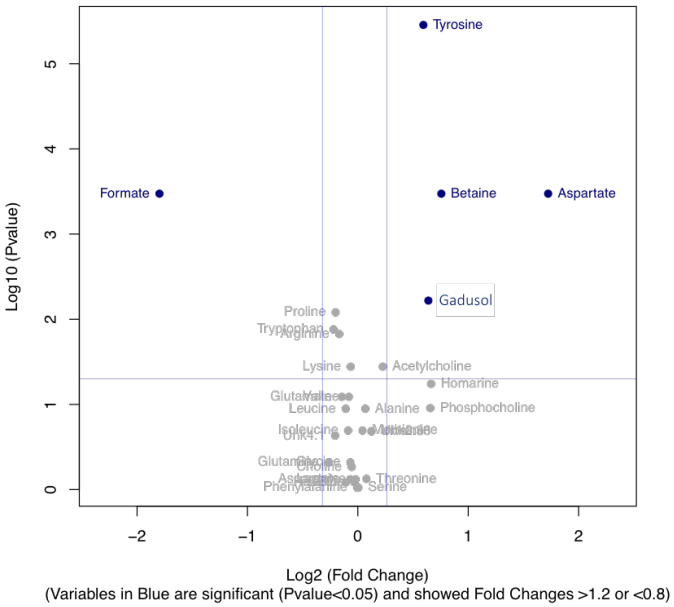

b

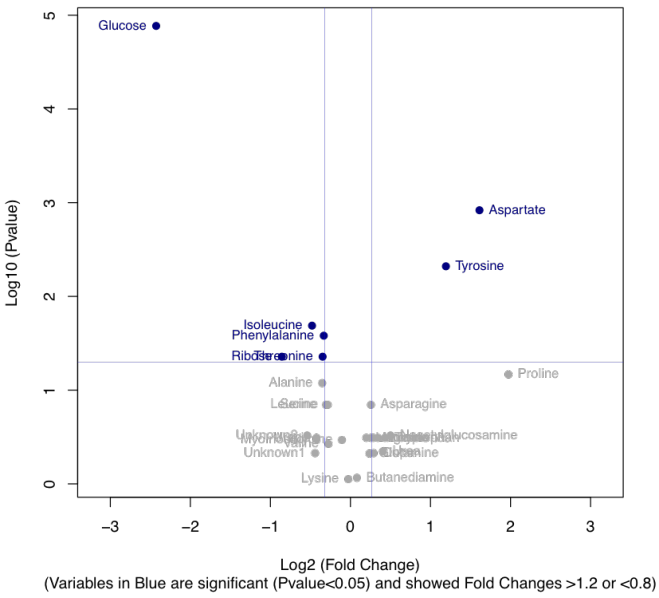

Figure 3.9. Volcano Plots for Control vs 100 ppm Roundup® exposure for metabolites identified by GC-MS (a) and NMR (b). Variables in blue are significant (p-value < 0.05) and exhibit fold changes > 1.2 or < 0.8 (constructed in muma). On the x-axis, negative values are metabolites with a positive fold change compared to the control.

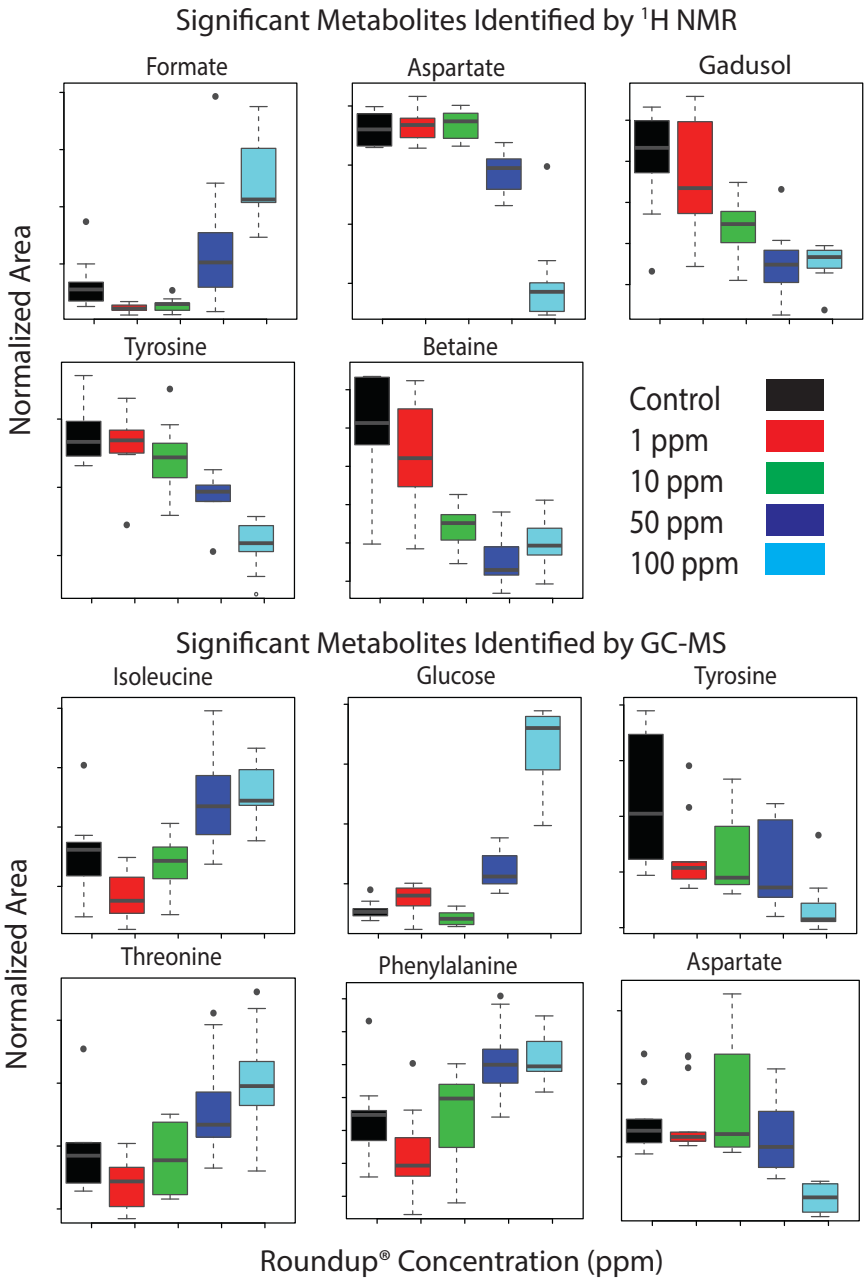

Figure 3.10. Box and whisker plots of significant variables for each Roundup® dose in ^{1}H NMR and GC-MS analysis. The box represents the interquartile range, the bar represents the median of the dataset, the whiskers extend to the highest and lowest observations, and black circles represent statistical outliers (Constructed in muma).

Table 3.4. Univariate statistics: Roundup® dose versus control p-value for each metabolite

	1 PPM		10 PPM		50 PPM		100 PPM	
Metabolite	**GC**	**NMR**	**GC**	**NMR**	**GC**	**NMR**	**GC**	**NMR**
Amino Acid								
Alanine	0.474	**0.78**	**0.113**	0.39	0.193	0.411	0.026	0.012
Arginine	**0.968**	**0.211**	0.271	0.226	0.011	0.111	0.218	**0.013**
Asparagine	0.170	0.094	0.315	0.769	0.348	0.533	0.059	0.964
Aspartate	**1.000**	**0.842**	0.393	0.323	0.435	0.000	0.000	**0.000**
Glutamate		0.139		0.569		0.190		
Glutamine	0.548	0.088	0.529	0.026	0.577	0.26	0.442	**0.604**
Glycine	**0.043**	0.185	**0.053**	0.057	**0.113**	0.857	**0.258**	0.441
Histidine		0.073		0.01		0.351		0.842
Isoleucine	0.022	0.069	0.615	0.442	0.022	0.433	0.003	0.076
Leucine	0.020	0.408	0.043	0.753	0.64	0.032	0.059	0.082
Lysine	0.280	0.003	0.294	0.004	0.321	0.713	0.890	0.077
Methionine		**0.400**		**0.529**		**0.912**		**0.065**
Phenylalanine	0.056	0.804	0.922	**0.481**	0.009	**0.280**	0.005	0.009
Proline	**0.968**	0.315	**0.095**	0.338	**0.001**	0.247	**0.019**	0.001
Serine	0.141	**0.315**	0.208	0.719	0.304	0.458	0.051	0.025
Threonine	**0.053**	0.49	**0.780**	0.348	**0.008**	0.129	**0.011**	0.059
Tryptophan	**0.035**	0.958	**0.053**	0.383	0.745	0.007	0.203	0.074
Tyrosine	**0.043**	0.207	**0.013**	0.151	0.023	0.000	**0.000**	0.000
Valine	0.962	0.08	0.125	0.207	**0.78**	0.132	0.103	0.039
Osmolyte								
Betaine		0.190		0.000		0.000		0.000
Formate		0.003		0.008		**0.063**		0.000
Lactate		**0.842**		**0.739**		**0.579**		**0.780**
Sugar								
Glucose	0.057		0.066		0.000		0.000	
Myo-Inositol	0.391		0.536		0.008		0.243	
Gadusol	0.111		**0.002**		**0.013**		0.406	
N-Acetyl Glucosamine	0.516		0.552		0.841		0.147	
Nucleic Acid								
Inosine	0.197		0.003		0.015		0.213	
Uracil	0.321		0.010		0.063		0.21	
Polyamine								
Butanediamine	0.611		0.486		0.943		0.832	
Urea	0.053		0.036		0.041		0.373	
Other								
L-Dopa	0.024		0.003		**0.035**		0.422	
Linolenic acid	**0.400**		**0.010**		**0.604**		**0.222**	

*** Wilcoxon-Mann-Whitney U Test P-Value**

*Statistically Significant P-Value (P < 0.05)

3.3.2. Positive Control Exposures

To verify the metabolic perturbation is due to the Roundup® formulation, a dose-response experiment was conducted on *Artemia* exposed to 100 ppm glyphosate and 100 ppm glycine as a positive control using the same conditions as the Roundup® exposure. Multivariate analysis was performed using SIMCA. PCA resulted in no apparent separation with PC1 = 25.3% and PC2 = 14.1 (Figure 3.11). Univariate statistics was performed to identify statistically significant metabolites between the control, glycine exposure, and glyphosate exposure. The only significant variable identified in the positive control experiments was the metabolite glycine when comparing the *Artemia* exposed to 100 ppm glycine and 100 ppm glyphosate. Higher levels of glycine were measured in *Artemia* exposed to 100 ppm glycine in both GC-MS and NMR (Figure 3.12). Isoleucine, serine, and L dopa had $p < 0.05$ for several conditions, but not a significant fold change.

3.3.3. Isopropylamine, Roundup®, Control Exposures

An exposure of *Artemia* following the same procedure as the positive control experiments was performed to identify the effects of the Roundup® formulation ingredients. Namely, isopropylamine, since it has shown to bioaccumulate based on the ^{1}H NMR spectra (Figure 3.13). Multivariate analysis was performed in SIMCA 14.1 and univariate analysis was performed with the muma R package. The loading plot (Figure 3.14) indicate which metabolites contribute most to the clustering predicted by the PCA score plots. The optimum separation for PCA was predicted with PC 1 (25.7%) and PC 2 (20.9 %). Metabolites that were significant from the control to the isopropylamine or Roundup®

exposure include aspartate, glucose, and glycine. Metabolites that were significant only in control versus isopropylamine include threonine, glycerophosphocholine, ornithine, and L dopa. Metabolites that were significant from the control to isopropylamine and between isopropylamine and Roundup® include proline, glucose, and homarine. This indicates that isopropylamine contributes to an effect on aspartate, glycine, proline, threonine, glucose, and homarine within the Roundup® formulation. Aspartate, threonine, and glucose were identified as metabolites that change significantly from the 100 ppm Roundup® exposure, so it is notable that isopropylamine also affects these metabolites.

a

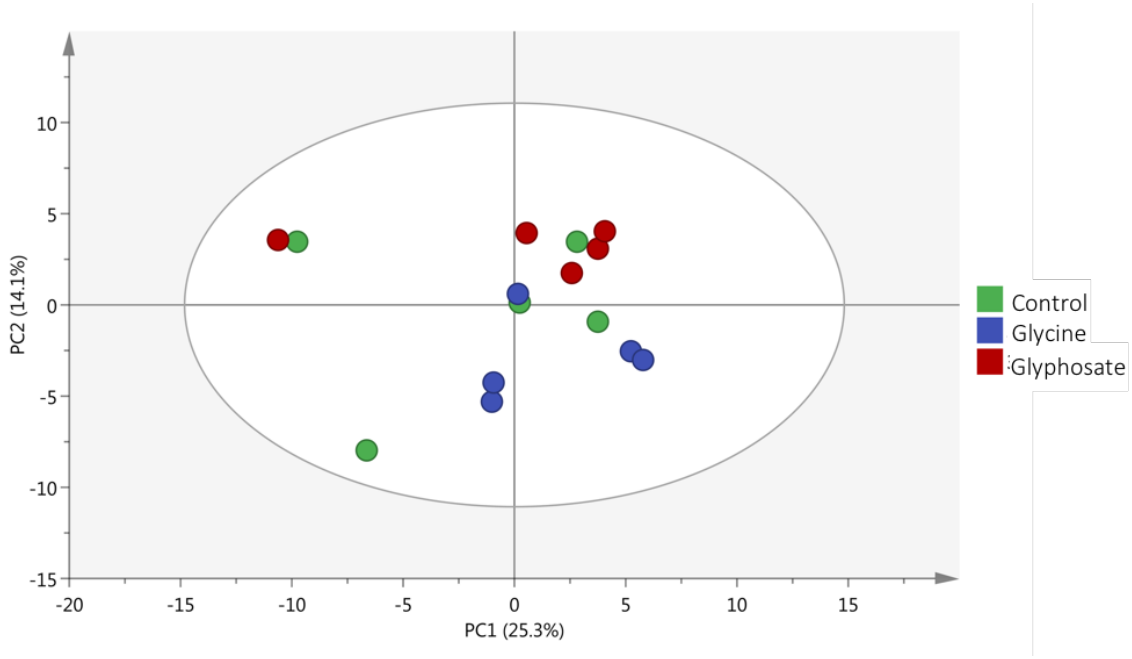

b

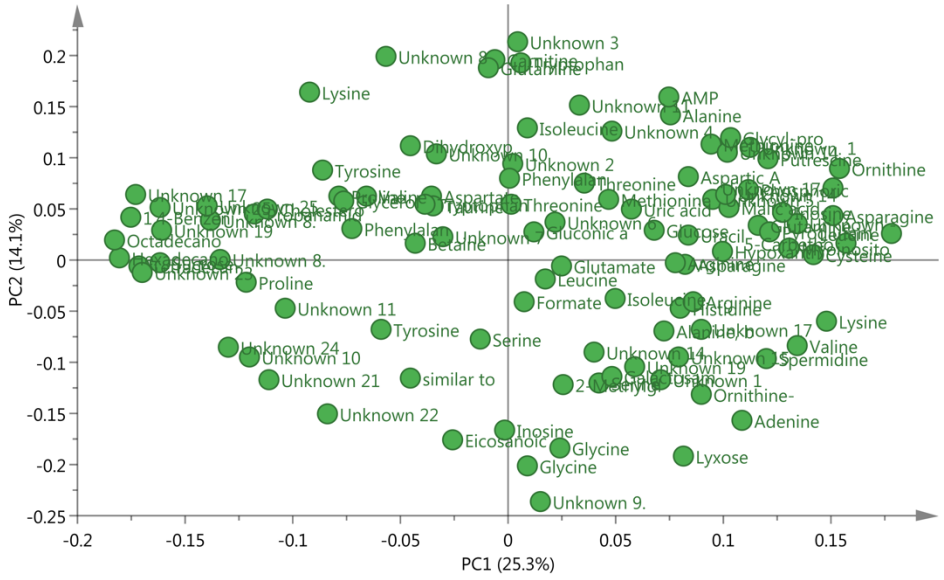

Figure 3.11. Multivariate analysis of GC-MS and NMR results for positive control experiments comparing control, 100 ppm glycine exposure, and 100 ppm glyphosate exposure. (a) Multiblock-PCA Score Plot (PC1=25.3%, PC2=14.1) and (b) loading plot (compiled in SIMCA).

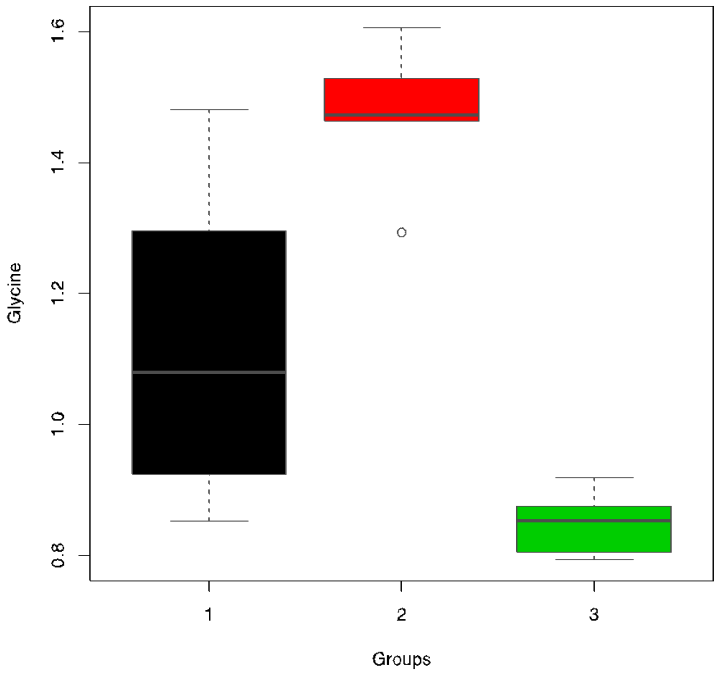

Figure 3.12. Boxplot showing glycine levels in the control (1, black), 100 ppm glycine (2, red), and 100 ppm glyphosate (3, green) exposures.

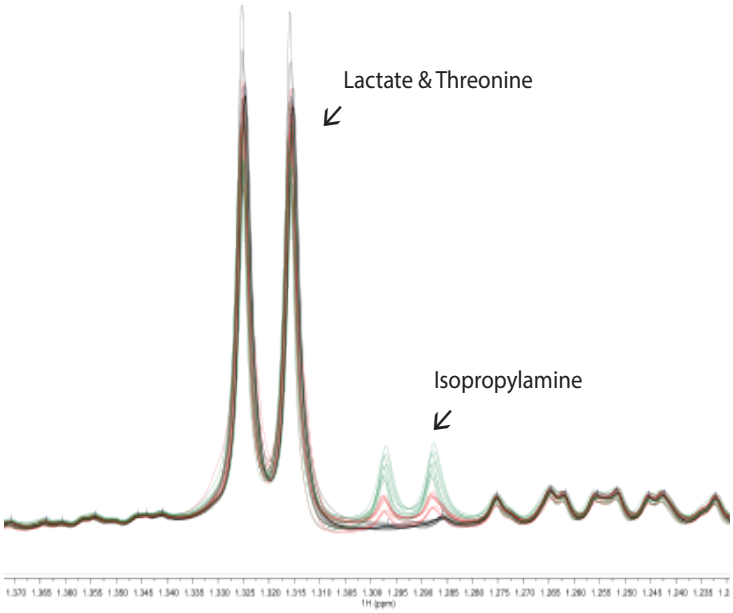

Figure 3.13. Overlaid ^{1}H NMR spectra of control (black), isopropylamine exposed (red), and Roundup® exposed (green) *Artemia* extracts.

a

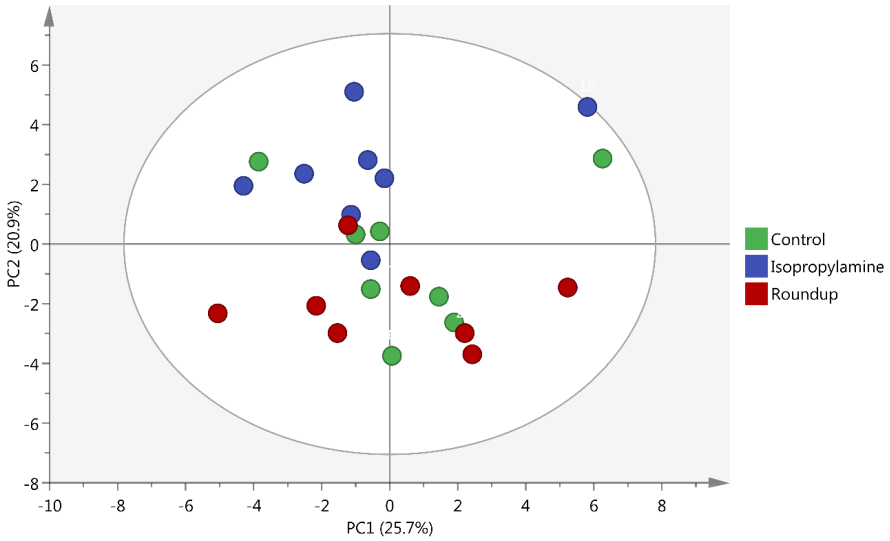

b

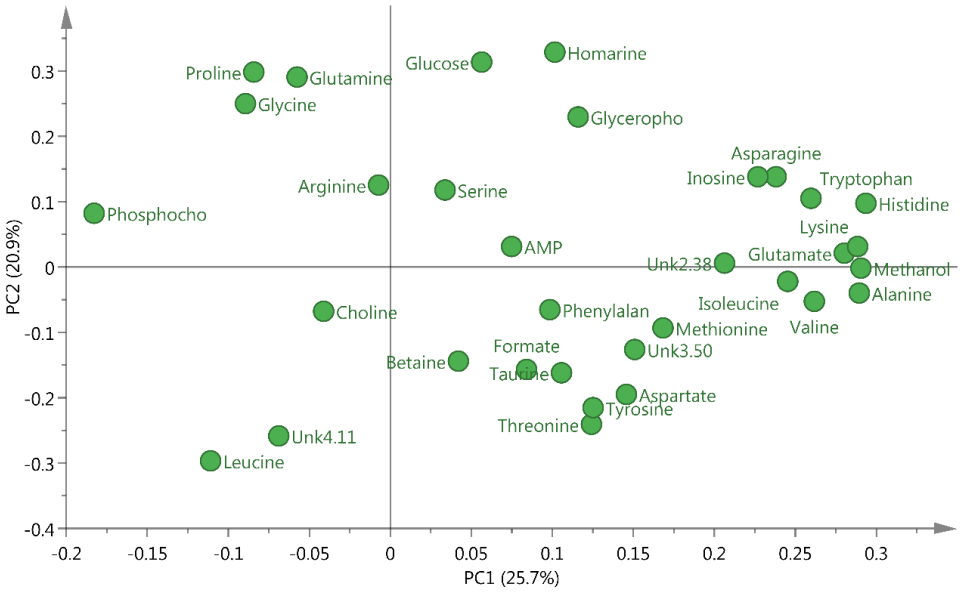

Figure 3.14. Multiblock PCA score plot (a) for control (green), 50 ppm isopropylamine (blue), 50 ppm Roundup® exposure (red). PC1 contributes 25.7% and PC2 contributes 20.9%. (b) Loading plots indicate how metabolites contribute to each component.

Table 3.5. Univariate statistics: control, 50 ppm isopropylamine (IPA), 50 ppm Roundup® p-value

Metabolites	**Con vs IPA**		**Con vs Roundup®**		**IPA vs Roundup®**	
Amino Acids	**NMR**	**GC-MS**	**NMR**	**GC-MS**	**NMR**	**GC-MS**
Alanine	0.278		0.805		0.130	
Arginine	**0.328**	0.807	0.000	0.106	**0.000**	0.071
Asparagine	0.679	0.880	0.043	0.089	0.230	0.155
Aspartate	0.170	**0.029**	0.395	**0.009**	0.562	0.284
Glutamine	0.067	0.872	**0.382**	**0.043**	**0.001**	**0.043**
Glutamate	0.414	**0.684**	0.169	**0.353**	0.323	**0.075**
Glycine	0.015	0.543	0.760	0.031	0.029	0.097
Histidine	**0.195**	0.864	0.164	0.001	**0.798**	0.000
Isoleucine	0.316	**0.853**	0.609	**0.684**	0.615	**0.315**
Leucine	0.220		0.488		0.036	
Lysine	0.611	0.443	0.385	0.016	0.894	0.001
Methionine	0.060	**0.075**	**0.382**	**0.631**	**0.328**	0.097
Phenylalanine	0.086	0.431	0.003	0.025	0.040	0.081
Proline	0.021	**0.143**	0.728	0.279	0.001	**0.019**
Serine	**0.234**	0.495	0.568	0.314	**0.105**	0.644
Threonine	0.004	0.018	0.243	0.438	0.050	0.059
Tryptophan	**0.959**	**0.853**	**0.878**	**0.035**	0.708	**0.007**
Tyrosine	0.146	0.180	0.005	0.390	0.000	0.483
Valine	0.612	**0.739**	0.614	**0.796**	0.932	**0.631**
Osmolyte						
Betaine	0.115		0.000		0.017	
Formate	0.296		0.000		0.021	
Choline	0.141		0.004		0.113	
Phosphocholine	0.473		0.791		0.135	
Glycerophosphocholine	0.023		**0.721**		**0.195**	
Sugar						
Glucose	0.019	0.082	0.580	0.002	0.013	0.028
Myo-inositol		0.451		0.000		0.000
Gadusol	0.634		0.452		0.246	
Nucleic Acid						
Inosine	**0.645**	0.611	**0.959**	0.001	**0.798**	0.001
Uracil		0.407		0.393		**0.853**
Polyamine						
Ornithine		0.031		**0.739**		**0.105**
Other						
L Dopa		0.001		0.004		0.677
Taurine	**0.161**		0.007		**0.000**	
Homarine	0.042		0.964		0.019	
Glycyl proline		0.828		0.423		0.318
N Acetyl Glucosamine		0.997		**0.393**		**0.796**
Uric Acid		**0.971**		**0.019**		0.399

***Wilcoxon Mann Whitney U-Test p-value**

*Statistically significant p-value ($p < 0.05$)

3.4. Contribution of Roundup® ingredients to metabolic perturbation

The Roundup® formulation of glyphosate contains a polyethoxylated tallow amine (POEA) surfactant and isopropylamine stabilizing salt. The exogenous biomarker, isopropylamine (1.29 ppm, d), was identified in the ^{1}H NMR spectrum of *Artemia* exposed to 50 ppm and 100 ppm Roundup®.[36] As the naupliar *Artemia* feed solely off vitelline (yolk platelets), the route of exposure for environmental contaminants is most likely not through consumption but rather through absorption or diffusion through the chitin exoskeleton. An assessment of the environmental impact quotient of active and inert pesticide ingredients found that POEA and isopropylamine have higher dermal toxicity than glyphosate.[33] The ratio of glyphosate salt to isopropylamine is expected to be 1:1, however the isopropylamine doublet at 1.29 ppm does not encompass the same spectral area in the 50 ppm Roundup® and 50 ppm isopropylamine exposure (Figure 3.13) suggesting that either the ratio is not exactly 1:1 in our store-bought Roundup® formulation or that there is less isopropylamine uptake in the absence of the POEA surfactant. PCA indicates that there is variation among the isopropylamine and Roundup® exposures, but there is an effect on many of the same metabolites which indicates that some of the effect that we see from the Roundup® formulation can be attributed to isopropylamine toxicity.[34] POEA is essential for facilitating the uptake of glyphosate by plants and was found to be toxic in certain frog, bacteria, algae, protozoa, and crustacea species.[4,12,34] There was also no significant difference in the metabolome of *Artemia* in control conditions compared to *Artemia* exposed to 100 ppm glyphosate. This leads us to surmise that POEA contributes significantly to *Artemia* toxicity either by facilitating the uptake of glyphosate and

isopropylamine though the *Artemia* chitin exoskeleton or because the surfactant is toxic on its own. Unfortunately, we were unable to obtain samples of the POEA surfactant for further testing.

3.5. Biological interpretation of endogenous metabolic perturbations

Pathway activity profiling was used to provide biological insights for metabolomics results using the PAPi R package. Global metabolite shifts from the 100 ppm Roundup® exposure were correlated with metabolic pathway information found in the Kyoto Encyclopedia of Genes and Genomes (KEGG) to predict biochemical pathways and compare their activity between the dosed and control experimental conditions.[28] A negative activity score (AS) indicates the pathway is down-regulated compared to the control group and a positive AS indicates the pathway is up-regulated. The GC-MS and NMR results were analyzed separately but similar pathways were identified in both datasets. Between GC and NMR, 87 unique pathways may have been significantly altered from Roundup® exposure with only 10 pathways identified in both NMR and GC metabolome. Many of the pathways are not likely relevant to the *Artemia* metabolome, such as alcoholism and nicotine addiction, since the KEGG includes the genome for many different organisms (Figure 3.15).

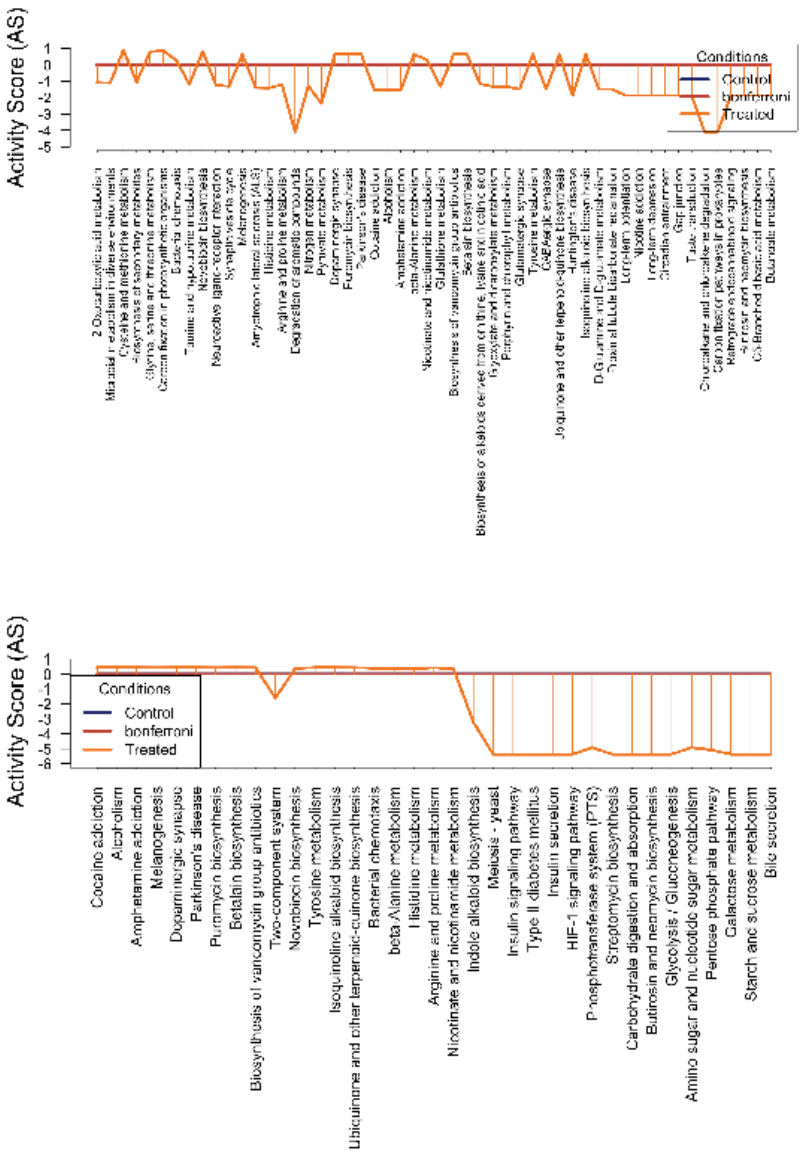

Figure 3.15. Line graph showing predicted pathways perturbed by 100 ppm Roundup® exposure (orange) from GC-MS (top) and NMR (bottom) metabolite shifts compared to the control condition (blue). A Bonferroni correction (red) was used for normalization.

The metabolites that were significantly affected ($p < 0.05$) by Roundup® exposure (100 ppm vs control) include aspartate, betaine, tyrosine, phenylalanine threonine, isoleucine, formate, gadusol, and glucose (Figure 3.10). These molecules are related to many of the metabolic pathways identified by PAPi. Although 87 different pathways were identified as significant by PAPi analysis, we will only focus on the pathways that can be explained by the measured changes to the significant variables because these were identified in our analysis as potential biomarkers of Roundup® exposure. PAPi analysis indicates that Roundup® exposure may significantly alter pathways related to amino acid metabolism, carbohydrate metabolism, energy metabolism, vitamin metabolism, and biosynthesis of secondary metabolites.

Glucose levels increased significantly with Roundup® exposure. PAPi analysis predicted down regulation of pathways involved in carbohydrate metabolism, such as glycolysis. Glucose has been identified as a cryoprotectant in earthworm species and in *Artemia franciscana,* our observations show that large amounts of glucose accumulate in cold-stressed naupliar *Artemia* (Chapter 2, section 3.4), therefore it may protect internal structures from damage from other xenobiotic stressors or adverse environmental conditions.[29,35,36] In the encysted *Artemia* embryo, energy is stored in the form of trehalose. As the embryo emerges and develops through the naupliar stages, trehalose is converted to glucose with the help of the proteolytic trehalase enzyme.[29,36,37] Trehalase and the other proteolytic enzymes that are involved in *Artemia* development are highly sensitive to environmental conditions, such as temperature, oxygen levels, and pH.[37,39]

Glucose accumulation may indicate suspended development and increased energy storage in response to the poor environmental conditions from the Roundup® exposure.

Amino acids are readily identified by NMR and GC-MS and they are abundant in *Artemia,* therefore it is reasonable that many of the pathways identified by PAPi are related to amino acid metabolism. Many of these pathways were suggested to be down-regulated at the high dose Roundup® exposure, which may indicate a protective stress response. Cysteine proteases (CP) are essential enzymes in *Artemia* for yolk utilization and growth in the early stages of pre- and post-emergence development.[29,39,40] When *Artemia* are under stress from unfavorable environmental conditions, these proteolytic enzymes may be inhibited to prevent nutrient and energy loss. Inhibition of CP may account for the overall observed decrease in metabolite concentration at higher Roundup® doses and for the down-regulation in pathways related to amino acid metabolism.

The negative activity score assigned to the degradation of aromatic compounds metabolic pathway and the positive activity score assigned to tyrosine metabolism may be related to the decreasing levels of tyrosine with Roundup® exposure. Tyrosinase is an enzyme located in crustacean hemolymph that is active during crustacean molt cycles and is important for converting tyrosine into *N*-acetyldihydroxyphenylalanine, which ultimately forms the chitin exoskeleton.[29,42] The developing *Artemia* nauplii are expected to undergo two molt cycles within the timeframe of the experiment (48 hr hatch, 48 hr exposure).[29,43,44] Upregulation of tyrosine metabolism may indicate that the *Artemia* exposed to Roundup®

were in the process of molting when they were sacrificed for the experiment. This could indicate either faster or slower development compared to the control group. Tyrosinase is also an important enzyme for wound healing in arthropods. Early juvenile crayfish exposed to glyphosate had elevated aspartate transaminase to alanine transaminase levels (ASAT:ALAT).[16] *Artemia* exposed to Roundup® may correlate to elevated ASAT:ALAT which would necessitate upregulation of tyrosinase activity to counter tissue damage. Tissue damage may be a result of isopropylamine accumulation and the reported dermal toxicity of isopropylamine and POEA.[33]

Gadusol and betaine levels decreased with Roundup® exposure. Gadusol is an interesting metabolite that is prevalent in marine organisms as a sunscreen-like molecule that absorbs UV radiation.[43–45] A study on *Artemia* in Lake Urmia has determined that the bioaccumulation of mycosporine-like amino acids, such as gadusol, is affected by salinity and UV radiation, indicating that gadusol also contributes to osmoregulatory function.[45] Considering betaine is an osmolyte and gadusol has a similar dose-dependent response (Figure 3.10), Roundup® or POEA exposure may affect osmoregulation.

Formate concentrations increase significantly with the increasing Roundup® concentration. Formate is an essential intermediate in folate-mediated one-carbon metabolism. Formate has been identified as a possible biomarker for deficiency in folate and vitamin B_{12} and downregulation of one-carbon metabolic processes.[48,49] One-carbon metabolism involves metabolic processes where methyl groups from donors, such as

serine, choline, glycine, betaine, and methionine, are interchanged and transferred using folate cofactors.[49–51] Thiamine, nicotinamide, vitamin B_{12}, pantothenate, riboflavin, pyridoxine, folic acid, biotin, and inositol have been identified as necessary vitamins for successful *Artemia* cultures.[41] Formic acid is a toxic metabolite so accumulation brought on by vitamin deficiency from Roundup® exposure may cause delayed development and lead to toxic results.[48,49]

Many of the pathways identified through PAPi are related to plant and bacteria metabolic pathways. Carbon fixation in prokaryotes, porphyrin and chlorophyll metabolism, and microbial metabolism in diverse environments were suggested to be down-regulated while bacterial chemotaxis, puromycin biosynthesis, and novobiocin biosynthesis were upregulated (Figure 3.15). These pathways are correlated to the changes measured in aromatic amino acids, such as tyrosine, L Dopa, and phenylalanine, and also gadusol. *Artemia* either obtain gadusol from the consumption of algae, from gut microbes, or through a biosynthetic pathway that has been identified in zebrafish.[44,48–50] Microbes synthesize gadusol through the shikimate pathway, which is the targeted pathway for the herbicidal activity of glyphosate so reduced expression of gadusol with increased Roundup® exposure may indicate an effect on the microbial community.[43,48,50,51] Gut microbes play an important role in the *Artemia* life cycle and the genome of this community has been sequenced.[52,53] However, the literature about the impact of Roundup® on the soil and gut microbiome has produced inconsistent and contradictory results. Some studies point to an increase in bacterial diversity and abundance, other studies report that prolonged

Roundup® exposure causes a shift in bacterial community composition towards glyphosate-tolerant species, and some studies report no effect on gut or soil microbes.[54–59] Further studies on the gut microbes in *Artemia* are necessary to elucidate the impact of Roundup® exposure.

4. Conclusion

Artemia franciscana is an aquatic crustacean that thrives in hypersaline environments. This organism is an interesting biological model due to its unique development and sensitivity to environmental conditions. We have characterized the metabolome of naupliar *Artemia* extracts using NMR and GC-MS and we have shown that *Artemia* can be used as a model species to characterize sublethal stressors for saltwater aquatic systems using environmental metabolomics. Although glyphosate was found to have no measurable effect on the metabolite profile of naupliar *Artemia*, the other commercial ingredients such as isopropylamine and the herbicidal formulation which includes isopropylamine and POEA cause metabolic perturbation at concentrations below the LD_{50} of Roundup®. Aspartate, betaine, tyrosine, phenylalanine, formate, isopropylamine, and glucose are potential bioindicators for Roundup® exposure. The effects on these metabolites correlate with impairment of carbohydrate and energy metabolism, folate-mediated one-carbon metabolism, *Artemia* molting and development, and microbial metabolism. Future work will involve using *Artemia* metabolomics to characterize the sublethal mode of action for other aquatic stressors that have been identified as emerging environmental contaminants.

5. References

1. Dugan, H. A. *et al.* Salting our freshwater lakes. *Proc. Natl. Acad. Sci.* **114,** 4453–4458 (2017).

2. Williams, W. D. Salinisation: A major threat to water resources in the arid and semi-arid regions of the world. *Lakes Reserv. Res. Manag.* **4,** 85–91 (1999).

3. Williams, W. D. Conservation of salt lakes. *Hydrobiologia* **267,** 291–306 (1993).

4. Williams, W. d. Environmental threats to salt lakes and the likely status of inland saline ecosystems in 2025. *Environ. Conserv.* 154–167 (2002).

5. Kaushal, S. S. *et al.* Increased salinization of fresh water in the northeastern United States. *Proc. Natl. Acad. Sci. U. S. A.* **102,** 13517–13520 (2005).

6. Watson, S. B. *et al.* The re-eutrophication of Lake Erie: Harmful algal blooms and hypoxia. *Harmful Algae* **56,** 44–66 (2016).

7. Martínez-Jerónimo, F. & Martínez-Jerónimo, L. Chronic effect of NaCl salinity on a freshwater strain of Daphnia magna Straus (Crustacea: Cladocera): a demographic study. *Ecotoxicol. Environ. Saf.* **67,** 411–416 (2007).

8. Schuytema, G. S., Nebeker, A. V. & Stutzman, T. W. Salinity tolerance of Daphnia magna and potential use for estuarine sediment toxicity tests. *Arch. Environ. Contam. Toxicol.* **33,** 194–198 (1997).

9. Nunes, B. S., Carvalho, F. D., Guilhermino, L. M. & Van Stappen, G. Use of the genus Artemia in ecotoxicity testing. *Environ. Pollut. Barking Essex 1987* **144,** 453–462 (2006).

10. Kerster, H. W. & Schaeffer, D. J. Brine shrimp (Artemia salina) nauplii as a teratogen test system. *Ecotoxicol. Environ. Saf.* **7,** 342–349 (1983).

11. Nitrogen Metabolism in Non-Insect Arthropods. in *Comparative Biochemistry of Nitrogen Metabolism* (ed. Campbell, JW) 299–372 (Academic Press INC, 1970).

12. Libralato, G. The case of Artemia spp. in nanoecotoxicology. *Mar. Environ. Res.* **101,** 38–43 (2014).

13. Nagato, E. G. *et al.* (1)H NMR-based metabolomics investigation of Daphnia magna responses to sub-lethal exposure to arsenic, copper and lithium. *Chemosphere* **93,** 331–337 (2013).

14. Nagato, E. G., Lankadurai, B. P., Soong, R., Simpson, A. J. & Simpson, M. J. Development of an NMR microprobe procedure for high-throughput environmental metabolomics of Daphnia magna. *Magn. Reson. Chem.* n/a-n/a (2015). doi:10.1002/mrc.4236

15. Clegg, James & Trotman, Clive. Physiological and Biochemical Aspects of Artemia Ecology. in *Artemia Basic and Applied Biology* **1,** (Kluwer Academic Publisher, 2002).

16. Lankadurai, Brian P, Nagato, Edward G & Simpson, M. J. Environmental metabolomics: an emerging approach to study organism responses to environmental stressors. *Environ. Rev.* **21,** 180–205 (2013).

17. Larive, C. K., Barding, G. A. & Dinges, M. M. NMR Spectroscopy for Metabolomics and Metabolic Profiling. *Anal. Chem.* **87,** 133–146 (2015).

18. Bundy, J. G., Ramløv, H. & Holmstrup, M. Multivariate Metabolic Profiling Using 1H Nuclear Magnetic Resonance Spectroscopy of Freeze-Tolerant and Freeze-Intolerant Earthworms Exposed to Frost. *Cryoletters* **24,** 347–358 (2003).

19. Siciliano, A., Gesuele, R., Pagano, G. & Guida, M. How Daphnia (Cladocera) Assays may be used as Bioindicators of Health Effects? *J. Biodivers. Endanger. Species* **0,** (2015).

20. OECD. *Test No. 211: Daphnia magna Reproduction Test*. (Organisation for Economic Co-operation and Development, 2012).

21. Watson, S. B., Jüttner, F. & Köster, O. Daphnia behavioural responses to taste and odour compounds: ecological significance and application as an inline treatment plant monitoring tool. *Water Sci. Technol. J. Int. Assoc. Water Pollut. Res.* **55,** 23–31 (2007).

22. Guilhermino, L., Diamantino, T., Silva, M. C. & Soares, A. M. Acute toxicity test with Daphnia magna: an alternative to mammals in the prescreening of chemical toxicity? *Ecotoxicol. Environ. Saf.* **46,** 357–362 (2000).

23. Battaglin, W. A., Kolpin, D. W., Scribner, E. A., Kuivila, K. M. & Sandstrom, M. W. Glyphosate, Other Herbicides, and Transformation Products in Midwestern Streams, 20021. *JAWRA J. Am. Water Resour. Assoc.* **41,** 323–332 (2005).

24. Battaglin, W. a., Meyer, M. t., Kuivila, K. m. & Dietze, J. e. Glyphosate and Its Degradation Product AMPA Occur Frequently and Widely in U.S. Soils, Surface Water, Groundwater, and Precipitation. *JAWRA J. Am. Water Resour. Assoc.* **50,** 275–290 (2014).

25. US EPA, O. National Primary Drinking Water Regulations. *US EPA* (2015). Available at: https://www.epa.gov/ground-water-and-drinking-water/national-primary-drinking-water-regulations. (Accessed: 1st June 2017)

26. Mercurio, P., Flores, F., Mueller, J. F., Carter, S. & Negri, A. P. Glyphosate persistence in seawater. *Mar. Pollut. Bull.* **85,** 385–390 (2014).

27. Carlisle, S. M. & Trevors, J. T. Glyphosate in the environment. *Water. Air. Soil Pollut.* **39,** 409–420 (1988).

28. Schuette, Jeff. Environmental Fate of Glyphosate.

29. Surgan, M., Condon, M. & Cox, C. Pesticide Risk Indicators: Unidentified Inert Ingredients Compromise Their Integrity and Utility. *Environ. Manage.* **45,** 834–841 (2010).

30. Howe, C. M. *et al.* Toxicity of glyphosate-based pesticides to four North American frog species. *Environ. Toxicol. Chem.* **23,** 1928–1938 (2004).

31. Theodoridis, G. *et al.* LC-MS based global metabolite profiling of grapes: solvent extraction protocol optimisation. *Metabolomics* **8,** 175–185 (2012).

32. Barding, G. A., Béni, S., Fukao, T., Bailey-Serres, J. & Larive, C. K. Comparison of GC-MS and NMR for Metabolite Profiling of Rice Subjected to Submergence Stress. *J. Proteome Res.* **12,** 898–909 (2013).

33. Gaude, E. *et al.* muma, An R Package for Metabolomics Univariate and Multivariate Statistical Analysis. *Current Metabolomics* (2013). Available at: http://www.eurekaselect.com/107837/article. (Accessed: 29th October 2017)

34. Aggio, R. B. M. Pathway Activity Profiling (PAPi): A Tool for Metabolic Pathway Analysis. in *Yeast Metabolic Engineering* 233–250 (Humana Press, New York, NY, 2014). doi:10.1007/978-1-4939-0563-8_14

35. Nakamura, K., Iwaizumi, K. & Yamada, S. Hemolymph patterns of free amino acids in the brine shrimp Artemia franciscana after three days starvation at different salinities. *Comp. Biochem. Physiol. A. Mol. Integr. Physiol.* **147,** 254–259 (2007).

36. Cartigny, B. *et al.* Quantitative determination of glyphosate in human serum by 1H NMR spectroscopy. *Talanta* **74,** 1075–1078 (2008).

37. Brausch, J. M. & Smith, P. N. Toxicity of Three Polyethoxylated Tallowamine Surfactant Formulations to Laboratory and Field Collected Fairy Shrimp, Thamnocephalus platyurus. *Arch. Environ. Contam. Toxicol.* **52,** 217–221 (2007).

38. Teets, N. M., Kawarasaki, Y., Lee, R. E. & Denlinger, D. L. Expression of genes involved in energy mobilization and osmoprotectant synthesis during thermal and dehydration stress in the Antarctic midge, Belgica antarctica. *J. Comp. Physiol. B* **183,** 189–201 (2013).

39. Warner, A. *Cell and Molecular Biology of Artemia Development*. (Springer Science & Business Media, 2013).

40. Ezquieta, B. & Vallejo, C. G. The trypsin-like proteinase of Artemia: Yolk localization and developmental activation. *Comp. Biochem. Physiol. Part B Comp. Biochem.* **82,** 731–736 (1985).

41. Shimomura, Y., Obayashi, M., Murakami, T. & Harris, R. A. Regulation of branched-chain amino acid catabolism: nutritional and hormonal regulation of activity and expression of the branched-chain alpha-keto acid dehydrogenase kinase. *Curr. Opin. Clin. Nutr. Metab. Care* **4,** 419–423 (2001).

42. Avigliano, L. *et al.* Effects of Glyphosate on Growth Rate, Metabolic Rate and Energy Reserves of Early Juvenile Crayfish, Cherax quadricarinatus M. *Bull. Environ. Contam. Toxicol.* **92,** 631–635

43. Mycosporine-Like Amino Acids and Related Gadusols: Biosynthesis, Accumulation, and UV-Protective Functions in Aquatic Organisms | Annual Review of Physiology. Available at: http://www.annualreviews.org/. (Accessed: 23rd January 2018)

44. Grant, P. T., Middleton, C., Plack, P. A. & Thomson, R. H. The isolation of four aminocyclohexenimines (mycosporines) and a structurally related derivative of cyclohexane-1:3-dione (gadusol) from the brine shrimp, Artemia. *Comp. Biochem. Physiol. Part B Comp. Biochem.* **80,** 755–759 (1985).

45. Khosravi, S., Khodabandeh, S., Agh, N. & Bakhtiarian, M. Effects of salinity and ultraviolet radiation on the bioaccumulation of mycosporine-like amino acids in Artemia from Lake Urmia (Iran). *Photochem. Photobiol.* **89,** 400–405 (2013).

46. Lamarre, S. G., Morrow, G., Macmillan, L., Brosnan, M. E. & Brosnan, J. T. Formate: an essential metabolite, a biomarker, or more? *Clin. Chem. Lab. Med.* **51,** 571–578 (2013).

47. Fox, J. T. & Stover, P. J. Chapter 1 Folate-Mediated One-Carbon Metabolism. in *Vitamins & Hormones* **79,** 1–44 (Academic Press, 2008).

48. Brotherton, C. A. & Balskus, E. P. Biochemistry: Shedding light on sunscreen biosynthesis in zebrafish. *eLife* **4,** e07961 (2015).

49. Osborn, A. R. *et al.* De novo synthesis of a sunscreen compound in vertebrates. *eLife* **4,**

50. Carreto, J., Carignan, M. & Montoya, N. *A high-resolution reverse-phase liquid chromatography method for the analysis of mycosporine-like amino acids (MAAs) in marine organisms*. **146,** (2005).

51. MetaCyc gadusol biosynthesis. Available at: https://biocyc.org/. (Accessed: 22nd January 2018)

52. Riddle, M. R., Baxter, B. K. & Avery, B. J. Molecular identification of microorganisms associated with the brine shrimp Artemia franciscana. *Aquat. Biosyst.* **9,** 7 (2013).

53. Nougue, O., Gallet, R., Chevin, L.-M. & Lenormand, T. Niche Limits of Symbiotic Gut Microbiota Constrain the Salinity Tolerance of Brine Shrimp. *Am. Nat.* **186,** 390–403 (2015).

54. Imparato, V., Santos, S. S., Johansen, A., Geisen, S. & Winding, A. Stimulation of bacteria and protists in rhizosphere of glyphosate-treated barley. *Appl. Soil Ecol.* (2016).

55. Pizarro, H. *et al.* Glyphosate input modifies microbial community structure in clear and turbid freshwater systems. *Environ. Sci. Pollut. Res. Int.* **23,** 5143–5153 (2016).

56. Allegrini, M., Gomez, E. del V. & Zabaloy, M. C. Repeated glyphosate exposure induces shifts in nitrifying communities and metabolism of phenylpropanoids. *Soil Biol. Biochem.* **105,** 206–215 (2017).

57. Newman, M. M. *et al.* Changes in rhizosphere bacterial gene expression following glyphosate treatment. *Sci. Total Environ.* **553,** 32–41 (2016).

58. Riede, S. *et al.* Investigations on the possible impact of a glyphosate-containing herbicide on ruminal metabolism and bacteria in vitro by means of the 'Rumen Simulation Technique'. *J. Appl. Microbiol.* **121,** 644–656 (2016).

59. Zabaloy, M. C., Carné, I., Viassolo, R., Gómez, M. A. & Gomez, E. Soil ecotoxicity assessment of glyphosate use under field conditions: microbial activity and community structure of Eubacteria and ammonia-oxidising bacteria. *Pest Manag. Sci.* **72,** 684–691 (2016).

TDCIPP exposure affects *Artemia* growth and osmoregulation

CHAPTER FOUR

I would like to acknowledge Professor David C Volz for his help developing an *Artemia* imaging system and for the use of his microscope for the work presented in this chapter.

Abstract

Environmental monitoring has demonstrated widespread occurrence of the flame retardant tris(1,3-dichloro-2-propyl) phosphate (TDCIPP), raising concerns about its impact on aquatic life.[1–4] Using ^{1}H NMR and GC-MS metabolomics and 20-day body length experiments, we have determined that chronic exposure to environmentally relevant concentrations of TDCIPP affects *Artemia* development. Acute exposure (48 hr) to 50 % of the LC_{50} did not affect *Artemia* body length but it did elicit a metabolic change. TDCIPP exposure triggered a significant response in the level of expression in metabolites of the osmolyte class, namely betaine, phosphocholine, gadusol, and taurine, and also glycerol and trehalose, metabolites that are essential osmoprotectants in extremophile species.[5] Other pathways that may be perturbed by TDCIPP exposure include one carbon, glycine, serine, and threonine, and glycerophospholipid metabolism.

1. Introduction

Flame retardants are chemicals that are added to manufactured materials to prevent combustion and delay the spread of fire after ignition.[4] The production and use of flame retardants is continually increasing due to strict fire safety standards for furniture and appliances, such as the California Technical Bulletin (TB) 117. In 2015 the worldwide consumption of flame retardants reached a volume of 2.49 million tonnes, valued at $6.29 billion. By 2025, it is projected that use will reach 4.0 million tonnes and value $11.96 billion.[24] Brominated flame retardants (BFR), such as pentabromodiphenyl ether (PBDE), were one of the most widely used classes of flame retardants until they were phased out in the EU and US due to being highly persistent, bioaccumulative, and toxic.[4,25,26] In addition to detection in human breast milk, adipose tissue, and serum, a number of flame retardants have been detected in aquatic animals including orcas, indicating their potential to accumulate in the aquatic environment.[27]

Tris(1,3-dichloro-2-propyl) phosphate (TDCIPP, Figure 4.1) is a high-production volume organophosphate-based flame retardant (OPFR). TDICPP is widely used in automotive industry for upholstery and seat cushions; it is also used in household textiles like curtains.[25] In the 1960s-70s, it was used in children's pajamas until mutagenic properties were reported.[25] It is applied as an additive flame retardant, meaning it is not chemically bonded to the surface of the product, which may result in easy release to the environment. OPFRs have been detected in household air, dust, clothes, and baby products, but TDCIPP is the most commonly detected.[7,28] It was found that many OPFRs end up in aquatic

systems, such as the Columbia River, from laundry wastewater.[28] OPFRs had been accepted as a safe alternative to BFRs, but recent studies have raised concerns about the safety of some of these formulations. TDCIPP was voluntary phased out of production by ICL Industrial Products in 2015, but many products with TDCIPP are still in use.[3,4,25] Growing use of flame retardants and increasing evidence of environmental prevalence has created a concern for the effects of exposure in humans and other animals.

Studies have shown that TDCIPP exposure may cause endocrine disruption, neurotoxicity, carcinogenicity, infertility and developmental toxicity.[4,6,8–12] TDCIPP exposure has been linked to infertility in women and decreased fecundity in zebrafish and *Daphnia magna*. Bis(1,3-dichloro-2-propyl) phosphate (BDCIPP), the primary metabolite of TDCIPP, was detected in 87% of urine samples from a study of participants undergoing IVF treatment. The level of BDCIPP was correlated with decreased pregnancy success.[9] Exposure did not cause birth defects in rats exposed to TDCIPP during pregnancy but it did affect the growth and development of *Daphnia magna* and zebrafish embryos.[4,10,14–16] It has been identified as an endocrine disruptor in chicken and zebrafish embryos and the MCF-7 human breast cancer cell line.[29–31]

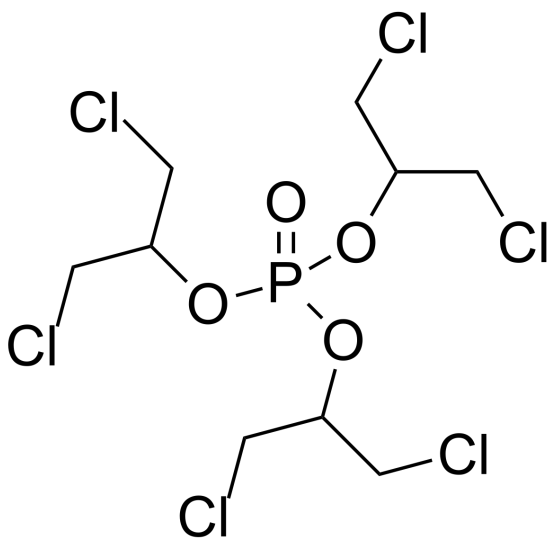

Figure 4.1. Structure of tris(1,3-dichloro-2-propyl) phosphate (TDCIPP)

The effects of TDCIPP have not been well studied in natural waters. Studies report detectable levels of TDCIPP in natural water systems ranging from 9 to 353 ngL^{-1}, but little is known of the impact on aquatic life.[1–3] Risk assessments from the WHO and EU report that TDCIPP is very persistent in the environment and that fish rapidly metabolize this compound.[4,11,12] However, studies with zebrafish embryos and *Daphnia magna* report that TDCIPP affects development.[1,6,12–15] Studies with zebrafish embryos have used developmental and genotoxicity assays and targeted genomics analysis to determine that TDCIPP affects DNA methylation during embryonic development.[12–14] Han et al. used *Daphnia magna* as a model to analyze fecundity, growth, and gene transcription and determined that TDCIPP decreased fecundity and body length and affected pathways related to protein synthesis, endocytosis, and metabolism.[10] While targeted genomics studies with aquatic species have revealed much about TDCIPP toxicity, untargeted studies may provide further insight into global metabolic effects. In order to further elucidate the mode of action of TDCIPP in aquatic organisms, we hope to complement these targeted studies using untargeted ^{1}H NMR and GC-MS metabolomics analysis of the effects of TDCIPP exposure on the *Artemia* metabolome.

Artemia franciscana is a saltwater aquatic crustacean that is native to inland saltwater lakes but is often used for ecotoxicity assays representing the marine environment. They are closely related to *Daphnia magna*; therefore, we hypothesized that TDCIPP would similarly affect *Artemia* growth and metabolism. However, TDCIPP may trigger an entirely different metabolic response in saltwater compared to freshwater aquatic species.

The metabolic response of *Artemia* was measured using ^{1}H NMR and GC-MS metabolomics. NMR is a rapid, robust, and quantitative technique that requires minimal sample preparation.[17–19] GC-MS requires derivatization, but its low limit of detection and well-established libraries make it a great complementary technique.[20,21] We monitored changes to *Artemia's* small-molecule metabolite profile before and after exposure to TDCIPP. We then applied data reduction and statistical analysis to extract meaningful information about the potential mode of action and identify biomarkers of stress corresponding to TDCIPP exposure.

The aims of this study were to determine the effect of TDCIPP exposure on *Artemia* mortality and growth, characterize the metabolic response of *Artemia* to chronic and acute TDCIPP exposure, and apply Principal Component Analysis to identify small molecule biomarkers of exposure and metabolic pathways perturbed by chronic and acute TDCIPP exposure.

2. Materials and Methods

2.1. Determination of TDCIPP LC_{50}

To evaluate toxicity, we determined the lethal concentration of TDCIPP for 50% of the naupliar *Artemia* population (LC_{50}) in a 48 hr exposure. *Artemia* cysts were hatched in 300 mL tanks containing 35 g/L sea salt with 0-300 μM TDCIPP (Sigma Aldrich, St. Louis, MO) and 0.1% dimethylsulfoxide (DMSO, EMD, Burlington, MA). During the hatch period, the cysts were exposed to constant light and aeration. Nauplii were transferred to

aquariums containing 20 mL salt water with TDCIPP with 20 *Artemia* per aquarium and 10 aquariums per dose exposed to a 16:8 hr light:dark cycle. The number of living and dead shrimp in each aquarium was recorded to calculate the mortality rate. Mortality plots were constructed in GraphPad Prism 7 (San Diego, CA).

2.2. Sublethal acute exposures to 20 µM TDCIPP for metabolomics analysis

Artemia cysts (1 oz) were hatched for 24 hr in 1 L control sea salt solution or 20 µM TDCIPP with 0.1% DMSO-d_6 (Sigma Aldrich) in sea salt solution. The hatched nauplii were divided into 6 aquariums containing 300 mL media, 3 control and 3 treated, with constant aeration and a 16:8hr light cycle. After the 48 hr exposure, the nauplii were transferred to 2 mL microvials (3 samples per aquarium, 9 samples per dose) and flash frozen in liquid nitrogen. The protocols for metabolite extraction and NMR and GC-MS sample preparation can be found in Chapter 2, sections 2.2.1, 2.3.3, and 2.3.6.

2.3. Sublethal chronic exposure to 0.5 µM TDCIPP for imaging

Artemia cysts (1 oz) were hatched for 48 hr in 1 L control sea salt solution or 0.5 µM TDCIPP (0.1% DMSO) in sea salt solution. The hatched nauplii were divided into 20 aquariums, 10 treated and 10 control, containing 20 mL media and 20 nauplii per aquarium. The media was exchanged every 48 hr. After the first 96 hr of exposure, we began feeding algae to the *Artemia* by adding it to the fresh media. The number of living and dead *Artemia* was recorded each time the media was exchanged and the dead *Artemia* were removed

from the aquarium. At the end of the 20-day exposure, the living *Artemia* were fixed with 4% paraformaldehyde (Spectrum, Gardena, CA) and 10 mM phosphate-buffered saline.

2.4. *Artemia* body length measurements

Fixed *Artemia* were stained with Rhodamine 6-G (JT Baker Chemical Co, Phillipsburg, NJ) and transferred to a well-plate, one specimen per well. For the 48 hr experiment, a 384 well plate was used, and for the 20-day exposure a 96 well plate was used. An image acquisition protocol was optimized on an ImageXpress Micro (IXM) XLS Widefield High-Content Screening System equipped with MetaXpress 6.0.3.1658 (Molecular Devices, Sunnyvale, CA). A 4X objective (384-well plate) or a 2X objective (96-well plate) and TRITC filter cube was used to acquire one frame per entire well. Images were then used to measure body length.[22] *Artemia* images were exported to ImageJ (National Institute of Health, Bethesda, MD) and the body length measurements were taken from the head to the tail along the thorax and abdomen. An average body length (in pixels) was calculated for control and exposed *Artemia*.

2.5. Sublethal chronic exposure to 0.5 µM TDCIPP for metabolomics analysis

Artemia cysts (1 oz) were hatched for 48 hrs in 1 L control (0.1% DMSO-d_6) sea salt or 0.5 µM TDCIPP (0.1% DMSO-d_6) sea salt. The hatched nauplii were divided into 6 aquariums containing 300 mL media, 3 control and 3 treated, with constant aeration and a 16:8 hr light cycle. The nauplii were transferred to fresh solution and also fed algae after the first 96 hr of the exposure period. After 1 week, the nauplii were transferred to 2 mL

microvials (3 samples per aquarium, 9 samples per dose) and flash frozen in liquid nitrogen. Metabolite extracts were prepared for NMR and GC-MS metabolomics analysis.

2.6. Metabolomics statistical methods

Multivariate analysis was performed using SIMCA 14.1.[48] NMR and GC-MS results for each sample were combined in SIMCA for multiblock PCA. Univariate statistical analysis was performed using GraphPad Prism. Boxplots were constructed, and the normalized data was processed using one-way ANOVA with Tukey's post-hoc.

3. Results and Discussion

Artemia were subjected to acute and chronic TDCIPP stress to identify effects on growth and development and metabolic perturbation resulting from exposure.

3.1. Determination of the LC_{50} for 48 hr TDCIPP exposure

The LC_{50} for 48 hr TDCIPP exposure was determined to be 37.1 ± 1.3 μM TDCIPP in 0.1% DMSO (Figure 4.2). An initial 48 hr period involved hatching the *Artemia* cysts in TDCIPP media. This lethal concentration is approximately 10 times less toxic than the reported toxicities for *Daphnia magna* or fish species.[4] This value was determined to identify a starting point for studying sublethal TDCIPP stress in *Artemia*. The remaining exposures were conducted at 20 μM and 0.5μM TDCIPP for acute and chronic stress, respectively.

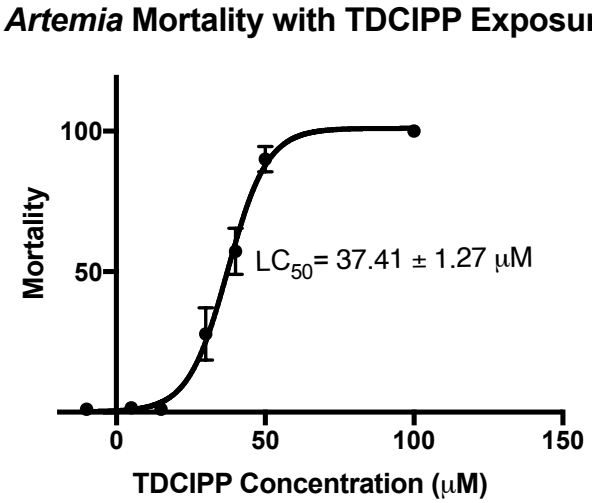

Figure 4.2. *Artemia* mortality over a 48 hr TDCIPP exposure ranging from 0-300 μM. The LC_{50} was determined to be 37.4 ± 1.3 μM.

3.2. Impact of acute and chronic TDCIPP exposure on *Artemia* mortality and development

Acute exposure to 0-20 μM TDCIPP caused no significant difference in *Artemia* body length (Figure 4.3). However, chronic exposure to 0.5 μM TDCIPP decreased body length significantly (Figure 4.4). Mortality was also higher in TDCIPP-exposed *Artemia* over the 20-day exposure. 109 of the initial 200 *Artemia* were still living on day 20 of the exposure, 41 from the TDCIPP exposures and 68 from the control group. Initially, we set out to test chronic exposure to 5 μM TDCIPP, but we observed 100% mortality for TDCIPP within 14 days. Naupliar and juvenile *Artemia* were identified in both the control and treated specimens (Figure 4.5), but there were 10% more juvenile *Artemia* in the control condition which likely contributed to a larger body length average in the controls versus the *Artemia* exposed to TDCIPP. This suggests that the ability of *Artemia* to molt may be impeded by TDCIPP exposure.

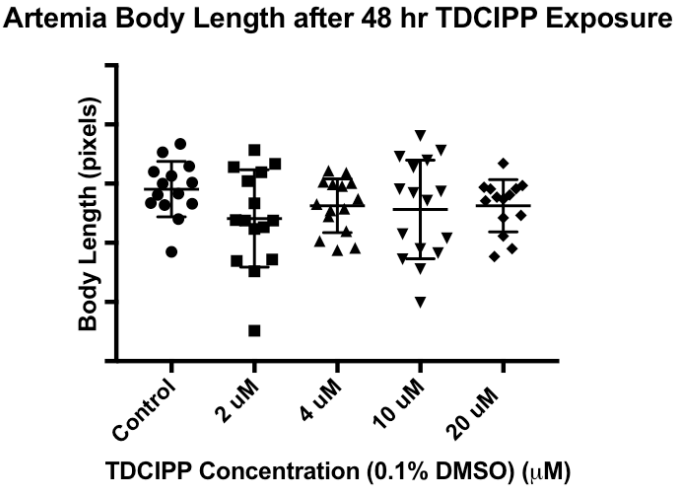

Figure 4.3. *Artemia* body length after 48 hr TDCIPP exposure. No statistically significant difference in body length was measured between doses.

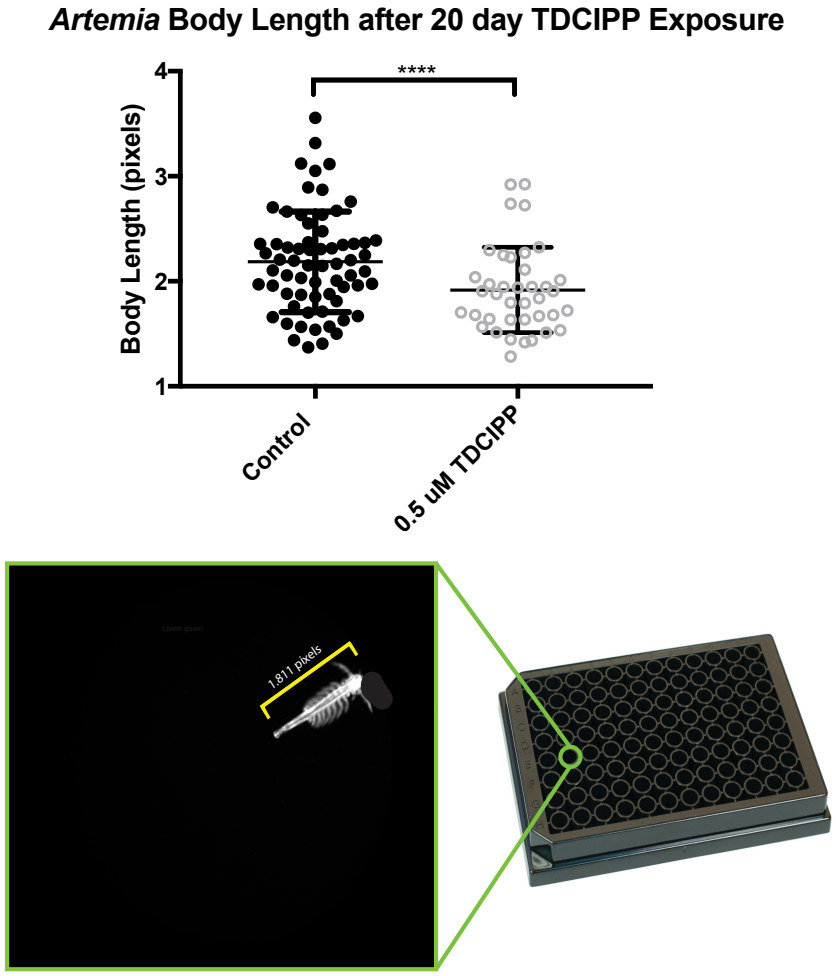

Figure 4.4. Body length measurements for 20-day Artemia exposed to 0.5 µM TDCIPP. The body length for TDCIPP exposed *Artemia* are significantly shorter than the body length for Control Artemia (**** $p<0.0001$). Body length measurements (measured in pixels) are taken from the top of the head to the tip of the tail.

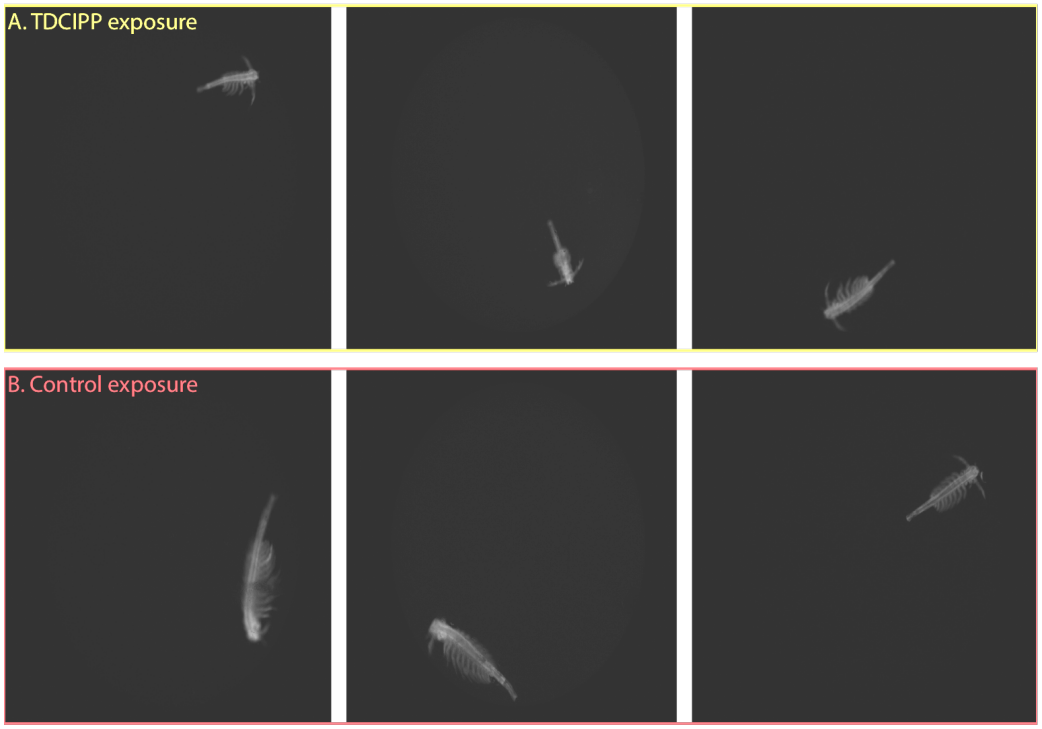

Figure 4.5. Sample images of fixed *Artemia* taken after 20-day exposure. (A) *Artemia* exposed to 0.5 uM TDCIPP. All of the specimens are in the naupliar stage. (B) *Artemia* in control conditions. Two specimens are juveniles and 1 is a nauplii.

3.3. NMR and GC-MS metabolite profiles

The *Artemia* metabolite profile was reported in Chapter 2. Representative ^{1}H NMR spectra of extracts of control and TDCIPP-exposed *Artemia* are shown in Figure 4.6. The spectra are labeled to highlight the resonances of several significant metabolites including gadusol, glycine, taurine, homarine, and glucose. A representative GC-MS TIC is shown in Figure 4.7, with the C24 internal standard and triclosan surrogate peaks labeled. Not all metabolites reported in the *Artemia* metabolome in Chapter 2 were quantified in this study due to the smaller number and age of the specimens. The extracts of 1-week old *Artemia* have slight differences in metabolite profile because they have started feeding on algae rather than relying on their own yolk stores. These samples are smaller because older specimens are harder to collect in large quantities. To collect the 48 hr nauplii, we take advantage of their phototaxis behavior which causes them to swim towards light sources to find food. When a point source of light is shone through the aquarium, the nauplii crowd around the light, making it easy to pipet the nauplii as a dense mass. 1-week old nauplii are developing new sight and swimming appendages that do not rely on a bright light source, so they are less likely to exhibit this behavior, as a result, it is harder to collected dense samples of *Artemia* as they age.

3.4. Multi- and Univariate statistical analysis of TDCIPP-induced metabolite shifts

Metabolite data represented by peak-fitted ^{1}H NMR resonances and GC-MS ion count, normalized by total spectral area were used for multi- and univariate analysis. The ^{1}H NMR

resonances and GC-MS peaks used for analysis are reported in Table 2.2. The variance in metabolite expression for Multiblock-PCA of acute and chronic TDCIPP exposure is best shown by PC 1 (36.4%) and PC 2 (17.4%) (Figure 4.8a). Principal component analysis of acute and chronic TDCIPP exposure indicates variance in metabolite expression for each condition. The loading plot (Figure 4.8b) indicates that inosine, glutamine, methionine, glutamate, taurine, and homarine contribute to the separation of the samples from the 1-week exposure along PC1 and betaine, choline, lysine, arginine, and alanine contribute to the segregation of the 48 hr exposure samples along PC1. Glucose, ornithine and taurine contribute to the separation of the TDCIPP exposure samples along PC1 and threonine, tryptophan, and leucine contribute to the segregation of the control group along PC1. Loading plots are hard to interpret when there are many overlapping metabolites, so univariate analysis was used to clarify the individual metabolite changes for these four groups and to evaluate the significance of those changes.

One-Way ANOVA identified metabolites that increased or decreased significantly ($p < 0.05$) from the acute (48 hr, 20 μM TDCIPP) and chronic (0.5 μM TDCIPP, 1 week) exposures. For the acute exposure, aspartate, phenylalanine, glycine, phosphocholine, betaine, taurine, gadusol, glycerol and trehalose levels increased, while methanol, methionine, and leucine levels decreased. For the chronic exposure, the levels of glucose, phosphocholine, betaine, taurine, and gadusol increased, whereas tyrosine, serine, threonine, aspartate, glutamate, phenylalanine, glycerol, trehalose, and glycerophosphocholine decreased (Figure 4.9). For NMR, glycerophosphocholine was not

detected in 48 hr-old *Artemia* and resonance overlap by glycerol prevented the determination of glycine for 1-week old *Artemia*. For GC, taurine was not detected in 48 hr old *Artemia* and methionine was not detected in 1-week old *Artemia*. There remains one unidentified peak in the GC chromatogram at 15.59 min that did change significantly from the 1-week exposure. Unfortunately, we were not successful in determining the compound responsible for this feature.

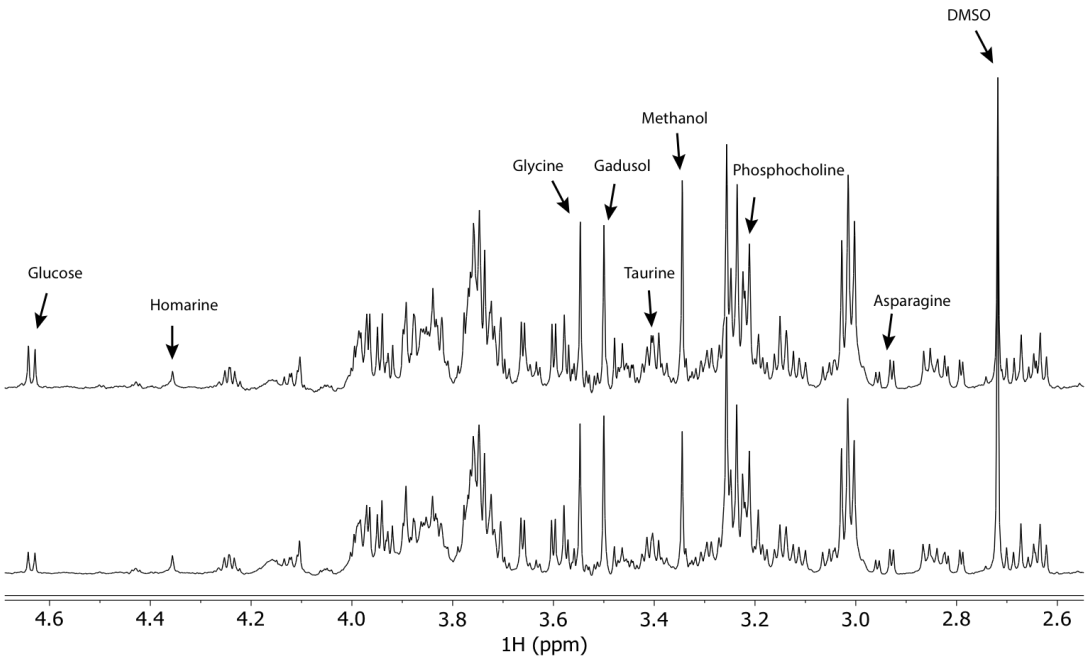

Figure 4.6. Representative ^{1}H NMR spectra showing the region from 2.60 to 4.65 ppm for *Artemia* extracts for 48 hr exposure to TDCIPP (bottom) and control (top). The labeled resonances indicate metabolites that were affected significantly by exposure. The vehicle DMSO was also identified in the spectra.

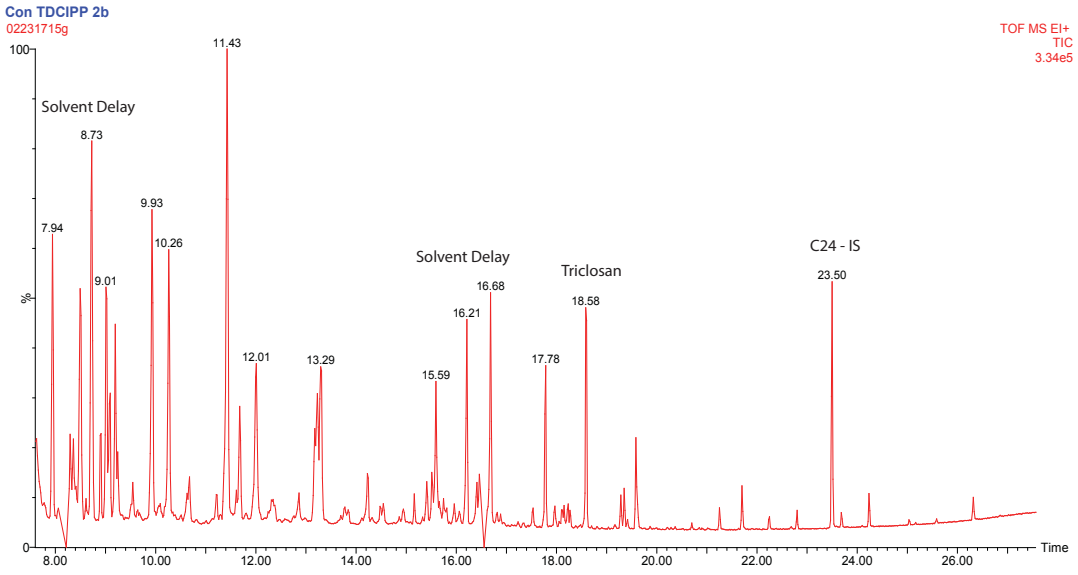

Figure 4.7. GC-MS TIC of an extract of control *Artemia* labeled with the internal standards and solvent delay regions.

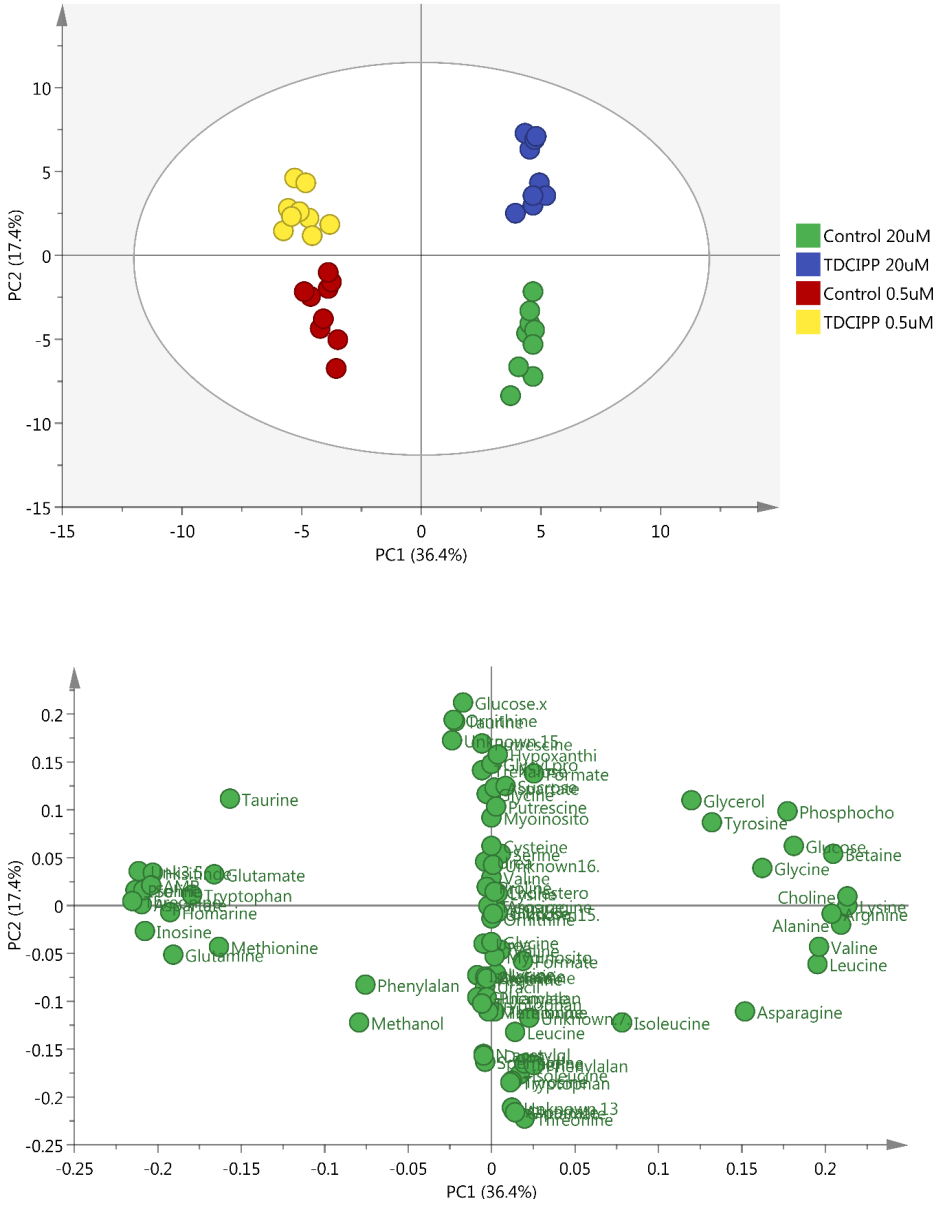

Figure 4.8. Multiblock-PCA Score Plot (a) for acute (48 h, 20 µM) and chronic (1 week, 0.5 µM) exposure to TDCIPP. The variance between control and TDCIPP-stressed *Artemia* is best explained by PC 1 (36.4 %) and PC 2 (17.4 %). The loading plot (b) indicates how metabolites contribute to each component. Data points are labeled by metabolite identity as determined by GC-MS and ^{1}H NMR.

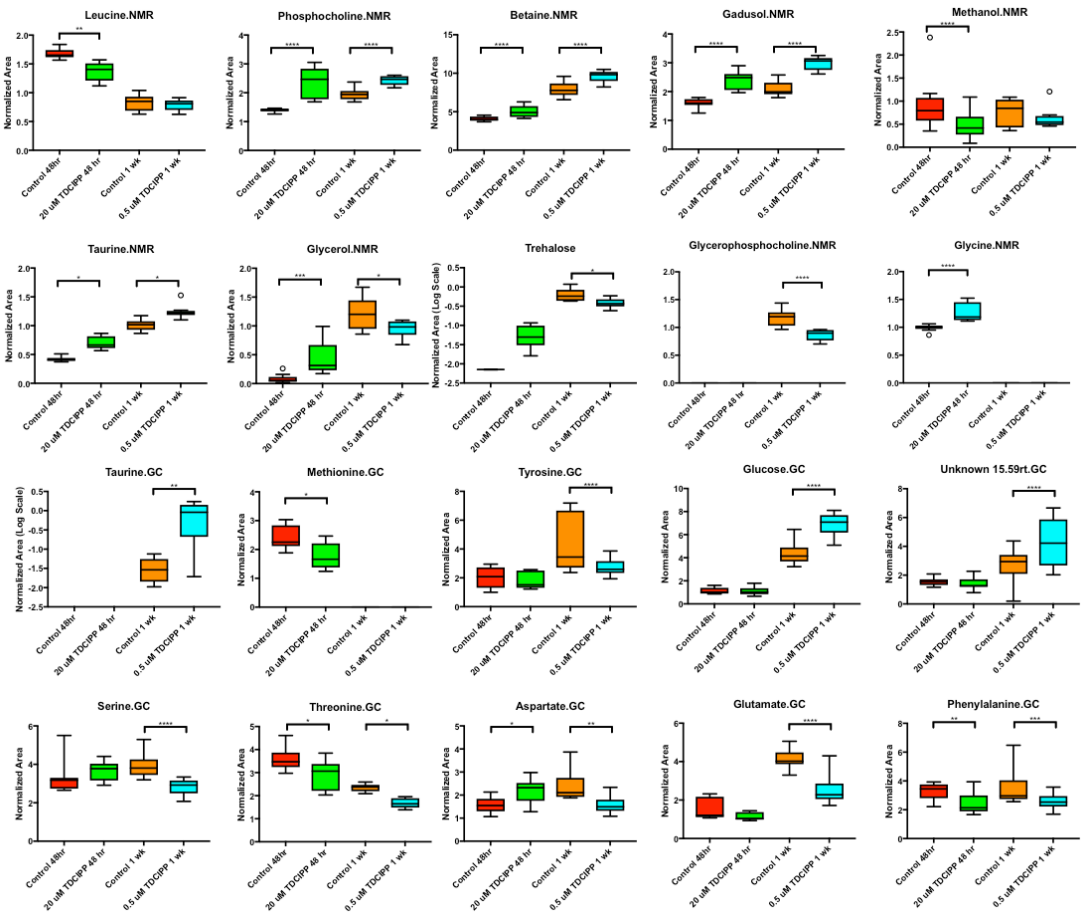

Figure 4.9. Univariate box plots indicating how significant variables change with acute (20 µM, 48 hr) and chronic (0.5 µM, 1 wk) TDCIPP exposure. Variables are labeled by metabolite name and instrument used for detection. One-way ANOVA with Tukey's HSD was used to identify significant differences between control and dosed. (*p<0.1, **p<0.01, ***p<0.001**** p<0.0001)

3.5. Biochemical interpretation of acute and chronic TDCIPP exposure

In agreement with studies on zebrafish and *Daphnia magna*, our study finds that chronic exposure to sublethal TDCIPP impedes *Artemia* development.[10,13,14] Over a 20-day exposure, we observed increased mortality and decreased body length in TDCIPP-exposed *Artemia* compared to the control group. We were unable to collect samples for metabolomics analysis of the 20-day exposure due to low survival of specimens in both the control and treated conditions; however, samples taken after 1 week of exposure to 0.5 μM TDCIPP reveal metabolic perturbation that may lead to the decreased growth that was observed downstream. During the 20-day exposure, each specimen was expected to molt several times in order to grow and develop to adulthood. The lack of growth in the TDCIPP-exposed *Artemia* may indicate an effect on the molt cycle. Acute exposure (48 hr) to 20 μM TDCIPP did not have an impact on *Artemia* body length but the organisms are not expected to molt during this time.

Dormant *Artemia* cysts are preloaded with all the necessary components for initial life stages.[32,33] These cysts are also impervious to environmental conditions and will only activate once conditions are suitable for hatching.[32,34] Our cysts were hatched in media containing TDCIPP, and the hatch rate was unaffected by TDCIPP exposure. Studies with zebrafish indicate that TDCIPP affects early embryogenesis.[14] Embryogenesis was already completed by the time the cyst was formed, so embryogenesis was not affected in *Artemia*.[33,35] In a study with *Daphnia magna*, fecundity and growth were affected in subsequent generations following maternal TDCIPP exposure, which may result from an

impact on *Daphnia* embryogenesis.[6] It would be interesting to study the effects of maternal TDCIPP exposure on the reproduction (oviparity vs ovoviparity), growth rate, fecundity, and metabolome of future generations to elucidate the impact on embryogenesis in *Artemia*.

Acute exposure did have considerable impact on the expression of several metabolites, namely osmolytes such as glycerol, betaine, phosphocholine, taurine, gadusol, and trehalose. Acute exposure to TDCIPP may cause osmotic stress, which triggers increased expression of glycerol and trehalose. Glycerol and trehalose play an important role in *Artemia* for both development and stress protection.[5,32,33,36] In the encysted *Artemia* embryo, energy is stored in the form of trehalose. As the embryo emerges and develops through the naupliar stages, trehalose is converted to glucose with the help of the proteolytic trehalase enzyme.[5,32,35] Trehalase and the other proteolytic enzymes that are involved in *Artemia* development are highly sensitive to environmental conditions, such as temperature, oxygen levels, and pH. Trehalose also serves as a substrate for the synthesis of glycerol and glycogen. In some extremophile organisms, glycerol and trehalose serve as osmoprotectants and cryoprotectants to protect internal structures of the organism from extreme conditions, such as temperature, dehydration, and salinity. In contrast, glycerol, trehalose, and glycerophosphocholine were decreased in *Artemia* experiencing chronic exposure to TDCIPP. Glucose levels increased with chronic TDCIPP exposure, indicating that trehalose may have been converted to glucose at higher rates.

Phosphocholine, taurine, gadusol, and betaine levels were increased with chronic and acute exposure to TDCIPP. Gadusol is a mycosporin-like amino acid (MAA) that has been categorized as a natural sunscreen in marine species because it absorbs UV radiation.[26–30] MAAs are also related to salinity, thermal, and desiccation stress.[27,28] A study with *Artemia* in Lake Urmia observed bioaccumulation of MAAs with UV radiation and salinity stress; therefore, we hypothesize that gadusol bioaccumulation in *Artemia* is related to an effect on osmoregulation.[31] *Artemia* is adapted to hypersaline environments and is an excellent osmoregulator; therefore, the high expression of these metabolites is likely a contributing factor in the considerably higher lethal concentration for TDCIPP in *Artemia* versus *Daphnia* and fish.[2,4,10,32]

The metabolites that were significantly ($p < 0.05$) affected by TDCIPP exposure are also involved in one carbon metabolism, glycine, serine, and threonine metabolism, and glycerophospholipid metabolism. Glycerophosphocholine and glycerol decreased while phosphocholine increased. This indicates that glycerophospholipid metabolism may be downregulated in chronic TDCIPP exposure, which may result in an alteration to energy storage mechanisms and lipid structures.[4,10,43] Lipid metabolism was also perturbed in chicken embryos exposed to TDCIPP.[30] One carbon metabolism involves metabolic processes where methyl groups are transferred using folate cofactors to many biochemical pathways.[44,45] Methanol is an intermediary of one carbon metabolism and downregulation of this metabolite may indicate perturbation of this pathway in response to oxidative stress.[44,45] Phosphocholine is a precursor to choline in the glycine, serine, threonine,

metabolic pathway and betaine is another intermediary, the measured changes to these metabolites may be an indication that combating TDCIPP-induced stress is an energy priority over amino acid metabolism.[44,46] These pathways and metabolites are interrelated and the measured patterns in metabolite shifts may indicate a perturbation in *Artemia* experiencing acute or chronic TDCIPP exposure.

4. Conclusion

Environmental monitoring has demonstrated widespread occurrence of TDCIPP, raising concerns about the impact on aquatic life. Using ^{1}H NMR and GC-MS metabolomics and 20-day body length experiments, we have determined that chronic exposure to environmentally relevant concentrations of TDCIPP affects *Artemia* development, which may indicate an effect on their molt cycle. TDCIPP exposure triggered a significant response in the expression in metabolites of the osmolyte class, namely betaine, phosphocholine, gadusol, and taurine and also glycerol and trehalose, metabolites that are essential osmoprotectants in extremophile species. Other pathways that may be perturbed by TDCIPP exposure include one carbon, glycine, serine, and threonine, and glycerophospholipid metabolism.

5. References

1. van der Veen, I. & de Boer, J. Phosphorus flame retardants: Properties, production, environmental occurrence, toxicity and analysis. *Chemosphere* **88,** 1119–1153 (2012).

2. Environmental Health Perspectives – Exposure to TDCPP Appears Widespread.

3. Stapleton, H. M. *et al.* Identification of Flame Retardants in Polyurethane Foam Collected from Baby Products. *Environ. Sci. Technol.* **45,** 5323–5331 (2011).

4. Feng, L. *et al.* Levels of Urinary Metabolites of Organophosphate Flame Retardants, TDCIPP, and TPHP, in Pregnant Women in Shanghai. *J. Environ. Public Health* **2016,** (2016).

5. Environmental Health Perspectives – Urinary Concentrations of Organophosphate Flame Retardant Metabolites and Pregnancy Outcomes among Women Undergoing in Vitro Fertilization.

6. Li, H. *et al.* Effects of Tris(1,3-dichloro-2-propyl) Phosphate on Growth, Reproduction, and Gene Transcription of Daphnia magna at Environmentally Relevant Concentrations. *Environ. Sci. Technol.* **49,** 12975–12983 (2015).

7. European Union. *Tris[2-chloro-1-(chloromethyl)ethyl]phosphate (TDCP)*. (2008).

8. WHO. *EHC 209: Flame Retardants: Tris-Chloropropyl)Phosphate and Tris-(2-chloroethyl)phosphate*. (1998).

9. Andresen, J. A., Grundmann, A. & Bester, K. Organophosphorus flame retardants and plasticisers in surface waters. *Sci. Total Environ.* **332,** 155–166 (2004).

10. Hu, M. *et al.* Regional distribution of halogenated organophosphate flame retardants in seawater samples from three coastal cities in China. *Mar. Pollut. Bull.* **86,** 569–574 (2014).

11. Zhong, M. *et al.* Occurrences and distribution characteristics of organophosphate ester flame retardants and plasticizers in the sediments of the Bohai and Yellow Seas, China. *Sci. Total Environ.* **615,** 1305–1311 (2018).

12. Volz, D. C. *et al.* Tris(1,3-dichloro-2-propyl) phosphate Induces Genome-Wide Hypomethylation Within Early Zebrafish Embryos. *Environ. Sci. Technol.* (2016). doi:10.1021/acs.est.6b03656

13. McGee, S. P., Cooper, E. M., Stapleton, H. M. & Volz, D. C. Early Zebrafish

Embryogenesis Is Susceptible to Developmental TDCPP Exposure. *Environ. Health Perspect.* **120,** 1585–1591 (2012).

14. Kupsco, A., Dasgupta, S., Nguyen, C. & Volz, D. C. Dynamic Alterations in DNA Methylation Precede Tris(1,3-dichloro-2-propyl)phosphate-Induced Delays in Zebrafish Epiboly. *Environ. Sci. Technol. Lett.* **4,** 367–373 (2017).

15. Dasgupta, S. *et al.* Tris(1,3-dichloro-2-propyl) phosphate disrupts dorsoventral patterning in zebrafish embryos. *PeerJ* **5,** e4156 (2017).

16. Lankadurai, Brian P, Nagato, Edward G & Simpson, M. J. Environmental metabolomics: an emerging approach to study organism responses to environmental stressors. *Environ. Rev.* **21,** 180–205 (2013).

17. Larive, C. K., Barding, G. A. & Dinges, M. M. NMR Spectroscopy for Metabolomics and Metabolic Profiling. *Anal. Chem.* **87,** 133–146 (2015).

18. Bundy, J. G., Ramløv, H. & Holmstrup, M. Multivariate Metabolic Profiling Using 1H Nuclear Magnetic Resonance Spectroscopy of Freeze-Tolerant and Freeze-Intolerant Earthworms Exposed to Frost. *Cryoletters* **24,** 347–358 (2003).

19. Yozzo, K. L., McGee, S. P. & Volz, D. C. Adverse outcome pathways during zebrafish embryogenesis: a case study with paraoxon. *Aquat. Toxicol. Amst. Neth.* **126,** 346–354 (2013).

20. Clegg, James & Trotman, Clive. Physiological and Biochemical Aspects of Artemia Ecology. in *Artemia Basic and Applied Biology* **1,** (Kluwer Academic Publisher, 2002).

21. *Artemia: Basic and Applied Biology | Th.J. Abatzopoulos | Springer*.

22. Warner, A. *Cell and Molecular Biology of Artemia Development*. (Springer Science & Business Media, 2013).

23. Teets, N. M., Kawarasaki, Y., Lee, R. E. & Denlinger, D. L. Expression of genes involved in energy mobilization and osmoprotectant synthesis during thermal and dehydration stress in the Antarctic midge, Belgica antarctica. *J. Comp. Physiol. B* **183,** 189–201 (2013).

24. Yancey, P. H. Organic osmolytes as compatible, metabolic and counteracting cytoprotectants in high osmolarity and other stresses. *J. Exp. Biol.* **208,** 2819–2830 (2005).

25. Verduyn, C., Postma, E., Scheffers, W. A. & van Dijken, J. P. Physiology of

Saccharomyces cerevisiae in anaerobic glucose-limited chemostat cultures. *J Gen Microbiol* **136,** (1990).

26. Carreto, J. I. & Carignan, M. O. Mycosporine-Like Amino Acids: Relevant Secondary Metabolites. Chemical and Ecological Aspects. *Mar. Drugs* **9,** 387–446 (2011).

27. Brotherton, C. A. & Balskus, E. P. Biochemistry: Shedding light on sunscreen biosynthesis in zebrafish. *eLife* **4,** e07961 (2015).

28. Osborn, A. R. *et al.* De novo synthesis of a sunscreen compound in vertebrates. *eLife* **4,**

29. Grant, P. T., Middleton, C., Plack, P. A. & Thomson, R. H. The isolation of four aminocyclohexenimines (mycosporines) and a structurally related derivative of cyclohexane-1:3-dione (gadusol) from the brine shrimp, Artemia. *Comp. Biochem. Physiol. Part B Comp. Biochem.* **80,** 755–759 (1985).

30. Arbeloa, E. M., Uez, M. J., Bertolotti, S. G. & Churio, M. S. Antioxidant activity of gadusol and occurrence in fish roes from Argentine Sea. *Food Chem.* **119,** 586–591 (2010).

31. Khosravi, S., Khodabandeh, S., Agh, N. & Bakhtiarian, M. Effects of salinity and ultraviolet radiation on the bioaccumulation of mycosporine-like amino acids in Artemia from Lake Urmia (Iran). *Photochem. Photobiol.* **89,** 400–405 (2013).

32. KEGG PATHWAY: Glycerophospholipid metabolism - Reference pathway. Available at: http://www.genome.jp/kegg-bin/show_pathway?map=map00564&show_description=show. (Accessed: 10th January 2018)

33. Fox, J. T. & Stover, P. J. Chapter 1 Folate-Mediated One-Carbon Metabolism. in *Vitamins & Hormones* **79,** 1–44 (Academic Press, 2008).

34. Codd, G. A., Dijkhuizen, L. & Tabita, F. R. *Autotrophic Microbiology and One-Carbon Metabolism*. (Springer Science & Business Media, 2012).

35. Lamarre, S. G., Morrow, G., Macmillan, L., Brosnan, M. E. & Brosnan, J. T. Formate: an essential metabolite, a biomarker, or more? *Clin. Chem. Lab. Med.* **51,** 571–578 (2013).

36. Locasale, J. W. Serine, glycine and the one-carbon cycle: cancer metabolism in full circle. *Nat. Rev. Cancer* **13,** 572–583 (2013).

Metabolic perturbations from PFOS and PFOA in *Artemia franciscana*

CHAPTER FIVE

Abstract

Perfluoroalkyl salts (PFAS) are fluorinated organic compounds that have many industrial uses due to their strong carbon-fluorine bonds that repel oil and water. Perfluorooctane sulfonic acid (PFOS) and perfluorooctanoic acid (PFOA) are types of PFAS that have been widely detected in the environment from industrial application and also as a breakdown produce of larger PFAS compounds. PFOS and PFOA are persistent contaminants that cause significant health concerns such as liver damage and infertility. PFOA is universally detected in human serum and breastmilk and PFOS bioaccumulates in fatty tissue of terrestrial and marine species. Uptake of these compounds has been measured in many higher trophic level aquatic species, raising concerns about the impact of biomagnification in the food chain. As *Artemia franciscana* is often used as a feedstock for fish farms, the effect of PFOS and PFOA on this lower trophic level organism may play an important role on transfer through the food chain. Using NMR and LC-MS environmental metabolomics, the *Artemia* metabolic profile was measured after a 68 hour exposure to sublethal PFOS and PFOA. It was determined that the 48 hr LC_{50} for *Artemia franciscana* is 20 ± 9 ppm for PFOS and approximately 60 ppm for PFOA. Exposures were conducted at the LC_5 and LC_{25} of both compounds, 59 metabolites were significantly affected by PFOS and 64 metabolites were affected by PFOA. Using pathway analysis with the PAPi R package, 35 metabolic pathways in the KEGG database were perturbed by PFOS and 116 pathways were perturbed by PFOA. Affected pathways were related to fatty acid oxidation and lipid

metabolism, protein synthesis, oxidative stress, and carbohydrate metabolism. PFOA also affected these mechanisms in addition to nitrogen and methane metabolism and the TCA cycle.

1 Introduction

Perfluorooctane sulfonic acid (PFOS) and perfluorooctanoic acid (PFOA) are fully fluorinated, organic compounds that are a type of perfluoroalkyl salt (PFAS). These compounds have been widely used for industrial applications such as surfactants, fire-fighting foam, and pesticides because of their ability to repel oil and water.[1] These products work well in these applications due to the highly strong and stable nature of the carbon-fluorine bond.[2] However, this stable nature has also created a health and environmental challenge.

PFOS and PFOA are detected in drinking water, indoor dust, food, environmental media, and biota in many parts of the world.[3] PFASs are extremely persistent in the environment and have the potential to bioaccumulate in humans and animals.[1] Toxicological studies indicate that PFAS exposure may be linked to preeclampsia, liver damage, increase in serum lipids, thyroid disease, infertility, asthma, decreased birth weight, and decreased antibody response to vaccines.[4] The primary route of exposure for humans is through the consumption of water and food contaminated with PFASs.[2,3] In 2002, the main producer of PFOS and PFOA, 3M, voluntarily phased out production of these compounds after a study found PFAS in samples from the global blood bank.[1–3] PFOS was added to the Persistent Organic Pollutant list at the Stockholm Convention in 2009.[1] In 2015, the EPA

lowered the drinking water standards for PFASs from 400 ppt to 70 ppt. Counties in Southern California had to take some of their water sources permanently offline in order to meet this new standard.[5] A report by the EPA and the Agency for Toxic Substances and Disease Registry released in June 2018 suggested decreasing the maximum risk level even further, but the exact recommendations have not been released.[4,6,7]

PFAS are globally distributed in our aquatic environment, with PFOS and PFOA being the most thoroughly studied in this class. PFOS or PFOA was detected in rivers in 100% of samples tested from 41 cities in North America, Asia, and Europe.[8] PFOA is more soluble in water and has a lower bioaccumulation potential than PFOS, so it is usually reported at higher levels in water.[8–10] PFOS is more often detected in sediment and biota.[11,12] Although the highest levels are reported in freshwater surrounding industrial areas, PFOS and PFOA are also reported in open-ocean and coastal seawater samples in the Atlantic Ocean, Pacific Ocean, and smaller seas like the Japan Sea and the Labrador Sea.[11] PFOS and PFOA have been detected in aquatic species and PFOS has been detected in higher trophic level species, including porpoises and turtles, indicating that it biomagnifies up the food chain.[9,12]

Biomagnification in the food chain is a result of the concentration of toxins in an organism as a result of ingesting other plants or animals in which the toxins bioaccumulate. *Daphnia* are small planktonic crustacea that are low on the food chain and are an important keystone species in many freshwater ecosystems. They are often used for toxicology testing to

identify aquatic stressors.[13] Several PFAS compounds, including PFOS and PFOA, were shown to bioaccumulate in *Daphnia magna*.[14] In separate studies, PFOS was also shown to affect the individual fitness of daphnids, inhibit metabolic enzymes, and decrease reproduction.[14–16] The consumption of daphnids or other low trophic level organisms is likely the source of PFAS detected in fish organs, such as tilapia, carp, and salmon.[17–19] *Artemia franciscana* is another important crustacean that is found in saltwater lakes. This organism is a globally important food source for aquacultures. The effects of PFAS on *Artemia* have not been reported, but if PFOS and PFOA have a similar effect on *Artemia* as *Daphnia*, it could be a human health concern. Due to the widespread detection of PFOS and PFOA in all environmental media, it is important to understand the effects of these contaminants for both the health of aquatic ecosystems and humans.

This study uses nuclear magnetic resonance (NMR) and liquid chromatography – mass spectrometry (LC-MS) to evaluate changes in *Artemia* metabolite levels in response to exposure to PFOS and PFOA. NMR is a rapid, robust, and quantitative technique that requires minimal sample preparation and has well-established libraries for metabolite identification.[20,21] In this dissertation, the *Artemia* metabolome was characterized using untargeted NMR and GC-MS, and at the start of this project, the UCR Metabolomics Core became available. LC-MS methods at the Core were utilized to explore the different metabolites that can be identified due to its broad range of metabolite classes, low limits of detection, and high mass resolution.[22–24] LC lacks standardized acquisition methods and robust libraries, so targeted methods compiled by the Core were utilized for this study. The

complementarity of NMR and LC-MS produce a more comprehensive analysis of the *Artemia* metabolome than could be obtained with either method alone. [25,26] The aims of this study are to characterize the molecular response of *Artemia* to sub-lethal PFOS and PFOA exposure and to identify metabolites and metabolic pathways that are perturbed by exposure using multivariate and univariate statistical analysis and biochemical pathway analysis.

2 Materials and Methods

2.1 PFOS and PFOA LC_{50} determination

Artemia cysts were hatched into nauplii according to the protocol from chapter 2 section 2.1.2. Perfluorooctane sulfonic acid (PFOS, Sigma Aldrich) and perfluorooctanoic acid (PFOA, Sigma Aldrich) dose solutions were prepared from a 1000 ppm stock solution in 35 g/L saltwater at pH 8.0. To determine the lethal concentration for 50% of the *Artemia* population (LC_{50}) of PFOS and PFOA, 20 nauplii were transferred into 50 mL jars for 3 replicates per dose. Initial range finding experiments tested PFOA concentrations of 0, 0.100, 1.00, 10.0, 100, and 1000 ppm and PFOS concentrations of 0, 0.100, 1.00, 10.0, and 250 ppm. The number of living and dead shrimp was recorded after 48 and 96 hr. The range finding exposures were followed by triplicate exposures with 0, 15.6, 31.2, 62.5, 125, 250, 500, and 1000 ppm PFOA and 0, 0.781, 1.56, 3.12, 6.25, 12.5, 25.0, 50.0, 100 ppm PFOS. The 48 hr LC_{50} was determined from mortality plots using the Dose-response -Stimulation: [Agonist] vs response (Variable slope – 4 parameters) non-linear regression in GraphPad Prism 7.0 (San Diego, CA).

2.2 PFOS and PFOA exposures

PFOS and PFOA metabolomics exposures were conducted at approximately 25% (LC_{25}) and 5% (LC_5) of the lethal concentration for both PFOS and PFOA, as determined by mortality plots. The LC_{25} for PFOA was 30.0 ppm and the LC_5 was 6.00 ppm. The LC_{25} for PFOS was 10.0 ppm and the LC_5 was 2.00 ppm.

Artemia cysts (1 oz) were hatched for 48 hrs in 1 L control sea salt. The hatched nauplii were divided into 9 aquariums containing 300 mL media: 3 control, 3 LC_{25}, and 3 LC_5, with constant aeration and a 16:8 hr light cycle. After 68 hrs, 10 samples were taken for each treatment. For each sample, nauplii were transferred to 2 mL screw top microvials and flash frozen in liquid nitrogen. The samples were thawed, and the media exchanged 3x with ultrapure water. The samples were re-frozen and lyophilized to dryness then stored at – 80 °C.

2.3 Sample preparation

Sample preparation for LC-MS analysis was performed at the UCR Metabolomics Core. Freeze-dried brine shrimp pellets were weighed in 1.5 mL Eppendorf tubes. The extraction solvent was added (1 mL per 10 mg shrimp) and samples were vortexed for 20 min, sonicated for 15 min, then vortexed for an additional 60 min. Samples were then centrifuged for 15 min at 4° C at 16,000 × g. The supernatant was transferred to a 2 mL glass vial and analyzed by LC-MS.

2.4 Metabolomics measurements

Untargeted metabolomics analysis was performed using ^{1}H NMR and targeted metabolomics measurements was performed using LC-MS in the UCR Metabolomics Core. The procedure for ^{1}H NMR acquisition can be found in chapter 2, section 2.3.3, and the procedure for ^{1}H NMR processing can be found in chapter 2, section 2.4.2.1. The NMR buffer contained 0.26 mM fluoxetine (Sigma Aldrich) at pH 7.61 as a chemical shift reference. ^{1}H NMR spectra were acquired with a Bruker Avance NMR spectrometer (Billerica, MA) equipped with a 5mm BBO broadband tunable probe operating at 599.88 MHz.

2.4.1 LC-MS analysis, targeted metabolomics

Targeted metabolomics of polar, primary metabolites was performed on a TQ-XS triple quadrupole mass spectrometer (Waters) coupled to a I-class UPLC system (Waters). Separations were carried out on a ZIC-pHILIC column (2.1 x 150 mm, 5 µM) (EMD Millipore). The mobile phases were (A) water with 15 mM ammonium bicarbonate adjusted to pH 9.6 with ammonium hydroxide and (B) acetonitrile. The flow rate was 200 µL/min and the column was held at 50° C. The injection volume was 2 µL. The gradient was as follows: 0 min, 90% B; 1.5 min, 90% B; 16 min, 20% B; 18 min, 20% B; 20 min, 90% B; 28 min, 90% B.

The MS was operated in selected reaction monitoring mode. Source and desolvation temperatures were 150° C and 500° C, respectively. Desolvation gas was set to 1000 L/hr

and cone gas to 150 L/hr. Collision gas was set to 0.15 mL/min. All gases were nitrogen except the collision gas, which was argon. Capillary voltage was 1 kV in positive ion mode and 2 kV in negative ion mode. System stability was monitored by analyzing a quality control sample (generated by pooling together equal volumes of all sample extracts) throughout the sample set. To prevent artifactual metabolite changes between groups, samples were analyzed in random order.

2.5 Data analysis

At the UCR Metabolomics Core, LC-MS data were processed and peaks integrated with the open source software Skyline (University of Washington)[27]. Statistical analyses and data visualizations were performed and generated in MetaboAnalyst except for principal component analysis, which was performed using SIMCA (Umetrics).[28–31] Univariate analysis was conducted between the high dose and control to identify metabolites that change significantly. A t-test was run between the mean of the control and the high dose to determine the p-value. For non-normally distributed data, the Wilcoxon-Mann Whitney U-test was performed. The fold change was calculated. One-way ANOVA with Fisher's LSD post hoc was performed for all three treatments and metabolites with p-value < 0.05 were identified along with the intertreatment significance. Heatmaps were also constructed in MetaboAnalyst for all three treatments. The heatmaps are plotted with Euclidean distance, Ward clustering and show with group averages and the colors correspond to z-score.[30]

Pathway analysis was conducted using the PAPi R package with metabolites that have a designated KEGG code. Ophthalmic acid, lauroyl-carnitine and glutarylcarnitine were excluded from analysis because they do not have designated KEGG codes. Glucose-6-phosphate was used in place of hexose-phosphate, trehalose was used in place of disaccharide hexose, glucose was used in place of hexose monomer, and ribose 5 phosphate was used in place of pentose phosphate. Metabolic pathway charts were constructed from MetaboAnalyst pathway analysis using the *Danio rerio* (zebrafish) reference metabolome. The figures are labeled by KEGG code. Metabolites that are present in the dataset are outlined in red and metabolites that are missing are outlined in blue. Box plots were constructed using GraphPad Prism 7.03.

3 Results and Discussion

3.1 PFOS and PFOA toxicity

Due to the widespread detection of PFOS and PFOA in aquatic systems and the importance of *Artemia* in aquacultures, we aimed to determine the toxic effects of these compounds. PFOS range-finding exposures estimated the approximate 48 hr LC_{50} as 15 ± 34 ppm and 96 hr LC_{50} as 0.5 ± 0.3 ppm. An exposure with a narrower range of concentrations identified the PFOS LC_{50} as 20 ± 9 ppm (Figure 5.1a). The reported 48 hr LC_{50} for PFOS is 37.36 ± 6.64 ppm for *D. magna* and 17.95 ± 3.22 ppm for *M. macrocopa*.[32] Our estimated lethal concentration is closer to *M. macrocopa*, which is a freshwater water flea like *D. magna*.

PFOA mortality was variable for the exposures, this prevented the calculation of precise LC_{50} values because the nonlinear regression did not fit the data. PFOA range-finding exposures identified the approximate 48 hr LC_{50} as ~130 ppm with an undetermined standard error and 96 hr LC_{50} as 44 ± 42 ppm. An exposure with a narrower range of concentrations was still statistically ambiguous and the PFOA LC_{50} was identified as ~ 60 ppm. The reported 48-hour LC_{50} for PFOA is 476.52 ± 101.2 ppm for *D. magna* and 199.51 ± 45.62 ppm for *M. macrocopa*. The NOEC for *M. macrocopa* is 62.5 ppm and LOEC is 125 ppm.[32] The PFOA result that was extrapolated from our data is much lower than reported values for these other similar water fleas. It is unexpected that the difference in mortality should be so great between *D. magna* and *Artemia*, considering *Artemia* is more tolerant of environmental toxins such as TDCIPP and adapted to harsh conditions.

Variable mortality results were observed for both PFOS and PFOA. The exposures were repeated three times, and each repetition yielded different results. Since the goal of the project was to study sublethal effects, it was decided that an exact LC_{50} was not essential. We ultimately combined these results to obtain averaged data. We hypothesize that some of this variability is due to the physicochemical nature of PFAS compounds. PFAS self-assemble into micelles at the critical micelle concentration (CMC). Below the CMC, monomers act as single molecules and above this point they aggregate into micelles. Micelle formation affects solubility. PFOA is soluble in water (~3.4 g/L) and its' CMC is 25 mM (~10 g/L).[33–35] PFOS is less soluble in water (550 mg/L) and its CMC is 8 mM (~4 g/L) than PFOA.[33–35] Micelle formation depends on many conditions such as fluorocarbon

chain length, the type and concentration of ions present, and temperature.[33] It is unclear to what extent the saltwater and temperature in the *Artemia* aquarium affects the solubility and micelle formation of these compounds, but both factors are known to decrease CMC and solubility for fluorocarbon surfactants.[33–35] There remains a lack of available physicochemical and kinetic information about PFAS compounds because it is challenging to obtain experimental data due to their surface active properties.

Other factors that may play a role in the variability in the dataset is the potential for partitioning, adsorption, and bioaccumulation. The octanol:water partition coefficient (log K_{ow}) for PFOS (2.45) and PFOA (1.92) indicates that these compounds are likely to partition into a non-aqueous phase or adsorb to a surface, such as tissue from *Artemia* or the walls of the aquarium.[33,35] Bioaccumulation factors for rainbow trout livers indicate that PFOS (5.40 x 10^3 L/kg) and PFOA (8.0 L/kg) have the tendency to biaccumulate.[12,33] PFOS and PFOA were measured in *Artemia* extracts using LC-MS. The 498.93 m/z ion in the *Artemia* extracted ion chromatogram corresponds to the same mass in the PFOS reference standard (Figure 5.2). Increased levels were measured at 2.00 ppm and 10.0 ppm PFOS. The 412.96 m/z ion from the extracted ion chromatogram corresponds to PFOA. Increased levels were measured at 6.00 and 30.0 ppm PFOA (Figure 5.3). This may indicate that both compounds have the potential for bioaccumulation in *Artemia*, however, further quantitative studies are needed to determine that uptake is occurring.

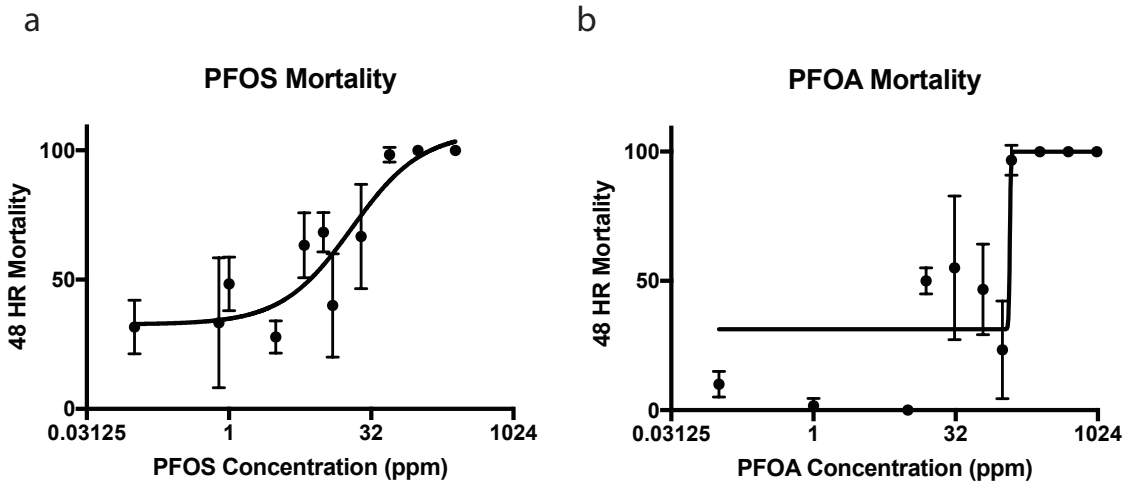

Figure 5.1. *Artemia* mortality plots after 48 hr exposure to PFOS (a) and PFOA (b) (n = 20 *Artemia* per sample). Concentrations in ppm are transformed by Log2. (a) PFOS LC_{50} = 20 ± 9 ppm. (b) LC_{50} was ~60 ppm as determined by non-linear regression. This regression did not fit the data, so standard error was not determined.

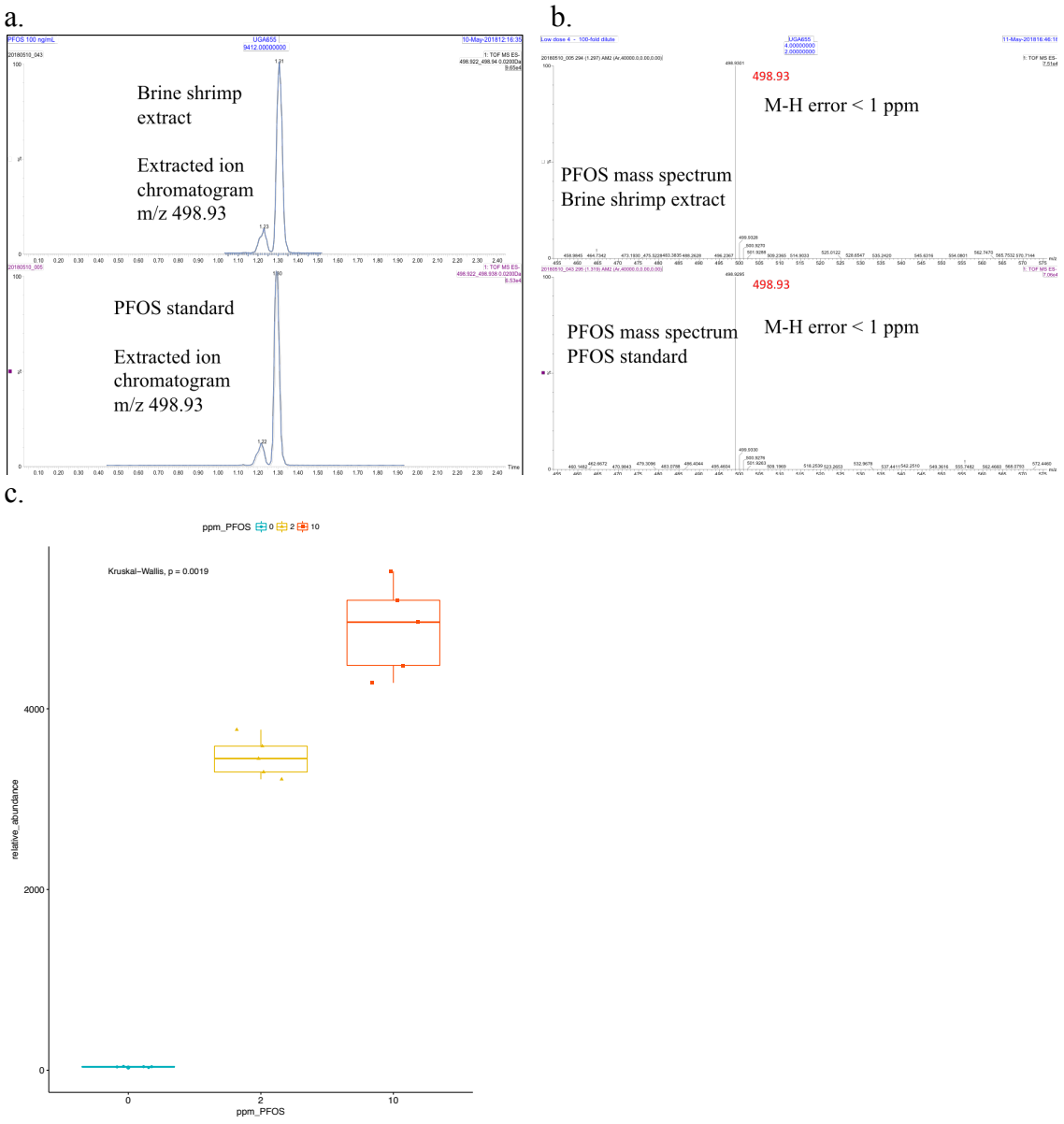

Figure 5.2. Identification of PFOS in *Artemia* extracts. (a) extracted ion chromatogram of Artemia sample and PFOS standard showing the same ion at m/z 498.93. (b) Mass spectrum of PFOS molecular ion with M-H less than -1 ppm mass error. (c) Box plots of PFOS relative abundance for the control (blue), 2.00 ppm (yellow), and 10.0 ppm (orange) doses.

a.

b.

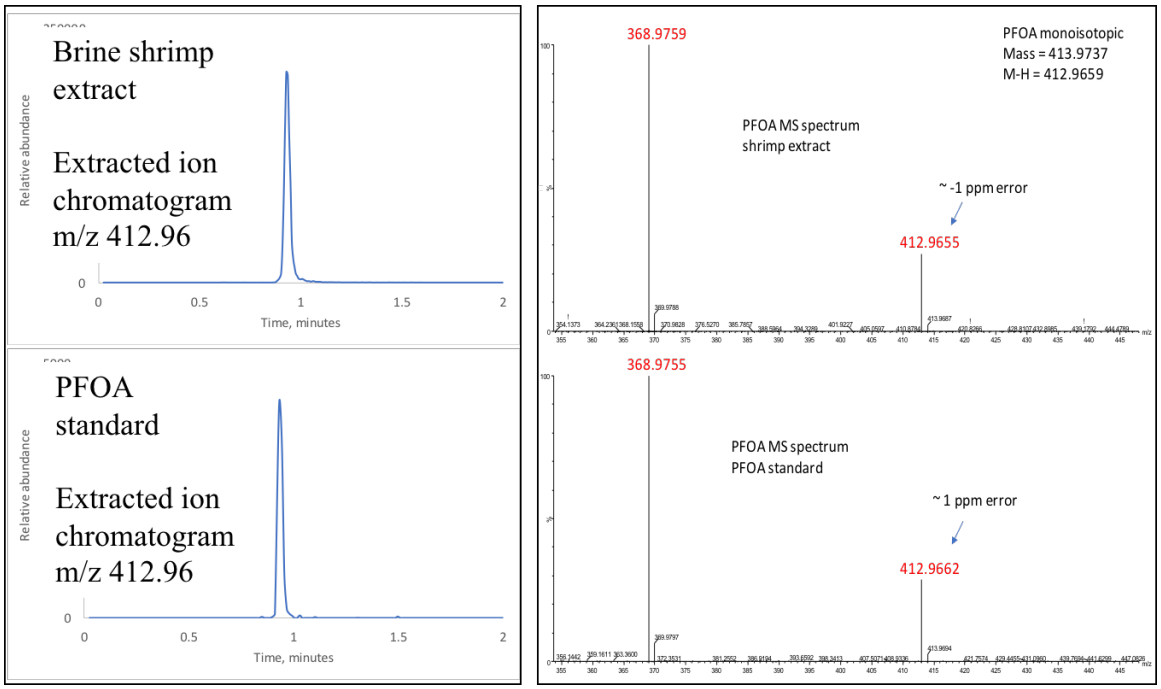

c.

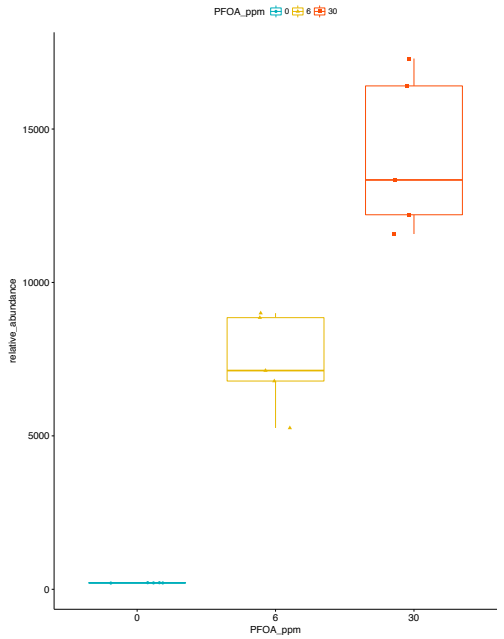

Figure 5.3. Identification of PFOA in *Artemia* extracts. (a) extracted ion chromatogram of *Artemia* sample and PFOA standard showing the same ion at m/z 412.96. (b) Mass spectrum of PFOA molecular ion and base peak with M-H less than -1 ppm mass error. (c) Box plots of PFOA relative abundance for the control (blue), 6.00 ppm (yellow), and 30.0 ppm (orange) doses.

3.2 Metabolites identified by LC-MS and NMR

LC-MS analysis of *Artemia* extracts led to the identification and relative quantitation of 100 metabolites for PFOS and 86 metabolites for PFOA (Table 5.1). These compounds were identified by their retention time, a precursor ion, and a product ion, from either positive or negative mode targeted metabolomics methods. These metabolites include amino acids, amino acid derivatives, polyamines, nucleotides, nucleoside, sugars, and sugar phosphates. Of the 29 metabolites quantified by NMR, asparagine, formate, methanol, gadusol and homarine were not identified by LC-MS. Asparagine was removed from the targeted method because contaminants interfered with its retention time and identifying ions. The molecular weight of formate and methanol was too low for the mass spectrometer, this is the case for several small organic acids and alcohols.[26] Gadusol and homarine are not common metabolites and a standard was not available to add to the targeted library.

Several metabolites were not able to be differentiated between their isomers by LC-MS. These include citrate and isocitrate, disaccharide hexose, pentose phosphate, and hexose monomer. Based on our NMR results, the disaccharide hexose might be trehalose and the hexose monomer might be glucose. NMR is advantageous for identifying isomers because it can differentiate these structures based on j-coupling and chemical shift. However, MS is able to differentiate many isomers based on fragmentation patterns in MS^2 and MS^3.[20,36] The identity of metabolites measured between PFOS and PFOA LC-MS analysis also differed. Carnosine, cysteinesulfinic acid, folic acid, glutathione (GSH), glutathione

disulfide (GSSG), lauroyl-carnitine, N-acetylalanine, NADP, N-methylglutamate, thymidine, glutarate, glycerol-3-phosphate, hexose phosphate, phosphoenolpyruvate, and succinate were only detected in PFOS samples. UMP was only detected in PFOA samples.

Although NMR is invaluable for metabolome characterization due to its strength for untargeted applications and structural elucidation of unknown metabolites, as was demonstrated by the elucidation of gadusol in chapter 2, section 2.3.5, LC-MS will be the primary focus of the remaining work. Due to the large number of primary and secondary metabolites that had not been previously elucidated by NMR or GC-MS there is more information from which to draw biochemical mode of action hypotheses from metabolic perturbations. However, more variables also add more complexity to the statistical analysis and there is no streamlined procedure for interpreting these large datasets.

Table 5.1. Metabolites quantified by LC-MS for PFOS and PFOA

Metabolite	RT	precursor	product	ionization	PFOA*	PFOS*
4-guanidinobutyric acid	12.5	146.0	86.0	Positive	Q	Q
4-Hydroxyproline	12.0	132.0	68.0	Positive	Q	Q
5-aminovaleric acid	12.6	118.0	101.0	Positive	Q	Q
5-hydroxylysine	15.8	163.0	128.0	Positive	Q	Q
Acetylcarnitine	8.9	204.0	85.0	Positive	Q	Q
Adenine	6.0	136.0	119.0	Positive	Q	Q
Adenosine	6.4	268.0	136.0	Positive	Q	Q
ADP	13.6	428.0	136.0	Positive	Q	Q
ADP ribose	12.8	560.0	348.0	Positive	Q	Q
Alanine	12.1	90.0	44.0	Positive	Q	Q
Allantoin	11.2	157.0	114.0	Negative	Q	Q
alpha-ketoglutarate	12.6	145.0	101.0	Negative	Q	Q
Aminoadipate	12.5	162.0	98.0	Positive	Q	Q
AMP	12.3	348.0	136.0	Positive	Q	Q
Arginine	16.4	175.0	70.0	Positive	Q	Q
Argininosuccinic acid	13.3	291.0	70.0	Positive	Q	Q
Aspartic	12.5	132.0	88.0	Negative	Q	Q
Betaine	8.8	118.0	58.0	Positive	Q	Q
Carnitine	11.0	162.0	103.0	Positive	Q	Q
Carnosine	12.5	227.0	110.0	Positive		Q
CDP-choline	12.6	489.1	184.0	Positive	Q	Q
CDP-ethanolamine	13.2	447.0	324.0	Positive	Q	Q
Choline	15.4	104.0	60.0	Positive	Q	Q
Citrulline	12.7	176.0	113.0	Positive	Q	Q
cyclic GMP	11.4	346.0	152.0	Positive	Q	Q
Cystathionine	13.4	223.0	134.0	Positive	Q	Q
Cysteinesulfinic acid	12.0	154.0	74.0	Positive		Q
Cystine	13.1	241.0	74.0	Positive	Q	Q
Cytidine	10.1	244.0	112.0	Positive	Q	Q
dAMP	11.2	332.0	136.0	Positive	Q	Q
dCMP	12.8	306.0	79.0	Negative	Q	Q
Deoxyadenosine	4.6	252.0	136.0	Positive	Q	Q
Deoxycytidine	8.8	226.0	93.0	Negative	Q	Q
Deoxyguanosine	9.9	266.0	150.0	Negative	Q	Q
Deoxyuridine	4.5	227.0	184.0	Negative	Q	Q
dGMP	13.2	348.0	152.0	Positive	Q	Q
Dimethylarginine	15.1	203.0	70.0	Positive	Q	Q
Disaccharide hexose	12.7	341.0	89.0	Negative	Q	Q
FAD	11.0	786.2	348.0	Positive	Q	Q
Folic acid	13.3	442.1	295.0	Positive		Q
gamma-aminobutyrate	12.4	104.0	87.0	Positive	Q	Q
GDP	14.3	444.0	152.0	Positive	Q	Q
Gln-6-P	13.4	258.0	79.0	Negative	Q	Q
Glutamate	12.1	146.0	102.0	Negative	Q	Q
Glutamine	12.3	147.0	130.0	Positive	Q	Q
Glutaric acid	12.1	131.0	87.0	Negative		Q
Glutarylcarnitine	10.9	276.0	115.0	Positive	Q	Q
Glycerol-3-P	12.4	171.0	97.0	Negative		Q
GSH	12.0	308.0	76.0	Positive		Q
GSSG	13.6	613.2	231.0	Positive		Q
Guanosine	11.1	284.0	152.0	Positive	Q	Q

Hexose dimer	10.7	367.0	157.0	Negative	Q	
Hexose monomer	10.7	179.0	71.0	Negative	Q	Q
Hexose-P	13.4	259.0	79.0	Negative		Q
Hypoxanthine	7.7	137.0	110.0	Positive	Q	Q
Inosine	9.5	267.0	135.0	Negative	Q	Q
Iso/Citrate	14.8	191.0	111.0	Negative	Q	Q
Isoleucine	9.4	132.1	86.0	Positive	Q	Q
Kynurenine	9.9	209.0	94.0	Positive	Q	Q
Lauroyl carnitine	3.4	344.0	285.0	Positive		Q
Leucine	9.4	132.1	86.0	Positive	Q	Q
Lysine	16.1	147.0	84.0	Positive	Q	Q
Malate	13.2	133.0	115.0	Negative	Q	Q
Malonic acid	4.6	103.0	59.0	Negative	Q	Q
Methionine	9.9	150.0	133.0	Positive	Q	Q
Myo-inositol	13.1	179.0	161.0	Negative	Q	Q
N-acetylalanine	3.3	132.0	44.0	Positive		Q
N-acetyllysine	12.2	189.0	84.0	Positive	Q	Q
N-acetylphenylalanine	1.6	208.0	120.0	Positive	Q	Q
N-acetylputrescine	15.1	131.0	72.0	Positive	Q	Q
N-methylglutamate	10.2	162.0	116.0	Positive		Q
NAD	12.2	664.1	136.0	Positive	Q	Q
NADP	13.7	744.1	136.0	Positive		Q
Nicotinamide	3.6	123.0	80.0	Positive		Q
Nicotinamide mononucleotide	12.9	335.0	123.0	Positive	Q	Q
Nicotinic acid	3.5	122.0	78.0	Negative	Q	Q
Opthalmic acid	11.4	290.0	161.0	Positive	Q	Q
Ornithine	15.1	133.0	70.0	Positive	Q	Q
Pentose-P	13.3	229.0	79.0	Negative	Q	Q
Phenylalanine	8.4	166.0	103.0	Positive	Q	Q
Phosphocholine	12.5	184.0	86.0	Positive	Q	Q
Phosphoenolpyruvate	14.2	167.0	79.0	Negative		Q
Proline	10.6	116.0	68.0	Positive	Q	Q
S-adenosylhomocysteine	11.7	385.0	136.0	Positive	Q	Q
S-adenosylmethionine	13.4	399.0	250.0	Positive	Q	Q
Serine	12.6	106.0	60.0	Positive	Q	Q
Succinate	12.1	117.0	73.0	Negative		Q
Taurine	11.6	124.0	80.0	Negative	Q	Q
Thiamine	15.4	265.0	122.0	Positive	Q	Q
Thiamine monophosphate	12.1	345.0	122.0	Positive	Q	Q
Threonine	11.7	120.0	74.0	Positive	Q	Q
Thymidine	3.5	243.0	117.0	Positive		Q
Trimethyllysine	15.2	189.0	84.0	Positive	Q	Q
Tryptophan	10.3	205.0	188.0	Positive	Q	Q
Tryptophanamide	3.7	204.0	159.0	Positive	Q	Q
Tyrosine	11.2	182.0	136.0	Positive	Q	Q
UDP-glucose	13.4	565.0	323.0	Negative	Q	Q
UDP-glucuronic acid	14.6	579.0	403.0	Negative	Q	Q
UMP	12.8	323.0	111.0	Negative	Q	
Uridine	7.5	243.0	110.0	Negative	Q	Q
Valine	10.4	118.0	72.0	Positive	Q	Q
Xanthine	9.2	151.0	108.0	Negative	Q	Q

*Q indicates a metabolite that was quantified in the PFOS or PFOA dataset

3.3 Statistical analysis of PFOS and PFOA exposure

Multivariate analysis was conducted on metabolites detected by LC-MS to visualize global differences in the metabolite profiles of *Artemia* exposed to PFOS and PFOA. We were unable to do multiblock multivariate analysis with NMR because the samples were treated and analyzed differently from the LC-MS samples. PCA indicates that there is clear separation between doses for each compound. For PFOS, PC1 explains 53.8% of the variance, which corresponds to a separation between the control and the two doses. PC2 explains 24.4% of the variance which corresponds to the difference between 2 ppm and 10 ppm PFOS (Figure 5.4a). The loading plot (Figure 5.4b) indicates that the iso/citrate, pentose phosphate, and guanosine may contribute to the control, hexose phosphate, GSH, and GDP contribute to 2 ppm, and deoxyadenosine, adenosine, and malonic acid contribute to 10 ppm PFOS. For PFOA, PC1 explains 62.1% and PC2 explains 25.7% (Figure 5.4c). PC1 separates the control from 30 ppm PFOA and PC2 separates 6 ppm PFOA from the control and from 30 ppm. The loading plot indicates that N-acetyllysine, citrulline, and disaccharide hexose contribute to the control, cystine, malate and aminoadipate contribute to 30 ppm, and adenosine, cytidine, and deoxycytidine contribute to 6 ppm (Figure 5.4d).

Univariate analysis was performed to identify how individual metabolites are affected by PFOS and PFOA exposure and to evaluate significance. Univariate analysis was conducted for the control versus 10 ppm PFOS and 30 ppm PFOA (high dose) treatments. 49 metabolites were significantly affected by PFOS and 58 metabolites were significantly affected by PFOA. The majority of the metabolites had a negative fold change from PFOS

exposure, 12 of which had a fold change greater than 2.0, and a positive fold change from PFOA exposure, and 43 of which had a fold change greater than 2.0.

One-way ANOVA with Fisher's LSD post hoc was calculated for each treatment to identify metabolites that were significantly affected ($p < 0.05$) between two or three conditions. For these exposures, 77 out of 101 detected metabolites were significantly affected; 13 metabolites were significant in PFOS, 18 were significant in PFOA, and 46 were significant in both exposures (Figure 5.5). Arginine, asparagine, betaine, leucine, phosphocholine, gadusol, and homarine were significant in NMR for PFOS exposures and lysine was significant by NMR and LC-MS for PFOS. ADP, alanine, taurine, and hexose monomer/glucose were significant by both PFOS and PFOS and identified by NMR and LC-MS. Glutamate and methionine were significant in PFOA and identified by NMR and LC-MS.

Heat maps were also constructed to visualize metabolite changes with each treatment. The metabolites are arranged by hierarchal clustering to indicate which metabolites are similarly affected. The heat map plotted with average metabolite response for each treatment shows an overall trend of metabolite levels increasing slightly from control to 2 ppm PFOS and then decreasing from 2 ppm to 10 ppm PFOS (Figure 5.6a). In contrast, the PFOA heat map indicates that overall metabolite levels increase with exposure (Figure 5.6b). However, N-acetylputrescine, 5-aminovaleric acid, glucosamine-6-phosphate, adenine, N-acetyllysine, disaccharide hexose, S-adenosylhomocysteine, hexose monomer,

alpha-ketoglutarate, and ophthalmic acid trend opposite from the majority and decrease with PFOA dose. The trends plotted in the heat map for control and the high dose agree with the univariate statistics (Table 5.2), however it is not clear why the levels of many metabolites would increase from control to 2 ppm PFOS but decrease from 2 ppm to 10 ppm.

a.

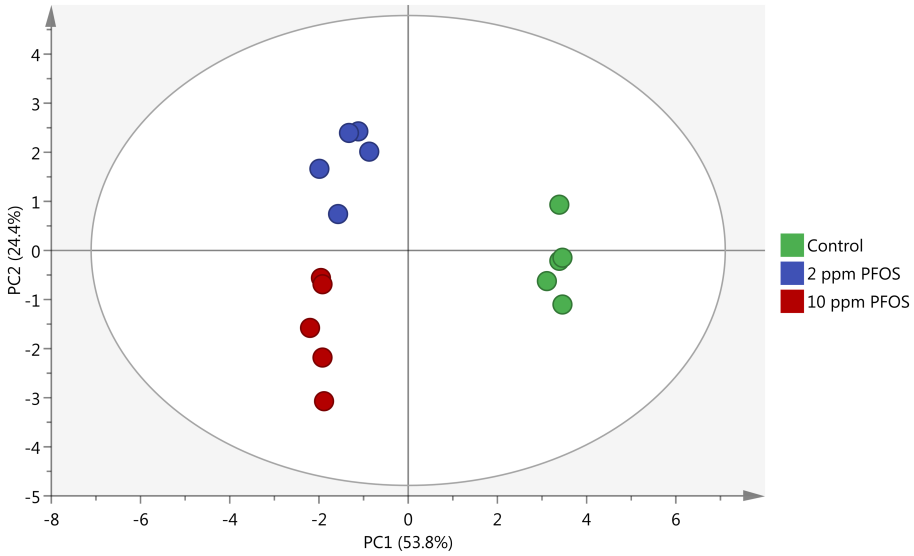
PC2 (24.4%)
PC1 (53.8%)
Control
2 ppm PFOS
10 ppm PFOS

b.

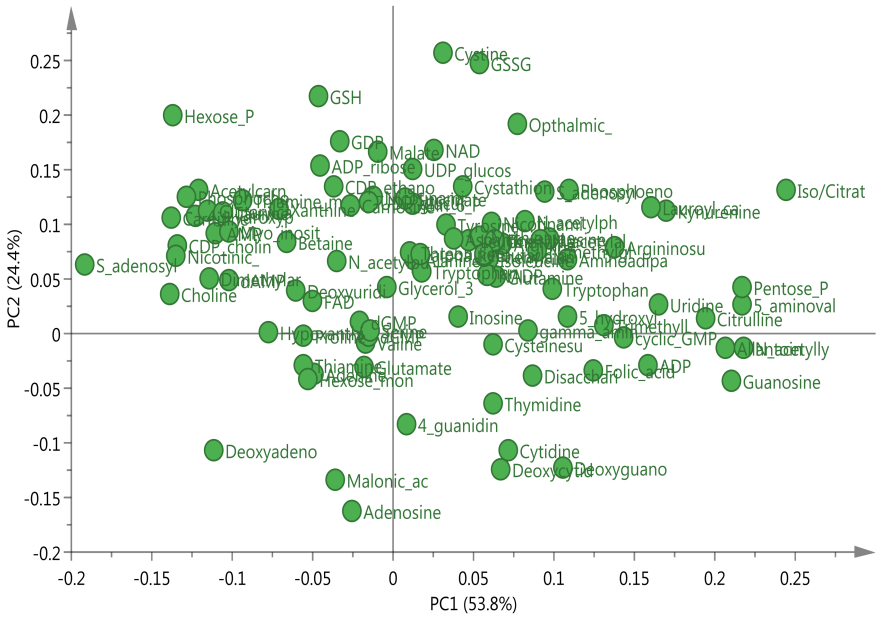
PC2 (24.4%)
PC1 (53.8%)
Cystine
GSSG
GSH
Hexose_P
Opthalmic_
NAD
ADP_ribos
UDP_glucos
Iso/Citrat
Betaine
S_adenosyl
Choline
Deoxyurid
FAD
Glycerol_3
Tryptophan
Pentose_P
5_aminoval
Uridine
Citrulline
Inosine
Cysteinesu
cyclic_GMP
ADP
Guanosine
Disaccharn
Thymidine
4_guanidin
Deoxyadeno
Cytidine
Deoxyguano
Malonic_ac
Adenosine

c.

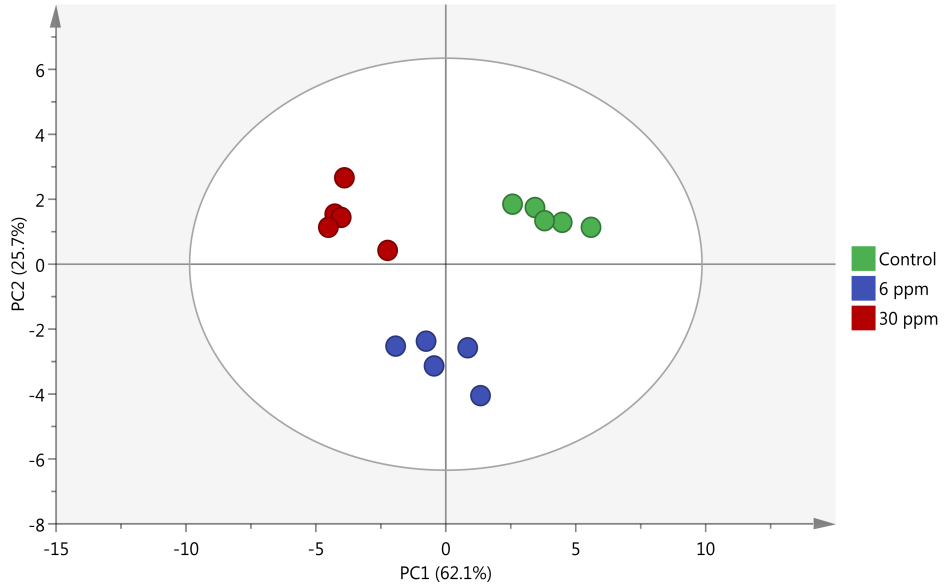

d.

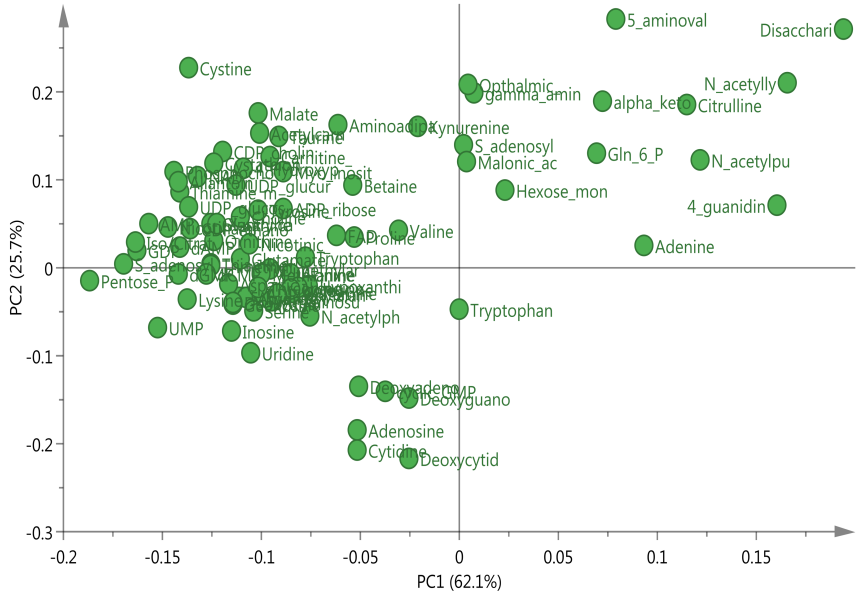

Figure 5.4. PCA plots for the LC-MS metabolite response from PFOS and PFOA exposures. Ellipse represents 95% confidence interval. The PCA score plot (a) and loading plot (b) for PFOS indicates that PC1 = 53.8 % and PC2 = 24.4 % explained variance. The score plot (c) and loading plot (d) for PFOA indicates that PC1 = 62.1% and PC2 = 25.7% explained variance.

Table 5.2. Univariate analysis of LC-MS metabolites for control versus 10 ppm PFOS and 30 ppm PFOA

Name	PFOS p-value	Fold Change	10 ppm PFOS/ Control	PFOA p-value	Fold Change	30 ppm PFOA/ Control
4_guanidinobutyric_acid	0.3535	1.09	Up	< 0.0001	-6.35	Down
4_Hydroxyproline	0.0037	1.53	Up	0.0002	2.38	Up
5_aminovaleric_acid	< 0.0001	-4.68	Down	0.0046	-2.45	Down
5_hydroxylysine	0.0001	-1.47	Down	0.0079 (W)	2.2	Up
Adenine	0.0385	1.18	Up	0.0003	-1.94	Down
Adenosine	0.002	1.35	Up	0.0017	1.64	Up
ADP	0.0079	-2.23	Down	0.0027	2.04	Up
ADP_ribose	0.9016	1.02	Up	0.0091	1.88	Up
Alanine	0.1168	-1.05	Down	< 0.0001	1.55	Up
Allantoin	0.014	-4.29	Down	0.0801	5.47	Up
alpha_ketoglutarate	0.4863	-1.16	Down	0.0079 (W)	-1.91	Down
Aminoadipate	< 0.0001	-1.57	Down	0.038	1.67	Up
AMP	0.0023	1.42	Up	0.0006	5.45	Up
Arginino succinic_acid	0.0079 (W)	-2.03	Down	0.0008	1.76	Up
Aspartate	0.1206	-1.24	Down	0.0079 (W)	2.41	Up
Carnosine	0.8796	-1.02	Down			
CDP_choline	0.0016	1.69	Up	< 0.0001	3.11	Up
CDP_ethanolamine	0.7881	-1.02	Down	0.0011	3.51	Up
Citrulline	0.0079 (W)	-3.39	Down	0.0079 (W)	-3.39	Down
cyclic_GMP	0.0007	-1.92	Down	0.0918	1.27	Up
Cystathionine	0.0096	-1.29	Down	0.0079 (W)	3.01	Up
Cysteinesulfinic_acid	0.0036	-1.22	Down			
Cystine	0.0097	-1.88	Down	0.0045	6.14	Up
Cytidine	0.0721	-1.16	Down	0.0159 (W)	1.52	Up
dAMP	0.0014	1.36	Up	< 0.0001	3.61	Up
dCMP	0.8595	1.02	Up	0.0007	3	Up
Deoxyadenosine	0.0002	1.96	Up	0.0079 (W)	1.46	Up
Deoxycytidine	0.2852	-1.16	Down	0.1904	1.28	Up
Deoxyguanosine	0.0283	-1.42	Down	0.277	1.19	Up
Deoxyuridine	0.1836	1.16	Up	0.001	2.45	Up
dGMP	0.7966	1.04	Up	0.0003	3.72	Up
Disaccharide_hexose	0.0815	-1.55	Down	< 0.0001	-12.41	Down
FAD	0.104	1.12	Up	0.0002	1.31	Up
Folic_acid	0.0048	-1.77	Down			
gamma_aminobutyrate	< 0.0001	-1.26	Down	0.3045	-1.11	Down
GDP	0.5511	-1.05	Down	0.0003	5.29	Up
Gln_6_P	0.1356	-1.16	Down	0.0021	-1.83	Down
Glutamate	0.5153	1.06	Up	< 0.0001	2.1	Up
Glutaric_acid	0.066	-1.3	Down			
Glutarylcarnitine	0.0016	1.44	Up	0.0029	2.9	Up
Glycerol_3_P	0.6856	-1.03	Down			
GSH	0.6745	-1.06	Down			
GSSG	0.001	-1.95	Down			
Guanosine	< 0.0001	-3.63	Down	0.0283	2.77	Up

Hexose_monomer	0.0066	1.18	Up	0.1472	-1.12	Down
Hexose_P	0.0075	1.65	Up			
Inosine	0.2163	-1.12	Down			
Iso/Citrate	0.0129	-9.94	Down	0.0119	6.56	Up
Kynurenine	< 0.0001	-3.26	Down	0.2822	1.13	Up
Lauroyl_carnitine	< 0.0001	-3	Down			
Lysine	< 0.0001	-1.52	Down			
Malate	0.2844	-1.13	Down	0.0001	2.53	Up
Malonic_acid	0.0008	1.31	Up	0.9282	1.03	Up
Myo_inositol	0.0085	1.37	Up	0.0011	1.93	Up
N_acetylalanine	< 0.0001	-1.48	Down			
N_acetyllysine	< 0.0001	-4.4	Down	0.0079 (W)	-8.61	Down
N_acetylphenylalanine	0.0044	-1.51	Down	0.0005	2.05	Up
N_acetylputrescine	0.4535	1.08	Up	0.0001	-3.4	Down
N_methylglutamic_acid	0.0001	-1.43	Down			
NAD	0.0159 (W)	-1.28	Down	0.0079 (W)	3.58	Up
NADP	0.0261	-1.26	Down			
Nicotinamide	0.1678	-1.07	Down			
Nicotinamide_ mononucleotide	0.0021	-1.29	Down	< 0.0001	3.83	Up
Nicotinic_acid	< 0.0001	1.68	Up	0.0037	2.12	Up
Opthalmic_acid	0.0002	-1.81	Down	0.7888	-1.03	Down
Ornithine	0.0032	-1.27	Down	0.0021	2.65	Up
Pentose_P	0.0002	-4.65	Down	0.0014	9.74	Up
Phosphoenolpyruvate	0.0749	-2.15	Down			
Proline	0.0104	1.13	Up	0.0099	1.2	Up
S_adenosylhomocysteine	< 0.0001	2.86	Up	0.6356	-1.02	Down
S_adenosylmethionine	< 0.0001	-1.67	Down	< 0.0001	6.04	Up
Serine	0.6905 (W)	1.02	Up	0.0023	2.07	Up
Succinate	0.391	-1.14	Down			
Taurine	0.0044	1.38	Up	0.0005	2.01	Up
Thiamine	0.0114	1.2	Up	< 0.0001	2.66	Up
Thiamine_ monophosphate	0.0074	1.28	Up	< 0.0001	3.79	Up
Threonine	0.2976	-1.07	Down	< 0.0001	1.87	Up
Thymidine	0.1981	-1.17	Down			
Trimethyllysine	< 0.0001	-1.71	Down	0.0003	2.59	Up
Tryptophan	0.2237	-1.08	Down	0.0002	1.44	Up
Tryptophanamide	0.0002	-1.45	Down	0.6169	-1.05	Down
UDP_glucose	0.2163	-1.19	Down	0.0079 (W)	3.31	Up
UDP_glucuronic_acid	0.6951	-1.05	Down	0.0004	2.54	Up
UMP				0.0012	4.53	Up
Uridine	< 0.0001	-2.39	Down	< 0.0001	2.28	Up
Valine	0.4559	1.04	Up	0.0038	1.1	Up
Xanthine	0.1961	1.15	Up	0.0003	2.78	Up
*p-value is calculated with t-test as a default, significant p-values are highlighted in blue						
*p-value with (W) is calculated by the Wilcoxon Mann Whitney test						
*fold change > |2.0| are highlighted in blue						

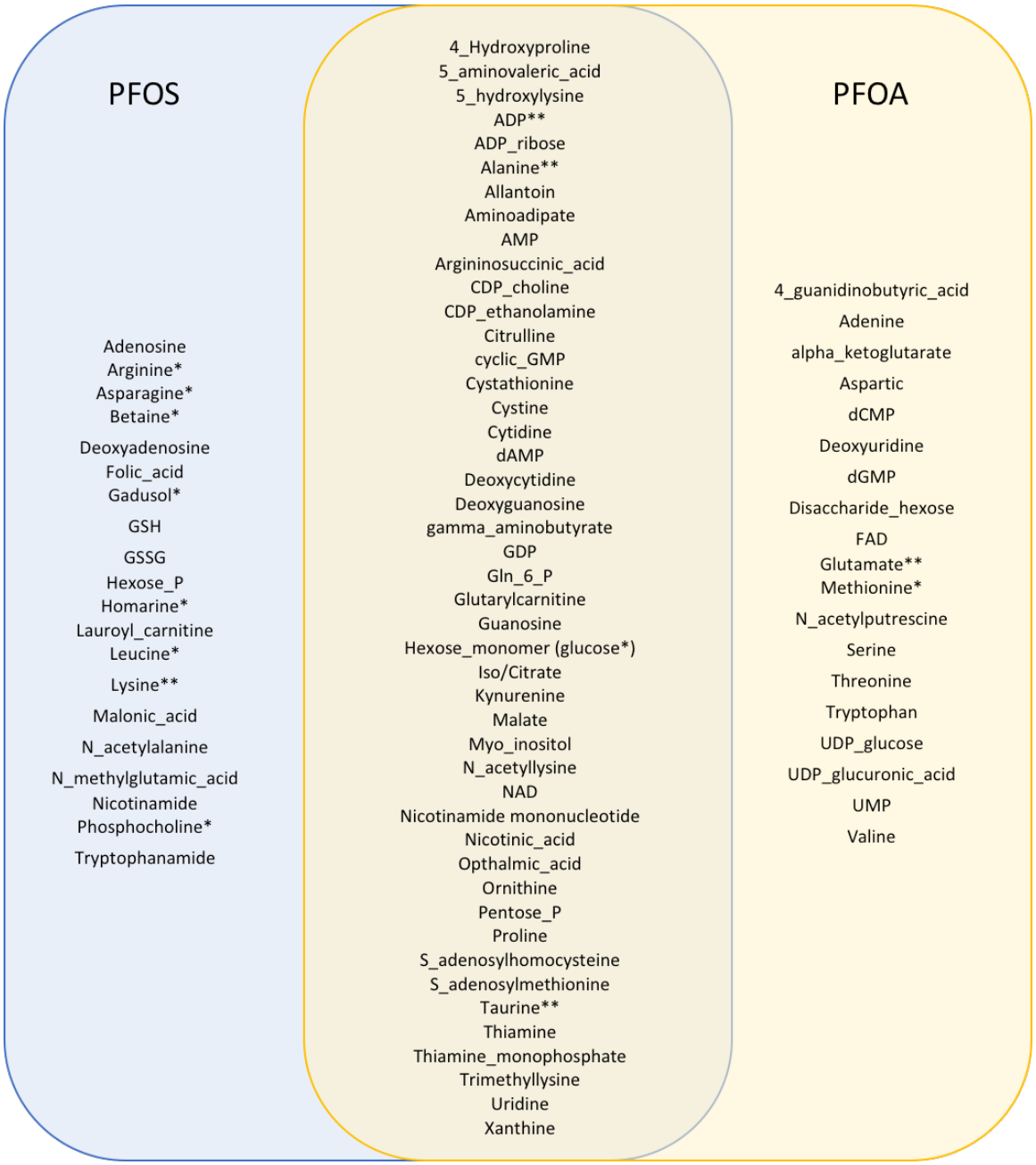

Figure 5.5. Venn diagram indicating metabolites that were significantly affected ($p < 0.05$) by PFOS and PFOA exposure. Metabolites that were significant by NMR are indicated by *, and metabolites that were significant by both NMR and LC-MS are indicated by **.

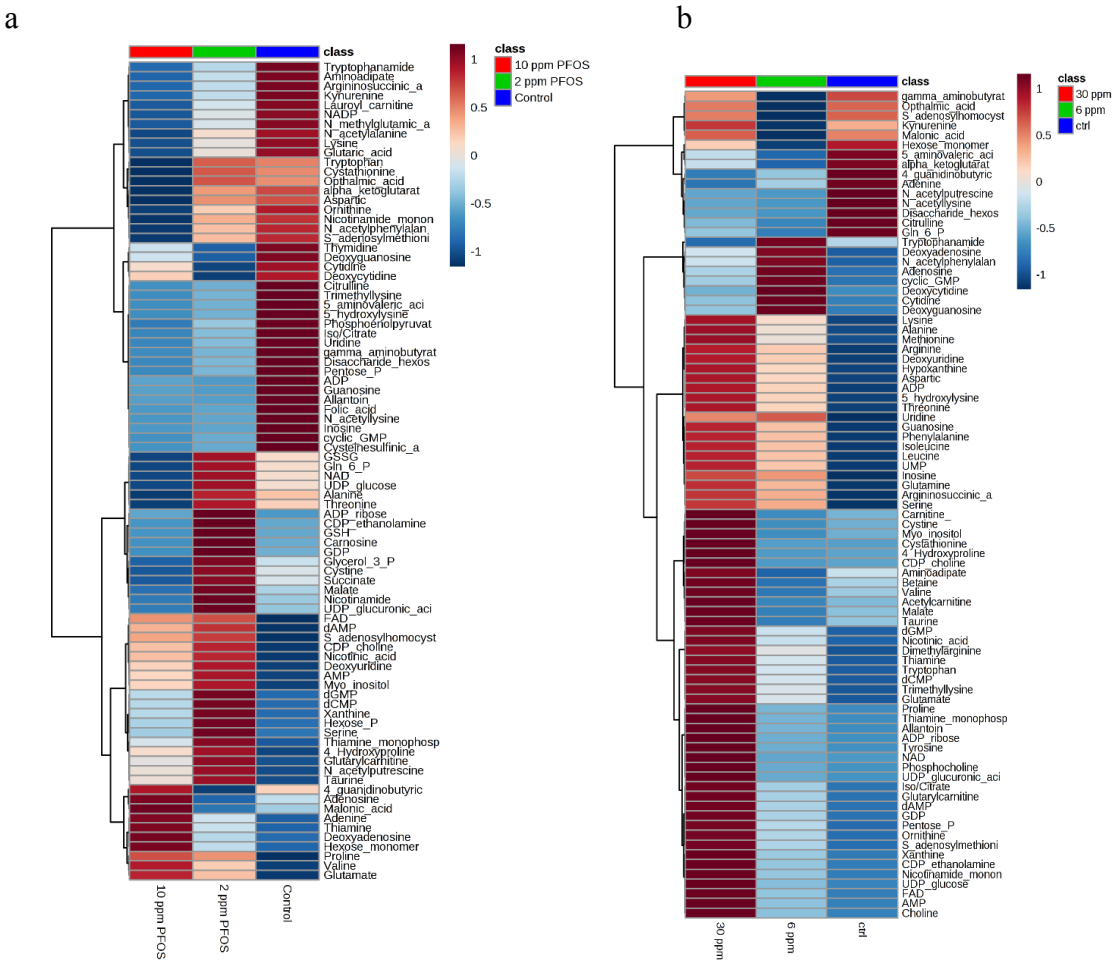

Figure 5.6. Heat map of group average metabolite concentration measured by LC-MS from PFOS exposures (a) and PFOA exposures (b). Blue indicates decreased concentration and red indicates increased concentration with respect to the average metabolite concentration. Metabolites are arranged by hierarchal clustering.

3.4 Biochemical pathway analysis of PFOS and PFOA metabolites

Pathway analysis (PAPi) was performed to identify biochemical pathways that might be affected from PFOS and PFOA exposure. PAPi indicated that 35 pathways were altered by PFOS and 116 pathways were altered by PFOA (Figure 5.7). These pathways are related to amino acid, nucleic acid, lipid, and carbohydrate metabolism in addition to signaling pathways and diseased states. Pathways with a positive activity score are considered upregulated and a negative activity score indicates down regulation. Upregulated pathways have decreased metabolite levels compared to the control and pathways and downregulated pathways have increased metabolite levels. Increased metabolite levels indicates that the activity of the pathway has slowed and is causing accumulation of metabolites.[37] The heat maps show that metabolite accumulation increases with PFOA concentration, which indicates that more pathways may be downregulated. Less accumulation is evident at the high dose for PFOS, which may indicate more pathways are upregulated (Figure 5.6). This trend is also confirmed by the PAPi line graph, which shows more upregulated pathways in PFOS than PFOA (Figure 5.7). Identified pathways in which three or more metabolites were identified were mapped to show individual metabolite changes.

a.

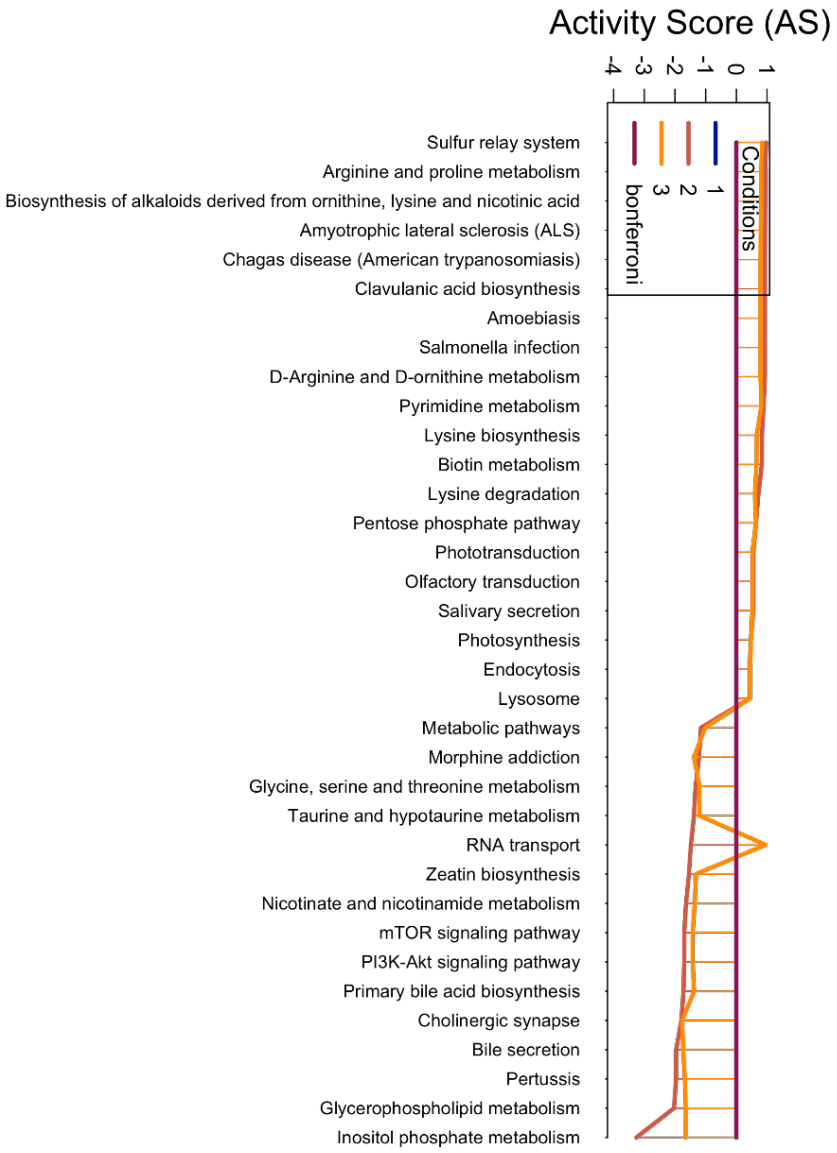
Activity Score (AS)
-4
-3
-2
-1
0
1
bonferroni
3
2
1
Conditions
Sulfur relay system
Arginine and proline metabolism
Biosynthesis of alkaloids derived from ornithine, lysine and nicotinic acid
Amyotrophic lateral sclerosis (ALS)
Chagas disease (American trypanosomiasis)
Clavulanic acid biosynthesis
Amoebiasis
Salmonella infection
D-Arginine and D-ornithine metabolism
Pyrimidine metabolism
Lysine biosynthesis
Biotin metabolism
Lysine degradation
Pentose phosphate pathway
Phototransduction
Olfactory transduction
Salivary secretion
Photosynthesis
Endocytosis
Lysosome
Metabolic pathways
Morphine addiction
Glycine, serine and threonine metabolism
Taurine and hypotaurine metabolism
RNA transport
Zeatin biosynthesis
Nicotinate and nicotinamide metabolism
mTOR signaling pathway
PI3K-Akt signaling pathway
Primary bile acid biosynthesis
Cholinergic synapse
Bile secretion
Pertussis
Glycerophospholipid metabolism
Inositol phosphate metabolism

b.

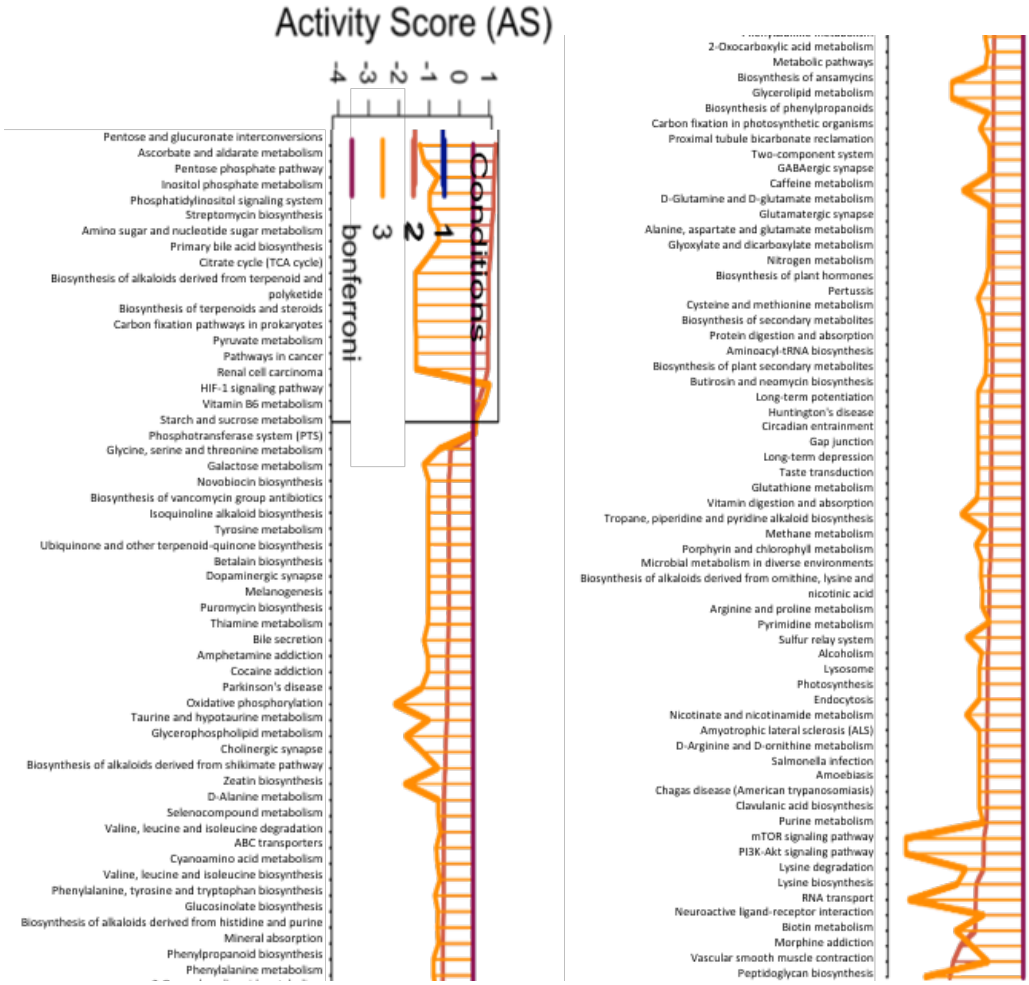

Figure 5.7. PAPi pathway analysis line plots indicating metabolic pathways that are significantly affected ($p < 0.05$) by PFOS (a) and PFOA (b) exposure. The activity score for each pathway is calculated with the control group (1) set as a reference compared to the low dose (2) and the high dose (3) for each treatment and normalized using the Bonferroni correction. Graphs were constructed in the PAPi r package.[37]

Toxicological studies with PFAS consistently report effects on glucose, urea/uric acid metabolism, lipid metabolism, and hepatotoxicity in model organisms.[4,38] We have found that both PFOS and PFOA affect glycerophospholipid metabolism and pathways related to carbohydrate metabolism in *Artemia* after 68 hrs of exposure. *Artemia* are ammonotetic, meaning they excrete waste in the form of nitrogen instead of urea.[39] We found that nitrogen metabolism was downregulated by PFOA exposure (Figure 5.8), which may be related to an effect on waste excretion or an overall impact on metabolism which results in reduced waste production, which would be consistent with reported findings. Phenylalanine, tyrosine, cystathione, aspartate, AMP, glutamine and glutamate increased, and taurine decreased at 6 ppm and increased at 30 ppm. Methane metabolism was also downregulated with PFOA exposure, this is another important route of waste removal.

Glycerophospholipid metabolism was downregulated by PFOS exposure, with 2 ppm PFOS having a lower activity score than 10 ppm PFOS (Figure 5.9), and PFOA exposure. Choline increases, phosphocholine, CDP-choline, and CDP-ethanolamine increase at 2 ppm and decrease at 10 ppm. Glycerol-3-phosphate does not change. In PFOA, choline, phosphocholine, CDP-choline, and CDP-ethanolamine increased with exposure. This pathway is associated with the metabolism of fatty acids that make up lipid bilayers.[40] The impairment of lipid metabolism is a commonly hypothesized pathway of toxicity for PFOS. It is known to bioaccumulate in fatty tissue and is attributed to liver toxicity in many organisms, including chickens, fish, and rats.[19,41–43] PFOS affects fatty acid metabolism in

fish species, such as fathead minnows and rainbow trout.[44] PFOS and PFOA induced hepatotoxicity in tilapia, in which liver glycogen accumulation was measured.[19]

The acylcarnitines, lauroylcarnitine and glutarylcarnitine, are involved in processes related to carnitine biosynthesis, transport, and utilization.[45] Carnitine is essential for fatty acid oxidation. It was found to increase with PFOS and PFOA. Glutarylcarnitine and lauroylcarnitine were not identified by the KEGG database and could not be considered for pathway analysis. Glutarylcarnitine increases with PFOS and PFOA exposure and lauroylcarnitine decreases with PFOS but was not detected in PFOA. The accumulation of carnitine with PFOS and PFOA exposures indicates that pathways related to fatty acid oxidation were likely downregulated. The effects on these polyamine compounds may also be related to downregulation of nitrogen metabolism measured in PFOA exposures.

Several pathways related to carbohydrate metabolism were perturbed by PFOS and PFOA. These pathways are important for energy conservation or utilization. *Artemia* are highly sensitive and responsive to environmental conditions and this is reflected in the carbohydrate and osmolyte profile.[39,46] In the studies described in earlier chapters of this dissertation, we have found that several of these metabolites are consistently affected by exposure to environmental toxins. These include the metabolites that are involved with osmoregulation, including taurine, betaine, glucose, phosphocholine, gadusol, homarine, and choline.[39] This indicates that these metabolites are likely important for defending growing *Artemia* from environmental stress. Additionally, inositol phosphate metabolism

had the largest negative activity score for PFOS. Myo-inositol, ATP and ADP are involved in this pathway along with many other inositol compounds that are absent from our dataset. Starch and sucrose metabolism (Figure 5.10) and pentose and glucuronate interconversions were upregulated with PFOA. In the starch and sucrose metabolism pathway, trehalose (disaccharide hexose) and glucose (hexose monomer) decreased, UDP-glucose increased, and UDP-glucuronic acid decreased at 6 ppm and increased at 30 ppm.

Several pathways involved in amino acid metabolism were affected by PFOS and PFOA exposure. Alanine, aspartate, and glutamate metabolism (Figure 5.11) arginine and proline metabolism (Figure 5.12), lysine degradation (Figure 5.13), lysine biosynthesis, and D-arginine and D-ornithine metabolism were upregulated with PFOS. Glycine, serine and threonine metabolism (Figure 5.14), and taurine and hypotaurine metabolism were downregulated with PFOS. These same pathways were all downregulated with PFOA exposure. In the alanine, aspartate, and glutamate metabolism pathway, aspartate, argininosuccinate, and glutamine decreased with increasing exposure, glucosamine-6-phosphate and succinate increased for 2 ppm and decreased for 10 ppm PFOS. Alpha-ketoglutarate and glutamate did not change significantly. For PFOA, aspartate, argininosuccinate, glutamine, and glutamate increased, oxoglutarate, and glucosamine-6-phosphate decreased. In the arginine and proline metabolism pathway, glutamine, aspartate, argininosuccinate, arginine, citrulline and ornithine decrease with PFOS exposure. Proline and hydroxyproline increase at 2 ppm and decrease at 10 ppm PFOS. N-acetylputrescine, 4-guanidinobutyric acid, and glutamate do not change significantly. For

PFOA, glutamine, aspartate, argininosuccinate, arginine, ornithine, proline, hydroxyproline, and glutamate increased. N-acetylputrescine, citrulline, and 4-guanidinobutyrate decreased. In the lysine degradation pathway, lysine was only detected in the 10 ppm PFOS sample, N-acetyllysine, aminoadipate, 5-aminovaleric acid, and trimethyllysine decreased with exposure. For PFOA, lysine increased, aminoadipic acid decreased at 6 ppm and increased at 30 ppm, trimethyllysine increased at 6 ppm and was not detected at 30 ppm. N-acetyllysine and 5-aminopentanoic acid (5-aminovaleric acid) decreased. In the glycine, serine, and threonine metabolism pathway, choline increased, betaine and cystathione increased at 2 ppm and decreased at 10 ppm, serine and threonine did not change significantly. Choline and cystathione increased, serine increased at 6 ppm and decreased at 30 ppm. Betaine decreased at 6 ppm and increased at 30 ppm. Threonine was only detected in the control. The pathways that were upregulated by PFOS include amino acids with amine side-chains and polyamine metabolites. These pathways are important for protein synthesis and waste excretion and detoxication. Valine, leucine, and isoleucine degradation and cysteine and methionine metabolism were also downregulated with PFOA exposure.

Several studies have determined that PFOS and PFOA induce oxidative stress.[17–19] In a study where in which salmon were fed PFOS or PFOA, reactive oxygen species-induced damage was measured.[17] Glutathione metabolism was downregulated by PFOA by *Artemia* and glutathione (GSH) and oxidized glutathione (GSSG) were affected by PFOS. Additionally, ophthalmic acid levels decreased in PFOS and PFOA. This compound is not

in the KEGG database, but it is a tripeptide analog of glutathione. Ophthalmic acid has been identified as a possible biomarker of oxidative stress that is produced in higher quantities when glutathione is being consumed by oxidative stress.[47] The sulfur relay system and cysteine and methionine metabolism were identified by pathway analysis, indicating that many sulfur-containing compounds were affected in this study by both PFOS and PFOA.

The sulfur relay system was upregulated with PFOS and downregulated with PFOA exposure. This system includes many different pathways, including thiamine metabolism and cysteine metabolism.[48] Cysteine and methionine metabolism was downregulated from PFOA exposure (Figure 5.15). Cystine, methionine, S-adenosylmethionine, and cystathione increased. S-adenosylhomocysteine decreased at 6 ppm and increased at 30 ppm. And serine increased at 6 ppm and decreased at 30 ppm. For thiamine metabolism, three metabolites detected from this pathway include thiamine, thiamine monophosphate, and cysteine, but cysteine was not detected for PFOA exposures. Thiamine is produced from dephosphorylation of thiamine monophosphate. Thiamine levels increased and thiamine monophosphate decreased with PFOS. Both metabolites increased with PFOA exposure.

Other pathways that may have been affected by PFOS and PFOA include vitamin metabolism, nucleic acid metabolism, the TCA cycle, and signaling pathways. Pathways related to the metabolism of vitamins include nicotinate and nicotinamide metabolism

(Figure 5.16) and vitamin digestion and absorption. These pathways were downregulated by PFOS and PFOA. In the nicotinate and nicotinamide metabolism pathway, aspartate, nicotinamide mononucleotide, and NADP decrease with exposure, nictotinic acid, nicotinamide, and NAD increase at 2 ppm and decrease at 10 ppm PFOS. For PFOA, aspartate, nicotinic acid, NAD, and nicotinamide mononucleotide increased. Pathways related to nucleic acid metabolism were affected by PFOS and PFOA. Pyrimidine metabolism was upregulated with PFOS and PFOA (Figure 5.17). Glutamine and uridine decrease, cytidine, deoxycytidine, and thymidine decrease at 2 ppm and increase at 10 ppm, deoxyuridine increases at 2 ppm and decreases at 10 ppm PFOS. For PFOA, glutamine decreased, dCMP and deoxyuridine increased, deoxycytidine, cytidine, and uridine increased at 6 ppm and decreased at 30 ppm.

Purine metabolism (Figure 5.18), amino sugar and nucleotide sugar metabolism, and thiamine metabolism were downregulated by PFOA. ADP-ribose, GDP, xanthine, hypoxanthine, glutamine, ADP, and AMP increased. Cyclic GMP, deoxyguanosine, guanosine, inosine, and deoxyadenosine increased at 6 ppm and decreased at 30 ppm. These pathways are related to DNA synthesis and nucleotide interconversion from the exchange of phosphate. Pathways related to phosphate transfer were also affected by PFOA, including the phosphotransferase system and oxidative phosphorylation.

The TCA Cycle was upregulated in 6 ppm and downregulated at 30 ppm (Figure 5.19). Malate decreased at 6 ppm and increased at 30 ppm. Citrate and isocitrate (iso/citric acid) increased and oxoglutarate decreased. This pathway is central for many metabolic pathways and is essential for cellular respiration. Downregulation of this pathway in PFOA may have been the reason for the overall increase in measured metabolite levels that was identified in the heat map.

The mTOR signaling pathway and the PI3K-AKT signaling pathway were downregulated with PFOS and PFOA exposure. In humans, the mTORC1 gene is activated by the presence of growth factors, amino acids, energy status, stress and oxygen levels to regulate several biological processes, including lipid metabolism, autophagy, protein synthesis and ribosome biogenesis. The phosphatidylinositol 3'-kinase (PI3K)-Akt signaling pathway is activated by cellular stimuli or toxins and regulates cellular functions such as transcription, translation, proliferation, growth, and survival. PI3K catalyzes the production of phosphatidylinositol-3,4,5-triphosphate (PIP3) at the cell membrane. PIP3 serves as a second messenger that activates Akt. Akt controls key cellular processes by phosphorylating substrates involved in apoptosis, protein synthesis, metabolism, and cell cycle. It is not clear if these pathways are relevant for *Artemia*, but they may have been identified by PAPi because other pathways related to these cellular functions were affected by exposure.

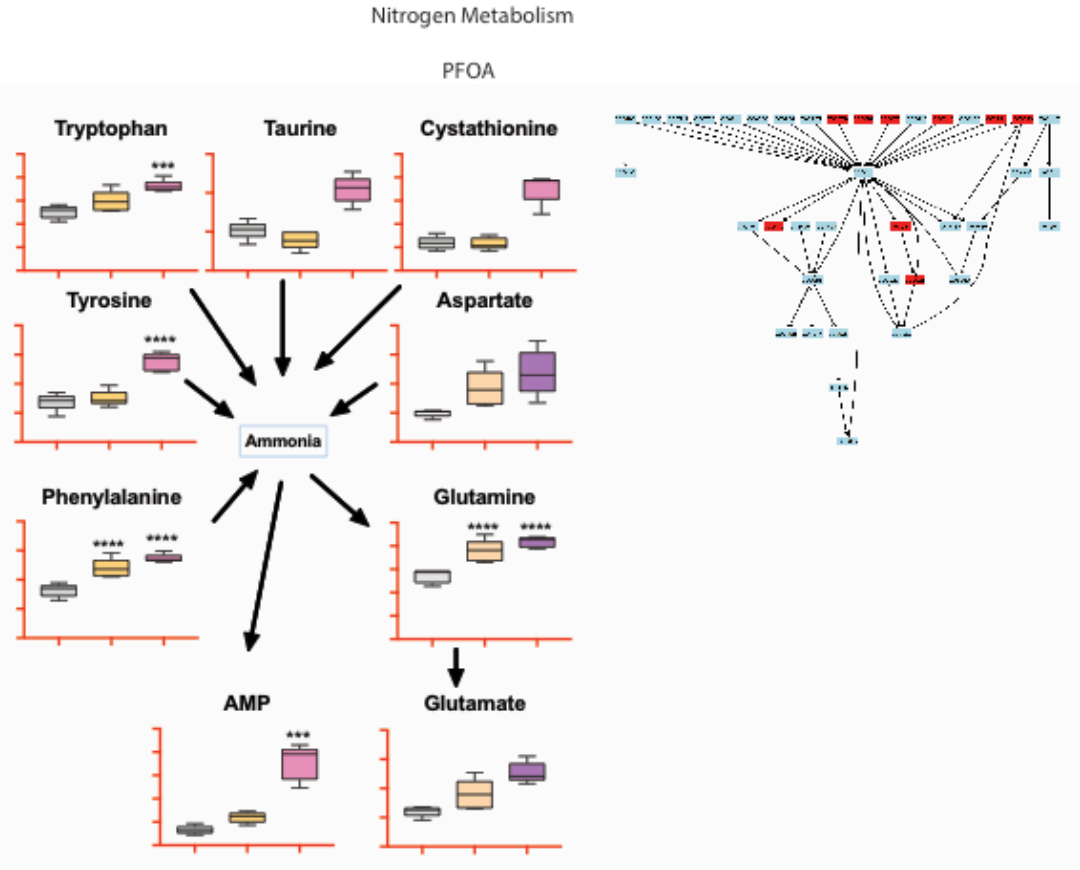

Figure 5.8. Metabolite changes induced by PFOA exposure (control=grey, 6 ppm= orange, 30 ppm = pink) from the nitrogen metabolism pathway. Nitrogen metabolism was downregulated with PFOA. The biochemical map indicates which metabolites were identified in the dataset, with blue rectangles indicating metabolites that were not identified and red rectangles indicating metabolites that were present. Asterisks indicate statistically significant difference in mean for the dose compared to the control mean (*p<0.5, **p<0.01, ***p<0.001, ****p<0.0001).

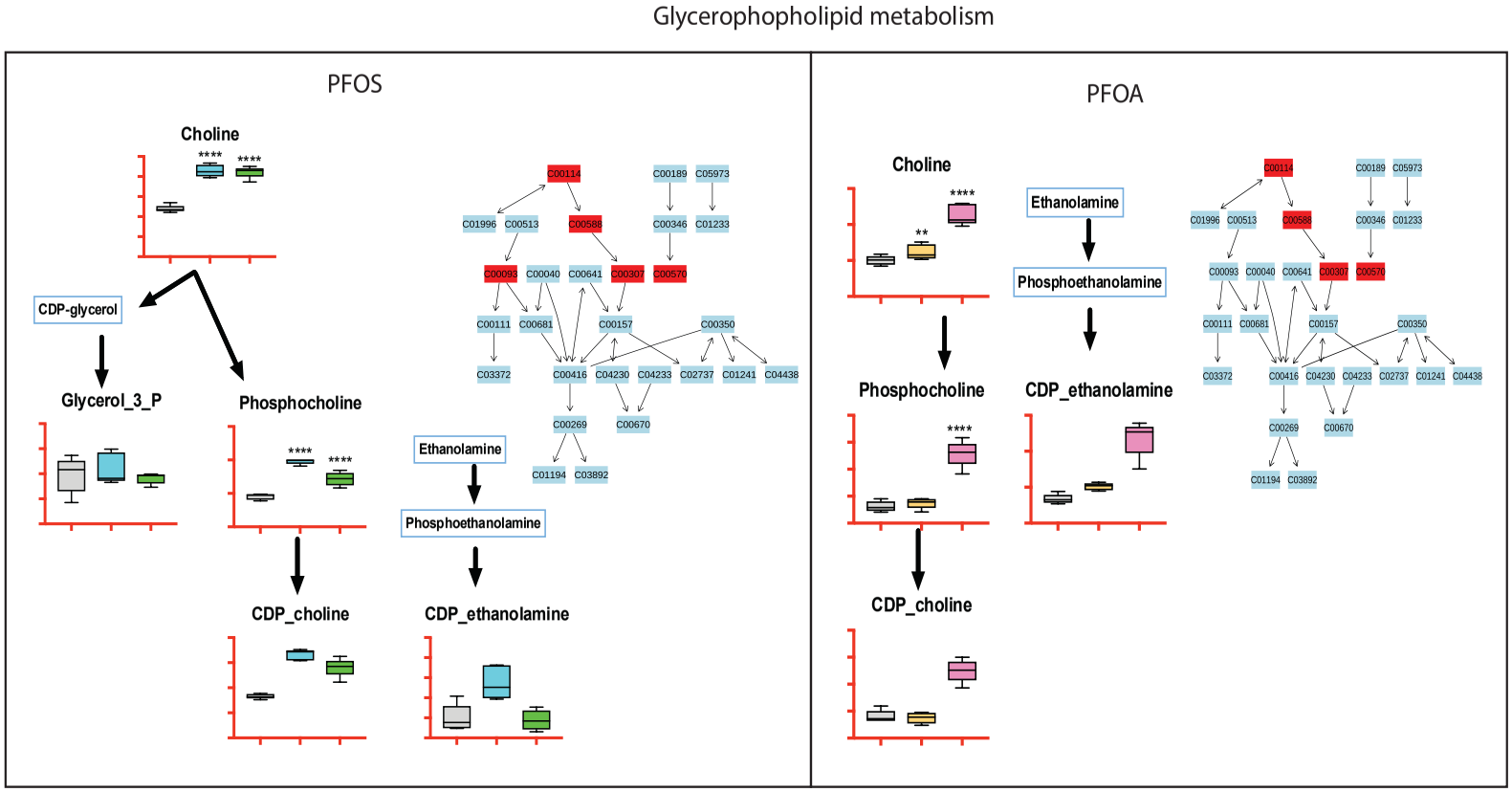

Figure 5.9. Metabolite changes induced by PFOS exposure (control=grey, 2 ppm= blue, 10 ppm = green) and PFOA (b) exposure (control=grey, 6 ppm= orange, 30 ppm = pink) from the glycerophospholipid metabolism pathway. This pathway was downregulated by PFOS exposure, with 2 ppm PFOS having a lower activity score than 10 ppm PFOS, and PFOA exposure. The biochemical map indicates which metabolites were identified in the dataset, with blue rectangles indicating metabolites that were not identified and red rectangles indicating metabolites that were present. Asterisks indicate statistically significant difference in mean for the dose compared to the control mean (*p<0.5, **p<0.01, ***p<0.001, ****p<0.0001).

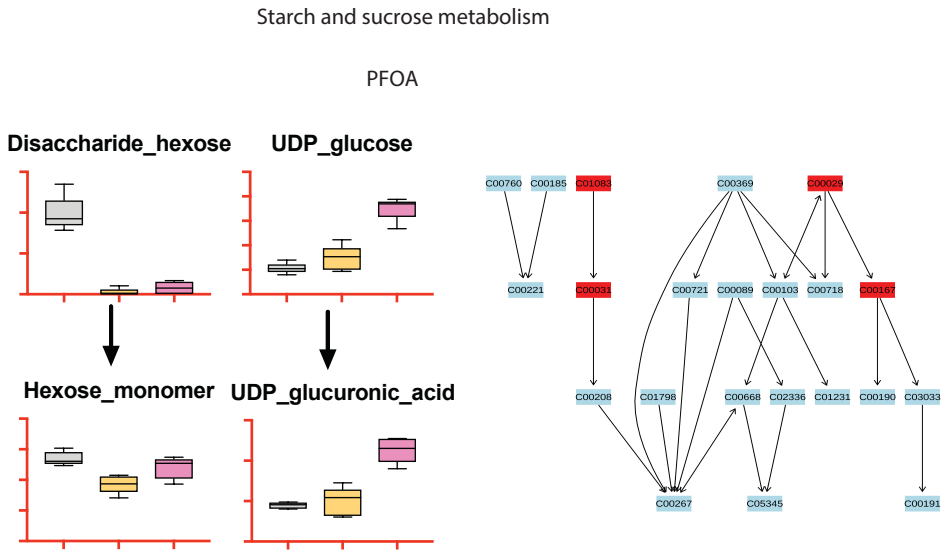

Figure 5.10. Metabolite changes induced by PFOA exposure (control=grey, 6 ppm= orange, 30 ppm = pink) from starch and sucrose metabolism pathway. This pathway was upregulated with PFOA. The biochemical map indicates which metabolites were identified in the dataset, with blue rectangles indicating metabolites that were not identified and red rectangles indicating metabolites that were present. Asterisks indicate statistically significant difference in mean for the dose compared to the control mean (*p<0.5, **p<0.01, ***p<0.001, ****p<0.0001).

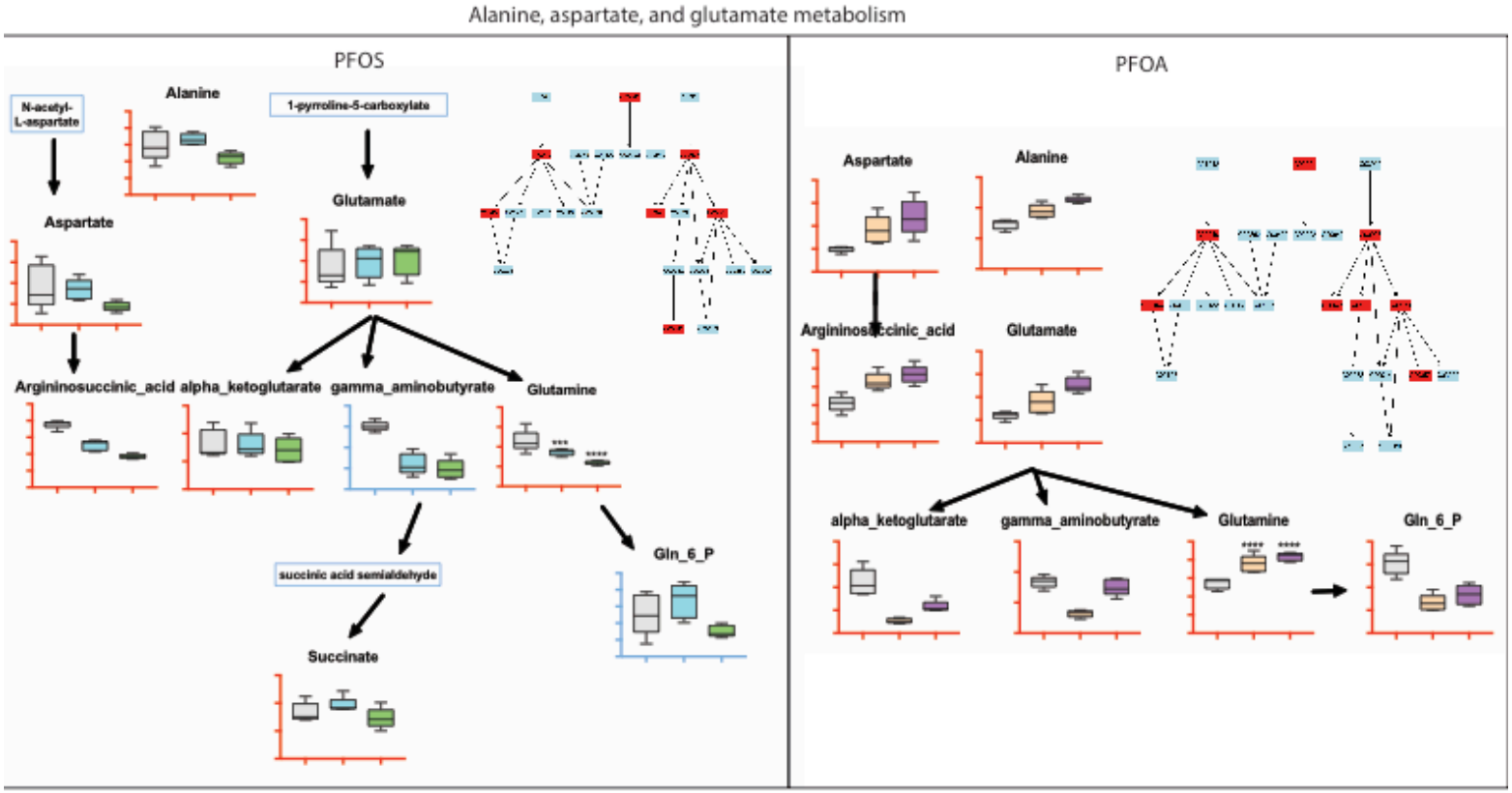

Figure 5.11. Metabolite changes induced by PFOS exposure (control=grey, 2 ppm= blue, 10 ppm = green) and PFOA (b) exposure (control=grey, 6 ppm= orange, 30 ppm = pink) from the alanine, aspartate, and glutamate metabolism pathway. This pathway was not significantly affected by PFOS but it was downregulated with PFOA. The biochemical map indicates which metabolites were identified in the dataset, with blue rectangles indicating metabolites that were not identified and red rectangles indicating metabolites that were present. Asterisks indicate statistically significant difference in mean for the dose compared to the control mean (*p<0.5, **p<0.01, ***p<0.001, ****p<0.0001)

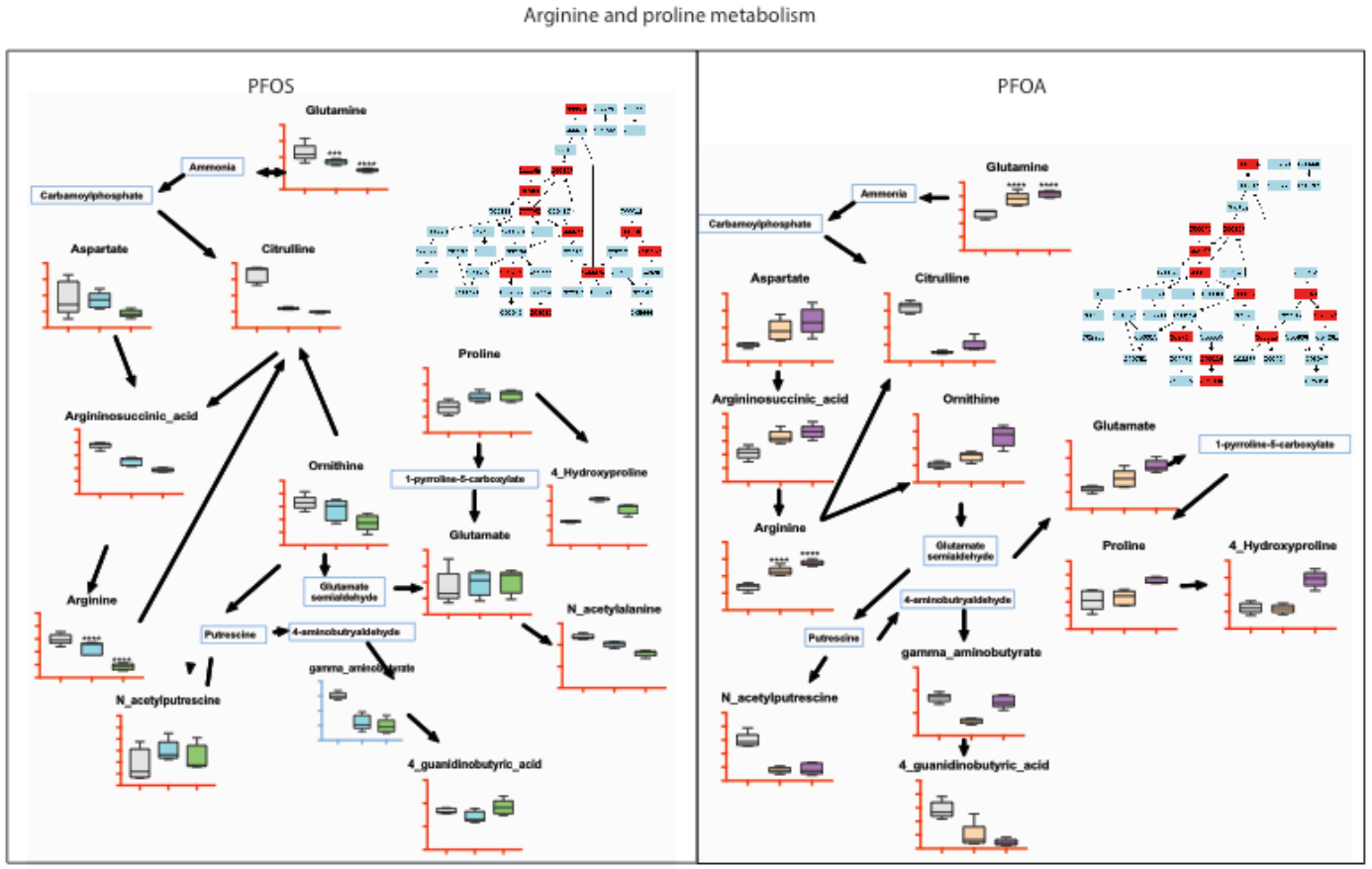

Figure 5.12. Metabolite changes induced by PFOS exposure (control=grey, 2 ppm= blue, 10 ppm = green) and PFOA (b) exposure (control=grey, 6 ppm= orange, 30 ppm = pink) from the arginine and proline metabolism pathway. This pathway was upregulated with PFOS and downregulated with PFOA. The biochemical map indicates which metabolites were identified in the dataset, with blue rectangles indicating metabolites that were not identified and red rectangles indicating metabolites that were present. Asterisks indicate statistically significant difference in mean for the dose compared to the control mean (*p<0.5, **p<0.01, ***p<0.001, ****p<0.0001).

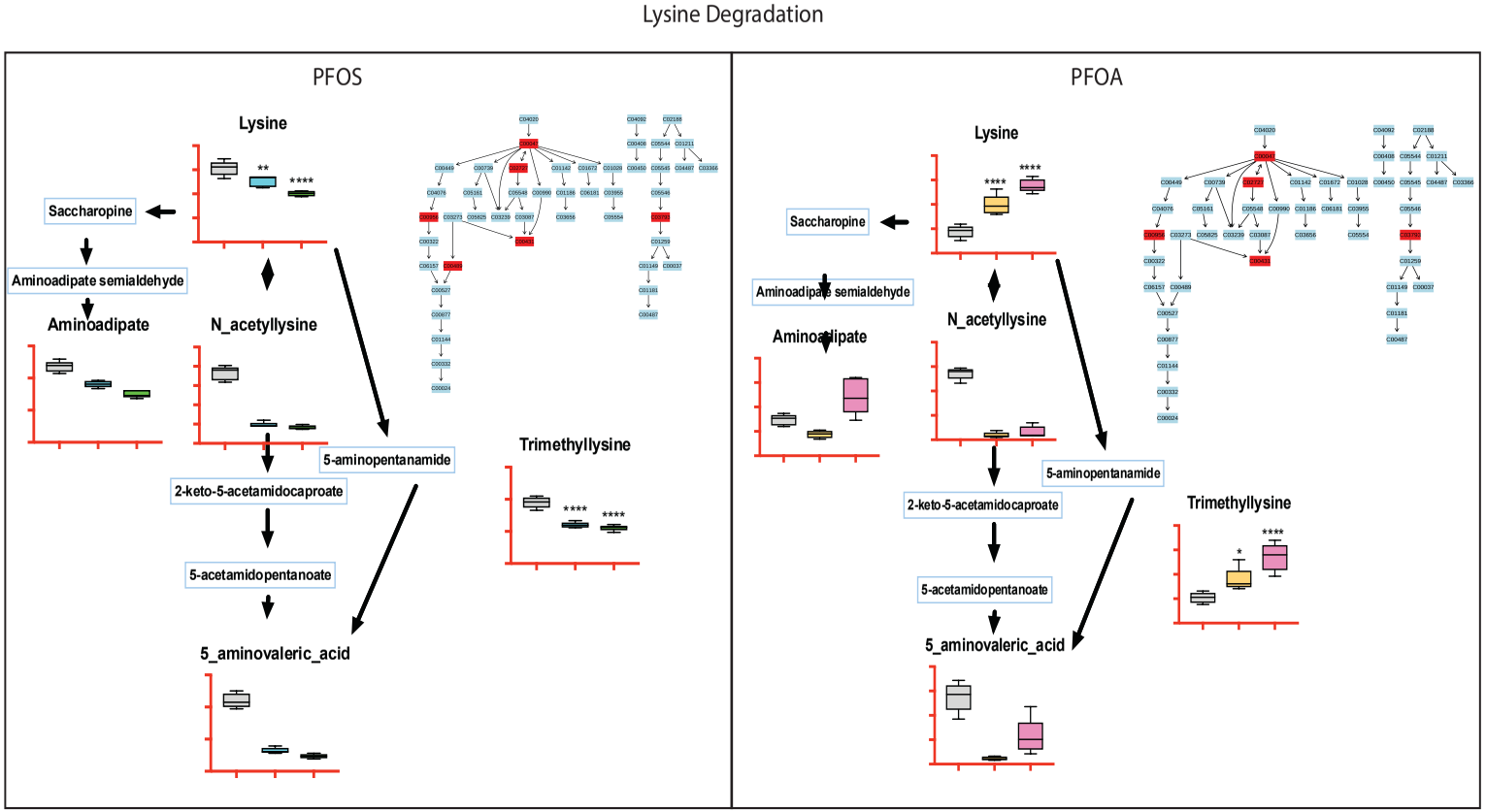

Figure 5.13. Metabolite changes induced by PFOS exposure (control=grey, 2 ppm= blue, 10 ppm = green) and PFOA (b) exposure (control=grey, 6 ppm= orange, 30 ppm = pink) from the lysine degradation pathway. This pathway was upregulated by PFOS and PFOA. The biochemical map indicates which metabolites were identified in the dataset, with blue rectangles indicating metabolites that were not identified and red rectangles indicating metabolites that were present. Asterisks indicate statistically significant difference in mean for the dose compared to the control mean (*p<0.5, **p<0.01, ***p<0.001, ****p<0.0001).

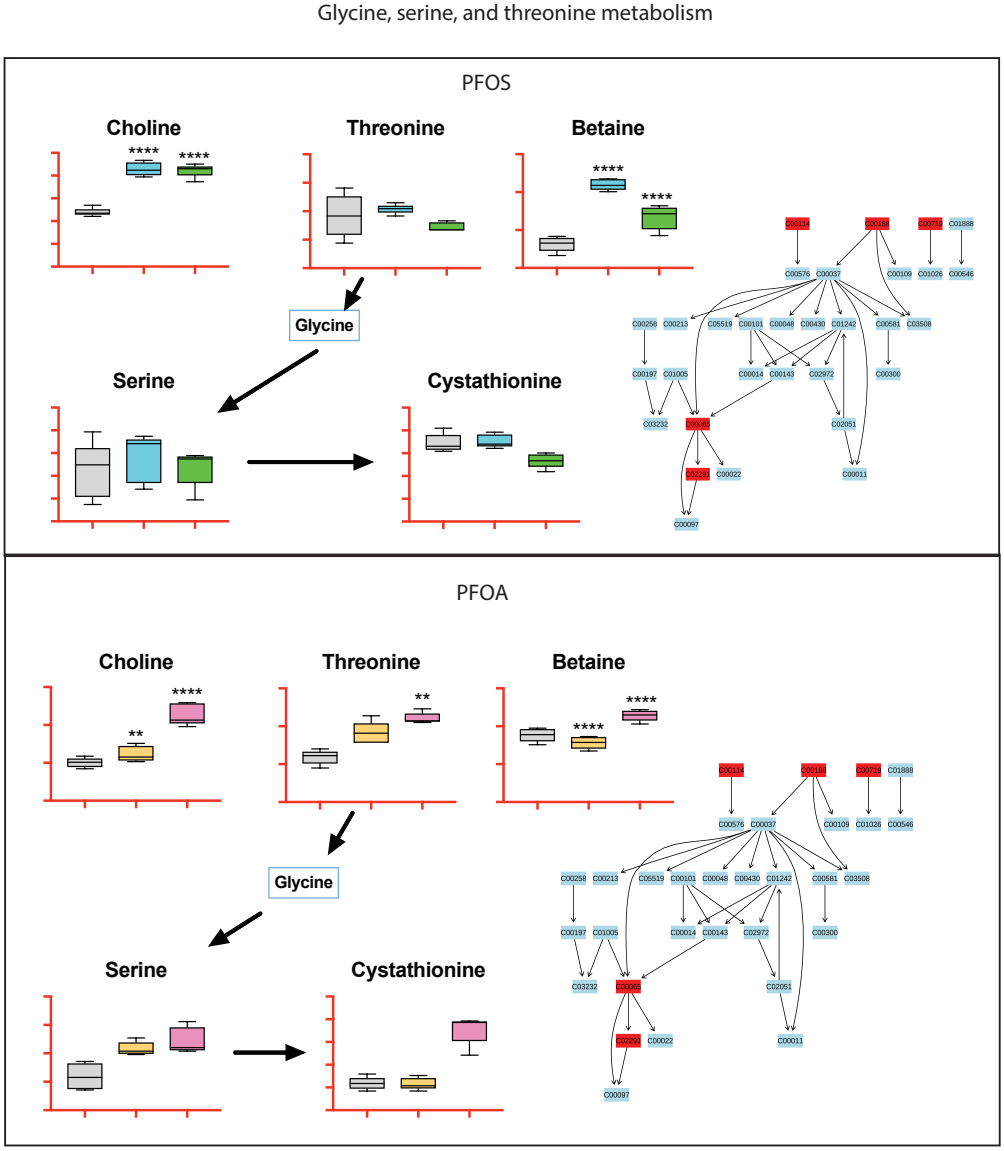

Figure 5.14. Metabolite changes induced by PFOS exposure (control=grey, 2 ppm= blue, 10 ppm = green) and PFOA (b) exposure (control=grey, 6 ppm= orange, 30 ppm = pink) from the glycine, serine, and threonine metabolism pathway. This pathway was downregulated in PFOS and PFOA. The biochemical map indicates which metabolites were identified in the dataset, with blue rectangles indicating metabolites that were not identified and red rectangles indicating metabolites that were present. Asterisks indicate statistically significant difference in mean for the dose compared to the control mean (*p<0.5, **p<0.01, ***p<0.001, ****p<0.0001).

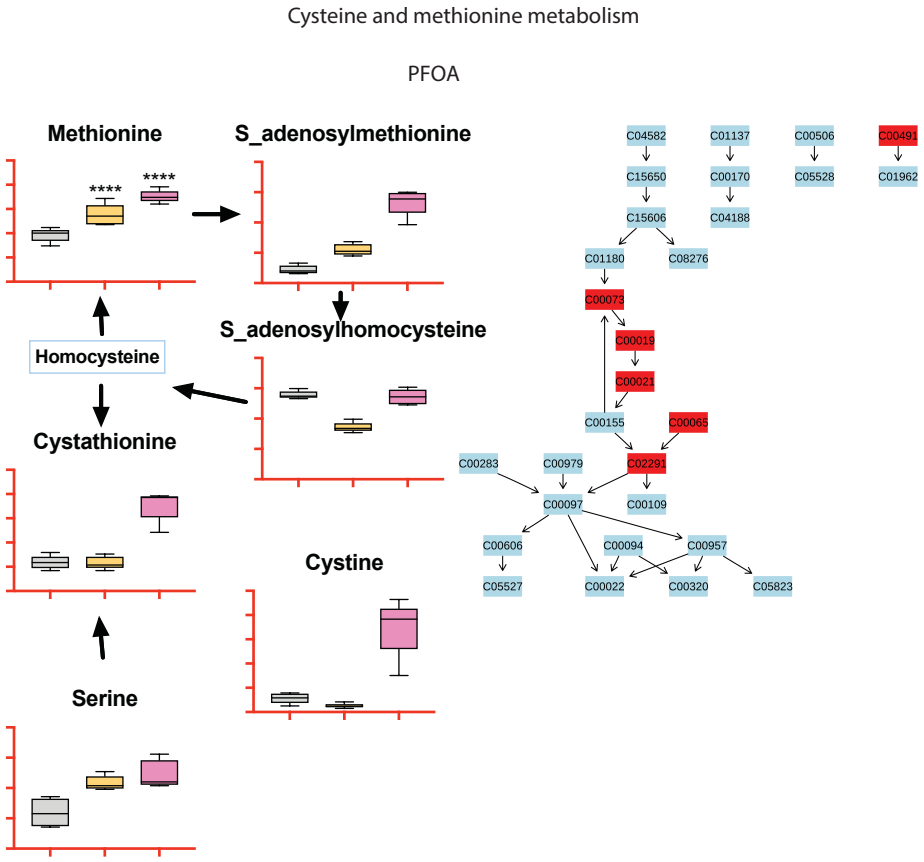

Figure 5.15. Metabolite changes induced by PFOA exposure (control=grey, 6 ppm= orange, 30 ppm = pink) from the cysteine and methionine metabolism pathway. This pathway was downregulated with PFOA. The biochemical map indicates which metabolites were identified in the dataset, with blue rectangles indicating metabolites that were not identified and red rectangles indicating metabolites that were present. Asterisks indicate statistically significant difference in mean for the dose compared to the control mean (*p<0.5, **p<0.01, ***p<0.001, ****p<0.0001).

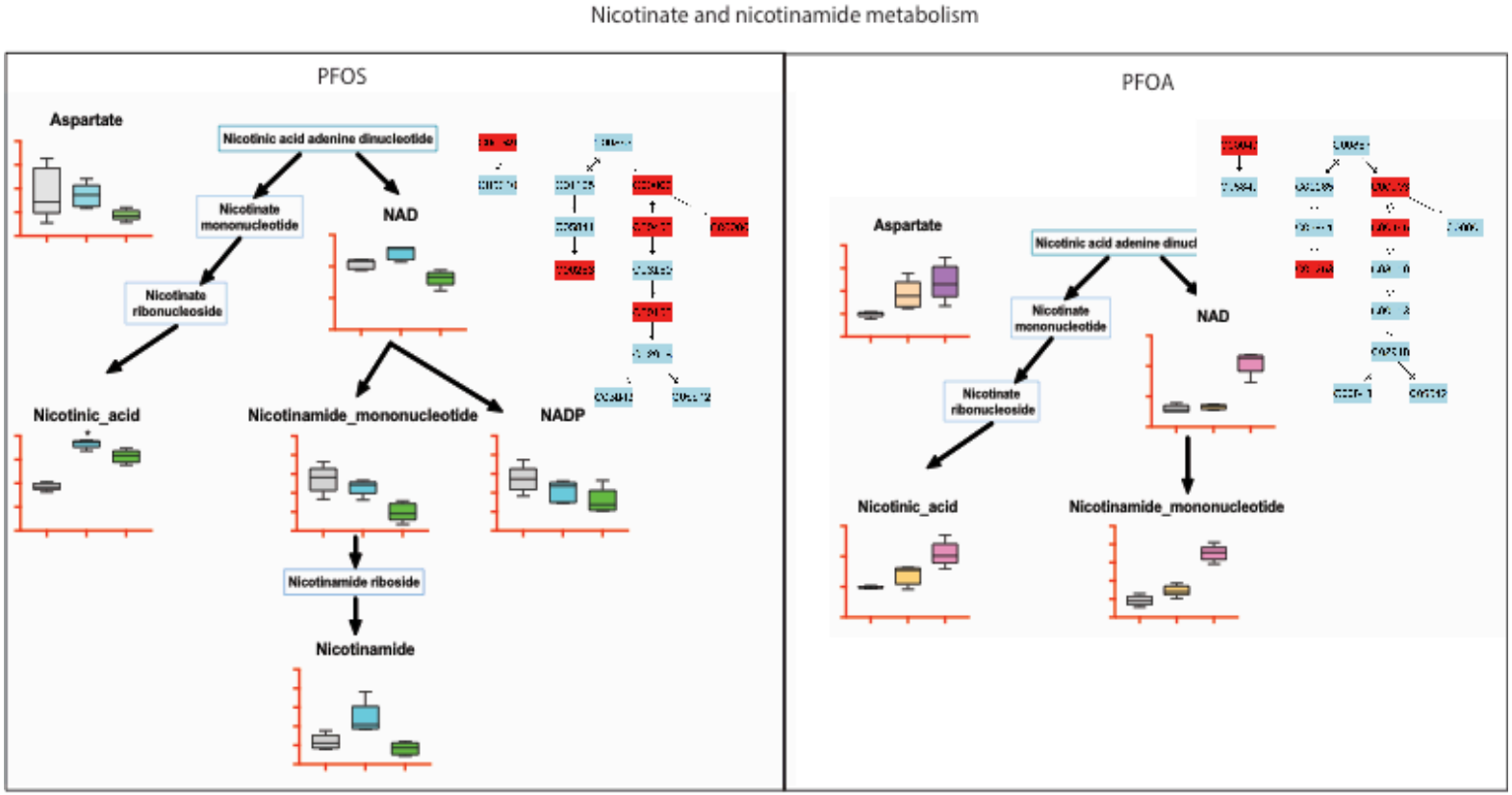

Figure 5.16. Metabolite changes induced by PFOS exposure (control=grey, 2 ppm= blue, 10 ppm = green) and PFOA (b) exposure (control=grey, 6 ppm= orange, 30 ppm = pink) from the nicotinate and nicotinamide metabolism pathway. This pathway was downregulated by PFOS and PFOA. The biochemical map indicates which metabolites were identified in the dataset, with blue rectangles indicating metabolites that were not identified and red rectangles indicating metabolites that were present. Asterisks indicate statistically significant difference in mean for the dose compared to the control mean (*p<0.5, **p<0.01, ***p<0.001, ****p<0.0001).

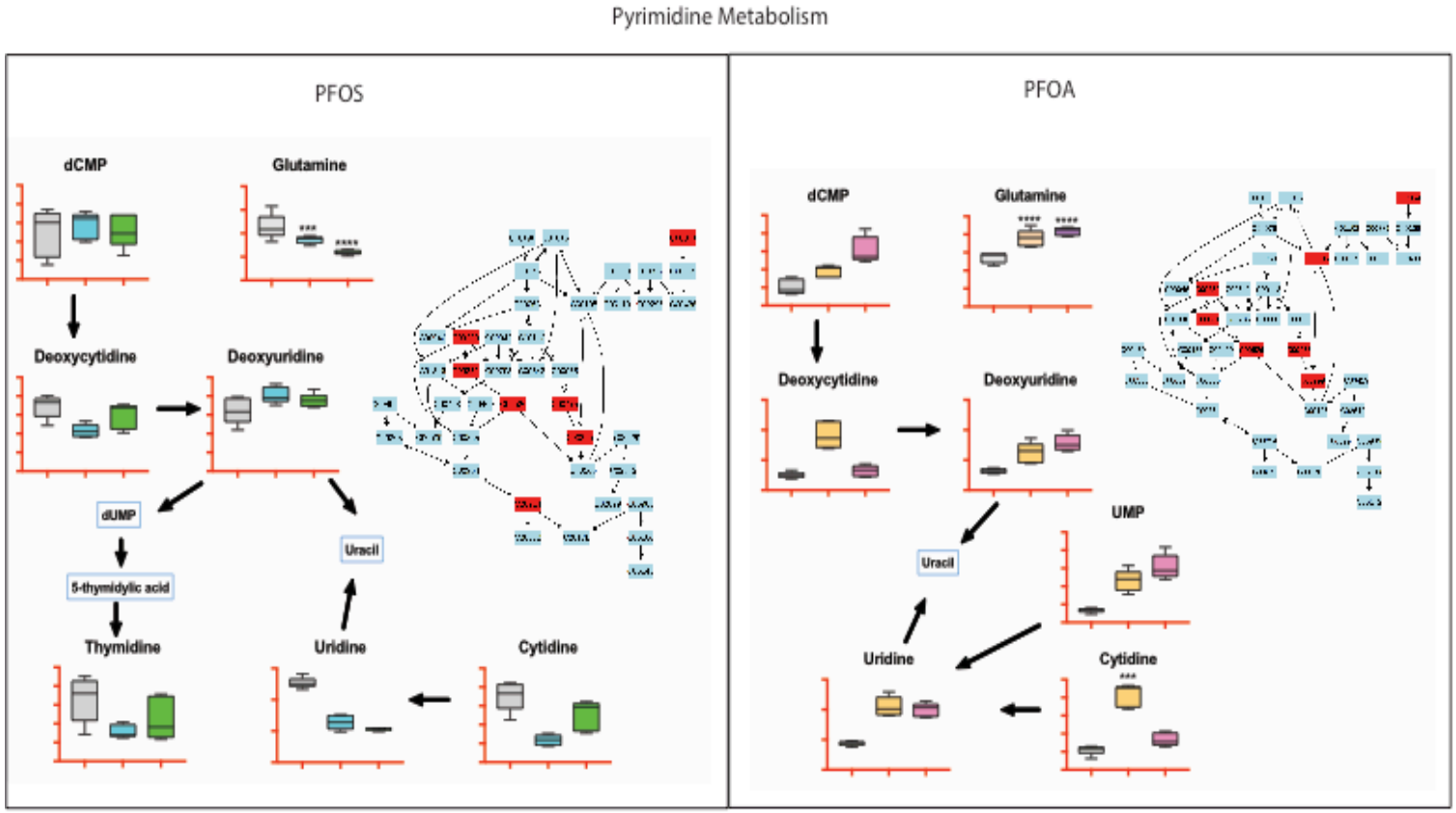

Figure 5.17. Metabolite changes induced by PFOS (control=grey, 2 ppm= blue, 10 ppm = green) and PFOA (b) exposure (control=grey, 6 ppm= orange, 30 ppm = pink) from the pyrimidine metabolism metabolic pathway. This pathway was upregulated by PFOS and PFOA. The biochemical map indicates which metabolites were identified in the dataset, with blue rectangles indicating metabolites that were not identified and red rectangles indicating metabolites that were present. Asterisks indicate statistically significant difference in mean for the dose compared to the control mean (*p<0.5, **p<0.01, ***p<0.001, ****p<0.0001).

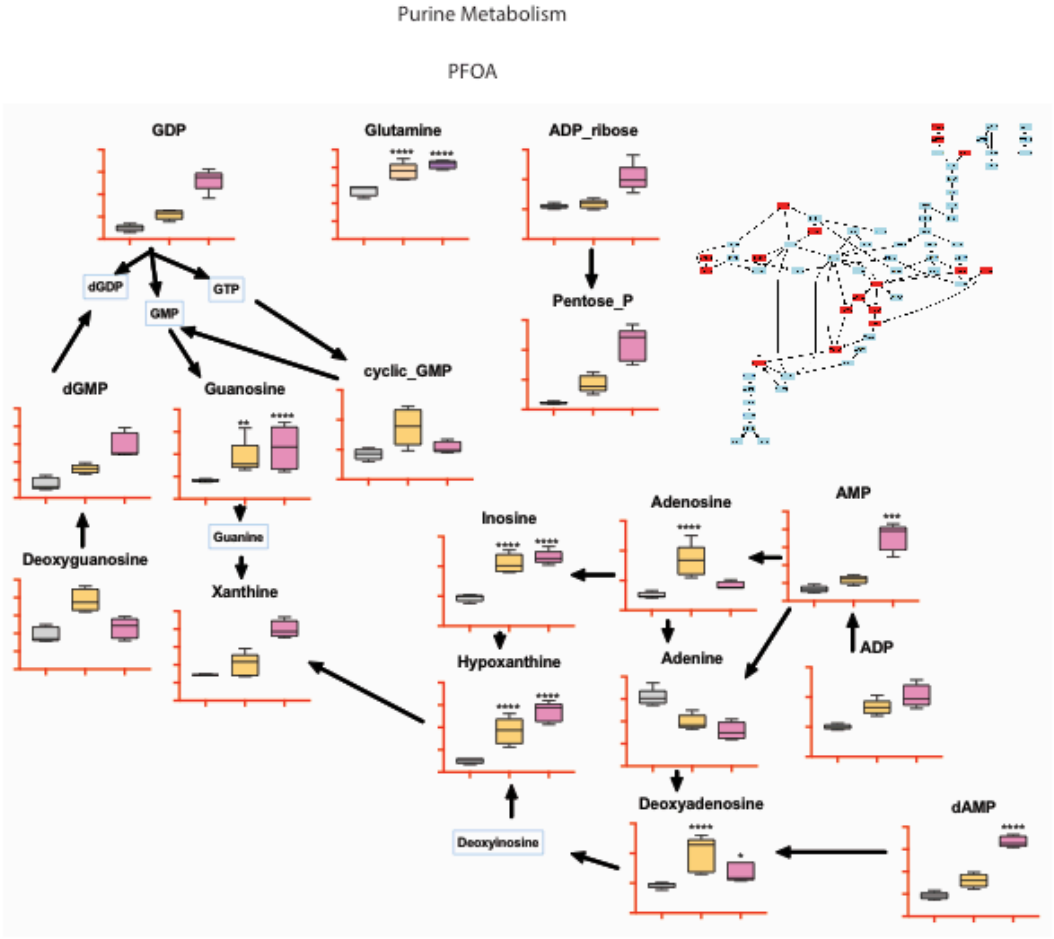

Figure 5.18. Metabolite changes induced by PFOA exposure (control=grey, 6 ppm= orange, 30 ppm = pink) from the purine metabolism pathway. This pathway was downregulated with PFOA. The biochemical map indicates which metabolites were identified in the dataset, with blue rectangles indicating metabolites that were not identified and red rectangles indicating metabolites that were present. Asterisks indicate statistically significant difference in mean for the dose compared to the control mean (*p<0.5, **p<0.01, ***p<0.001, ****p<0.0001).

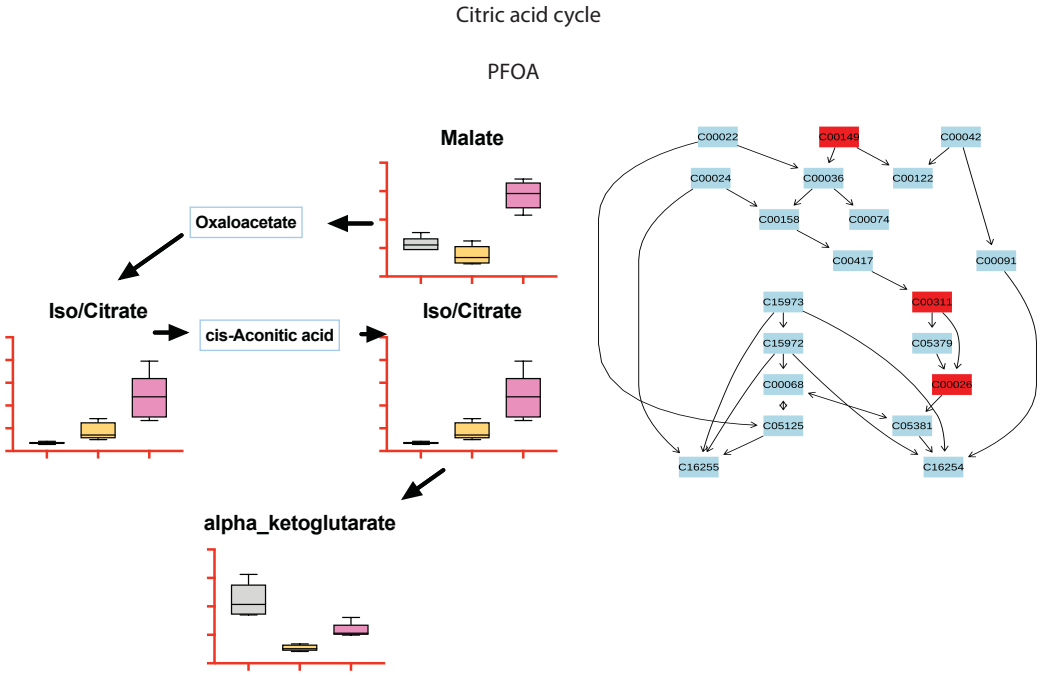

Figure 5.19. Metabolite changes induced by PFOA exposure (control=grey, 6 ppm= orange, 30 ppm = pink) from the TCA cycle. This pathway was downregulated with PFOA. The biochemical map indicates which metabolites were identified in the dataset, with blue rectangles indicating metabolites that were not identified and red rectangles indicating metabolites that were present. Asterisks indicate statistically significant difference in mean for the dose compared to the control mean (*p<0.5, **p<0.01, ***p<0.001, ****p<0.0001).

4 Conclusion

PFAS are widely distributed contaminants of the indoor and outdoor environment. Uptake in humans and animals has raised concerns about the effects of chronic exposure. PFOS and PFOA are found in many aquatic systems and in drinking water all over the world. The tendency of PFOS to bioaccumulate in fish has led to many studies on the potential toxic effects in aquatic species. Since *Artemia* are used as feedstock for aquacultures, we set out to determine the effect of PFOS and PFOA exposure on these saltwater crustaceans. From this study, we estimated that the 48 hr LC_{50} is 20 ± 9 ppm for PFOS. We did not identify an LC_{50} for PFOA due to inconsistent results, but it was approximately 60 ppm. Exposures at LC_{25} and LC_5 were conducted to identify sublethal metabolic effects. It was determined from pathway analysis that PFOS affected pathways and metabolites related to fatty acid oxidation and lipid metabolism, protein synthesis, oxidative stress, and carbohydrate metabolism. PFOA also affected these mechanisms in addition to nitrogen and methane metabolism and the TCA cycle. Many pathways related to phosphate transfer and sulfation were identified in both exposures, which are related to signal transduction, energy metabolism, and drug metabolism.[49]

5 References

1. US EPA, O. Technical Fact Sheet – Perfluorooctane Sulfonate (PFOS) and Perfluorooctanoic Acid (PFOA). *US EPA* (2017). Available at: https://www.epa.gov/. (Accessed: 21st June 2018)

2. Andersen, M. E. *et al.* Perfluoroalkyl acids and related chemistries--toxicokinetics and modes of action. *Toxicol. Sci. Off. J. Soc. Toxicol.* **102,** 3–14 (2008).

3. ATSDR - ToxFAQs™: Perfluoroalkyls. Available at: https://www.atsdr.cdc.gov/Toxfaqs/TF.asp?id=1116&tid=237. (Accessed: 21st June 2018)

4. Breysse, P. N. *Toxicological Profile: Perfluoroalkyls*. (ATSDR, 2018).

5. Radio, S. C. P. Hazardous chemical discovered in groundwater of 5 SoCal water agencies. *Southern California Public Radio* (700). Available at: https://www.scpr.org/news/2016/08/12/63545/water-agencies-shut-down-wells-after-discovering-h/. (Accessed: 21st June 2018)

6. Up to 110 Million Americans Could Have PFAS-Contaminated Drinking Water, EPA Testing Data Kept Secret. *EWG* Available at: https://www.ewg.org/research/report-110-million-americans-could-have-pfas-contaminated-drinking-water. (Accessed: 24th June 2018)

7. HHS Releases 'Nightmare' PFAS Chemical Study Suppressed by Scott Pruitt, White House. *EWG* Available at: https://www.ewg.org/release/hhs-releases-nightmare-pfas-chemical-study-suppressed-scott-pruitt-white-house. (Accessed: 24th June 2018)

8. Kunacheva, C. *et al.* Worldwide surveys of perfluorooctane sulfonate (PFOS) and perfluorooctanoic acid (PFOA) in water environment in recent years. *Water Sci. Technol. J. Int. Assoc. Water Pollut. Res.* **66,** 2764–2771 (2012).

9. Nakata, H. *et al.* Perfluorinated Contaminants in Sediments and Aquatic Organisms Collected from Shallow Water and Tidal Flat Areas of the Ariake Sea, Japan: Environmental Fate of Perfluorooctane Sulfonate in Aquatic Ecosystems. *Environ. Sci. Technol.* **40,** 4916–4921 (2006).

10. Lin, A. Y.-C., Panchangam, S. C., Tsai, Y.-T. & Yu, T.-H. Occurrence of perfluorinated compounds in the aquatic environment as found in science park effluent, river water, rainwater, sediments, and biotissues. *Environ. Monit. Assess.* **186,** 3265–3275 (2014).

11. Ahrens, L. Polyfluoroalkyl compounds in the aquatic environment: a review of their occurrence and fate. *J. Environ. Monit. JEM* **13,** 20–31 (2011).

12. Ahrens, L. & Bundschuh, M. Fate and effects of poly- and perfluoroalkyl substances in the aquatic environment: a review. *Environ. Toxicol. Chem.* **33,** 1921–1929 (2014).

13. OECD. *Test No. 211: Daphnia magna Reproduction Test*. (Organisation for Economic Co-operation and Development, 2012).

14. Xia, X., Rabearisoa, A. H., Jiang, X. & Dai, Z. Bioaccumulation of perfluoroalkyl substances by Daphnia magna in water with different types and concentrations of protein. *Environ. Sci. Technol.* **47,** 10955–10963 (2013).

15. Jeong, T.-Y., Yuk, M.-S., Jeon, J. & Kim, S. D. Multigenerational effect of perfluorooctane sulfonate (PFOS) on the individual fitness and population growth of Daphnia magna. *Sci. Total Environ.* **569–570,** 1553–1560 (2016).

16. Liang, R. *et al.* Effects of Perfluorooctane sulfonate on immobilization, heartbeat, reproductive and biochemical performance of Daphnia magna. *Chemosphere* **168,** 1613–1618 (2017).

17. Arukwe, A. & Mortensen, A. S. Lipid peroxidation and oxidative stress responses of salmon fed a diet containing perfluorooctane sulfonic- or perfluorooctane carboxylic acids. *Comp. Biochem. Physiol. Toxicol. Pharmacol. CBP* **154,** 288–295 (2011).

18. Hagenaars, A. *et al.* Toxicity evaluation of perfluorooctane sulfonate (PFOS) in the liver of common carp (Cyprinus carpio). *Aquat. Toxicol. Amst. Neth.* **88,** 155–163 (2008).

19. Han, Z., Liu, Y., Wu, D., Zhu, Z. & Lü, C. Immunotoxicity and hepatotoxicity of PFOS and PFOA in tilapia (<Emphasis Type="Italic">Oreochromis niloticus</Emphasis>). *Chin. J. Geochem.* **31,** 424–430 (2012).

20. Schuhmacher, R., Krska, R., Weckwerth, W. & Goodacre, R. Metabolomics and metabolite profiling. *Anal. Bioanal. Chem.* **405,** 5003–5004 (2013).

21. Barding, G. A., Salditos, R. & Larive, C. K. Quantitative NMR for bioanalysis and metabolomics. *Anal. Bioanal. Chem.* **404,** 1165–1179 (2012).

22. Villas-Bôas, S. G. *Metabolome Analysis: An Introduction*. (John Wiley & Sons, Ltd, 2007).

23. Xiao, J. F., Zhou, B. & Ressom, H. W. Metabolite identification and quantitation in LC-MS/MS-based metabolomics. *Trends Anal. Chem. TRAC* **32,** 1–14 (2012).

24. Zhou, B., Xiao, J. F., Tuli, L. & Ressom, H. W. LC-MS-based metabolomics. *Mol. Biosyst.* **8,** 470–481 (2012).

25. Nagana Gowda, G. A. & Raftery, D. Recent Advances in NMR-Based Metabolomics. *Anal. Chem.* **89,** 490–510 (2017).

26. Gregory A. Barding, Jr. Comparison of GC-MS and NMR Metabolite Profiling of Rice Subjected to Submergence Stress. *J. Proteome Res* 898–909 (2013).

27. MacLean, B. *et al.* Skyline: an open source document editor for creating and analyzing targeted proteomics experiments. *Bioinforma. Oxf. Engl.* **26,** 966–968 (2010).

28. Chong, J. *et al.* MetaboAnalyst 4.0: towards more transparent and integrative metabolomics analysis. *Nucleic Acids Res.* (2018). doi:10.1093/nar/gky310

29. Xia, J. & Wishart, D. S. Using MetaboAnalyst 3.0 for Comprehensive Metabolomics Data Analysis. *Curr. Protoc. Bioinforma.* **55,** 14.10.1-14.10.91 (2016).

30. Xia, J., Sinelnikov, I. V., Han, B. & Wishart, D. S. MetaboAnalyst 3.0--making metabolomics more meaningful. *Nucleic Acids Res.* **43,** W251-257 (2015).

31. MetaboAnalyst. Available at: http://www.metaboanalyst.ca/MetaboAnalyst/faces/ModuleView.xhtml. (Accessed: 27th May 2018)

32. Ji, K. *et al.* Toxicity of perfluorooctane sulfonic acid and perfluorooctanoic acid on freshwater macroinvertebrates (Daphnia magna and Moina macrocopa) and fish (Oryzias latipes). *Environ. Toxicol. Chem.* **27,** 2159–2168 (2008).

33. Ding, G. & Peijnenburg, W. J. G. M. Physicochemical Properties and Aquatic Toxicity of Poly- and Perfluorinated Compounds. *Crit. Rev. Environ. Sci. Technol.* **43,** 598–678 (2013).

34. Rayne, S. & Forest, K. Perfluoroalkyl sulfonic and carboxylic acids: A critical review of physicochemical properties, levels and patterns in waters and wastewaters, and treatment methods. *J. Environ. Sci. Health Part A* **44,** 1145–1199 (2009).

35. Wang, F., Liu, C. & Shih, K. Adsorption behavior of perfluorooctanesulfonate (PFOS) and perfluorooctanoate (PFOA) on boehmite. *Chemosphere* **89,** 1009–1014 (2012).

36. Dettmer, K., Aronov, P. A. & Hammock, B. D. MASS SPECTROMETRY-BASED METABOLOMICS. *Mass Spectrom. Rev.* **26,** 51–78 (2007).

37. Aggio, R. B. M. Pathway Activity Profiling (PAPi): A Tool for Metabolic Pathway Analysis. in *Yeast Metabolic Engineering* 233–250 (Humana Press, New York, NY, 2014). doi:10.1007/978-1-4939-0563-8_14

38. Stahl, T., Mattern, D. & Brunn, H. Toxicology of perfluorinated compounds. *Environ. Sci. Eur.* **23,** 38 (2011).

39. Clegg, James & Trotman, Clive. Physiological and Biochemical Aspects of Artemia Ecology. in *Artemia Basic and Applied Biology* **1,** (Kluwer Academic Publisher, 2002).

40. Tocher, D. R. Chapter 6 Glycerophospholipid metabolism. in *Biochemistry and Molecular Biology of Fishes* (eds. Hochachka, P. W. & Mommsen, T. P.) **4,** 119–157 (Elsevier, 1995).

41. Nordén, M., Westman, O., Venizelos, N. & Engwall, M. Perfluorooctane sulfonate increases β-oxidation of palmitic acid in chicken liver. *Environ. Sci. Pollut. Res. Int.* **19,** 1859–1863 (2012).

42. Bjork, J. A., Lau, C., Chang, S. C., Butenhoff, J. L. & Wallace, K. B. Perfluorooctane sulfonate-induced changes in fetal rat liver gene expression. *Toxicology* **251,** 8–20 (2008).

43. Sinclair, E., Mayack, D. T., Roblee, K., Yamashita, N. & Kannan, K. Occurrence of Perfluoroalkyl Surfactants in Water, Fish, and Birds from New York State. *Arch. Environ. Contam. Toxicol.* **50,** 398–410 (2006).

44. Oakes, K. D. *et al.* Short-term exposures of fish to perfluorooctane sulfonate: acute effects on fatty acyl-coa oxidase activity, oxidative stress, and circulating sex steroids. *Environ. Toxicol. Chem.* **24,** 1172–1181 (2005).

45. Schooneman, M. G., Vaz, F. M., Houten, S. M. & Soeters, M. R. Acylcarnitines. *Diabetes* **62,** 1–8 (2013).

46. *Artemia: Basic and Applied Biology | Th.J. Abatzopoulos | Springer*.

47. Soga, T. *et al.* Differential metabolomics reveals ophthalmic acid as an oxidative stress biomarker indicating hepatic glutathione consumption. *J. Biol. Chem.* **281,** 16768–16776 (2006).

48. KEGG PATHWAY: Sulfur relay system. Available at: https://www.genome.jp/kegg-bin/show_pathway?map=ko04122&show_description=show. (Accessed: 2nd July 2018)

49. Sulfation - an overview | ScienceDirect Topics. Available at: https://www.sciencedirect.com/topics/neuroscience/sulfation. (Accessed: 4th July 2018)

Conclusions and Future Work

CHAPTER SIX

1 Conclusions

The work presented in this dissertation seeks to establish *Artemia franciscana* as a model organism for studying stress in saltwater lakes using environmental metabolomics. *Artemia* are an ideal model system because they are robust, easy to work with, have a short life cycle, and have a hemolymph rich with metabolites that exchange with the environment.[1,2] Metabolomics takes advantage of this rich hemolymph and extracts information about the metabolic state of the organism and how they respond to different environmental conditions.[3,4] Metabolomics offers many advantages as an analytical approach for studying environmental stress because it is high-throughput and produces content-rich information about metabolic perturbations and biomarkers of exposure.[5]

In order to determine the utility of *Artemia* as a model species, we studied the effects of environmental stressors of increasing complexity. We started with cold stress because it is well studied in *Artemia* and similar extremophile organisms, such as the Arctic midge and freeze tolerant frogs.[6,7] With this stressor we were able to optimize and verify our analytical methods as described in Chapter 2, including *Artemia* exposures, sample preparation, and NMR and GC-MS analysis. Two-dimensional NMR methods aided in the identification of metabolites with poorly resolved resonances and uncommon metabolites, such as gadusol. It was determined that a 48 hr cold temperature stress affected metabolites related to osmoregulation and cryoprotection, including glucose, trehalose, glycerol, and gadusol.

Next, Chapter 3, we described the impacts of glyphosate exposure. Though glyphosate is a well-studied herbicide, it's effects had not been reported in *Artemia* or many saltwater contexts. Glyphosate is applied terrestrially, but still has significance in salt water ecosystems due to its extensive global agricultural application and concerns over human exposure through food consumption and farm work.[8–10] Studies have determined that the formulation of glyphosate is more toxic than the active ingredient, especially the POEA adjuvant has been reported to be toxic to several North American frogs.[11] Using NMR and GC-MS metabolomics, we determined that *Artemia* exposed to the unformulated active ingredient did not have increased mortality or experience a measurable metabolic perturbation. However, the LC_{50} for the Roundup® formulation was 237 ± 23 ppm for a 48 hr exposure. Sublethal exposure caused a metabolic perturbation in pathways involving carbohydrate and energy metabolism, folate-mediated one-carbon metabolism, *Artemia* molting and development, and microbial metabolism. The stabilizing salt, isopropylamine also present in the Roundup® formulation, was also found to have toxic effects that contribute to this perturbation.

In Chapter 4, we focused on the impacts of the organophosphate flame retardant, tris(1,3-dichloro-2-propyl) phosphate (TDCIPP). This is an emerging contaminant that has been studied in zebrafish by our collaborator, Dr. David Volz, from UCR's environmental science department. TDCIPP affects embryogenesis in zebrafish embryos, so we hypothesized that if TDCIPP affects *Artemia* growth and development we would be able

to determine this by measuring the body length of developing nauplii.[12,13] We developed an imaging assay to measure *Artemia* body length after exposure to TDCIPP. The TDCIPP LC_{50} was determined to be 37.4 ± 1.3 μM, it was determined that *Artemia* exposed to sublethal TDCIPP for 20 days had a smaller body length than control specimens. The most significant metabolic perturbations related to osmoprotectant metabolites, such as betaine, gadusol, and taurine. Pathways involving one carbon metabolism, amino acid metabolism, and glycerophospholipid metabolism were also affected.

Lastly, in Chapter 5, the emerging contaminants perfluorooctane sulfonic acid (PFOS) and perfluorooctanoic acid (PFOA) were studied. These compounds have unique chemical characteristics as fully fluorinated compounds that bioaccumulate in humans and animals.[14] We introduced LC-MS metabolomics in this study and the metabolites that are elucidated by this method. This study showed the power of LC-MS metabolomics, which was able to quantify over 100 metabolites. Bioaccumulation of these compounds was demonstrated by LC-MS and it was determined that these compounds affect pathways involving lipid metabolism, amino acid metabolism, oxidative stress, carbohydrate metabolism, and the TCA cycle.

After subjecting *Artemia* to stress from 4 different environmental contaminants and temperature stress, we were able to learn a lot about how these organisms interact with their environment and respond to stress. In each study, it was clear that sugars and osmolytes play an important role in stress response. Glucose, betaine, taurine,

phosphocholine, choline, and gadusol were significantly affected by almost every condition. Glycerol, glycerophosphocholine, and trehalose were not detected in each study likely because their concentrations change with the age of the organism, but these compounds also changed significantly for cold stress and TDCIPP exposure. Osmolyte compounds play an important role in maintaining cell volume and fluid balance in many organisms.[15,16] These are especially important in *Artemia*, because they live in extremely saline environments, such as the Great Salt Lake which seasonally fluctuates between 50 to 270 parts per thousand.[17] Metabolic perturbations related to amino acids were also identified in each study. *Artemia* hemolymph has a high concentration of free amino acids that are involved in primary metabolism and osmoregulation.

Compared with GC-MS and LC-MS, fewer metabolites were detected by NMR-based metabolomics due to its higher limits of detection and problems arising from resonance overlap because NMR analysis is usually effected without a separation. Therefore, the NMR resonances of the abundant amino acids and primary metabolites overshadowed lower concentration metabolites leading to data bias because the interpretation of metabolic mode of action is skewed towards pathways related to abundant metabolites like amino acids. The addition of a separation step in GC-MS and the use of solvent delays for high concentration species permitted the detection of some lower concentration metabolites that were not observed by NMR. LC-MS metabolomics, which became available only near the end of this research, opened up many more possibilities for metabolic interpretation because the limit of detection is lower, and the range of metabolite classes accessed is

broader. Even though the untargeted approach of GC-MS and NMR has some advantages, with targeted LC-MS metabolomics 118 metabolites were identified in the *Artemia* metabolome compared to 49 metabolites for NMR and GC-MS combined. Gadusol is an important and unusual compound in *Artemia*, and it was not identified by GC-MS or LC-MS. Gadusol was not part of the libraries used for peak identification and it is also challenging to ionize. Also, LC-MS was not able to differentiate several compounds, including hexose, hexose phosphate, and disaccharide hexose. These compounds are likely glucose, glucose-6-phosphate, and trehalose based on our 1D and 2D NMR and GC-MS data. This demonstrates the importance of using multiple instrumental platforms for metabolic profiling.

Chapter 5 also highlighted the major challenge still remaining with chemometric analyses in metabolomics studies. LC-MS produces many variables and it is challenging to find the best way to manage all of that information and draw meaningful, unbiased conclusions. Principal component analysis, t-tests, hierarchal clustering, and heat maps provide valuable information but with so many variables, it is difficult to consider all the variables together. Pathway analysis is a useful way to derive meaning from this information, but many of the resources are still lacking and only focus on human genes and pathways, limiting their utility in environmental metabolomics studies. In our analysis of the *Artemia* metabolome, important metabolites impacted by the applied stress including gadusol, homarine, ophthalmic acid, glutaryl-carnitine, and lauroyl-carnitine could not be subjected to pathway analysis because they do not have designated KEGG codes. It is also likely that their

pathways are not completely elucidated. Future advances in bioinformatics, genomics, and metabolomics will likely lead to fewer gaps in knowledge in unresolved biochemical pathways and new and improved resources for making sound hypotheses to explain metabolic perturbations in environmentally important species.

Is *Artemia franciscana* a good model organism for environmental metabolomics? This was the big question posed by my research, and I believe that work described in this dissertation has demonstrated that the answer is unequivocally yes. *Artemia* has all of the right qualities to make it a good indicator species, it is abundant and common, easy to raise, has a short life cycle, is economically important, and provides measurable responses to a wide variety of environmental stressors.[18] Additionally, *Artemia* is a more suitable model for many studies compared to *Daphnia magna* because it is tolerant of salt and temperature changes. One other important quality for an indicator species is that they are well-studied.[19] *Artemia* have been studied for hundreds of years because they have an interesting and strange interaction with their environment. Enzymes and molecules that are important for early development were characterized back in the mid to late 1900s, especially those related to diapause and hatching.[2] Unfortunately, *Artemia* have not been a popular model in the omics age and the *Artemia* genome has not been sequenced. Many metabolomics studies with well-studied model organisms, such as zebrafish and *Daphnia*, are able to make metabolic interpretations based on known genetic pathways. Therefore, *Artemia* metabolomics suffers somewhat from a lack of supporting genetic information. Several researchers have been pushing for the use of *Artemia* in more ecotoxicological studies, but one challenge

with *Artemia* is lack of standardized methods and a decision for a unified subspecies.[20–22] Therefore, it is my hope that as more researchers employ *Artemia* as a model organism, standard methods will be established, and it will be easier to fill in some of the gaps in knowledge of *Artemia* metabolic pathways.

2 Future Work

The success of the experiments described herein paves the way for future environmental metabolomics studies using *Artemia*. Among the many opportunities for future work, four possibilities are discussed as important next steps: the study of different contaminants, especially ones that are important for saltwater ecosystems such as the Salton Sea and the Great Salt Lake. Second, determine the optimal instrumentation for *Artemia* metabolomics. Third, use different omics approaches, such as lipidomics or genomics to study environmental stress. Fourth, sample *Artemia* directly from the environment to compare metabolic profiles to lab grown shrimp.

Although the *Artemia* metabolomics experiments described in this dissertation led to important findings about the mode of action of several relevant environmental contaminants, the environmental stressors that were studied are not necessarily among the biggest threats facing saltwater lakes. In order to determine that *Artemia* is a good biological model for saltwater ecosystems, we wanted to be able to compare our results with those of better studied model organisms, and those are largely freshwater. My main motivation for this work was the Salton Sea, which is an inland lake in Southern California.

The surrounding agriculture operations produce run-off that flows into the lake, causing eutrophication, high salinity, and pesticide pollution. Therefore, in future work it would be interesting to study contaminants that are important for saltwater lakes, such as metals.

Selenium is one such metal of concern at the Salton Sea. Selenium levels vary greatly across the Sea, ranging from 1.1 μg/L in the Sea to 6.6 μg/L in the Alamo River.[23] These levels are non-toxic to fish, but biomagnification increases the toxicity in higher order species and has caused massive die-offs and developmental problems in the endangered birds that rely on this body of water as the last protected stop on the Pacific Flyway.[24] Selenium exists in four states in the Sea, the majority is in the form of selenate (VI) which is found in aerobic conditions such as irrigation water. In anoxic conditions, such as deeper water and bottom sediment, selenite (0) and metal and organically-bound selenide (-II) are the dominant forms.[25] It has been shown that *Artemia* accumulate Se, there have even been proposals to use *Artemia* for bioremediation of agricultural wastewater and a new technology used chitin to sequester Se.[26,27] Studying selenium bioaccumulation in *Artemia*, as well as the metabolic perturbations resulting from selenium exposure would be important to understand its role in biomagnification and potential for bioremediation. It would also be important in future studies to evaluate the effects of different oxidation states of selenium and how they transform throughout the exposure.

In addition to studying other pollutants, more work is needed to evaluate the optimal instrumentation to be used for *Artemia* environmental metabolomics. NMR, GC-MS, and

LC-MS were used at different times in this dissertation. While it was useful to characterize metabolome with these methods, it might not be important to use each instrument for every study. However, these studies were performed under slightly different time periods and conditions and the LC-MS samples were extracted by the UCR Metabolomics Core, so the protocol was different for this method than for NMR and GC-MS. In order to determine which instrumentation are optimal, it would be useful to conduct a study using all three instruments with *Artemia* raised under the same conditions and the solvents extracted in the same manner to compare the metabolite profiles directly. Targeted LC-MS metabolomics, which only became available in the last months of my dissertation research, quantified 101 metabolites in our study compared to 43 identified by NMR and GC-MS, therefore, LC-MS is the preferred technique as far as sensitivity and detecting a wide range of metabolite classes and it would be advantageous to continue to use this method for future studies in addition to NMR or GC-MS.

Another area of further study is to apply genomics or lipidomics to the *Artemia* model. Since the *Artemia franciscana* genome is not fully sequenced, this would be a useful addition to metabolomics for interpreting metabolic impacts. The Institute for Integrative Genome Biology at UCR assists researchers with sequencing genomes and transcriptomes using next generation sequencing. Using RNA-Seq at the genomics core, gene expression can be measured in *Artemia* exposed to different conditions.[28] The UCR Metabolomics Core is also developing methods for lipidomics analysis. This would be an interesting application for *Artemia* because the yolk platelets that are present in nauplii are high in fat,

which makes them a great food source for aquacultures.[2,29] Since many bioaccumulative compounds are taken up into fatty tissue and affect processes related to fatty acid oxidation and fat reserves, as was the case with PFOS, PFOA and TDCIPP, a lipidomics study could better identify which metabolites and pathways are affected.

Lastly, it would be interesting to compare the metabolite profile of *Artemia* raised under different environmental conditions, such as Salton Sea, Mono Lake, or Great Salt Lake water. The *Artemia* cysts used in this dissertation were collected from the Great Salt Lake but hatched in sea salt reconstituted in ultrapure water, so it would be interesting to study how the growth conditions affect metabolite expression for cysts that were hatched from the same source. These bodies of water suffer from many of the same pollutants but have different levels of important inorganic species. For example, the Great Salt Lake is known for high levels of mercury, Mono Lake is highly alkaline from high levels of carbonates and sulfates, and the Salton Sea has high selenium. All three lakes are shallow, have high salinity levels, and suffer from anthropogenic interference.[17,30,31]

Artemia franciscana is a versatile and promising model system that offers many opportunities for environmental omics research. It is a robust organism that can be used to study stressors from aquatic environments of varying salinity levels. Environmental metabolomics in particular is a promising approach to studying stressors that affect arthropods, such as *Artemia*, because these organisms have hemolymph that is rich in metabolites that are susceptible to changes and are readily measured with instrumental

methods. Further studies with this system have the potential to make advances in the understanding of how aquatic organisms interact with their environment and the impact of pollutants on these organisms.

3 References

1. *Artemia: Basic and Applied Biology | Th.J. Abatzopoulos | Springer*.

2. Clegg, James & Trotman, Clive. Physiological and Biochemical Aspects of Artemia Ecology. in *Artemia Basic and Applied Biology* **1,** (Kluwer Academic Publisher, 2002).

3. Browse, J. & Lange, B. M. Counting the cost of a cold-blooded life: Metabolomics of cold acclimation. *Proc. Natl. Acad. Sci.* **101,** 14996–14997 (2004).

4. Lankadurai, Brian P, Nagato, Edward G & Simpson, M. J. Environmental metabolomics: an emerging approach to study organism responses to environmental stressors. *Environ. Rev.* **21,** 180–205 (2013).

5. Bundy, J. G., Davey, M. P. & Viant, M. R. Environmental metabolomics: a critical review and future perspectives. *Metabolomics* **5,** 3 (2009).

6. Teets, N. M., Kawarasaki, Y., Lee, R. E. & Denlinger, D. L. Expression of genes involved in energy mobilization and osmoprotectant synthesis during thermal and dehydration stress in the Antarctic midge, Belgica antarctica. *J. Comp. Physiol. B* **183,** 189–201 (2013).

7. Storey, K. B. & Storey, J. M. Freeze tolerant frogs: cryoprotectants and tissue metabolism during freeze–thaw cycles. *Can. J. Zool.* **64,** 49–56 (1986).

8. Benbrook, C. M. Trends in glyphosate herbicide use in the United States and globally. *Environ. Sci. Eur.* **28,** (2016).

9. Shahl, P. V. Toxicological Monograph on Glyphosate. in *Pesticide residues in food-2016* 89–296 (JMPR, 2016).

10. Erickson, B & Bomgardner, M. Rocky Road for Roundup. *Chemical & Engineering News* **93,** 10–15 (2015).

11. Howe, C. M. *et al.* Toxicity of glyphosate-based pesticides to four North American frog species. *Environ. Toxicol. Chem.* **23,** 1928–1938 (2004).

12. Kupsco, A., Dasgupta, S., Nguyen, C. & Volz, D. C. Dynamic Alterations in DNA Methylation Precede Tris(1,3-dichloro-2-propyl)phosphate-Induced Delays in Zebrafish Epiboly. *Environ. Sci. Technol. Lett.* **4,** 367–373 (2017).

13. Volz, D. C. *et al.* Tris(1,3-dichloro-2-propyl) phosphate Induces Genome-Wide Hypomethylation Within Early Zebrafish Embryos. *Environ. Sci. Technol.* (2016). doi:10.1021/acs.est.6b03656

14. Breysse, P. N. *Toxicological Profile: Perfluoroalkyls*. (ATSDR, 2018).

15. Yancey, P. H., Clark, M. E., Hand, S. C., Bowlus, R. D. & Somero, G. N. Living with Water Stress: Evolution of Osmolyte Systems. *Science* **217,** 1214–1222 (1982).

16. Yancey, P. H. Organic osmolytes as compatible, metabolic and counteracting cytoprotectants in high osmolarity and other stresses. *J. Exp. Biol.* **208,** 2819–2830 (2005).

17. Great Salt Lake Ecosystem Program. Available at: https://wildlife.utah.gov/gsl/brineshrimp/babies.php. (Accessed: 15th May 2017)

18. Bioindicators: Using Organisms to Measure Environmental Impacts | Learn Science at Scitable. Available at: https://www.nature.com/scitable/knowledge/library/bioindicators-using-organisms-to-measure-environmental-impacts-16821310. (Accessed: 10th March 2018)

19. Bioindicators: the natural indicator of environmental pollution: Frontiers in Life Science: Vol 9, No 2. Available at: https://www.tandfonline.com/doi/full/10.1080/21553769.2016.1162753. (Accessed: 10th March 2018)

20. Nunes, B. S., Carvalho, F. D., Guilhermino, L. M. & Van Stappen, G. Use of the genus Artemia in ecotoxicity testing. *Environ. Pollut. Barking Essex 1987* **144,** 453–462 (2006).

21. Kerster, H. W. & Schaeffer, D. J. Brine shrimp (Artemia salina) nauplii as a teratogen test system. *Ecotoxicol. Environ. Saf.* **7,** 342–349 (1983).

22. Libralato, G. The case of Artemia spp. in nanoecotoxicology. *Mar. Environ. Res.* **101,** 38–43 (2014).

23. Holdren, G. C. & Montaño, A. Chemical and physical characteristics of the Salton Sea, California. *Hydrobiologia* **473,** 1–21 (2002).

24. Riedel, Ralf, Schlenk, Daniel, Frank, Donnell & Costa-Pierce, Barry. Analysis of organic and inorganic contaminants in Salton Sea fish. *Mar. Pollut. Bull.* **44,** 403–411 (2002).

25. Schroeder, R. A., Orem, W. H. & Kharaka, Y. K. Chemical evolution of the Salton Sea, California: nutrient and selenium dynamics. *Hydrobiologia* **473,** 23–45 (2002).

26. Schmidt, Radomir; Tantoyotai, Prapakorn; Fakra, Sirine C.; Marcus, Matthew A.; Yang, Soo In; Pickering, Ingrid J.; Banuelos, Gary S.; Hristova, Krassimira R.; Freeman, John L. Selenium Biotransformation in an Engineered Aquatic Ecosystem for Bioremediation of Agricultural Wastewater via Brine Shrimp Production. *Environ. Sci. Technol.* **47,** 5057–5065 (2013).

27. New Technology That Could Help Avert Toxicity Crisis at Salton Sea. *Water* Available at: https://www.newsdeeply.com/water/articles/2018/01/04/new-technology-that-could-help-avert-toxicity-crisis-at-salton-sea. (Accessed: 7th August 2018)

28. Horgan, R. P. & Kenny, L. C. 'Omic' technologies: genomics, transcriptomics, proteomics and metabolomics. *Obstet. Gynaecol.* **13,** 189–195 (2011).

29. Nitrogen Metabolism in Non-Insect Arthropods. in *Comparative Biochemistry of Nitrogen Metabolism* (ed. Campbell, JW) 299–372 (Academic Press INC, 1970).

30. Williams, W. D. Salinisation: A major threat to water resources in the arid and semi-arid regions of the world. *Lakes Reserv. Res. Manag.* **4,** 85–91 (1999).

31. Williams, W. d. Environmental threats to salt lakes and the likely status of inland saline ecosystems in 2025. *Environ. Conserv***,** 154–167 (2002).